OPEN ACCESS

University of BRISTOL

This electronic thesis or dissertation has been downloaded from Explore Bristol Research, http://research-information.bristol.ac.uk

Author:
Allen, Rachel Elizabeth

Title:
Controls on pyritization in recent sediments, and their role in fossilization.

General rights
Access to the thesis is subject to the Creative Commons Attribution - NonCommercial-No Derivatives 4.0 International Public License. A copy of this may be found at https://creativecommons.org/licenses/by-nc-nd/4.0/legalcode This license sets out your rights and the restrictions that apply to your access to the thesis so it is important you read this before proceeding.

Take down policy
Some pages of this thesis may have been removed for copyright restrictions prior to having it been deposited in Explore Bristol Research. However, if you have discovered material within the thesis that you consider to be unlawful e.g. breaches of copyright (either yours or that of a third party) or any other law, including but not limited to those relating to patent, trademark, confidentiality, data protection, obscenity, defamation, libel, then please contact collections-metadata@bristol.ac.uk and include the following information in your message:

• Your contact details
• Bibliographic details for the item, including a URL
• An outline nature of the complaint

Your claim will be investigated and, where appropriate, the item in question will be removed from public view as soon as possible.

Controls on pyritization in Recent sediments, and their role in fossilization.

Rachel Elizabeth Allen

Thesis submitted for the degree of Doctor of Philosophy to the University of Bristol.
Department of Geology, September 1996

Acknowledgements

This Ph.D project was funded by NERC studentship GT4/92/120/G.

I would like to thank Professors Derek Briggs and John Parkes for their supervisory assitance, and Drs Simon Bale, Peter Wellsbury, Barry Cragg, Phil Wilby and Steve Barnes, and Kim Goodman for the technical assistance I have recieved.

I would also like to thank the rest of the members of the geology department at Bristol University, especially those residing in the geomicrobiology and palaeontology laboratories for their advice, friendship, alcohol supplies and insults. Lastly, thanks to Steve Dewhurst, who has been remarkably supportive throughout this project.

Abstract

Pyrite is the most abundant authigenic sulphide mineral, commonly occurring in conjunction with organic matter in argillaceous sediments. It forms in anaerobic marine environments where sulphate-reducing bacteria metabolise organic matter and sulphate, producing hydrogen sulphide. Hydrogen sulphide reacts with iron minerals to form iron monosulphides; which react with hydrogen sulphide (Rickard, 1997), elemental sulphur (Berner, 1970) or polysulphides (Rickard, 1975) to form pyrite. In marine sediments, pyrite formation appears to be controlled by the concentrations of metabolisable organic matter, sulphate and reactive iron, with organic matter being the dominant control in terrigenous sediments (Berner, 1970). When cultures of sulphate-reducing bacteria were grown under conditions where sulphate and organic matter could become limiting, pyrite formation was controlled by the form of iron compounds and the possibility of oxygen leaking into the experiment, as these affected the dominant reaction to form pyrite and the proportion of the reduced sulphur pool represented by pyrite. Where lepidocrocite was the iron source, or oxygen leaked into the experiment, an actively metabolising culture of sulphate-reducing bacteria is required to prevent the oxidation of reduced sulphur species. High concentrations of iron also affected the iron sulphide pool as the high iron:hydrogen sulphide ratio meant that iron monosulphides were the dominant species. The iron sulphides produced in the bacterial cultures are poorly crystalline, and are bound to the bacterial cells and extra-cellular polysaccharides. The surfaces of organic particles added to cultures were rapidly colonised and covered with the iron sulphide film. This probably represents the mechanism for the formation of mineral coats, and may play a part in the initial nucleation of pyrite in association with organic matter.

Although low concentrations of iron in cultures favoured pyrite precipitation, the preservation of a decaying carcass requires high concentrations of iron to prevent hydrogen sulphide from diffusing out of the carcass. This process is assisted by the development of iron diffusion gradients into the carcass. Low iron concentrations produced diffuse halos and banded precipitates of iron sulphide. Liesegang banded precipitation is formed by a negative feedback reaction, where the consumption of hydrogen sulphide and iron monosulphides in a zone of pyrite precipitation prevents the formation of iron sulphides in areas surrounding this zone (Berner, 1969; Ortoleva, 1994). Higher concentrations of iron prevented the diffusion of hydrogen sulphide out of the carcass and produced pyrite biofilms and calcium carbonate bundles inside and around the shrimp carcass. This type of mineralization is similar to that seen in cases of soft tissue pyritization. Pyritization of soft tissues requires very high concentrations of dissolved iron to be present in the sediment porewaters (Raiswell *et al.*, 1993; Briggs *et al*, 1996). Previous models of soft tissue pyritization limited iron reduction by limiting the availability of metabolisable organic matter do not explain the production of high iron concentrations. However, when metabolisable organic matter is available, iron reduction can be dominant due to either the redox potential of the sediment or the availability of iron compounds. This would still generate high concentrations of dissolved iron in the sediment, and sulphate reduction could occur within carcasses, due to the higher pH and availablity of sulphate rather than reactive iron minerals.

Contents

Chapter One- General Introduction **Page No.**

1.A - Pyrite Mineralogy and Occurrences 1
1.B - Previous Work on the Chemistry of Pyrite Formation 6
1.C - Pyrite in Association with Organic Particles 10
1.D - Investigative Aims 11

Chapter Two - Development of Selective Digestion Procedures for Reduced Sulphur Species

2.A - Introduction 12
2.A.1 - Methods of determining the proportion of different types of reduced sulphur compounds in sediments 13
2.B - Methods
2.B.1 - Sample preparation and selection 16
2.B.2 - Analysis of samples 17
2.B.3 - The digestions 19
2.C - Results and Discussions 20
2.D - Conclusions 25

Chapter Three - Bacterial Experiments Modelling Controls upon the Formation of Pyrite

3.A - Introduction 28
3.B - The production of pyrite in bacterial cultures 29
3.B.1 - Experimental method 29
3.B.2 - Results 30
3.B.2.1 - Changes in sulphur compounds 30
3.B.2.2 - pH changes 32
3.B.2.2 - What form does the pyrite take? 33
3.C - Sulphate reduction and pyrite formation under different environmental conditions 37

Contents

3.C.1 - Introduction 37

3.C.2 - The effect of different iron compounds on the rate and amount of pyrite formation in bacterial cultures. 38

3.C.2.1 - Changes in the concentrations of sulphur compounds 38

3.C.2.2 - The effect on pH of changing the iron source 39

3.C.3 - The effect of changing the concentration of iron on the rate and amount of pyrite formation in bacterial cultures. 42

3.C.4 - The effect of changing the concentration of bacterial substrate on the rate and amount of pyrite formation in bacterial cultures. 43

3.C.5 - The effect of changing the concentration of sulphate on the rate and amount of pyrite formation in bacterial cultures. 44

3.C.6 - The effect of changing the medium type on the rate and amount of pyrite formation in bacterial cultures. 46

3.C.7 - The effect of changing the substrate and bacterial strain on the rate and amount of pyrite formation in bacterial cultures. 48

3.C.8 - The effect of sealing the experimental vials on the rate and amount of pyrite formation in bacterial cultures. 48

3.C.9 - Pyrite formation without bacterial metabolism 50

3.C.10 -The effect of combinations of variables on the rate and amount of pyrite formation in bacterial cultures. 52

3.D - Discussion 53

3.E - Conclusions 55

Chapter Four - Physical Controls upon Pyritization

4.A - Introduction 58

4.B - The Availability of Organic and Iron compounds 59

4.C - The Effect of Diffusion 60

4.D - Experimental Aims 61

4.E - Aqueous Cultures

4.E.1 - Methods for aqueous cultures 62

4.E.2 - Methods for Visking Tubing Experiments 64

4.E.3 - Results for Aqueous Experiments

4.E.3.1 - Set A 65
4.E.3.2 - Set B 68
4.E.3.3 - Set C 72
4.E.3.4 - Results from the Visking Tubing Experiments 74
4.E.3.5 - Discussion of Aqueous Experiments 74
4.F - Gel-stablised Systems 75
4.F.1 - Methods for gel-stablised systems 75
4.F.2 - Results of gel-stablised systems 79
4.F.2.1 - Set 1 79
4.F.2.2 - Set 2 79
4.F.2.3 - Set 3 82
4.F.2.4 - Set 4 82
4.F.2.5 - Set 5 82
4.F.3 - Using the data from the gel-stablised systems 85
4.F.4 - Discussion of gel-stablised systems 90
4.G - Sediment incubations 93
4.G.1 - Introduction 93
4.G.2 - Results of sediment incubations
4.G.3 - Conclusions drawn from sediment incubations 95
4.H - Conclusions of Physical Controls 95

Chapter Five - The Rock Record and Pyritization
5.A - Introduction 97
5.B - Stratigraphy of the Belemnite Marls 97
5.C - Lithologies and faunal elements collected from the Upper Belemnite Marls and Lower Clays of the Green Ammonite Beds
5.C.1 - The Basal Marls 100
5.C.2 - The Crinoid Limestone 100
5.C.3 - The Pyritic Marls 101
5.C.4 - The Bioturbated Marls and Belemnite Stone 102
5.C.5 - The Lower Clays of the Green Ammonite Beds 102
5.D - Analytical Methods
5.D.1 - Hand-specimen treatment 102
5.D.2 - Chemical Analysis 103

5.D.2.1 - Elemental analysis 103
5.D.2.2 - Sulphide analysis 103
5.D.2.3 - Percentage total organic matter (%TOM) 104
Measurements
5.E - Chemical Results 104
5.F - Discussion 104
5.F.1 - Limestone Bands 108
5.F.2 - The Lower Pyritic Marl 108
5.F.3 - The Upper Pyritic Marl 109
5.G - Conclusions 110

Chapter Six - General discussion and Conclusions 112
References 118
Appendices 128

Figures

Chapter One

Figure 1.1 - Pyrite forms and pyritization in sediments 2
Figure 1.2 - Profiles of AVS and pyritic sulphide (PS) concentrations found in different sedimentary environments 3
Figure 1.2 - Schematic representation of a sediment column showing summary of pyrite mechanisms 4
Figure 1.3 - Relationship between monosulphide and pyrite (Berner, 1969) 6
Figure 1.4 - Mechanisms of pyrite formation (Luther & Ferdelmann, 1993) 9

Chapter Two

Figure 2.1 - Apparatus used for solid sulphide digestions (1 bank of a bank of 6) 15
Figure 2.2 - Distribution of reduced sulphur species measured in Tamar Estuary sediments 22
Figure 2.3 - Distribution of reduced sulphur species in an experimental sample 25
Figure 2.4 - Schematic diagram of method for determining the concentration of reduced sulphur species 26

Chapter Three

Figure 3.1 - Decreases in sulphate concentrations and increases in TRIS and bacterial numbers; where TRIS concentrations are the sum of hydrogen sulphide, acid-volatile sulphide, pyritic sulphide and elemental sulphur concentrations. 31
Figure 3.2 - Changes in the concentrations of reduced sulphur species in a bacterial experiment. 31
Figure 3.3 - pH changes in bacterial experiments containing ferrous sulphate 32
Figure 3.4 - Bacterial biofilms in experiments 34
Figure 3.5 - SEM and Acridine-orange stainned micrographs of biofilms 35

Figure 3.6 - Microprobe results of samples from the bacterial experiments 36

Figure 3.7 - Changes in the concentration of sulphate and reduced sulphur species in an experiment containing lepidocrocite (an iron monosulphide) 39

Figure 3.8 - Changes in the concentration of sulphate and reduced sulphur species in an experiment containing mackinawite (an iron oxyhydroxide) 40

Figure 3.9 - pH changes in experiments containing ferrous sulphate, lepidocrocite and mackinawite 41

Figure 3.10 - Changes in the concentration of sulphate and reduced sulphur species in an experiment containing 15mM lepidocrocite 42

Figure 3.11 - Changes in the concentration of sulphate and reduced sulphur species in an experiment containing low lactate concentrations 44

Figure 3.12 - Changes in the concentration of sulphate and reduced sulphur species in experiments which had different sulphate concentrations throughout the experiments 45

Figure 3.13 - Changes in the concentration of sulphate and reduced sulphur species in an experiment containing Widdels medium 47

Figure 3.14 - Changes in the concentration of sulphate and reduced sulphur species in an experiment sealed with buytl or neoprene septa 49

Chapter Four

Figure 4.1 - Structures on the cuticle of a decaying shrimp in aqueous experiment A 66

Figure 4.2 - Structures on the organic particles in aqueous experiment A 67

Figure 4.3 - Structures on the cuticle of a freshly-killed shrimp 69

Figure 4.4 - Structures on the cuticle of a decaying shrimp in aqueous experiment B 70

Figure 4.5 - Structures on the organic particles in aqueous experiment B 71

Figure 4.6 - Structures on the organic particles in aqueous experiment C 73

Figure 4.7 - Starting conditions for gel-stablised systems 77

Figure 4.8 - Graphs showing variations in cumulative concentrations of AVS, pyritic sulphide and elemental sulphur in gel-stabilised set 1 80
Figure 4.9 - Graphs showing variations in cumulative concentrations of AVS, pyritic sulphide and elemental sulphur in gel-stabilised set 2 81
Figure 4.10 - Graphs showing variations in cumulative concentrations of AVS, pyritic sulphide and elemental sulphur in gel-stabilised set 3 83
Figure 4.11 - Graphs showing variations in cumulative concentrations of AVS, pyritic sulphide and elemental sulphur in gel-stabilised set 4 84
Figure 4.12 - Graphs showing variations in cumulative concentrations of AVS, pyritic sulphide and elemental sulphur in gel-stabilised set 5 86
Figure 4.13 - Details of structures associated with the hard interior of shrimps in gel-stabilised experiment 5 87
Figure 4.14 - Details of structures associated with the hard interior of shrimps in gel-stabilised experiment 5 88
Figure 4.15 - Cumulative reduced sulphur species profiles from incubations of Severn Estuary sediments 94

Chapter Five

Figure 5.1 - Sketch map of geology surrounding Seatown, Dorset, UK 98
Figure 5.2 - Log of sampled section beneath Golden Cap, Dorset, UK 99
Figure 5.3 - Distribution of faunal elements in the Crinoid Limestone 101
Figure 5.4 - Distribution of sulphur and organic carbon concentrations (%S and %TOC) in the Belemnite Marls 106
Figure 5.5 - Distribution of some major elements in the Belemnite Marls 107
Figure 5.6 - Some variations in the trace element distribution in the Belemnite Marls 110

Tables

Table I - Summary of previous work on pyrite formation 7

Table II - Mineral samples analysed 18

Table III - Recoveries obtained under various digestions 21

Table IV - Summary of Methods 29

Table V - A comparison of the rate of sulphate reduction and size of the bacterial population in a culture of sulphate-reducing bacteria 30

Table VI - Comparison of sulphate reduction and TRIS production rates in mM day-^{1} for ferrous sulphate, lepidocrocite and mackinawite experiments. 42

Table VII - Sulphate reduction and TRIS production rates in mM day-^{1} for experiments with high and low lactate concentrations. 43

Table VIII - Sulphate reduction and TRIS production rates in mM day-^{1} for experiments using Postgates and Widdels media 47

Table IX- Sulphate reduction and TRIS production rates in mM day-^{1} for experiments sealed with butyl and neoprene septa. 50

Table X - Concentrations of Hydrogen sulphide (H_2S), acid-volatile sulphide (AVS), pyritic sulphide (PS), elemental sulphide (ES) and TRIS in experiments injected with sodium sulphide solution. 70

Table XI - Medium receipe for aqueous and gel experiments 63

Table XII - Aqueous experiments variations 63

Table XII - Acid-volatile sulphide (AVS), total reduced inorganic sulphide (TRIS), Total organic matter (%TOM), iron and calcium concentrations and DOP values from the Belemnite Marls 105

Appendices

Appendix 1 -Abbreviations used 128

Appendix 2 - Preparing the Jones Reductor column 129

Appendix 3 - Methods of making artificial compounds 130

Appendix 4 - Media Receipes 132

Appendix 5 - Methods for determining the concentrations of dissolved sulphide, sulphate and thiosulphate ions 134

A5.1 - Sulphide Titration 134

A5.2 - Methods for determining the concentration of Reduced Sulphide Species in cultures 134

A5.3 - Bacterial Direct Counts (AODC) 135

A5.4 - Modified sulphide analysis 135

A5.3- Determination of sulphate and thiosulphate 136

Appendix 6 - Chapter Three Results 137

Appendix 7 - Chemical Drying for Scanning-Electron Microscopy 140

Appendix 8 - Results of the aqueous fossilization experiments 141

Appendix 9 - Results of the gel-stabised experiments 144

Appendix 10- Results from the analysis of sediment incubations 154

Appendix 11 - Results from the analysis of rock samples from the Lower Lias of Dorset, UK 155

Chapter One
General Introduction

1.A - Pyrite mineralogy and occurrences.

Pyrite is the most common sulphide mineral found in ancient and Recent argillaceous sediments, and as such is a major sink in the biogeochemical cycles of sulphur. It produces both economic metalliferous deposits and some of the commonest examples of fossilisation (Canfield and Raiswell, 1991). This iron bisulphide is cubic, metallic and has a brassy yellow colour in hand specimen (Deer *et al.*, 1966). Euhedral pyrite commonly occurs in masses of interlocking, striated cubes, but it can take a bladed or framboidal habit (Canfield and Raiswell, 1991) (Figure 1.1). Pyrite can be formed hydrothermally in sulphide rich systems such as mid-ocean ridges, or by reactions between bacterially-produced hydrogen sulphide and sedimentary iron minerals. Hydrogen sulphide is produced in anoxic sediments as a by-product of the bacterial reduction of sulphate. Under anaerobic conditions, sulphate-reducing bacteria utilise organic matter and sulphate in the following reactions:

$$2CH_2O + SO_4^{2-} = 2HCO_3^- + H_2S \qquad \text{Eq. 1.1}$$

This process is either assimilatory or dissimilatory. During the former the hydrogen sulphide produced is retained within the bacterial cell, while during the latter it is released into the surrounding porewaters. Dissimilatory bacterial sulphate reduction is one of the dominant decay processes in marine sediments, accounting for up to half of the breakdown of organic matter in coastal environments (Thode-Anderson and Jørgensen, 1989; Parkes and Buckingham, 1986). It has also been documented in a wide variety of environments including lakes (Bak and Pfennig, 1991), marsh land (Marnette *et al.*, 1993) and 500m below the Pacific floor (Parkes *et al.*, 1994) (Figure 1.2).

Generally, sulphate reducing environments occur where bacterial processes have exhausted the supplies of oxygen, nitrate, manganese and iron used as electron acceptors in organic matter degradation (Figure 1.3) (Froelich *et al.*, 1979; Nedwell, 1984). Sulphate reduction can also occur in oxic sediments within anoxic micro-environments such as decaying fragments of organic matter and animal burrow linings (Figure 1.2) (Froelich *et al.*, 1979; Jørgensen, 1977; Aller, 1982). These fragments

A

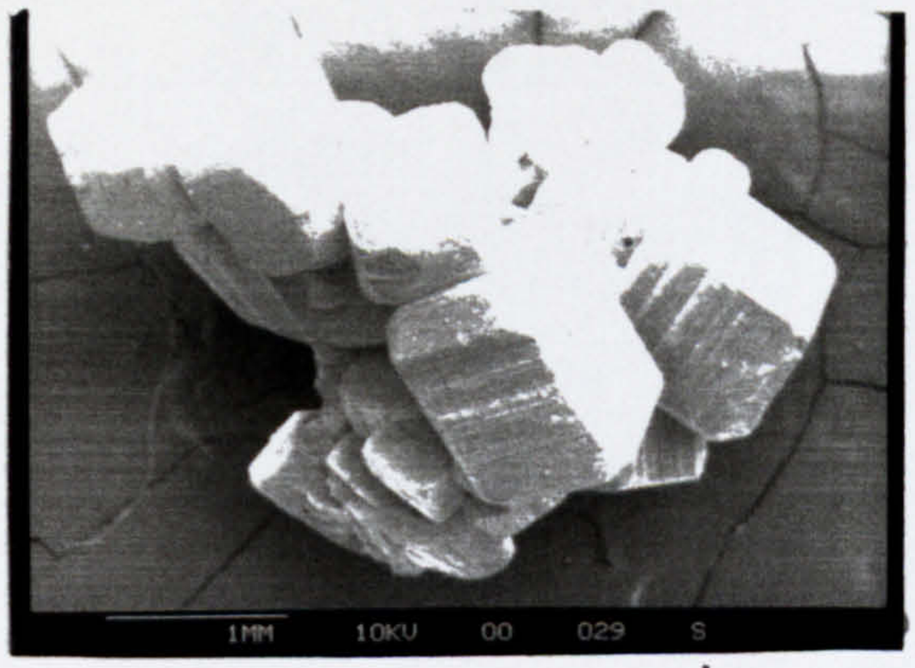

B

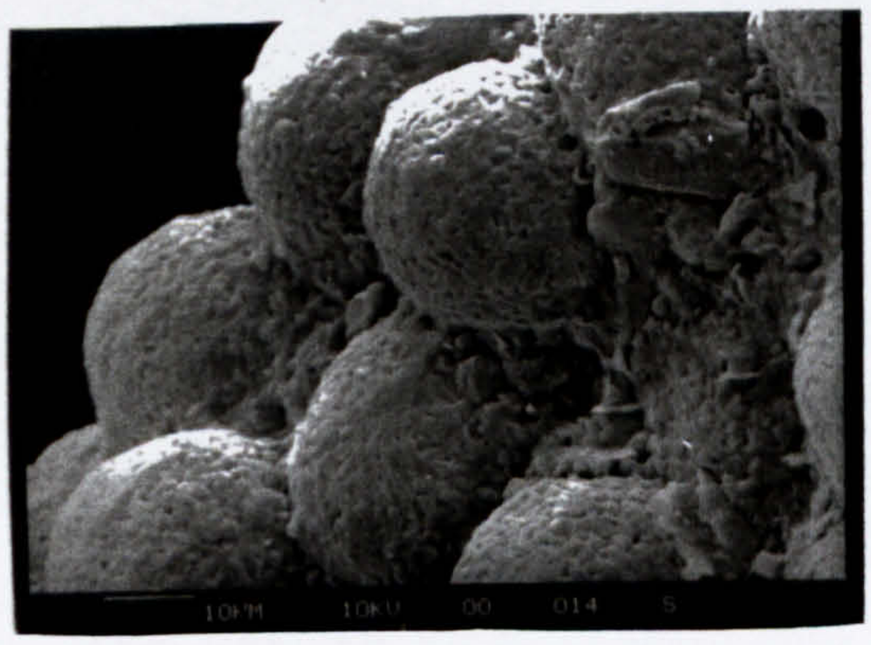

C

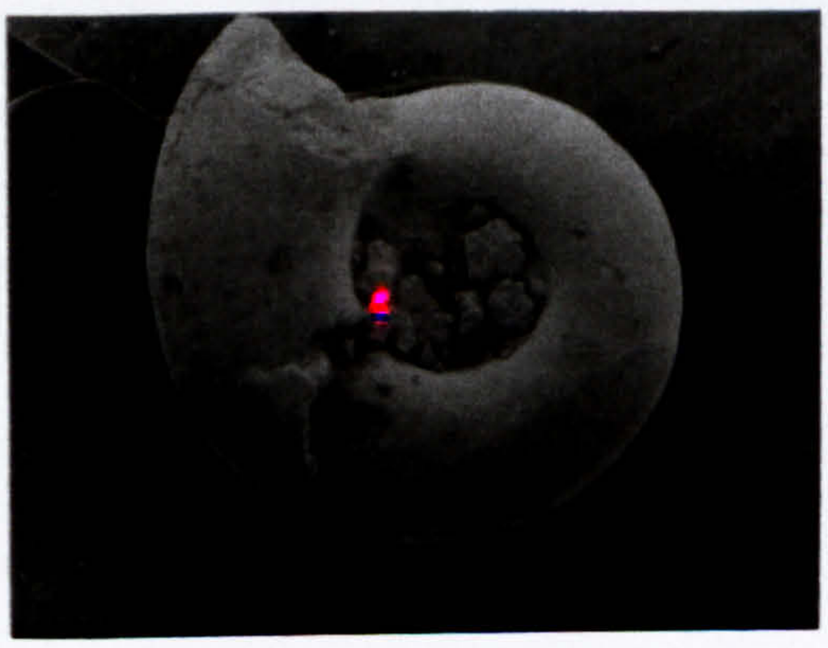

D

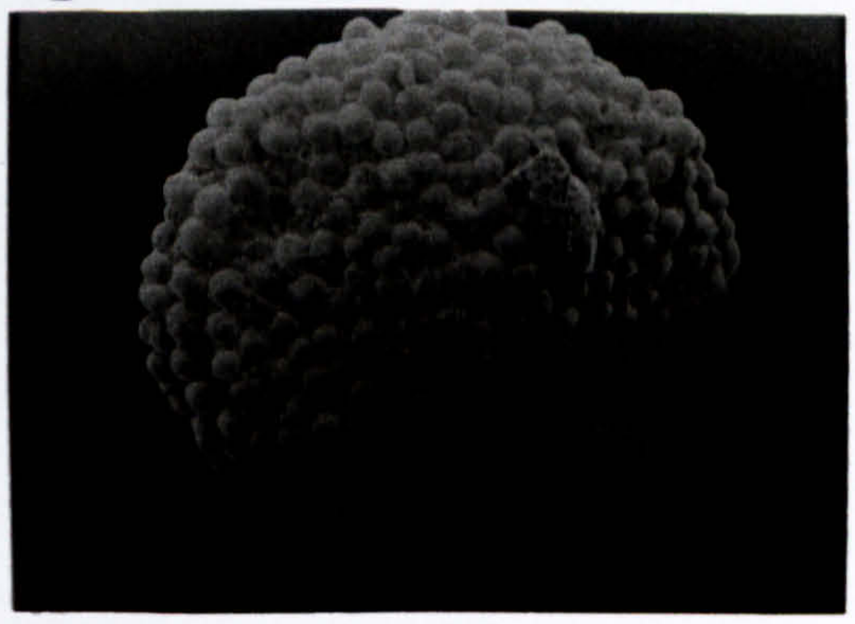

E

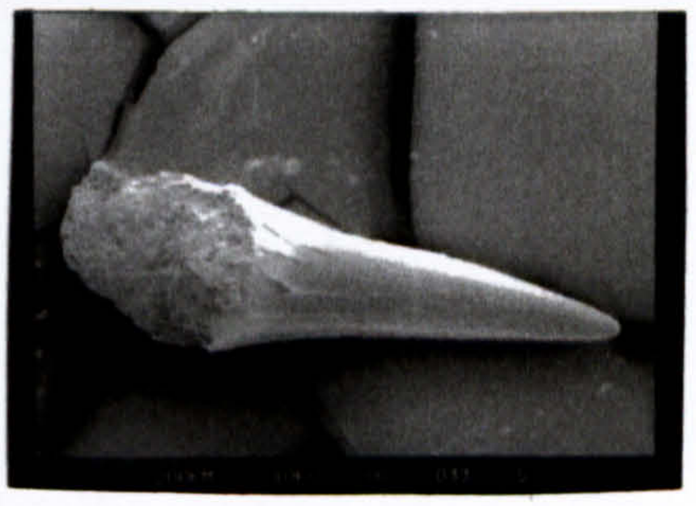

F

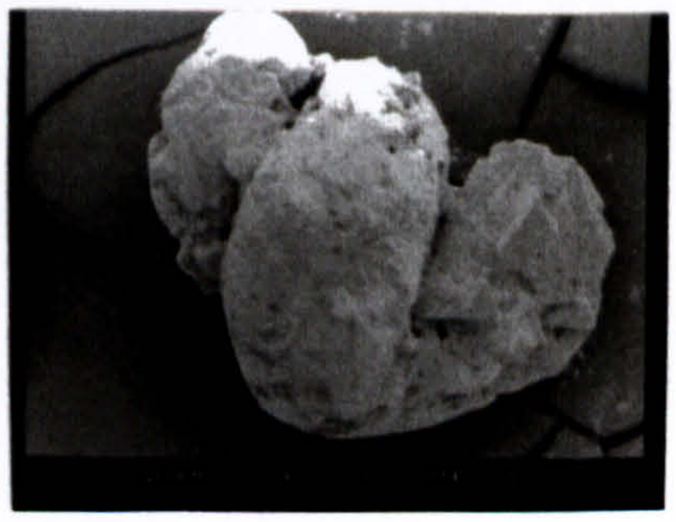

Figure 1.1-Pyrite forms and pyritization in sediments. A - Euhedral cubes, B - Framboids, C - Infill of ammonoid protoconch, D - Polyframboid, E - Infill of end of tooth, F - Gastropod infill

Figure 1.2 - Profiles of AVS and pyritic sulphide (PS) concentrations found in different sedimentary environments (A - Peru Margin Deep Sea Sediments (Cragg *et al.*, 1992), B - Limfjorden Fjord, Denmark (Howarth and Jørgensen, 1984), and C - Lake Constance, Switzerland (Bak and Pfennig, 1991), D - Moorland (Gerritsfles) sediment (Marnette *et al.*, 1993)).

A

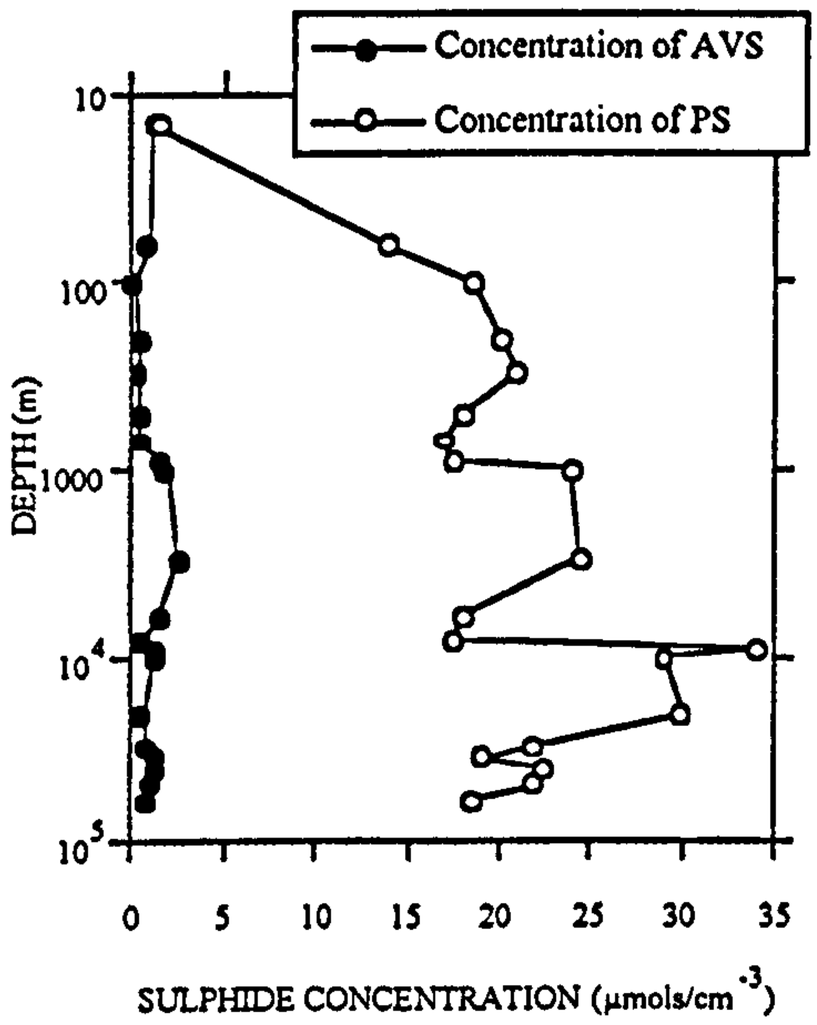

B

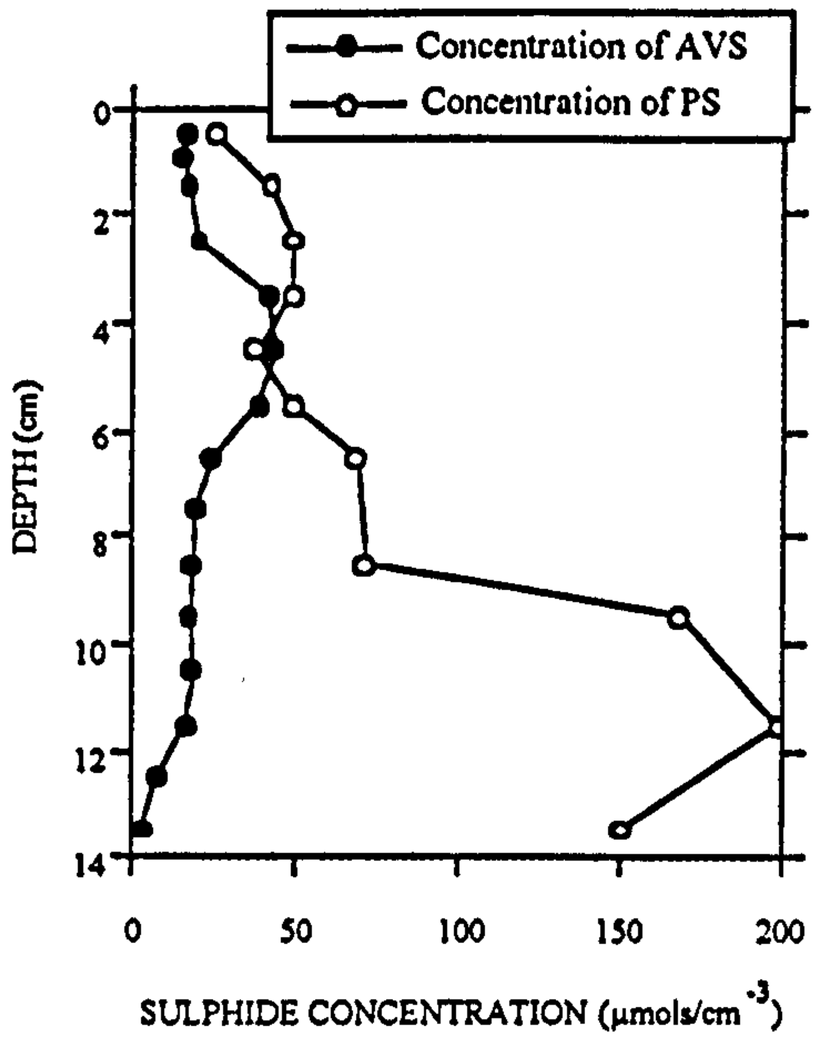

C

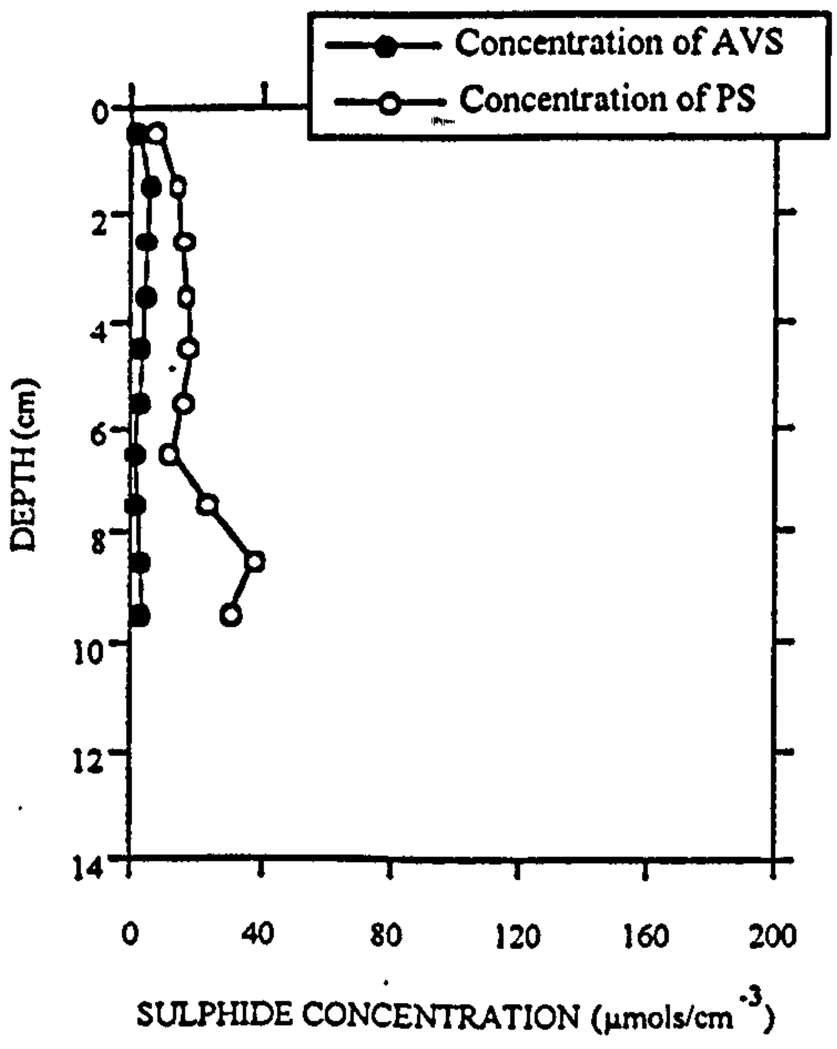

D

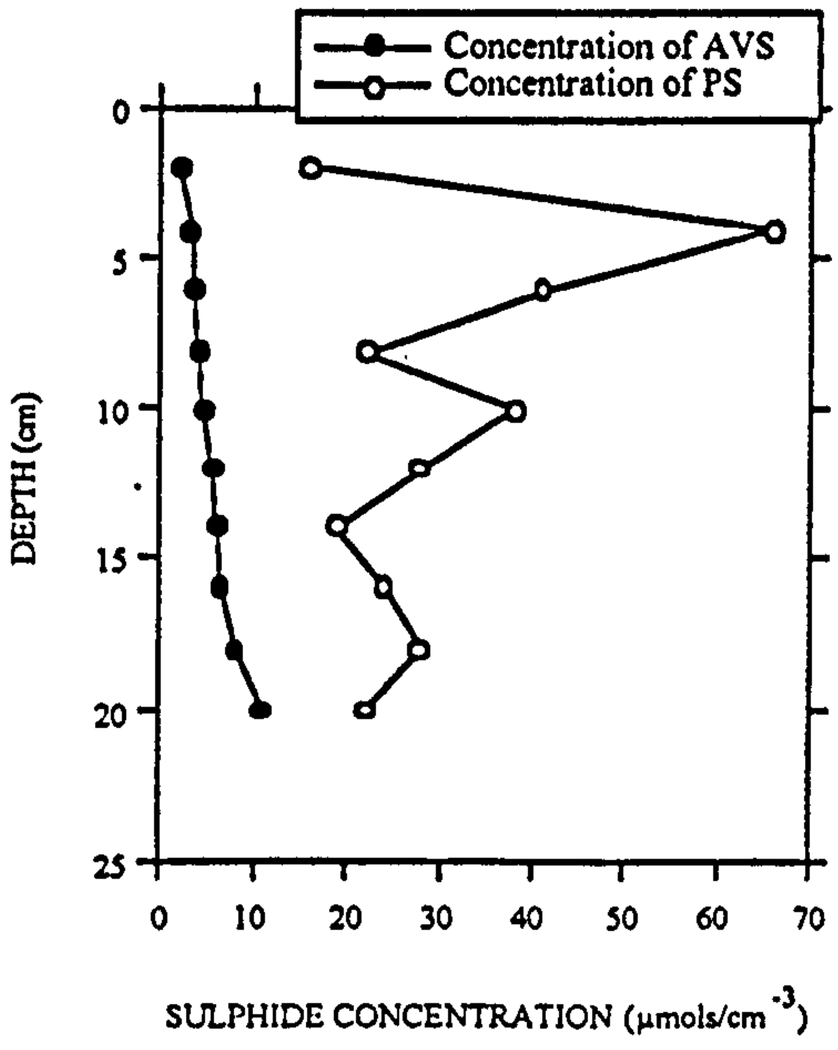

Figure 1.3 - Schematic representation of a sediment column showing zones of terminal electron acceptors used by bacteria and a summary of pyrite mechanisms.

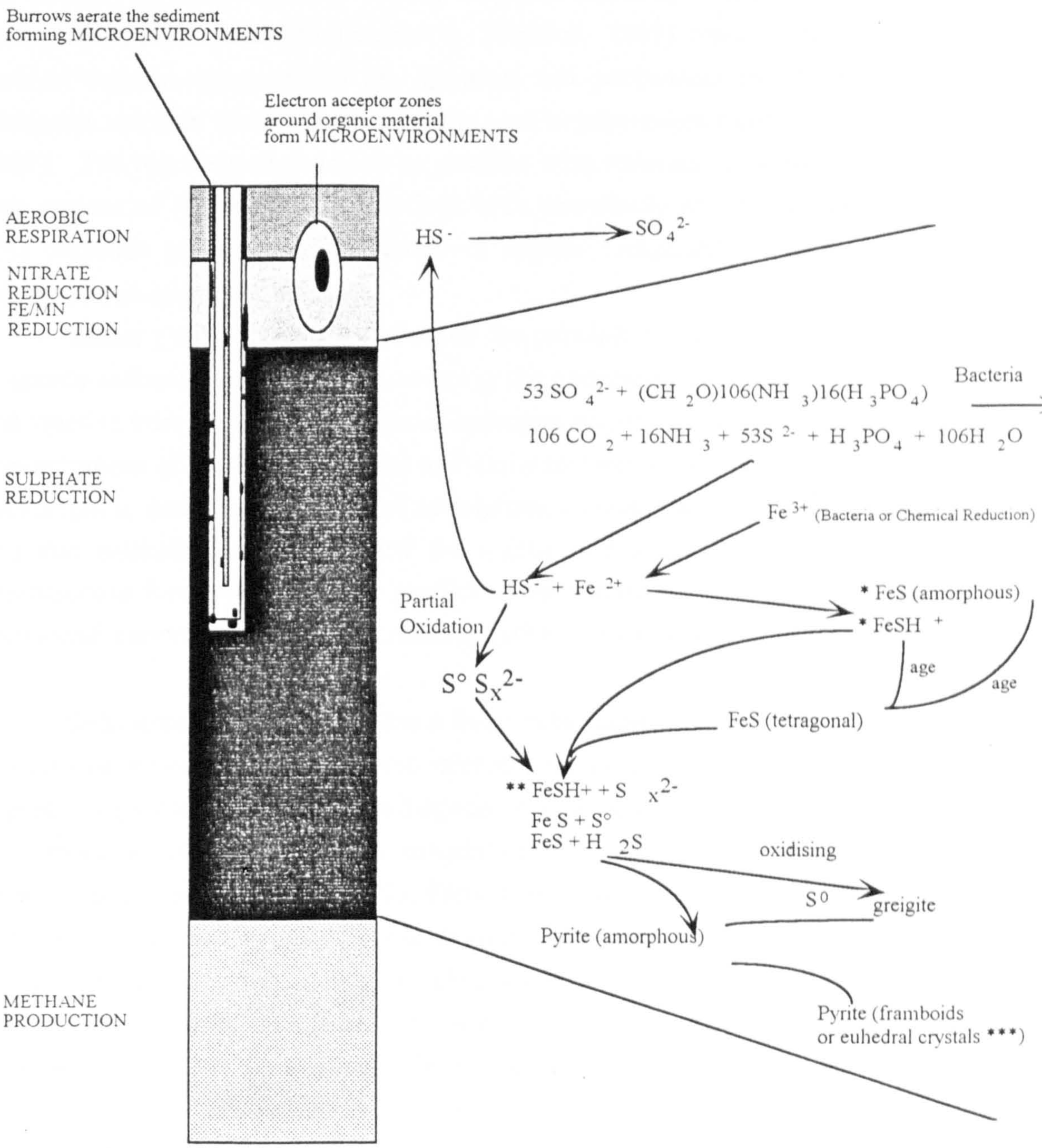

* The character of the first formed iron monosulphide precursors is undefined. ** The reaction may proceed via iron loss as suggested by Furakawa and Barnes (1995). *** The morphology of pyrite is dependant upon the supersaturation of the environment with respect to pyrite. At low values the pyrite formed is cubical, whereas at higher values pyrite crystals form spherical aggregates of crystals.

facilitate the consumption of oxygen and subsequent electron acceptors pushing the zone surrounding the organic particle towards sulphate reduction more rapidly than in the majority of the sediment. During sulphate reduction, a small fraction of the hydrogen sulphide produced (Berner & Westrich, 1985) reacts with metals and residual organic matter within the sediment and porewaters to produce various authigenic sulphide mineral, such as pyrite, and organo-sulphur compounds (Kohen, 1989). The remainder is oxidised by reaction with minerals, or diffuses into more oxic regions of the sediment where it is both microbially and chemically oxidised. This oxidation produces various forms of sulphur compounds, such as elemental sulphur, thiosulphate and sulphate.

Berner (1967; 1970; 1984) defined the principle controls on pyrite formation in anoxic sediments at neutral pH, as being the concentration of hydrogen sulphide and reactive iron. The concentration of hydrogen sulphide is also constrained by the concentrations of porewater sulphate and easily metabolisable organic material. The consumption, during sediment burial, of sulphate, organic matter and iron by bacteria and iron sulphide precipitation, and the reaction of acid-volatile sulphide (AVS) precursors to form pyrite, produce profiles of decreasing AVS, sulphate and organic compound concentrations, and increasing pyrite concentrations with depth (Figure 1.2).

Sedimentary pyrite usually has a framboidal, euhedral or anhedral habit but it has also been observed in unordered microcrystalline forms and in mixed sulphide aggregates (in the sediments of the Lagoon of Venice; Bertolin *et al.*, 1995) and as amorphous gel-like structures in association with bacteria (in several polluted environments; Konhauser *et al.*, 1993; Ferris *et al.*, 1987). Framboids are spherical to subspherical agglomerations of pyrite crystals, not more than 100μm in diameter, which form a raspberry-like structure. Their stable sulphur isotope signatures indicate that they were formed during early diagenesis (Raiswell, 1982) and they tend to be dispersed throughout the sediment. They may be centred upon short chain organic compounds which are utilised in micro-environments by sulphate reducing bacteria during iron or manganese reduction. Conversely, euhedral, anhedral and bladed authigenic pyrite may be associated with organic particles and later diagenesis of more complex compounds. Onema (1990) and Psenner (1983) suggested that this association is due to the organic particles acting as microsites of high sulphur concentrations within iron saturated sediments. The mixed sulphide aggregates and amorphous gels observed in sediments are also early diagenetic rather than later, and these may act as precursors for later pyrite formation.

1.B - Reactions forming pyrite from precursor compounds

The earliest research into pyrite formation (Allen *et al.*, 1912;1914) recorded the occurrence of amphorous material prior to the precipitation of pyrite and marcasite. Further work confirmed that when hydrogen sulphide reacts with detrital iron minerals, the initial precipitate is not normally pyrite but an intermediatory compound such as an iron monosulphide or iron-sulphide complex (Figure 1.3). The reaction pathways between these precipitates and pyrite are not fully defined in spite of extensive research over the last 80 years (see Table I). Three reaction pathways are currently suggested to operate with in sedimentary systems. These are:

i) a solid-solid reaction between an iron sulphide precipitate and sulphur,

ii) a reaction between polysulphide ions (formed by the reaction of sulphur and hydrogen sulphide) with either solid iron monosulphide or an aqueous iron sulphide complex,

and iii) a reaction between iron monosulphide solids and hydrogen sulphide where hydrogen sulphide acts an oxidising agent and hydrogen is produced as a by-product.

The initial work on pyrite reaction by Berner (1969) suggested that the reaction between microbial sulphide and ferrous ions proceeded:-

a) via a ferrous monosulphide precursor,

and b) involved elemental sulphur acting as an oxidising agent to produce pyrite from the precursor compounds, via a second intermediate, greigite (Figure 1.4).

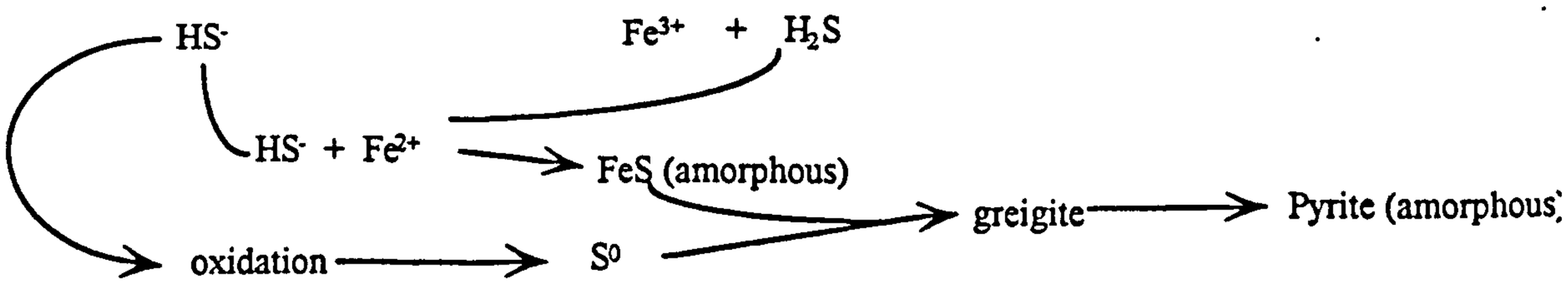

Figure 1.4 - The relationship between iron monosulphides and pyrite as suggested by Berner (1969)

Berner's experiments were performed over a range of pH values (3-9) and temperatures (20-90°C) using solutions of sodium sulphide or solutions saturated with hydrogen sulphide, and various iron compounds such as ground mineral goethite and steel. Pyrite and marcasite were only formed in vials where oxidation had

Table I - Summary of Previous Experimental Work on the Chemistry of Authigenic Pyrite Formation

AUTHORS	YEAR	IRON SOURCE	CONC	S^{2-} SOURCE	CONC	OXIDISING AGENT	CONC	TEMP(°C)	pH	TIME	NOTES
Allen et al.	1912	ferrous sulphate	0.18M	hydrogen sulphide gas	0.1M	elemental sulphur		25	2	1 year	Produced pyrite crystals at high temperatures
		ferrous sulphate	3g	sodium polysulphide	xs	elemental sulphur	5g	100		5 days	Pyrite formation also occured in a reaction
		ferric salt		hydrogen sulphide gas				100		5 days	where thiosulphate decomposed (also observed by Murrowchick & Barnes(1986))
Berner	1962	goethite		hydrogen sulphide gas	0.1M			25	4	2 days	Pyrite crystals and a pyritic film
		metallic iron		as above				>40	4	2 days	Pyrite only producted if T>40
		iron sulphate		sodium sulphide		Allowed oxygen in, elemental sulphur produced		25-65	3	5-200 days	Reaction increases with temperature Pyrite not observed at higher pHs
	1967	iron sulphate	2 5mM	hydrogen sulphide gas		Orthorhombic sulphur		65	7	14 days	Framboidal pyrite on the sulphur grains
	1970	iron sulphate		hydrogen sulphide gas NaHS		Flowers of sulphur		65	7.9 6.9		Framboids observed on sulphur surfaces Suggested reaction where FeS + S= Gregite, and Gregite + S = pyrite
Rickard	1969	iron sulphate		Sodium polysulphide				25	4 4-9.5	2 days	Suggested that Polysulphide + mackinawite=pyrite
		goethite		sodium sulphide				25	4 4-7 0	2 days	and sulphur + mackinawite = marcasite
		mackinawite		Sodium polysulphide				25	7	2 days	
	1975	iron sulphate		hydrogen sulphide gas		elemental sulphur		40	7.8	18 hours	Suggested that FeS dissolves to form ferrous ions which react with polysulphides to form pyrite.
	1989	Mohr's salt		sodium sulphide				20	7-8		Phosphate buffer Significant production of the H+ ion suggested formation of Fe(SH)+ (fast reaction) and Fe(SH)2 (slow reaction)
Roberts *et al*	1969	goethite		hydrogen sulphide gas	0.1M			25		1days	Single pyrite crystals
Sweeney and Kaplan	1973	ferrous chloride		hydrogen sulphide gas saturated solution		Allowed oxygen in, elemental sulphur produced		60 85	8		Produced pyrite framboids from gregite precursors
Taylor *et al*	1979	troilite		hydrogen sulphide gas				100		21 days	Single pyrite crystals
		mackinawite		hydrogen sulphide gas	0 3MPa			35		3 days	Single pyrite crystals
Drobner *et al*	1990	iron sulphate		hydrogen sulphide gas		H+ ion from hydrogen sulphide gas		100	7	14 days	FeS +Hydrogen sulphide (g)= Fe(HS)2 This then decays to pyrite emitting hydrogen. Forms crystals
Luther	1991	ferric iron	0.13mM 0.65mM	polysulphide	0.1mM 1.3mM			25	5.5 5 8	22 hours 48 hours	Single crystals of pyrite poduced Suggested a mechanism for pyrite
		ferrous iron	0.93mM 0.28mM 0.37mM 1.15mM		1.1mM 0.3mM 0.4mM 1 2mM				5.8 7 7 7.3	4 hours 4 months 4 months 24 hours	formation wheere the Fe(SH) complex reacts with polysulphide ions to produce pyrite, polysulphide and hydrogen ions
Schoonen and Barnes	1991	ferrous chloride	~0.03M	NaHS	0.03M	elemental sulphur	50mg	65	~8	varying	Formed crystals growing on sulphur grains
		Mohr's salt	0.033M	sodium polysulphide	0.07M	None		65	7.5	varying	Small, anhedral pyrite crystals dispersed throughout the solution
Rickard, Luther *et al*	1995 1996	mackinawite		hydrogen sulphide		hydrogen sulphide			various	varying	Low temperature formation of pyrite via the FeS + H_2S -> FeS_2 + H_2(g) mechanism.

occurred or a suitable oxidising agent (such as ferric iron) was present, while experiments at neutral pH and 25°C produced amorphous and tetragonal monosulphides after 5 and 22 days. Berner's (1967) explanation of this was that the dominant reaction between goethite and hydrogen sulphide changed from the production of iron monosulphides and pyrite at pH around 4 to a monosulphide dominated reaction at pH between 6 and 9. He also noted that lowering the pH, increasing temperatures and increasing the crystallinity of the iron source increased the crystallinity of the product, and suggested that the absence of pyrite in his experiments above pH 6 may due to the poor crystallinity of the pyrite making hard to identify. Schoonen and Barnes (1991b) also observed that pyrite produced in vials with a pH above 6 were small anhedral crystals, and noted that marcasite was dominant below pH 4 and pyrite the dominant form above pH 6. The role of intermediate compounds, such as greigite, may be important in this reaction, but work by Schoonen and Barnes (1991b) indicates that it's presence is dependant upon the redox of the environment in which the reaction is occurring. Although pyrite and other sulphide compounds are ostensibly produced in anaerobic micro-environments, a slight variation in the oxygen state will change the speciation of sulphur compounds in solution (Schoonen and Barnes, 1991b). This observation was confirmed by experimental work by Wang and Morse (1995) which indicated that is possible to form pyrite from greigite under conditions similar to those in a mackinawite dominated system.

Later experiments by Berner (1969) contained flowers of sulphur. These produced framboidal pyrite, on the surface of the sulphur crystals. This phenomenon was also observed by Rickard (1975) and was ascribed by him to the reactions which occur between the surface of elemental sulphur crystals and sulphide solutions, forming polysulphide compounds which then react to form ferrous mono/poly sulphide compounds. Schoonen and Barnes (1991b) have shown that either polysulphide or elemental sulphur is required in order to convert iron 'monosulphides' into pyritic compounds. The ferrous monosulphide was assumed to have disassocciated in order to facilitate this reaction. Rickard (1975) suggested that it is, however, unlikely that the amorphous iron monosulphide breaks down into its constituent ions and Rickard (1989) described an initial precipitate of a highly disordered gel with a formula close to $Fe(SH)_2$. The possibility of such an complex was also suggested by Taylor (1980) as an intermediate in the formation of mackinawite. Amorphous iron monosulphide precipitates are likely to exist as a combination of solid amorphous FeS and a $Fe(SH)_2$ complex which react to form iron-sulphide complexes (Figure 1.4). The occurrence of this sort of complex has

subsequently been confirmed by Luther (1991) who further suggested that iron sulphide complexes could react with both polysulphides and organic ligands. Organic compounds had previously been shown by Rickard (1969) to change the kinetics of the pyrite reaction. It seems likely from Luther's work that the polysulphides play a role in the production of pyrite from precursor compounds (Figure 1.5) and organics play a role in stabilising the iron-sulphydral complexes (Luther and Ferdelmann, 1993).

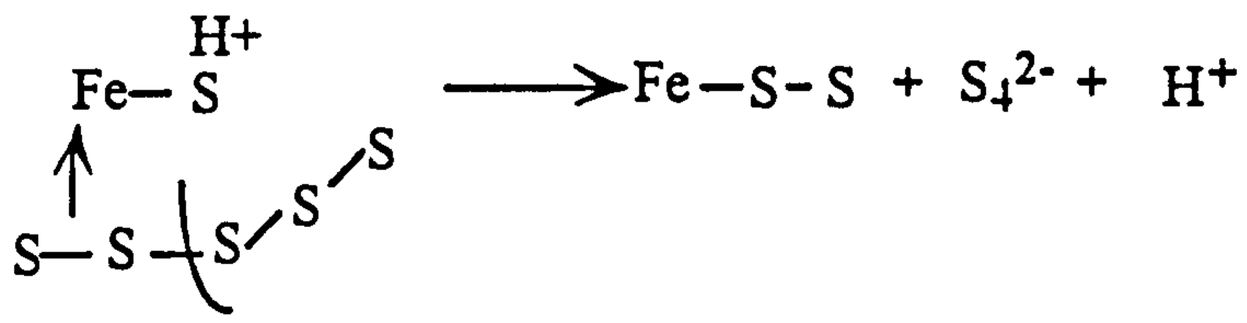

Figure 1.5 - Mechanism of pyrite formation (Luther and Ferdelmann, 1993)

Taylor et al. (1979) suggested a third mechanism for the iron monosulphide to pyrite reaction, utilising hydrogen sulphide as the oxidising agent. This mechanism involved the formation of a complex with two sulphide ions.

$$FeS + H_2S = FeS{->}SH_2 \qquad \text{Eq 1.3}$$

Hydrogen gas was then emitted from the complex leaving pyrite.

$$FeS{->}SH_2 = FeS_2 + H_2 \qquad \text{Eq 1.4}$$

(Rickard and Luther, 1996)

Drobner *et al.*, (1990) demonstrated that this mechanism worked at high temperatures, and although initial studies at low temperatures indicated that the rates of reaction to be slow below 65°C (Schoonen and Barnes, 1991b), the rate of reaction for hydrogen sulphide oxidation is significantly greater than that of either the polysulphide or elemental sulphur mediated reaction (rate of hydrogen sulphide oxidation reaction >>polysulphide>elemental sulphur mediated reaction; Rickard, Schoonen & Luther, 1995). Further work by Rickard and other workers (1996 and subsequent papers) showed that the reaction does occur at ambient temperatures, although it is more likely at pH values lower than pH 7, as the reaction rate is pH dependant. This means that it is likely to be more important in sedimentary environments such as salt marshes, rather than anoxic marine sediments.

It has also been suggested that pyrite forms without the precipitation of monosulphides and their subsequent sulphidation (Raiswell, 1982). Schoonen and Barnes (1991) experimented with solutions which were supersaturated and undersaturated with respect to iron monosulphides. They found that although pyrite

did nucleate directly from solution this was extremely slow, at low temperatures and neutral pH.

1.C - Pyrite in association with organic particles

As iron sulphide formation in sediments is intimately linked to the metabolic activities of sulphate-reducing bacteria, it is unsurprising that it is found in association with organic material, and is important in fossil preservation. It's comparative rarity in the preservation of soft tissues reflects the requirement for the rapid burial of sufficient easily metabolisable organics to fuel the consumption of oxygen and other electron acceptors from the sediment porewaters.

Commonly pyrite infills carbonate fragments and wood, encrusts fragments of organic material and occurs in concretions. Allison (1981) divided the types of pyrite preservation in association with organic material into three main groups; permineralization, mineral coats and mineral casts. These were then determined to vary only in the distance of the pyrite precipitation from the organic fragment, due to changes in the balance between the iron pool and the sulphide pool (Canfield and Raiswell, 1991). Permineralization occurs within the pore-spaces in organic particles and biomineralized tissues, and the less refractory material is the source of the organic material utilised by the bacteria. Examples of this occur in wood debris where the pore-spaces are infilled with pyrite and cellulose remains (Kenrick and Edwards, 1988) and in the carapaces of *Nephrophs norvegicus* (Allison, 1988). In mineral coats pyrite occurs as a thin layer on the surface of the organic structures. This outlines the organic material and is the commonest form of pyrite preservation of degradable soft parts, and occurs in Beecher's Trilobite Bed (New York State, USA), the Hunsrück Slate (Germany) and the Burgess Shale (British Columbia, USA). It has been suggested that pyrite preservation in this manner could be due to the permineralization of a layer of bacteria which have colonized the surface of the organic particle (Canfield and Raiswell, 1989). Similar mechanisms has also been suggested for the preservation of feathers in the rock record (Davis and Briggs, 1995) and preservation by siderite (Wüttke, 1983). The last and commonest preservation method is as a mineral cast. In this case, pyrite is precipitated around the outside of the organic particle preserving only the outline of the fossil.

Pyrite is also found in association with carbonate fossils, either within the internal sediment, as overgrowths, chamber linings or replacing sections of the skeletal material. Pyrite forming within the internal sediment precipitates as in the rest of the sedimentary column although the skeletal material may facilitate it's early formation, by forming micro-environment within it. Hudson (1982) suggested that

the chamber lining pyrite is initiated by the decay of either the organism or the organic matrix of the shell. Sulphate reduction by-products then precipitate upon the shell surfaces forming a thin layer of pyrite and pyrite precursors. This material will then increase in size and crystallinity during later diagenesis. The majority of the replacement of skeletal material also occurs in later diagenesis, with the initial precipitation being confined to the organic shell matrix. The initial formed pyrite is therefore similar to that formed during permineralisation. Crystallinity and bulk increases during later diagenesis with the introduction of sulphate and iron rich fluids. Fisher (1986a and b) observed that a pattern of pyrite formation similar to this is seen in Lower Oxford Clay ammonites, with initial precipitation occurring around the shelly material prior to compaction, and replacement occurring during growth after compaction.

1.D - Investigative aims

This thesis aims to elucidate the manner in which the concentration and availability of iron and sulphide affects the formation of pyrite under different sedimentary conditions by using cultures of sulphate-reducing bacteria and sediment incubations as micro-environment models. It then seeks to use these controls to show how pyritization occurs in association with organic particles, and to extrapolate the results to interpret pyritization in both Recent and ancient natural systems.

Chapter Two

Development of Selective Digestive Procedures for Reduced Sulphur Species*

2.A - Introduction

Microbiological cultures provide a model for pyrite formation as they produce suitable sulphide concentrations at low temperatures and under realistic chemical and biological conditions. However, the solid phases produced in microbiological cultures can be amorphous (see Chapter 3) and, as such, cannot be identified unequivocally either microscopically or using X-ray diffraction, although the elemental abundances of particles can be determined using an electron microprobe. It is essential, therefore, to identify the different forms of sulphur in the experiments chemically. It is also necessary to relate the forms of sulphur generated in bacterial cultures to those in sedimentary environments and geological samples in order to understand the role of bacteria in the formation of sedimentary sulphide minerals. In addition, the concentration of pyrite in an ancient sedimentary rock can be used as a palaeoenvironmental sediment redox indicator, by means of the degree of pyritization ratio (DOP, Raiswell *et al.*, 1988). This ratio relates the concentration of pyritized iron in the sediment to the concentration of reactive iron. Pyritic iron concentrations are usually determined from the concentration of pyritic sulphide (PS) or iron released during hot chromous chloride digestions.

$$DOP = \frac{PS \times 0.872}{(PS \times 0.872) + \text{reactive iron}} \qquad \text{Eq. 2.1}$$

In sediments where the solid sulphide pool is dominated by monosuphides the degree of sulphidation ratio (DOS: Boesen and Postma, 1988) is used as an indicator of the redox of the environment. This ratio relates the concentration of all the iron sulphides to the concentration of reactive iron in the sediment. Unlike DOP, DOS includes both the acid volatile sulphide and pyritic sulphide concentrations, as a means of expressing the amount of sulphide which has reacted with iron in a particular sediment.

---

* Published as Allen & Parkes 1995"An Evaluation of Digestion Procedures for Determining Reduced Sulfur Species in Bacterial Cultures and in Ancient and Recent Sediments" in "Sulfur transformations in sediments" ACS Symposium Volume 612, pages 243-259.

$$DOS = \frac{Total\ Reduced\ Inorganic\ Sulphur}{TRIS\ +\ reactive\ iron} \qquad \text{Eq. 2.2}$$

If these ratios are to be applied to the formation of pyrite and other sulphide minerals in sedimentary environments of all ages as well as bacterial cultures, then the techniques for the separation and quantification of each sulphur pool must be standardized for all conditions.

2.A.1 -Methods of Determining the Proportion of Different Types of Reduced Sulfur Compounds in Sediments

Although methods of determining both the Acid Volatile Sulphide (AVS) and the Total Reduced Inorganic Sulphide (TRIS) (Zhabina, 1978; Fossing and Jørgensen, 1989) have been checked previously with various sulphur compounds the details of the procedures have often varied considerably between research groups. Furthermore, a comprehensive range of reduced sulphur species and minerals has not been subjected to a standard procedure incorporating both chromous chloride (TRIS) and acid volatile digestions. Morse and Cornwell (1987) studied the greatest range of extraction conditions, but their study was limited to iron sulphides. TRIS digestions are a common method for determining the presence and quantity of bacterially reduced sulphur in a sediment and use reduced chromic chloride and concentrated HCl (Howarth and Jørgensen, 1984). The digestion reaction is conducted in an oxygen-free environment, and the hydrogen sulphide released is then actively transported into a chemical solution (e.g. zinc acetate) where it is trapped. The concentration of the trapped sulphide can then be determined spectrophotometrically (Cline, 1969), gravimetrically (Mossman *et al.*, 1991), by ICP-MS (Krairaponond *et al.*, 1992), polarographically (Luther *et al.*, 1985) or by titration (Fossing and Jørgensen, 1989). Nearly all the published methods for determining TRIS use 1M chromous chloride in an acidified solution, concentrated HCl, and ethanol (Fossing and Jørgensen, 1989; Canfield *et al.*, 1986). Heating of the solution and sediment is required to release any elemental sulphur in the sample although Fossing and Jørgensen (1989) observed the reduction of a small amount of elemental sulphur even under cold digestion conditions.

The AVS procedure is a less vigorous reaction, which uses acid to digest the more reactive sulphides, including iron monosulphides such as mackinawite, and

intermediate iron sulphides such as greigite. Cornwell and Morse (1987) compared different methods for extracting AVS using synthesized mackinawite, greigite and pyrite, with varying concentrations of hydrochloric acid, and with or without heat and stannous chloride. In their comparison of 6M HCl digestions, hot 6M HCl, cold 6M HCl, and cold 6M HCl in conjunction with $SnCl_2$ produced similar high recoveries of monosulphides and intermediate sulphides, although the last method may yield some sulphide from cryptocrystalline pyrite. Stannous chloride is added in order to negate the oxidation of the hydrogen sulphide produced in the digestion by ferric iron (Pruden and Bloomfield, 1968). Rice *et al.* (1993) suggested that stannous chloride should be included in AVS digestions for ancient sediments as it improved the recovery of monosulphides from their samples significantly, however the inclusion of stannous chloride in a cold AVS digestion followed by a cold chromous chloride digestion would lead to an over-estimation of AVS and an under-estimation of pyrite in Recent sediments and bacterial cultures. These errors are particularly significant in bacterial cultures and in $^{35}SO_4$ radiotracer measurements of sulphate reduction activity (Thode-Anderson and Jørgensen, 1989; Parkes and Buckingham, 1986; Fossing and Jørgensen, 1989; Jørgensen, 1982) as the initially formed amorphous and cryptocrystalline pyrite produced would be susceptible to breakdown (Cornwell and Morse, 1987). Chanton and Martens (1985) indicated that the use of stannous chloride in low concentrations at room temperatures will not extract pyrite. The euhedral (98% pure) hydrothermal pyrite, which they used as a standard, is not representative of the pyrite pool found in Recent sediment and bacterial cultures, which contain cryptocrystalline pyrite. Heating with excess 6M HCl appears to produce the greatest recovery of AVS and the lowest recovery of artificial pyrite (Cornwell and Morse, 1987). The recovery of the pyrite and elemental sulphur pools is minimal under hot 6M HCl digestion conditions, due to the stronger covalent bonds present in these reduced species. Elemental sulphur can be present in a sample, either as a primary component or as a by-product of the breakdown of more intermediate reduced sulphur compounds, such as greigite and polysulphide under acid conditions (Troelsen and Jørgensen, 1982). The AVS digestion method for determining the concentrations of monosulphides and intermediate sulphides is usually applied to sediments, but it can also be used for sedimentary rocks (Zhabina, 1978; Rice *et al.*, 1993).

As a small proportion of elemental sulphur is digested in cold chromous chloride (Fossing and Jørgensen, 1989), these digestions can be preceded by an extraction for elemental sulphur, so that pyrite concentrations can be estimated more accurately. The removal of elemental sulphur is apparently not necessary in most

sediments, as it occurs in very low concentrations (Fossing and Jørgensen, 1989). However, it is necessary in laboratory experiments, as elemental sulphur may be produced by oxidation within the incubation/reaction vessel, as well as during acid digestion. If sulphur is extracted before and after acid digestion, then the combined concentrations of polysulphide and greigite can be estimated independently of elemental sulphur as these two forms of sulphide breakdown into elemental sulphur and hydrogen sulphide under hot acid conditions.

There are three main methods of determining zero-valent sulphur concentrations in sediments. The first is the sodium cyanide method of Troelsen and Jørgensen (1982) which involves dissolving sulphur in carbon disulphide and reacting this with sodium cyanide in order to produce a compound which can then be measured spectrophotometrically. The second uses dichloromethane as a sulphur solvent, followed by a hot chromous chloride digestion. This was used by Mossman *et al.* (1991) who refluxed samples in a dichloromethane - methanol mixture, and Schimmelmann and Kastner (1993), who used two twelve hour extractions with 20 ml dichloromethane. Other nonpolar solvents, such as cyclohexane, may also be used to extract elemental sulphur from samples. The third method is a continuous extraction of sulphur in Soxhlet with acetone. The sulphur-bearing acetone reacts with copper to precipitate copper sulphide. The sulphide content of the trap is determined using an

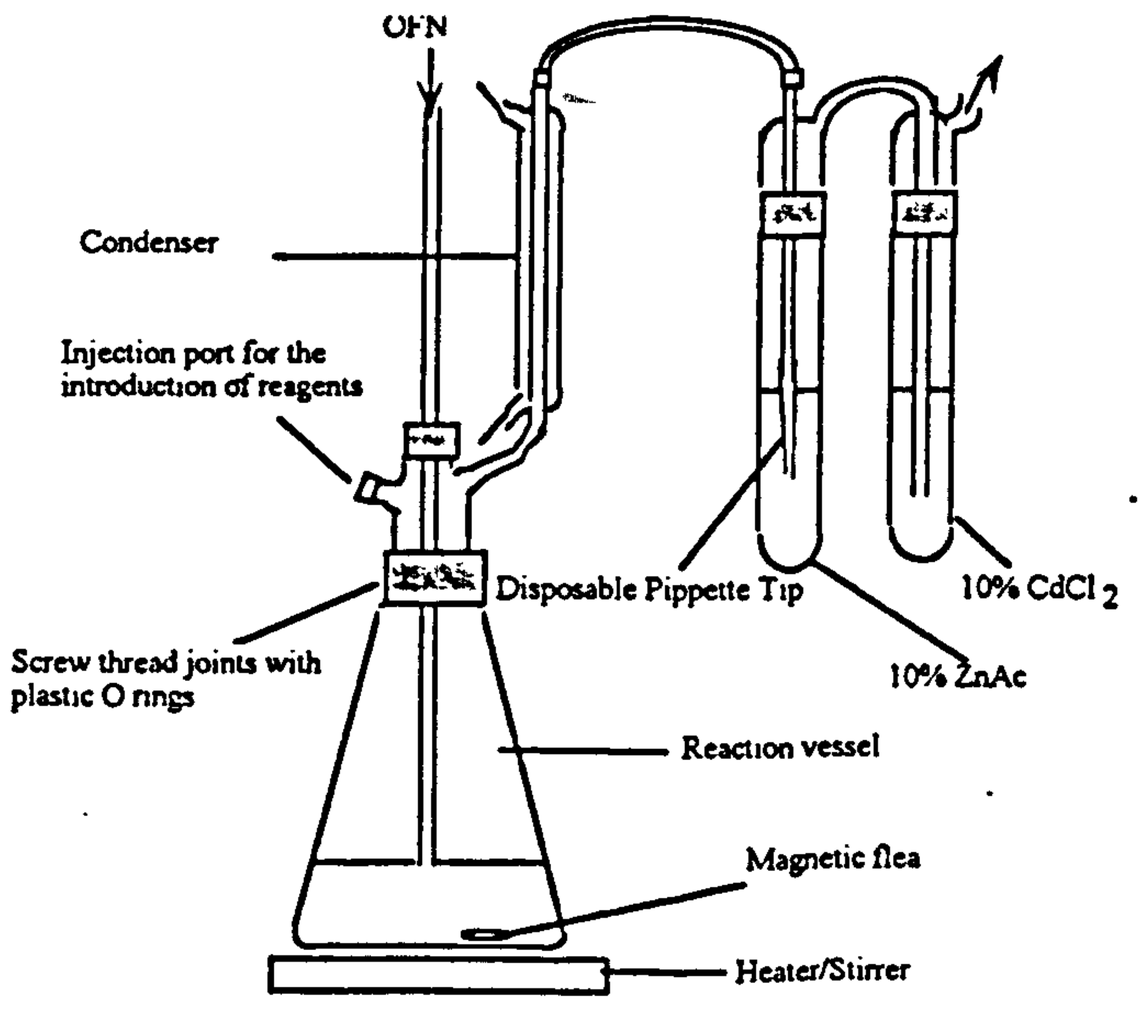

Figure 2.1 - Apparatus used for solid sulphide digestions (1 of a bank of six)

HCl digestion. Acetone digestions (Zhabina, 1978; Troelsen and Jørgensen, 1982) were not performed as acetone does not partition with water and is therefore not suitable for bacterial cultures or high porosity sediments.

2.B - Methods

2.B.1 - Sample Preparation and Selection.

In order to identify a consistent method of determining the distribution of different forms of sulphur within ancient, modern and bacterial systems, samples of each type were selected to validate previously used reaction schemes. Sedimentary sulphides, such as chalcopyrite, marcasite and galena were included in this study as previous work had been limited in the main to iron sulphide minerals. Sphalerite was used as a standard in Canfield *et al.* (1986) study, but was extracted under chromous chloride digestion conditions. Pyrrhotite, a monosulphide, was not included in this study as it is rare in normal sedimentary environments (Wada, 1977). A pyritic sedimentary rock from the Liassic of Devon, UK, and Recent sediments from the Tamar Estuary, Plymouth, UK were included in this study in order to provide a comparison between modern and ancient sedimentary sulphides. Sulphate-reducing bacterial cultures provide samples of the earliest formed iron sulphides and are analogous to those formed during $^{35}SO_4$ radiotracer incubations and early diagenesis. In addition artificial samples of the monosulphide mackinawite, and the intermediate sulphide greigite, were prepared along with elemental sulphur and polysulphide solutions, to check the separation of solid sulphide pool.

The rock and mineral samples listed in Table II were crushed in order to remove the matrix and increase the available reactive surface area. Rock samples were initially crushed in a jaw-crusher. Oxidised surfaces were removed by picking fragments from the interior of the samples and these fragments were then powdered to a 60μm mesh size. The composition of these samples was confirmed using XRD analysis. Digestions with unpowdered rock and mineral samples gave extremely poor recoveries compared to those which had been powdered. Sediment samples from the Tamar Estuary, Plymouth, UK, were used wet as the recovery of elemental sulphur pool is adversely effected by drying (Fossing and Jørgensen, 1989).. Sediment samples were stored frozen in 20% zinc acetate in order to minimize oxidation of the reduced sulphur. The artificial sulphides were prepared using the methods shown in Table II and Appendix 3. These were washed with deoxygenated water and

dichloromethane in order to remove residual reagents. Pyritic samples were also washed in 1M HCl in order to remove the monosulphides produced during the reaction. After drying in an anaerobic atmosphere at room temperature, the composition of each sample was confirmed using XRD.

The artificial samples were then stored in sealed deoxygenated vials prior to digestions. Samples were not stored for more than 4 days. Subsamples were then taken in an anaerobic cabinet (Forma Scientific, Marietta, Ohio, USA). Elemental sulphur and polysulphide solutions were prepared according to the methods shown in Table II and stored in a similar manner to the artificial sulphides. The sulphur content for each sample was calculated rom the purity of the phase in the XRD. Although this is not as accurate as a total sulphur analysis, in a comparison of digestion methods it was considered sufficient.

2.B.2 - Analysis of Samples.

All samples were treated in the same way. Three 15ml aliquots were removed from each liquid and sediment sample, while three 1.5g aliquots were removed from each solid sample. Two of the aliquots were mixed with either cyclohexane or dichloromethane in order to determine the concentration of elemental sulphur. The solvent to sample ratio used was 0.1g of sample to 20ml of solvent for solids and 1ml to 20 ml of solvent for bacterial cultures. The mixtures were shaken for 24 hours prior to the separation of the organic phase, and its subsequent removal using a pasteur pipette. This was digested with hot chromous chloride to determine the concentration of elemental sulphur. Each extraction was performed in triplicate. The third aliquot was stored in 15ml of 20% zinc acetate and then subsequently digested. Four types of digestions were performed; 6M HCl acid digestions with and without heating, and chromous chloride digestions with and without heating (Zhabina, 1978; Fossing and Jørgensen, 1989; Canfield *et al.*, 1986; Rice *et al.*, 1993; Chanton and Martens, 1985). Each digestion was performed in triplicate and the remainder of the aliquot was then used to run sequential digestions.

Additional samples from the bacterial cultures and sediment porewaters were filtered and stored in 10% zinc acetate so that the contribution from the free sulphide pool could be determined. . The concentration of sulphide was determined using a colorimetric method (Cline, 1969).

Table II. Mineral samples analysed

Mineral/ Sample	Characteristics	Preparation/Storage
Pyrite (euhedral) FeS_2	Brassy yellow striated cubes from a hydrothermal vein. Unknown age	Crushed to a 60μm powder after removing rock matrix
Pyrite (rock nodule)	Cryptocrystalline nodule from black Liassic marine shales.	As for euhedral pyrite
Pyrite (artificial)	Subhedral pyrite.	Made following the method of Cornwell and Morse (1987). Washed in deoxygenated water, 6M HCl and dichloromethane. . Dried anaerobically.
Pyrite (vein)	Cryptocrystalline vein from a black slate. Llandovery in age.	As for euhedral pyrite.
Sphalerite (ZnS)	Brown, resinous material showing subhedral crystal edges. With galena in a hydrothermal vein.	Crushed to 60 μm powder after removing galena from around the crystals
Chalcopyrite ($CuFeS_2$)	Subhedral yellow mineral. Softer than pyrite. In a hydrothermal vein.	As for euhedral pyrite.
Galena (PbS)	Silver, heavy metallic sulphide. Hydrothermal origin, age unknown.	Crushed after picking from fragments of the sphalerite sample.
Marcasite FeS_2	Orthorhombic dimorph of pyrite. Nodule from Liassic marine shales.	Crushed as for euhedral pyrite.
Iron Monosulphide FeS	Amorphous black mass of monosulphide.	Made following the method of Cornwell and Morse (1987). Washed with deoxygenated water and stored wet in the anaerobic cabinet.
Greigite Fe_3S_4	Intermediate sulphide in sediments.	Made following the method of Berner (1964). Washed with deoxygenated water and acetone Dried in the anaerobic cabinet and stored in a sealed nitrogen filled vial.
Polysulphide Solution S_n-S^{2-}	Colourless solution.	Made following the method of Wada (1977). Stored in a sealed vial filled with nitrogen.
Sulfur suspension S°	Yellow suspension in acetone.	Made following the method of Fossing and Jorgensen (1989) Stored as a suspension in a sealed vial with nitrogen
Flowers of Sulfur S°	Yellow, crystals of sulphur.	Precipitated by evaporating sulphur-bearing dichloromethane. Dried and stored anaerobically

2.B.2 - The Digestions.

It is clear that a protocol involving a hot 6M HCl digestion will separate the monosulphide from the pyritic sulphide pool (Cornwell and Morse, 1987). Despite the recommendation of Rice *et al.* (1993) stannous chloride was not used in the 6M HCl digestions as it has been shown to digest synthetic pyrite (Cornwell and Morse, 1987) and would probably remove the large amount of amorphous pyrite produced in bacterial cultures. Cold AVS digestions were only applied to those minerals with a metal to sulphur ratio of 1:1 to determine if there were any difference in reactivity between them. The pyrite and elemental sulphur pools were separated by a cold chromous chloride digestion as this removes a minimal amount of the elemental sulphur but the majority of the pyritic pool. To avoid delays when changing from hot to cold digestions, they were normally run in parallel on replicate samples. However, some sequential runs were conducted to assess subsample variability.

In the AVS digestions, 2ml of bacterial sample stored in zinc acetate, 1ml of sediment, or 0.1g of finely powdered rock or mineral sample was placed in a distillation flask. To each flask 5ml deoxygenated water, 5ml of 20% zinc acetate and a magnetic stirrer were added. The flasks were then attached to the distillation apparatus (Figure 2.1) where they were flushed with OFN (commercial oxygen-free nitrogen passed through an oxygen scrubber) and stirred. The system was checked for leaks. An all glass and PTFE apparatus was used for the distillations (Parkes and Buckingham, 1986).

The apparatus was left to flush for 10 minutes before 2ml, or excess, 6M HCl was injected into each flask. The amount of HCl required for the digestion depended upon the concentration of carbonate in the sediment. The volume required can be determined prior to the digestion by adding acid to a subsample of sediment until effervescence has stopped. In heated digestions, the temperature was then brought up to 80°C and the flasks left to react . The zinc acetate filled trap tubes were changed every 15 minutes in the case of artificial samples, and every 30 minutes for all other types of sample, and the reaction was continued until no noticeable change in colour of the trap tubes for two successive trap tubes. 1ml from the zinc acetate trap was then used to determine the AVS content of the sample using a colorimetric method (Cline, 1969).

The same amount of sample used in the AVS digestions was placed in a distillation flask for the chromous chloride digestions. 5ml of 95% ethanol, 5ml of 20% zinc acetate, and a magnetic stirrer were added to each flask. The flasks were

then attached to the distillation apparatus as previously described. The apparatus was left to flush for 10 minutes before 25ml of 1M chromous chloride in 0.5N HCl (reduced in a Jones Reductor column- see appendix 2) and 10ml of concentrated hydrochloric acid were injected into each flask. In heated digestions the temperature was then brought up to 80°C. Distillation times and sulphide concentrations were determined as in the AVS procedure.

Additional digestions were performed on mixtures of samples in order to determine whether they could be separated by using sequential and parallel digestions. In these cases mixtures of two or three samples were treated in a similar manner to the single digestions, with a cold AVS digestion followed by a hot AVS digestion. These digestions were then followed by a cold chromous chloride digestion prior to heating again. In sequential digestions such as these 20 minutes were allowed before the introduction of further reagents in order to allow the temperature changes to occur. Replicate samples were digested in parallel, cold and hot AVS extractions on one sample and cold and hot chromous chloride digestions on a replicate.

2.C - Results and Discussion

All four pyrite samples behaved similarly under different reaction conditions (Table III). Hot and cold chromous chloride digestions produced similar recoveries from all types of pyrite, except artificial which showed a increase from 75% recovery in cold digestions to 93% recovery in hot, due to some oxidation of pyrite to elemental sulphur. Only the length of digestion time required to obtain complete recovery varies. In previous studies (Parkes and Buckingham, 1986, Krairaponond *et al.*, 1992, and Parkes - unpublished results) it was found that between 40 minutes and 1 hour were sufficient to reduce all the sulphide compounds in a bacterial culture or $^{35}SO_4$ radiotracer incubation sample, while two hours was recommended for ancient shales (Canfield *et al.*, 1986). Canfield *et al.* (1986) considered this variation in digestion times to be due to the coating of pyrite crystals in lithified sediments, while Chanton and Martens (1985) and Rice *et al.* (1993) showed that grainsize is a contributing factor to digestion time. Rice *et al.* (1993) commented that the age of pyrite used effects its recovery in AVS digestions containing stannous chloride.

In this study, which is based on identifying a method of determining pyrite, elemental sulphur and AVS concentrations in samples ranging in age from 1 day to millions of years, crystallinity is likely to be the primary controlling factor. The difference in grainsize between Recent and ancient pyrite can be eliminated by

Table III - Recoveries of Various Mineral Samples under Different Digestion Conditions

Sample	Method	Digestion Time	Percentage recovery	Standard deviation
Pyrite (euhedral)	Hot $CrCl_2$	4 hours	105	19
FeS_2	Cold $CrCl_2$	4 hours	96	21
	Hot AVS	2 hours	0	0
Pyrite (rock nodule)	Hot $CrCl_2$	4 hours	112	12
	Cold $CrCl_2$	4 hours	91	25
	Hot AVS	2 hours	0	0
Pyrite (artificial)	Hot $CrCl_2$	2 hours	93	9
	Cold $CrCl_2$	2 hours	75	25
	Hot AVS	2 hours	0	0
Pyrite (vein)	Hot $CrCl_2$	4 hours	105	19
	Cold $CrCl_2$	4 hours	85	12
	Hot AVS	2 hours	0	0
Sphalerite (ZnS)	Hot $CrCl_2$	4 hours	93	12
	Cold $CrCl_2$	4 hours	92	13
	Hot AVS	2 hours	111	14
	Cold Avs	2 hours	68	15
Chalcopyrite ($CuFeS_2$)	Hot $CrCl_2$	4 hours	108	23
	Cold $CrCl_2$	4 hours	125	16
	Hot AVS	2 hours	12	7
	Cold Avs	2 hours	37	13
Galena (PbS)	Hot $CrCl_2$	4 hours	106	14
	Cold $CrCl_2$	4 hours	80	13
	Hot AVS	2 hours	119	8
	Cold Avs	2 hours	116	13
Marcasite	Hot $CrCl_2$	4 hours	72	13
FeS_2	Cold $CrCl_2$	4 hours	61	3
	Hot AVS	2 hours	1	1
Iron Monosulfide	Hot $CrCl_2$	1hour	87	13
FeS	Cold $CrCl_2$	1 hour	87	7
	Hot AVS	1 hour	81	3
	Cold Avs	1 hour	104	14
Greigite	Hot $CrCl_2$	1 hour	78	21
Fe_3S_4	Cold $CrCl_2$	1 hour	91	24
	Hot AVS	1 hour	88	4
	Cold Avs	1 hour	34	12
Polysulfide Solution	Hot $CrCl_2$	1 hour	93	4
$S_n - S^{2-}$	Cold $CrCl_2$	1 hour	50	1
	Hot AVS	1 hour	11	2
Sulfur suspension	Hot $CrCl_2$	1 hour	85	7
S°	Cold $CrCl_2$	1 hour	0	0
	Hot AVS	1 hour	0	0
Flowers of Sulfur	Hot $CrCl_2$	1 hour	105	28
S°	Cold $CrCl_2$	1 hour	1	2
	Hot AVS	1 hour	0	0

NB The distillation apparatus used had an internal error of 5-9% on standard sulphide solutions distilled under hot AVS conditions.

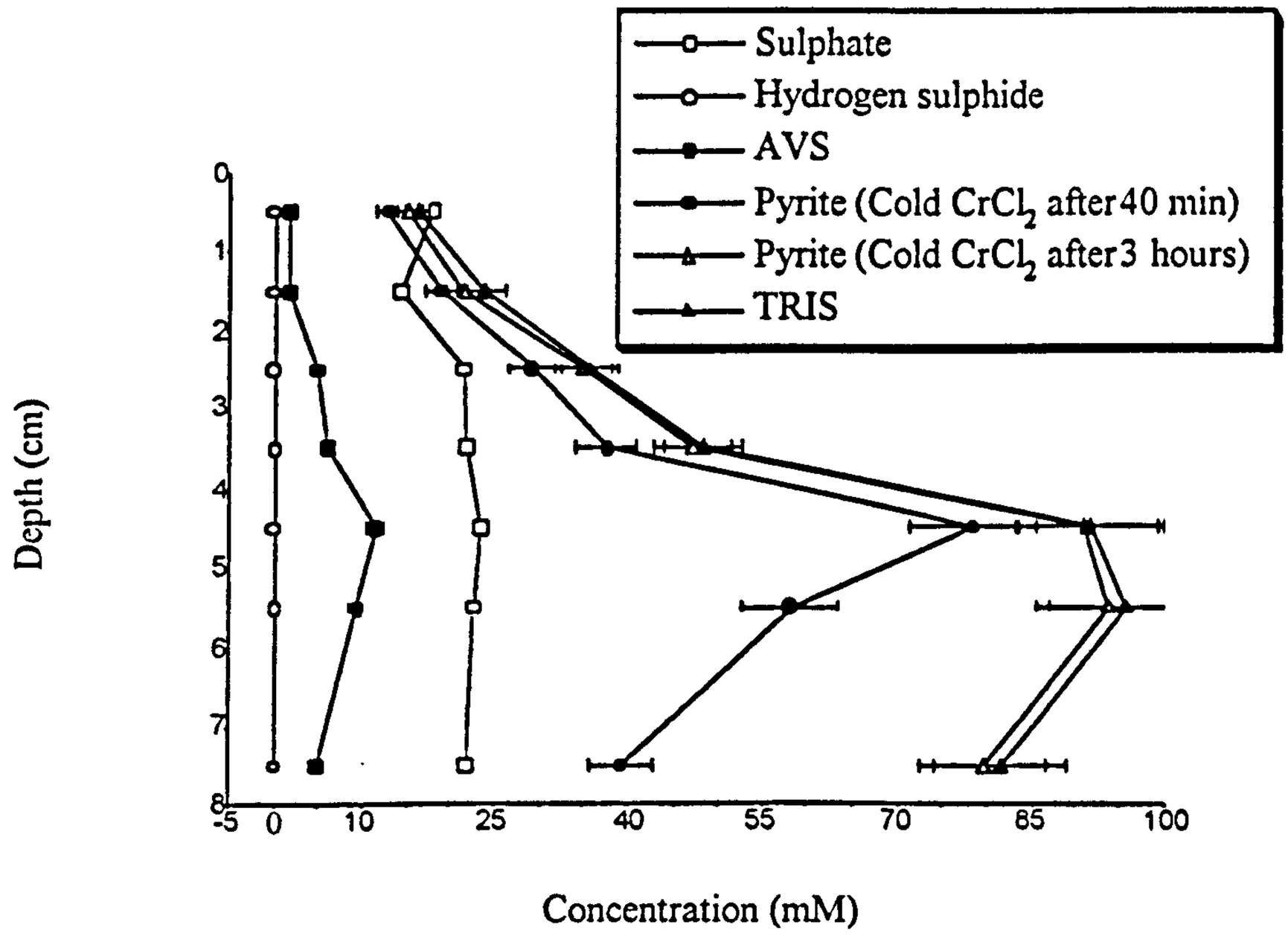

Figure 2.2 - Distribution of reduced sulphur species measured in Tamar Estuary sediments

crushing the rock samples. A 40 minute chromous chloride digestion will remove the least mature pyrite for a sediment, for example that which contains $^{35}S^{2-}$ in radiotracer experiments, but continuing the digestion for up to 3 hours removes the remaining pyrite fraction in sediments (Figure 2.2). This older or more crystalline pyrite fraction represented up to 35% of the total pyrite concentration in Tamar Estuary sediments (Figure 2.2), and is considered to be framboidal or euhedral, while the newly formed material is amorphous. The elemental sulphur content is low in these sediments and there is, therefore, a small increase in sulphide recoveries after heating with chromous chloride (shown by higher TRIS concentrations in Figure 2.2). The euhedral pyrite digestion times were similar to those of sedimentary pyrite with the majority of sulphide recovered within 3 hours (c. 85% +/- 20%), indicating that the sediment contains pyrite of a similar crystallinity. This behaviour indicates that the concentration of sulphide produced during $^{35}SO_4$ radiotracer incubations for sulphate reduction activity measurements is not synonymous with the concentration of iron sulphide minerals in a sediment (its degree of sulphidation; Boesen and Postma, 1988) when the digestion times used are short. In order to compare ancient and Recent sulphidic sediments the whole of the pyrite pool must be analysed and the pyrite from recovered by 40 minute cold chromous chloride digestion is not representative of this.

Results for marcasite were similar to those for pyrite. It is recovered under hot and cold chromous chloride digestions. However, the sample was a nodule from a sedimentary succession and it also contained clay. Thus the concentration of sulphide recovered was lower than the theoretical value for the pure sulphide standard (Table III). Chalcopyrite, unlike pyrite, does not contain sulphur-sulphur covalent bonds and hence should be recovered with AVS digestions. Only 37% was recovered under these conditions, however, while the remainder required chromous chloride digestion. Since chalcopyrite is usually found intergrown with pyrite this behaviour is likely to be due to the contamination of the sample with pyrite. This was later confirmed by XRD. The other mineral samples which contain a metal to sulphur ratio of 1:1, reacted as expected and in a similar manner to that of iron monosulphide minerals (Table III). Galena was digested completely in hot and cold acid digestions, while sphalerite required heating for complete recovery (Table III). The recovery of the non-iron monosulphide minerals (Table II and III) during AVS digestions is not unexpected, but it does indicate that the DOS ratio may be distorted. Hence, for a DOS ratio to accurately represent the sulphidation of the sediment, the concentration of the HCl-soluble metal fraction should be analysed for metals in addition to iron, as their sulphides contribute to the sulphide pool. This may be significant in DOS ratios in deposits such as the Kupferschiefer (copper shales) of Germany where large concentrations of copper are precipitated as sulphides (Deer *et al.*, 1966), or in sediments where anthropogenic influences are high (Bryan and Lanyton, 1992). The DOP ratio is also distorted as small amounts of iron are present in chalcopyrite and other sulphide minerals: sphalerite, for example, may contain up to 15% iron (Deer *et al.*, 1966), which are included in the reactive iron fraction (HCl-extractable) and in the sulphide pool if the contribution from the AVS pool is not included. Thus the proportion of other minerals must be taken into account in calculation of DOP because they contribute to the available iron pool although their sulphides are not included in the pyrite pool.

The artificial greigite showed recoveries of 34% in cold AVS and 88% in hot AVS digestions. In contrast at least 81% of iron monosulphide was recovered in each digestion (Table III). This clearly demonstrates that these two compounds cannot be separated on the basis of a cold and hot AVS digestion. Mixtures of different pyrite samples with greigite or FeS showed good separation when treated in hot AVS and cold chromous chloride digestions. During hot acid digestions, 92% (+/- 6%) FeS and 87% (+/- 21%) greigite were recovered while pyrite was only recovered during cold chromous chloride digestions (90% +/- 20%). Samples of other minerals and various pyrites showed similar behaviour when treated in this way.

The sulphur suspension in acetone and the flowers of sulphur were recovered only in hot chromous chloride digestions (Table III). Extractions for elemental sulphur using cyclohexane and dichloromethane were not particularly successful due to a poor partition between sulphur and the solvents, especially in bacterial cultures and artifical compounds, where it was difficult to get the suspensions sufficiently wet with the organic solvent. The particulate nature of bacterial cultures and the artifical compounds also made the separation of the phases difficult. After extracting sulphur for 24 hours the maximum sulphur recovered after 24 hours with dichloromethane was only 72% of the recovery of the whole sample under hot chromous chloride conditions. Dichloromethane consistently gave higher recoveries than cyclohexane, although both solvents gave unsatisfactory phase separation. Recoveries were especially poor when the extractions were applied to cultures of sulphate-reducing bacteria. Dichloromethane only recovered 20% of the elemental sulphur in this sample, while none was recovered with cyclohexane. When applied to Recent and ancient sedimentary samples the problem of separating the solvent from the sample was increased as there was often a suspension of sample at the interface. However, hot chromous chloride digestions recover the majority of elemental sulphur (between 85% and 105%, Table III). As most of the pyrite can be removed without heating (75% to 92%, Table III) a cold followed by a hot chromous chloride digestion provides a reasonable estimate of the concentration of elemental sulphur in a sample. This was tested with a mixture of elemental sulphur and pyrite. Although the recovery of pyritic sulphide increased slightly (possibly due to the recovery of some sulphur during cold chromous chloride digestions) this was within the experimental error.

Polysulphide breaks down into hydrogen sulphide and elemental sulphur upon acidification (Luther *et al.*, 1985). This means that the sulphide evolved during chromous chloride digestions is separated equally between cold and hot digestions, the additional sulphide being recovered during hot digestions (Table III). AVS digestions produce less sulphide than cold chromous chloride digestions. The increased yield in cold chromous chloride digestions is due to the increased reducing capacity of chromous chloride. Heating in chromous digestions breaks the sulphur-sulphur bonds in the polysulphide ion. Extractions on a polysulphide-elemental sulphur mixture confirmed that dichloromethane is better at extracting sulphur than cyclohexane.

When the hot AVS, and cold followed by hot chromous chloride digestions are applied to cultures of sulphate-reducing bacteria used to model sedimentary pyrite

formation (Figure 2.3) iron sulphide minerals including pyrite, elemental sulphur and hydrogen sulphide can be observed to coexist within 3 days. This digestion scheme (Figure 2.4) allows the chemical changes in the sulphides, and the ratio of various reduced sulphur species to pyrite, to be monitored despite the amorphous nature of the solid phases and the presence of organic films draping the minerals. The characterisation of solid phases was subsequently confirmed by electron microprobe analysis of precipitates from the samples. The same treatment of Recent sediments also produce reliable results and efficiently separated different sulphide pools, enabling the formation of authigenic sulphide minerals to be studied (Figure 2.2).

Figure 2.3 - Distribution of reduced sulphur species in a experimental sample

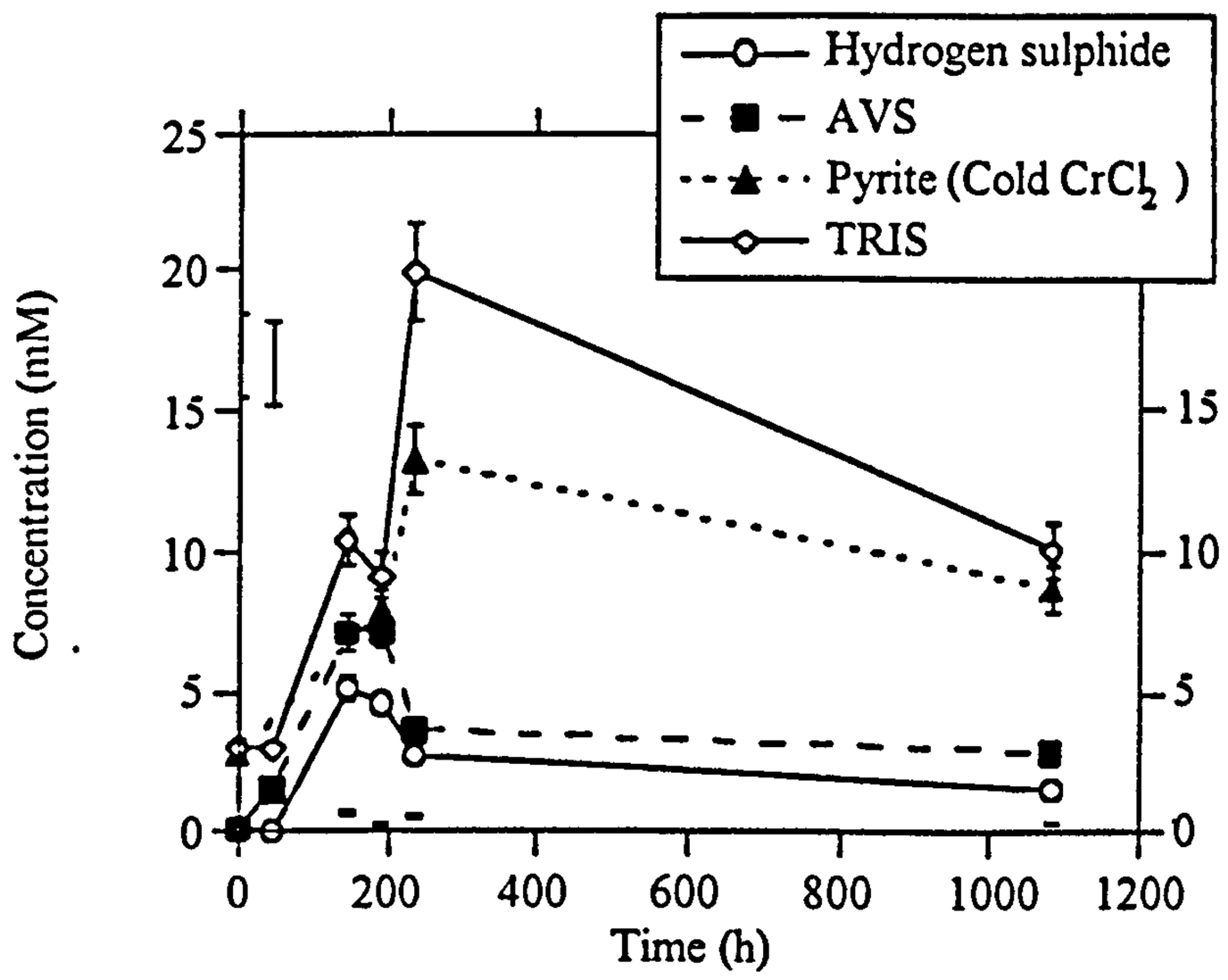

2.D - Conclusions

A hot acid digestion in addition to a cold/hot chromous chloride digestion appears to be applicable to sulphide mineralisation of all ages, allowing the separation of the reduced sulphide pool into AVS, pyritic sulphides and elemental sulphur. There is, however, a considerable difference between the digestion times required to recover mineral sulphides during early sulphide formation by bacteria (i.e. in bacterial cultures and $^{35}SO_4$ radiotracer incubations) and those in mature sulphide minerals (i.e. Recent sedimentary framboids, geological samples and fossils). Hot chromous chloride digestion appears to be a more accurate way of determining the concentration of elemental sulphur in the sample than the use of solvent extraction of

sulphur. As each environment or experimental sample varies it is recommended that precise digestion times are established prior to the determination of sulphur species.

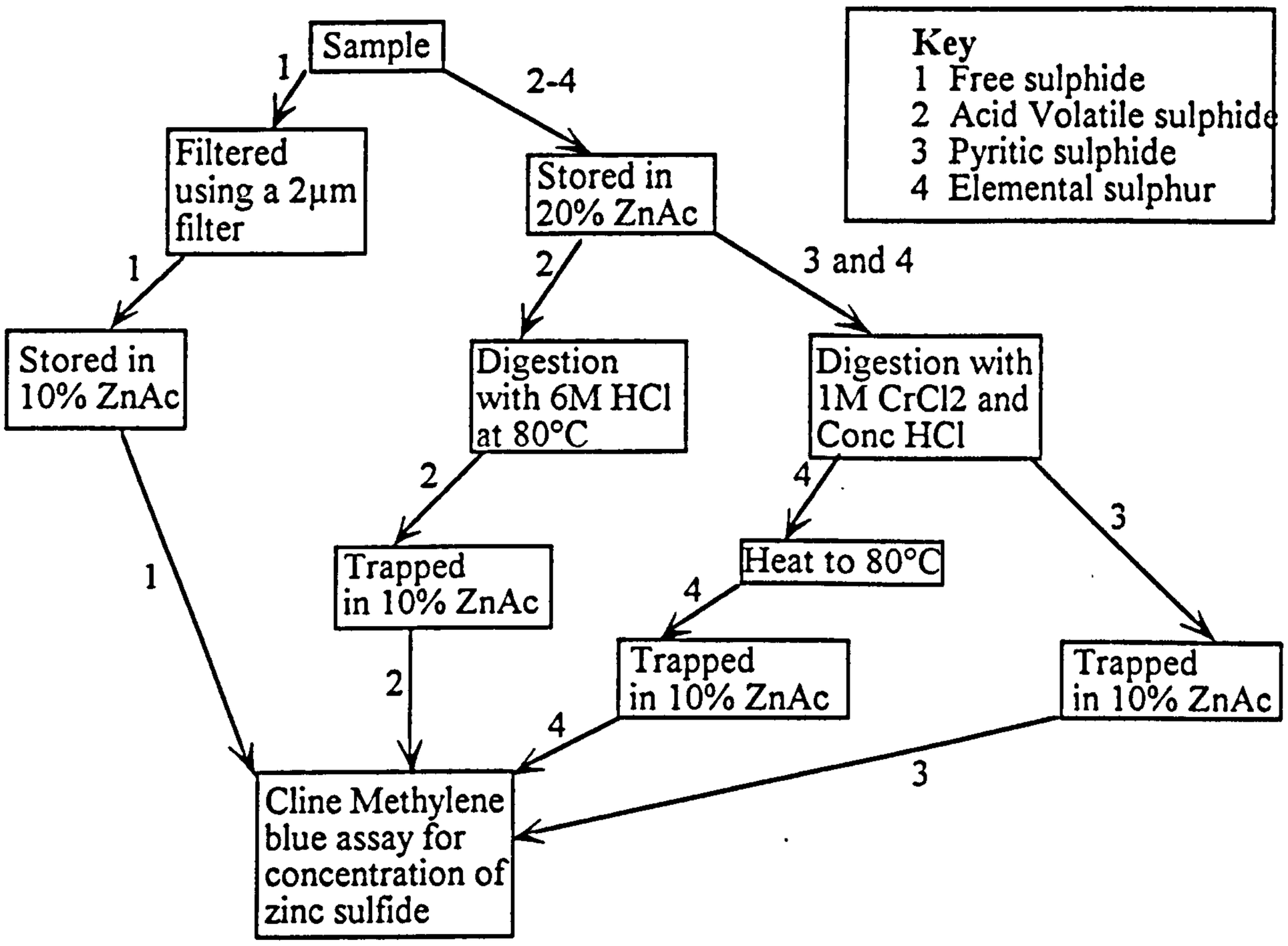

Figure 2.4 - Schematic diagram of method for determining the concentrations of reduced sulphur pools.

PAGE NUMBERING AS ORIGINAL

Chapter Three

Bacterial Experiments Modelling Controls upon the Formation of Pyrite

3.A - Introduction

Most previous experimental studies performed on pyrite formation have been restricted to laboratory experiments that exclude organic compounds and organisms. These allow the kinetics and the mechanisms of the reactions between hydrogen sulphide and iron, and forming pyrite from acid-volatile sulphide precursors to be determined, but they do not reflect sedimentary environmental conditions. This is pertinent as the studies of pyrite formation in the presence of organic compounds suggest that they altered both the kinetics of the reaction (Rickard, 1975) and the stability of the products (Kríbek, 1975). Experiments including organic material will therefore produce a more realistic view of the process of pyrite formation in sediments, and sedimentary sulphate-reducing bacteria provide a means of reproducing this in the laboratory at low temperatures. The use of bacterial cultures as an approach to the study of early sulphide mineralisation is therefore appropriate. The approach is especially relevant as the production of sulphide minerals in bacterial cultures has long been used as a method of detecting bacterial growth (Postgate, 1979), and pyrite formation in cultures of sulphate reducers was first reported in 1912 by Issatchencho.

The purpose of the experiments using bacterial cultures was to define the conditions under which bacterial-mediated pyritization occurs, rather than to define the reactions involved. The experiments also seek to define the chemical controls upon pyrite in a sedimentary environment, by altering the concentrations and form of the ingredients within the growth medium. Berner (1967;1970;1980) defined the controls on pyrite formation in anoxic environments at neutral pH to be the concentrations of sulphate, easily metabolisable organic matter and reactive iron. Changing the concentration of these variables, as well as altering less absolute variables such as the openness of the system, changes the environmental conditions. Each experiment can therefore be considered to represent a micro-environment and altering these variables allows different sedimentary conditions to modelled, and their effects assessed.

3.B - The production of pyrite in bacterial cultures

3.B.1 - Methods

In order to illustrate the changes in the chemistry of iron sulphide precipitation in a culture of sulphate reducing bacteria, an experiment containing Postgates medium (appendix 4) with 17.5ml l^{-1} sodium lactate syrup (Sigma), 0.14g ferrous sulphate, and *Desulfovibrio desulfuricans* was selected. The growth medium was made up in modified two litre durans; sterilized using an autoclave and cooled under oxygen-free nitrogen. The pH was checked prior to dispensing into sterile 100ml vials containing 0.14g of ferrous sulphate and the vials were then stoppered with sterile grey neoprene septa. The vials were inoculated with 2ml of a 5% inoculum of a standard culture of *Desulfovibrio desulfuricans* , prior to sampling and incubation at 25°C.

Samples were taken via a 0.8mm diameter needle, on days 0, 2, 4, 6, 8 and 10, and were stored for analyses. 1ml was filtered into 0.5ml 10% zinc acetate for free sulphides and sulphates, and 5ml was stored in 5ml 20% zinc acetate for solid sulphides and elemental sulphur. The latter were also frozen after sampling in order to prevent oxidation of the iron sulphide. Additionally, 0.5ml samples for bacterial enumeration (AODC; Fry *et al.*, 1990; Gibson *et al.*, 1987) analysis were stored in 0.5ml of filter sterilised 2% formalin solution. The methods used to determine the concentrations of hydrogen sulphide, reduced sulphur species, sulphate and thiosulphate ions are outlined in appendix 5 and individual methods of analysis are shown in Table IV.

Table IV - Summary of Methods

Species	Initial Method	2nd Method
Hydrogen sulphide	Modified sulphide assay	
Sulphate	Dionex	
Acid-volatile sulphide	Hot acid digestion	Methyl-blue sulphide assay
Pyritic sulphide	Cold chromous chloride digestion	Methyl-blue sulphide assay
Elemental sulphur	Hot chromous chloride digestion	Methyl-blue sulphide assay
Bacterial numbers	AODC	
Type of iron compound	Microprobe	
pH	pH electrode	

3.B.2 - Results

3.B.2.1 - Changes in Sulphur Compounds. Over 10 days, the concentrations of sulphur compounds varied considerably. Day 0 is taken to be the time of inoculation and the initial concentration of TRIS is greater than zero due to the reduced sulphur species contained in the inoculum. When the experiment was inoculated hydrogen sulphide in the inoculum reacted to form the AVS compounds observed on day 2 (Figure 3.1).

Table V - A comparison of the rate of sulphate reduction and size of the bacterial population in a culture of sulphate-reducing bacteria

Timespan	Rate of Sulphate Reduction	Size of the bacterial population
0-2 days	2.77 mM day^{-1}	5.2 x 10^7 cells per ml (day 2)
2-4 days	5.77 mM day^{-1}	7.6 x 10^7 cells per ml (day 4)
4-8 days	-0.38 mM day^{-1}	9 x 10^7 cells per ml (day 8)
8-10 days	0.29 mM day^{-1}	1.1 x 10^8 cells per ml (day 10)

Initially, the bacterial population was small, but sulphate concentrations still decreased as bacteria took sulphate ions into their cells. Sulphate concentrations decreased at varying rates, which corresponded to the size of the bacterial population within the experiment (Table V). As sulphate was metabolized the bacterial population increased, until the rate of population growth and the rate of sulphate reduction were rapid (Figure 3.1). However, as sulphate was consumed it reached low concentrations limiting the rate of sulphate reduction (Table V); the rate at which the bacterial population was increasing also slowed. Sulphate concentrations are considered to become limitng around 5mM (Boudreau & Westrich, 1984), however this threshold is dependant on the concentration of organic matter; in environments with high concentrations of organic matter the concentration of sulphate which is limiting is much lower than 5mM. 78% of the sulphate in the experiment was measured as reduced sulphur species on day 10 (Figure 3.1), meaning that sulphate did not limit sulphate reduction until it reached a concentration of 4mM. The sulphur mass balance in this experiment indicates that 20% of the sulphur species were not measured in the reduced sulphur and sulphate pool. In this experiment this is likely to be due to oxidation of hydrogen sulphide to an intermediate sulphur compound, such as thiosulphate, during sampling. Oxidation also caused a slight increase in sulphate concentrations around day 8, but this was rapidly reduced by day 10 (Figure 3.1). However, the standard deviation of reduced sulphur concentrations in this experiment is around 20%. This is due to the variations in bacterial inoculums and bacterial growth, rather than errors in the method.

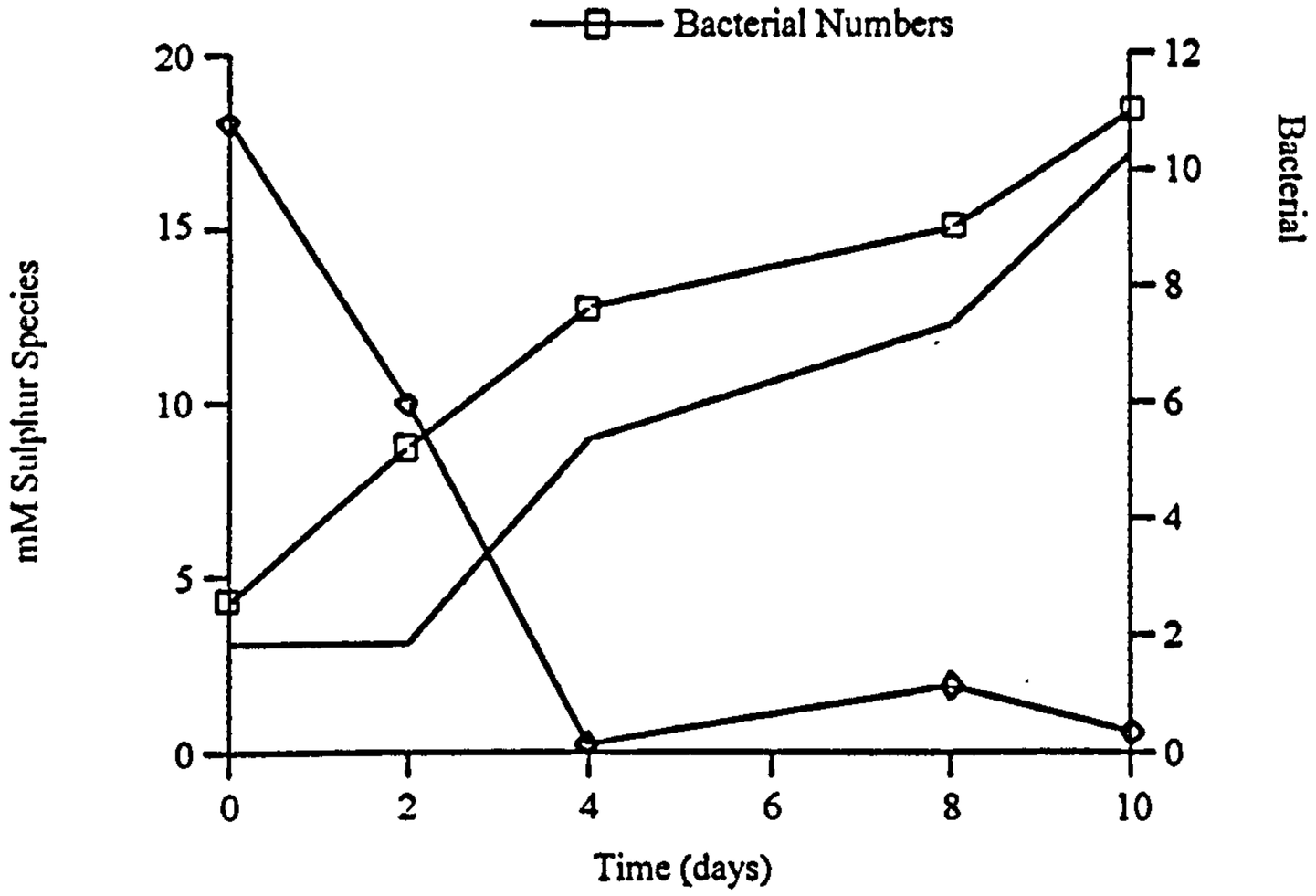

Figure 3.1 - Decreases in sulphate concentrations and increases in TRIS concentrations and bacterial numbers; where TRIS concentrations are the sum of the concentrations of hydrogen sulphide, AVS, pyritic sulphide and elemental sulphur.

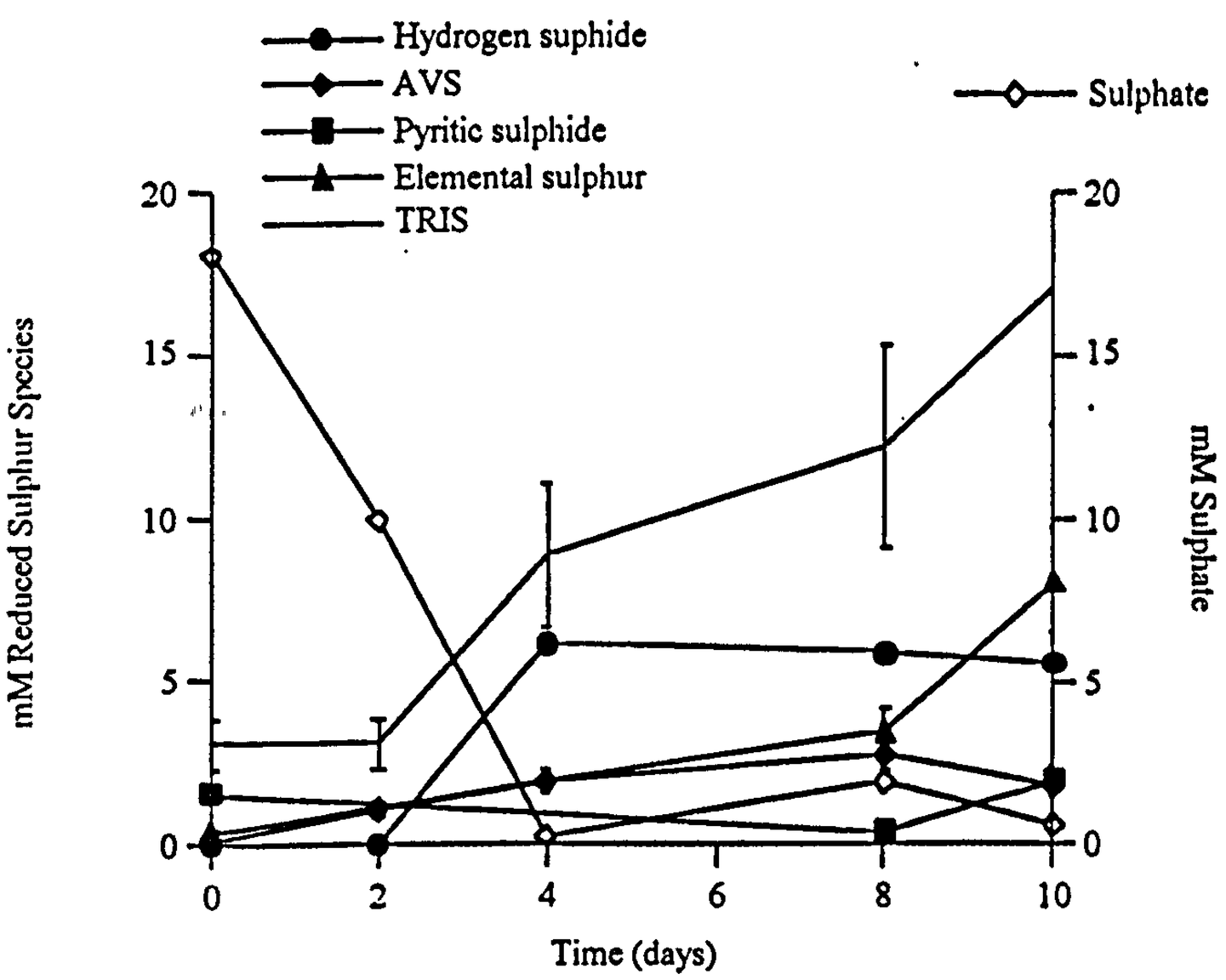

Figure 3.2 - Changes in the concentrations of reduced sulphur species in the bacterial experiment

During the initial phase of sulphate reduction there was little increase in the concentrations of hydrogen sulphide, AVS, pyrite and elemental sulphur from the concentrations in the inoculum (Figure 3.2). This was due to the lag phase where bacteria take sulphate into their cells, prior to metabolising it. After day 4, the

concentration of the reduced sulphur species increased, with hydrogen sulphide being the dominant phase (Figure 3.2). Hydrogen sulphide then reacted with iron within the medium to precipitate acid-volatile sulphides and pyrite. The concentrations of acid-volatile sulphide and elemental sulphur remained similar until day 10, when elemental sulphur concentrations increased sharply. The elemental sulphur concentrations increased due to the partial oxidation of hydrogen sulphide, AVS and the breakdown of pyritic sulphide. Oxidation occurs in the experiment as the amount of hydrogen sulphide produced in the experiment decreases, sue to bacterial metabolism becoming limited by organic and sulphate concentrations and as the septa is repeatedly pierced. This trend appears in the all of the duplicate experiments.

When pyrite is manufactured chemically the vessels in which the initial reaction take place are aged (see appendix 3) in order to increase the concentration and crystallinity of the product. However, when the bacterial experiments were left to age for 130 days at 30 °C the precipitates did not increase in crystallinity although the biofilms containing pyrite clumped together in blobs (Figure 3.4) and sulphide concentrations increased to 10mM in some experiments. Aged vials change from being pyrite-dominanted to having a dominant acid-volatile sulphide phase, due to the increase in the hydrogen sulphide concentrations, and although there may be a drop in the concentration of TRIS or pyritic sulphide concentrations this is not reflected in an increase in either sulphate or thiosulphate concentrations (appendix 6).

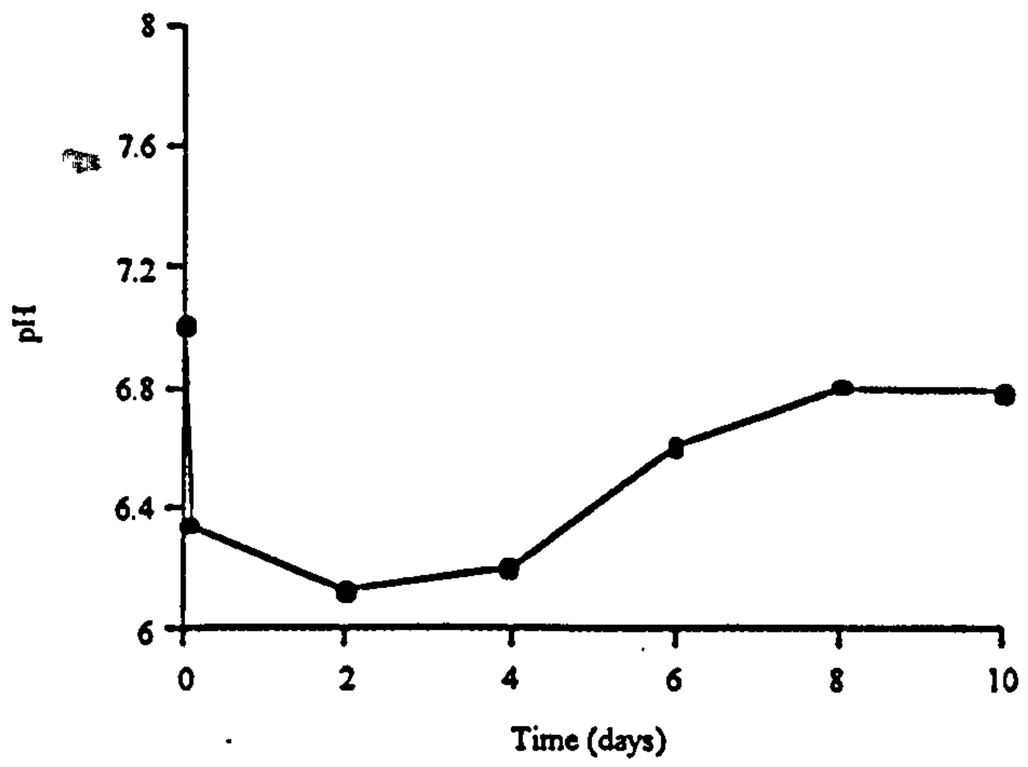

Figure 3.3 - pH changes in bacterial experiment containing ferrous sulphate

3.B.2.2 - pH changes. In general, when the medium was dispensed into the vials there was an initial decrease in the pH of the medium from around 7 to 6.1 (Figure 3.3). This was due to the introduction of iron ions into the medium; ferrous ions are a strong proton donor (ie., acid) and the high solubility of ferrous sulphate

means that the concentration of ferrous ions in solution is high. In bacterial media, and seawater, the iron ions may also form complexes with other aqueous ions which will alter their behaviour as electron acceptors/donors. Iron may form complexes with sulphate ions, hydroxyl ions, thioglycolatic acid, acetate, chloride and other halide ions, and hydrogen sulphide as well as oxygen and hydroxide ions (Davison, 1979).

As the bacterial culture began to metabolise the pH gradually recovered to around 6.5 (Figure 3.3). The pH of the medium, just as in natural systems, is dependant upon a complex interplay of several variables (Gardener, 1971) which are associated with the breakdown of organic matter within the experiments and the concurrent production of sulphide, ammonium and bicarbonate ions. In *Desulfovibrio* experiments, the pH was dependant upon the production of ions during the metabolism of lactate to acetate and bicarbonate ions.

$$2C_3H_5O_3Na + SO_4^{2-} \text{------>} 2CH_3COONa + H_2S + 2HCO_3^- \quad \text{Eq.3.1}$$

If this occurred in a medium where there was no iron sulphide precipitation a solution with a pH of approximately 6.9 was produced. This was due to the increase in concentration of hydrogen sulphide ions which act as an acid (Boudreau and Canfield, 1987). When iron sulphide precipitation occurred the pH increased to around 7.5 (Figure 3.1) due to the removal of hydrogen sulphide and iron ions. The pH is then reduced to around 7 by the precipitation of carbonate ions as calcium carbonate and the action of the buffers included in the medium.

3.B.2.3 - What form does the pyrite take? Pyrite formed in *Desulfovibrio desulfuricans* cultures was precipitated in association with other iron sulphides in an amorphous film. This was attached to the sides of vials, formed discrete blobs or floated on the surface of the medium (Figure 3.4). When films were floating or attached they are similar to the "oil" described by Rickard (1969b). This film became discrete, forming blobs, in experiments where the sulphide concentration was very high, or was observed stuck to the side of the vials (Figure 3.4). When the film was examined under the SEM it had a knobbly appearance, and when an Acridine Orange stain was applied it could be seen that there were a large numbers of bacteria in close association (Figure 3.5). The proximity of the bacteria suggested that the film may be associated with the extra-cellular polysaccharides which bacteria produce to attach themselves to surfaces and to protect themselves from inhospitable conditions, such as a high concentrations of hydrogen sulphide. These biofilms or glycocalyx are produced by many species of bacteria and can be observed in association with cells, as

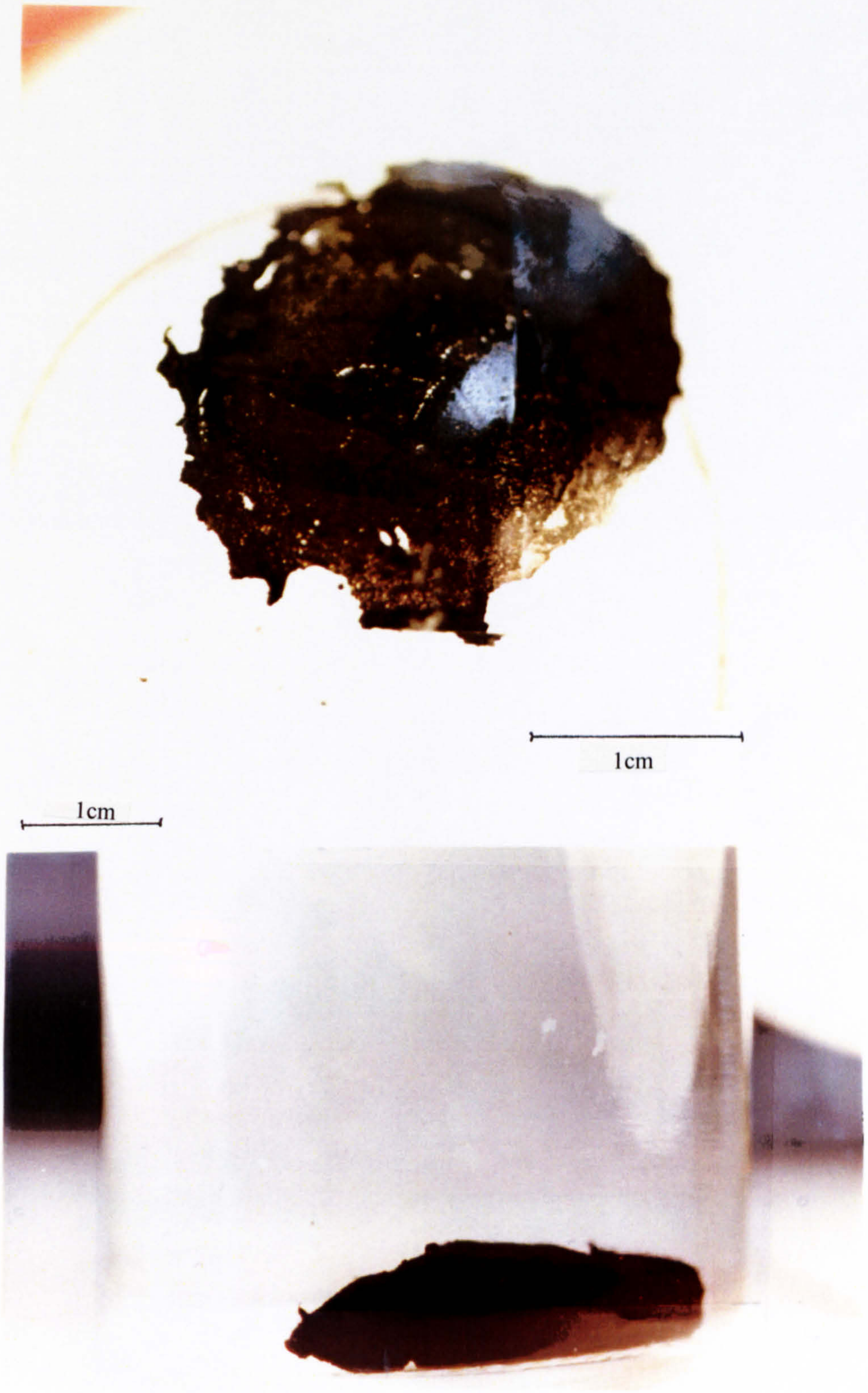

Figure 3.4 - Biofilms formed in vials of *Desulfovibrio desulfericans* after 40 days.

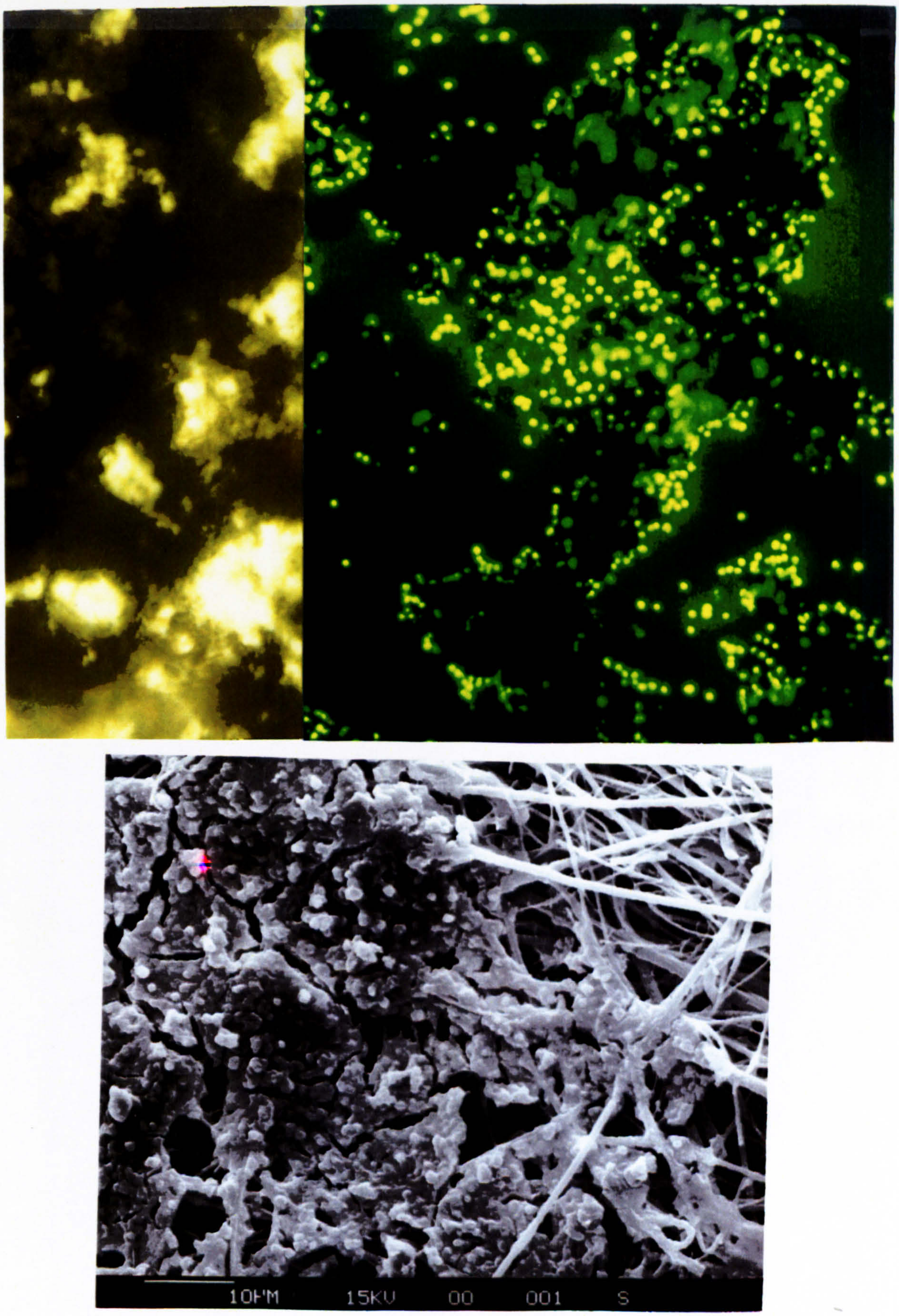

Figure 3.5 - Details of biofilms observed in figure . A - Acridine orange stained and light micrograph of sulphide precipitate, B - SEM of biofilm on filter paper.

Figure 3.6 - Microprobe scan results of samples from bacterial experiments. A is from a biofilm whereas B is from the surface of an organic fragment. Both samples are from lactate -rich Postgates media containing ferrous sulphate..

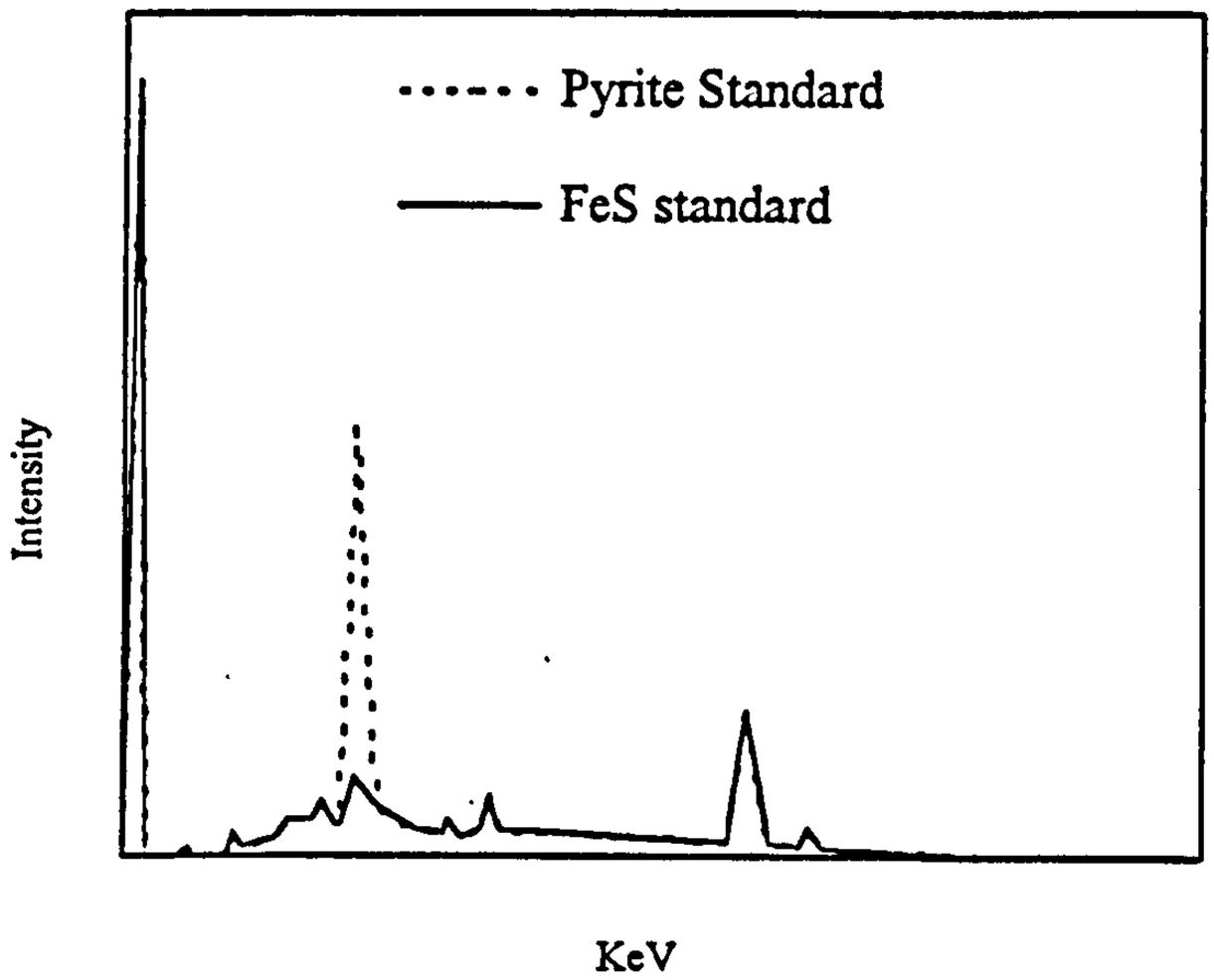

A

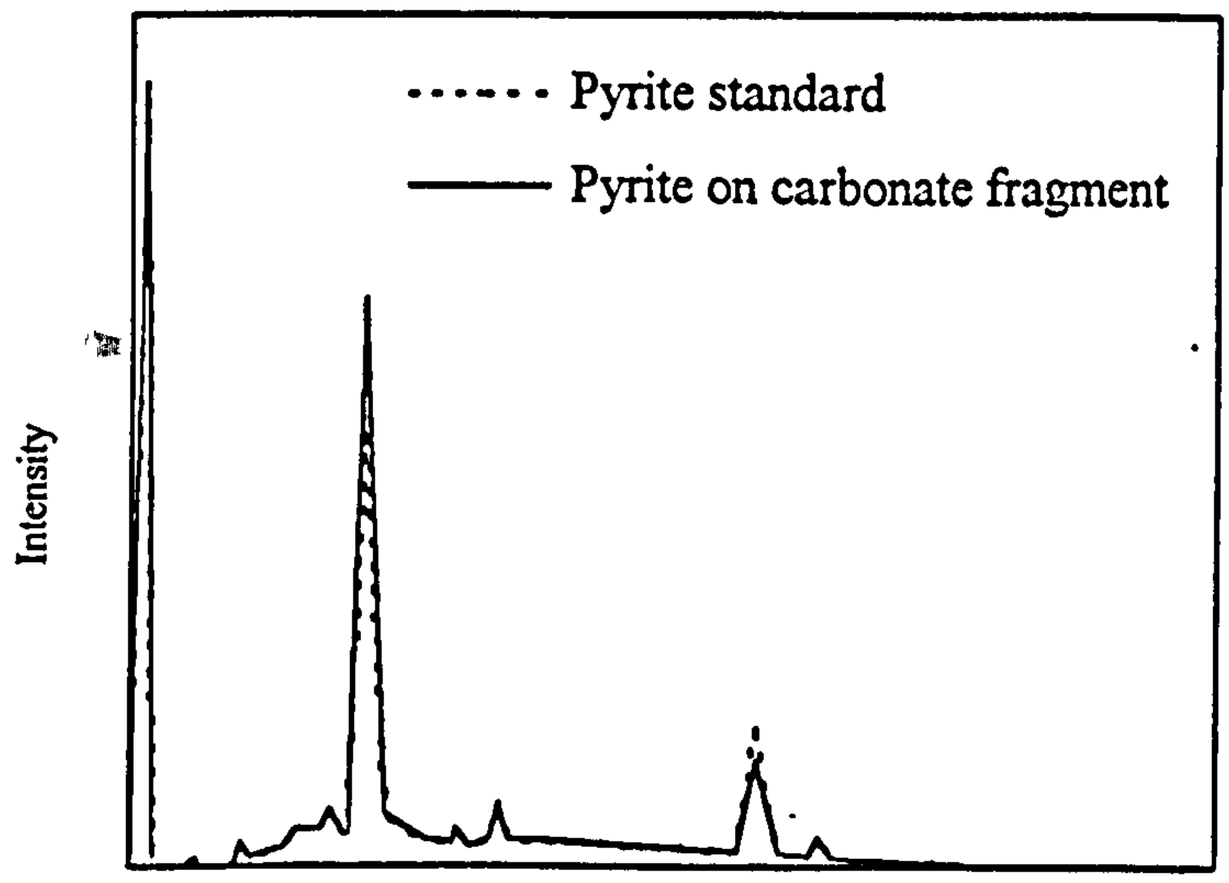

B

a capsule, or in the medium surrounding the bacteria (Costerton, 1981; Blenkinsopp and Costerton, 1991).

When the film in the *Desulfovibrio* vials was analysed using the electron micro-probe, it was found to have variable iron:sulphur ratios including some which match those of pyrite and mackinawite and many in between (Figure 3.6). These films formed in a similar fashion to those observed by Beveridge and co-workers (Beveridge, 1989; Konhauser *et al.*, 1993; Ferris *et al.*, 1987), who found bacterial capsules acting as nucleation sites for iron sulphides and other minerals. The precipitates associated with the bacteria and their remains occurred in a mixed mineral phases and frequently showed no crystal habit. The presence of compounds such as acetate (Luther, *et al.*, 1986) and humic acids (Krîbek, 1975) which form complexes with iron, also inhibits the formation of crystalline pyrite.

The presence of bacteria producing large quantities of extra-cellular polysaccharides is thought to prevent the formation of discrete pyrite crystals, although the pH of the system indicates that crystals would, in this case, be small and anhedral (Schoonen and Barnes, 1991). If the iron or the sulphide is complexing with the polysaccharides then the film will bear the sulphide minerals. This is probably the origin of the mixed sulphide films observed by Bertolin et *al.*, (1995) in the Lagoon of Venice, (and those observed in these experiments) and is consistent with the sulphidised biofilm suggested by Rickard (1970) as the source of organic material in framboids.

3.C - Sulphate reduction and pyrite formation under different environmental conditions

3.C.1 - Introduction

In natural systems the production of pyrite is suggested to be controlled, under neutral pH and anoxic conditions, by the rate of sulphate reduction and the availability of iron compounds. The rate of sulphate reduction is itself controlled by the concentration of easily metabolisable organic compounds and sulphate. Changing the concentrations of these components, and other variables, in a medium changed the conditions under which sulphate reduction and pyrite formation occurs. Microbial experiments were designed to answer the following questions.

a) What is the effect of changing the starting concentrations of i) sulphate, ii) organic substrate, and iii) iron ?

b) What is the effect of different strains of sulphate-reducing bacteria?
c) What is the effect of using different iron compounds?
d) What is the effect of other discrete variables such as system closure and media type?
e) Does the presence of bacteria facilitate the production of pyrite in microbial cultures ?
and f) Can microbial experiments be used to model changes in sediments?

3.C.2 - The effect of different iron compounds on the rate and amount of pyrite formation in bacterial cultures

Ferrous sulphate was replaced with ferric oxyhydroxide (lepidocrocite) or ferrous monosulphide (mackinawite) to determine whether changing the iron phase would increase the potential for pyrite formation, and change the sulphur chemistry. The experiments were prepared as before, with the ferrous sulphate being replaced by 0.05g of lepidocrocite or 0.044g of mackinawite.

3.C.2.1 - Changes in the concentrations of reduced sulphur compounds. The experiments containing lepidocrocite produced a similar pattern to the ferrous sulphate experiments, with sulphate decreasing and reduced sulphur compounds increasing over time. TRIS concentrations were nearer zero at the beginning of the experiment because the ferric iron did not react immedaiately with the hydrogen sulphide in the inoculum but oxidised it. The reduced sulphur species were still dominated by hydrogen sulphide, but the overall concentration of reduced sulphur species (TRIS) was as much as 50% lower than that in the ferrous sulphate experiments (Figure 3.7). The difference in the amount of TRIS produced in the lepidocrocite experiment may be explained by the presence of an oxidising agent, the oxyhydroxide in the experiment. This oxidised reduced sulphur species to intermediate sulphur compounds, such as thiosulphate (not measured in this experiment) causing the sulphur mass balance to be unequal (Figure 3.7). Between days eight and ten, elemental sulphur and acid-volatile sulphide concentrations increased, as pyritic sulphide decreased. This pattern of increasing elemental sulphur occurred at the end of the experiment when the sulphate reduction rate decreased; the lower concentrations of hydrogen sulphide facilitated the diffusion of oxygen into the experiment. This means that the concentrations of pyritic sulphide and acid-volatile sulphide were similar at the end of the incubation period to those in the ferrous sulphate experiment, but prior to day 8 the ferrous sulphate experiment was dominated by acid-volatile sulphide and the lepidocrocite experiment was dominated by pyritic sulphide. The PS/TRIS ratio indicated that pyritic sulphide formed 50% of

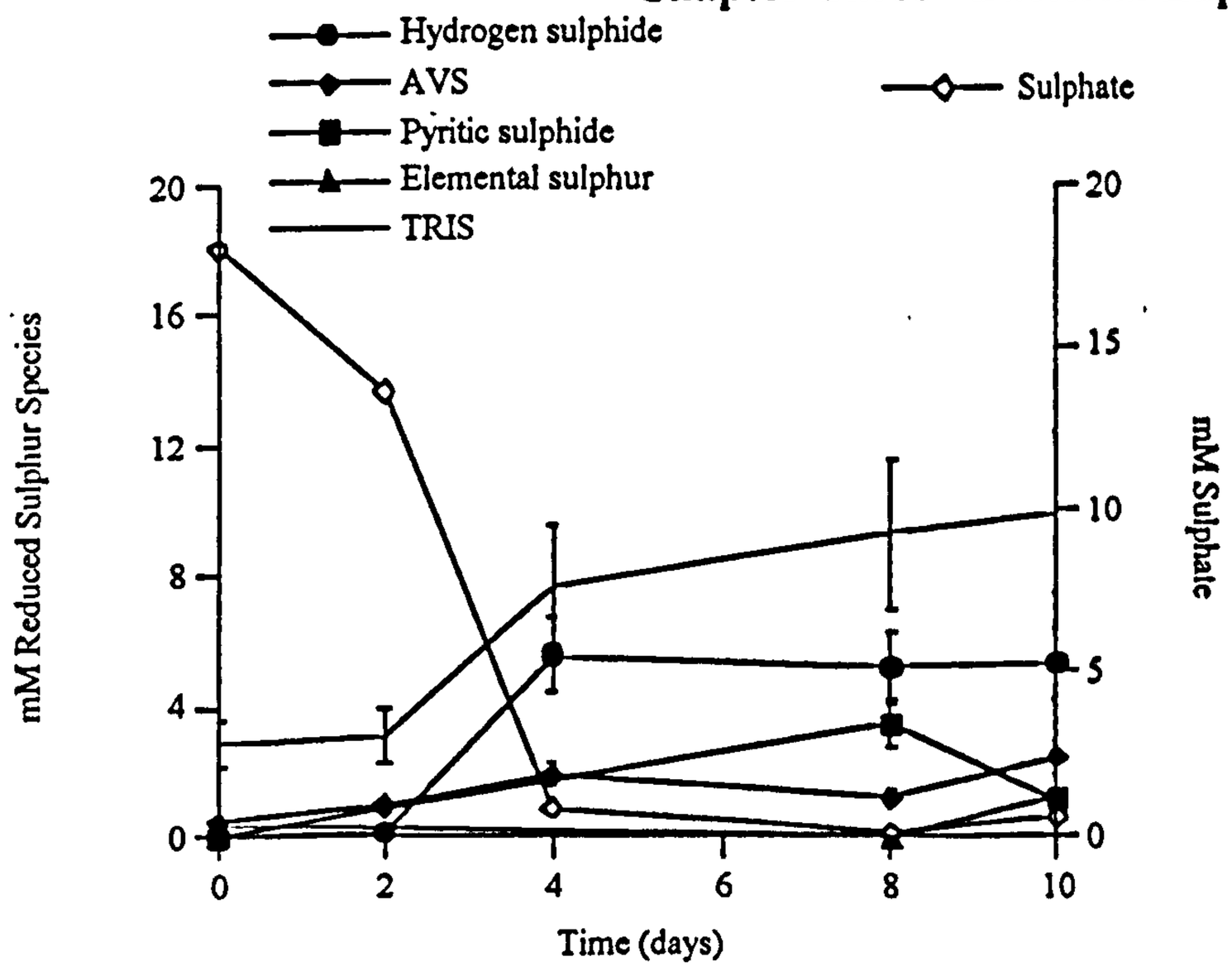

Figure 3.7 - Changes in the concentrations of sulphate and reduced sulphur species in an experiment containing lepidocrocite (an iron oxyhydroxide)

the TRIS pool in the lepidocrocite experiment rather than the 38% in the ferrous sulphate experiment.

In the experiments containing ferrous monosulphide (mackinawite), sulphate did not decrease in the same manner as in ferrous sulphate and ferric oxyhydroxide experiments (Figure 3.8). Between days 0 and 2, the initial drop in sulphate concentrations did occur but then the concentration maintained a constant level until day 8, when it decreased. The drop in sulphate concentrations at the beginning and end of the experiment indicated that bacterial sulphate reduction had occurred and the AODC bacterial numbers were in fact very similar to ferrous sulphate experiments. As the stabilization of sulphate concentration coincided with a decrease in the initially high TRIS concentration, it is likely that sulphate reduction was not slower in these experiments but that the rate of sulphate reduction was matched by the rate of sulphide oxidation (equation 3.2).

$$FeS\,(s) + 2O_2\,(aq) \rightarrow Fe^{2+}\,(aq) + SO_4^{2-}\,(aq) \qquad \text{Eq. 3.2}$$

As in the ferrous sulphate and lepidocrocite experiments, hydrogen sulphide was the dominant reduced sulphur phase; AVS, pyrite and elemental sulphur concentrations remained at lower concentrations throughout the experiment. Around day 10, acid-volatile sulphide concentrations then increased, so that the final concentrations of TRIS and acid-volatile sulphide were similar to those in the ferrous

sulphate experiments. Pyrite concentrations in this experiment remained very small (Figure 3.8).

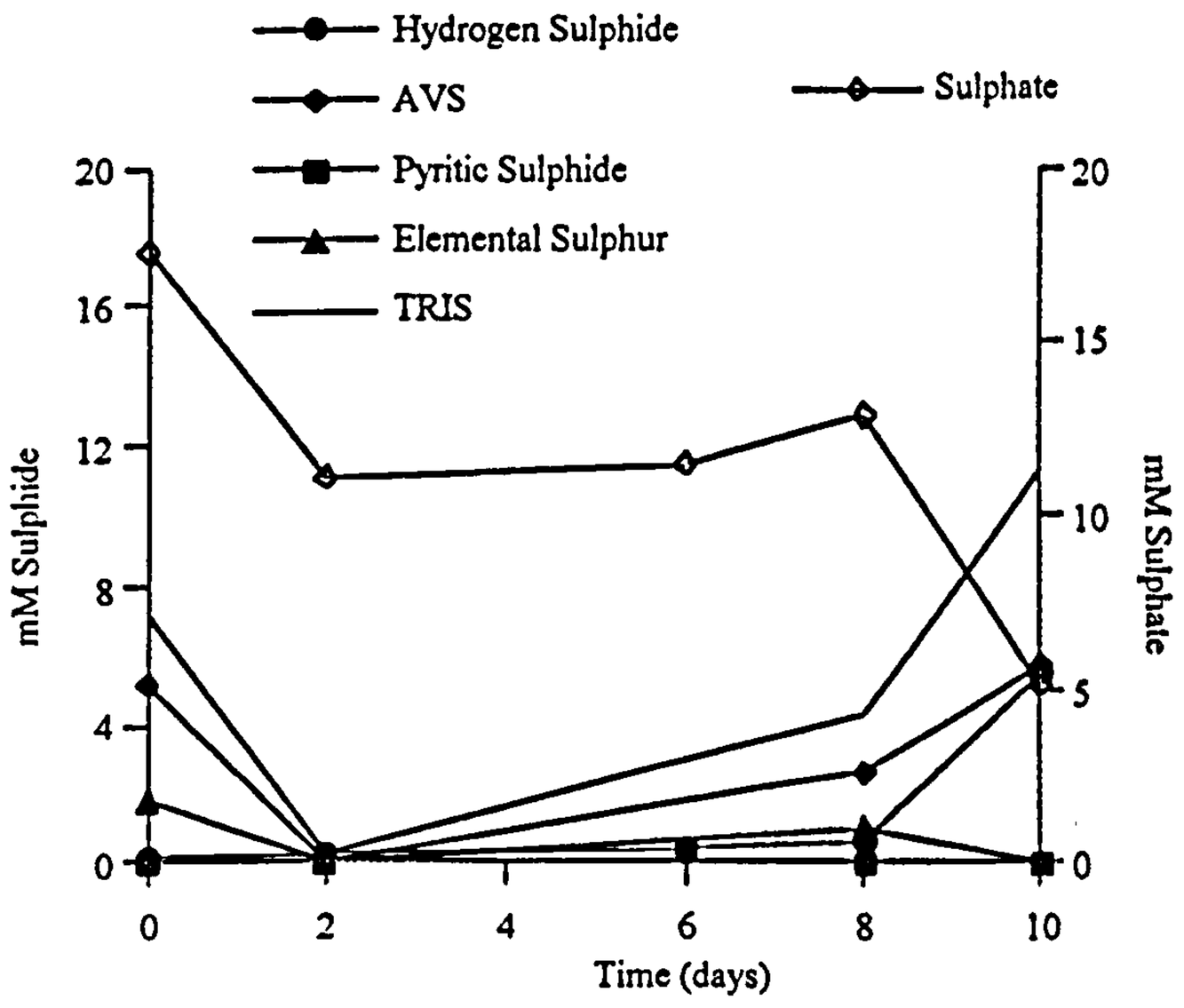

Figure 3.8 - Changes in the concentrations of sulphate and reduced sulphur species in an experiment containing mackinawite (an iron monosulphide).

3.C.2.2 - The effect on pH of changing the type of iron source. Changing the iron phase in an experiment affected the pH. For example, the experiments containing lepidocrocite did not show such a large decrease in the pH after the medium was dispensed into the vials. This was due to the interaction of two factors; firstly ferric iron ions are not as strong as electron acceptor as ferrous iron ions, and secondly, the low solubility of lepidocrocite meant that fewer iron ions were available to react with hydrogen sulphide. The pH of these experiments quickly increased and remained at around pH 6.9 for the majority of the experiment (Figure 3.9), unlike the experiments containing ferrous sulphate which remains at a lower pH for a longer period. The mackinawite experiments did not show an immediate decrease in pH for the first two days; after this time pH decreased to levels similar to the ferrous sulphate vials. This decrease was due to the oxidation of mackinawite to form ferrous ions and sulphate. Unlike the ferrous sulphate experiments, the pH of the mackinawite experiment did not increase greatly towards day 10 due to the high concentrations of hydrogen sulphide in the experiment.

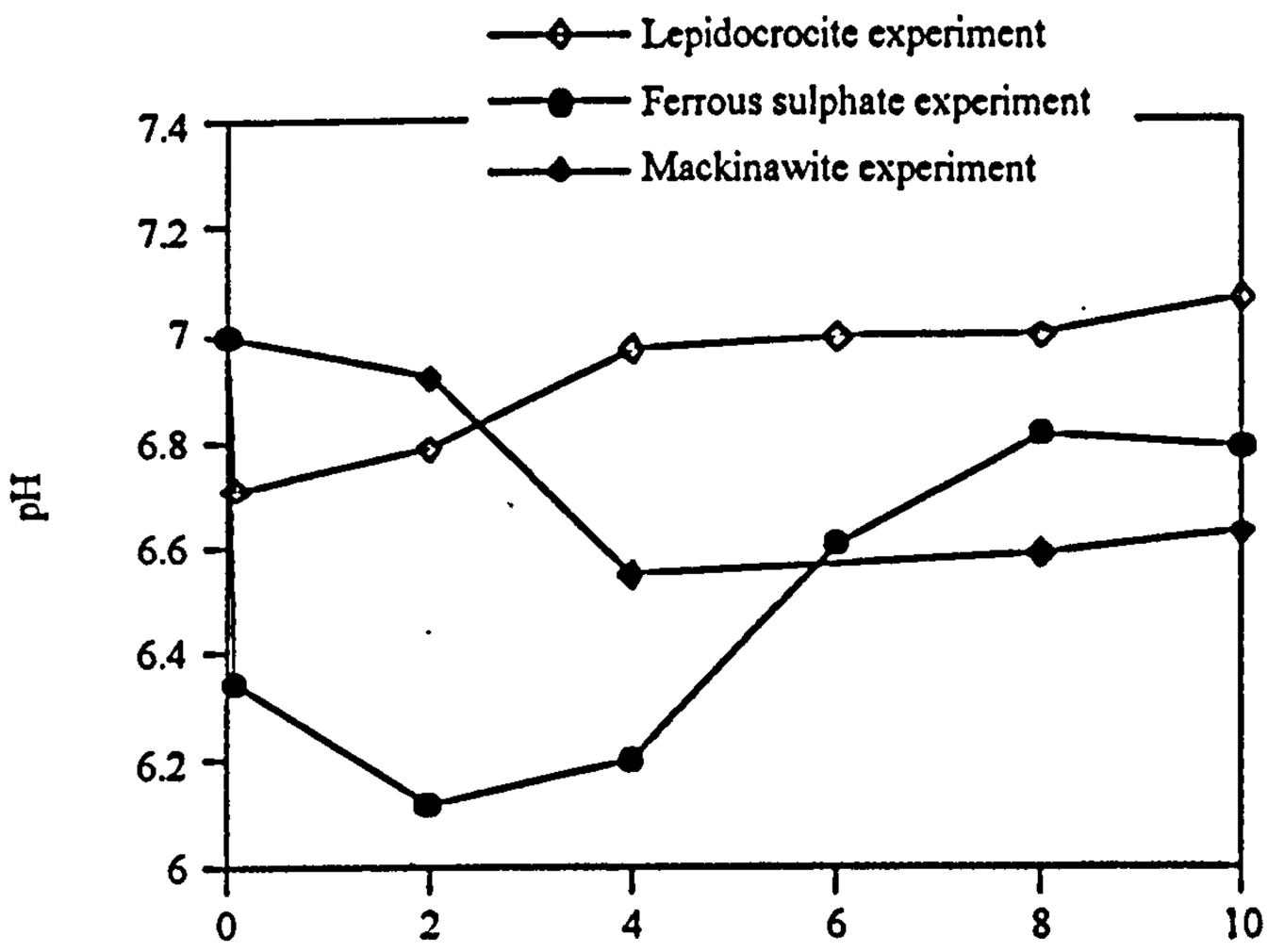

Figure 3.9 - pH changes in experiments containing ferrous sulphate, lepidocrocite and mackinawite

Changing the iron phase in the experiment from ferrous sulphate to lepidocrocite affected the amount of iron sulphide produced. Acid-volatile sulphide concentrations were higher in the ferrous sulphate experiment, while pyritic sulphide concentrations were higher in the lepidocrocite experiments. The experiment containing mackinawite had very low concentrations of pyritic sulphide throughout the experiment. By day 2, acid-volatile sulphide concentrations had dropped rapidly due to oxidation, but reached starting concentrations by day 10 due to rapid sulphate reduction.

The lepidocrocite experiment had higher sulphate reduction rates, due to higher bacterial numbers but this was not reflected in the TRIS concentrations, due to the oxidation of hydrogen sulphide to sulphate (Table VI). However, the proportion of the reduced sulphur species which was pyritic sulphide was greater in the lepidocrocite experiments. The lower pH in the ferrous sulphate and mackinawite experiments prevented the bacterial numbers from reaching such high levels but they produced more TRIS. This may have been due to the low pH keeping ferrous ions in solution and hence facilitating the reaction between iron and hydrogen sulphide, while inhibiting bacterial metabolism. In the lepidocrocite experiment, higher pH made conditions more suitable for sulphate reduction and the increased hydrogen sulphide flux faciliated the formation of pyrite despite oxidation by the iron compound.

Table VI - Comparison of sulphate reduction and TRIS production rates in mM day $^{-1}$ for ferrous sulphate, lepidocrocite and mackinawite experiments

	Sulphate Reduction Rates			TRIS Production Rates		
Time Period	$FeSO_4$ Expt	FeOOH Expt	FeS Expt	$FeSO_4$ Expt	FeOOH Expt	FeS Expt
Day 0-2	2.77	6.6	3.24	0.02	0.19	0
Day 2-4	5.77	8.73	0	5.87	4.51	
Day 4-8	0	0	0	3.48	1.61	0.68
Day 8-10	0.29	0.63	3.83	4.82	0.69	3.47

3.C.3 - The effect of changing the concentration of iron on the rate and production of pyrite and reduced sulphur species.

Iron concentrations in experiments containing either ferrous sulphate or lepidocrocite were increased from 5mM to 15mM to determine whether increasing iron concentrations enhanced the production of iron sulphides in a bacterial culture. However, due to the large pH drop caused by the ferrous ions (pH 5.08 after 2 hours) the experiment containing ferrous sulphate did not produce a large concentration of reduced sulphur.

Figure 3.10 - Distribution of sulphate and reduced sulphur species in an experiment containing 15mM lepidocrocite

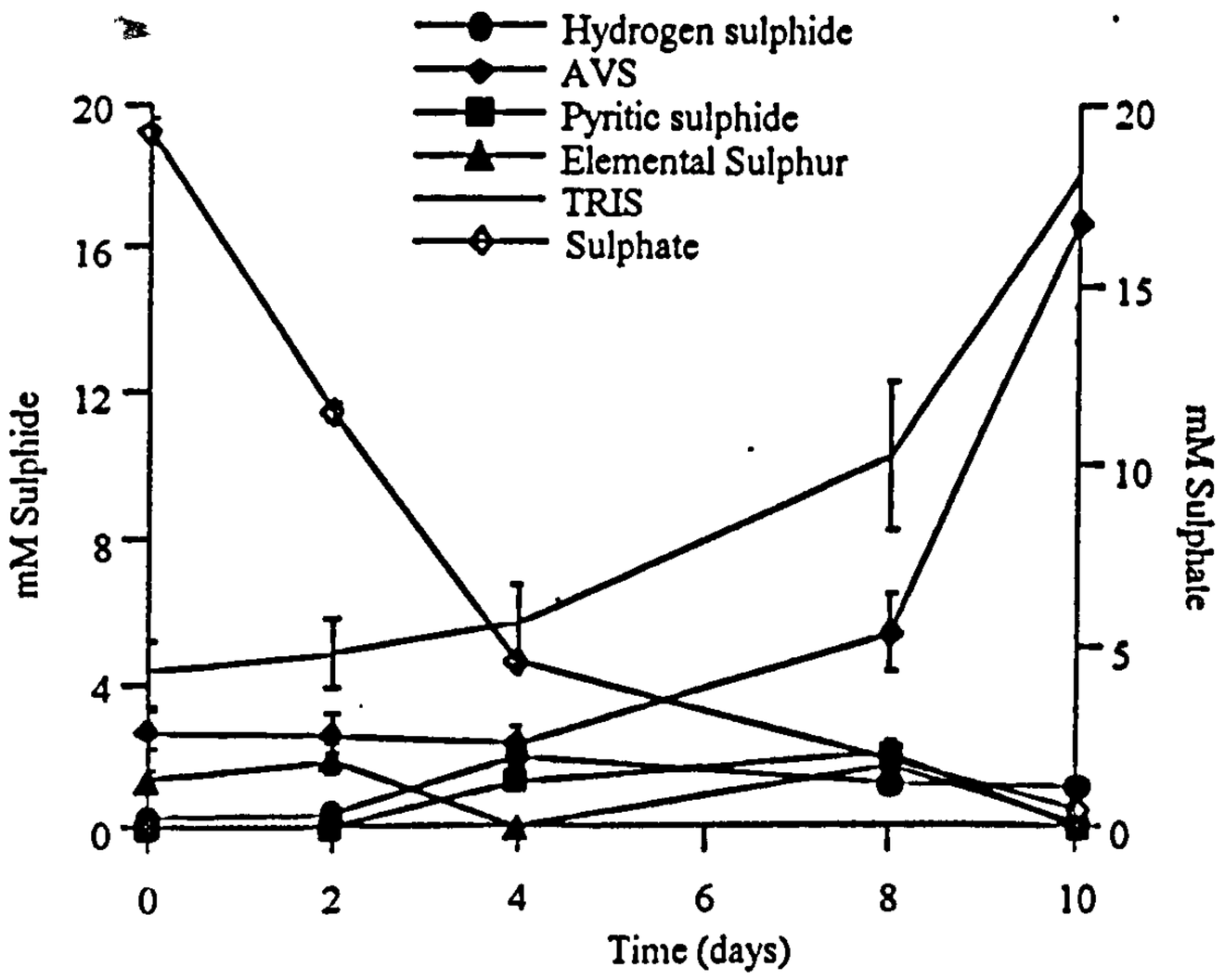

However, in the experiment containing lepidocrocite pH values remained higher (pH 5.95 to 7.04) and the bacteria were able to metabolise. This experiment produced large quantities of acid-volatile sulphides (Figure 3.10), when compared to the lepidocrocite experiments with 5mM iron (Figure 3.4). The experiment had lower sulphate reduction rates than the experiment containing 5mM iron and this contributed to the large iron to hydrogen sulphide ratio produced in the experiment.

3.C.4 - The effect of changing the concentration of bacterial substrate on the production of pyrite and other reduced sulphur species.

In order to determine the effect of lowering the bacterial substrate on the production of iron sulphides an experiment containing 2.8ml l^{-1}, rather than 17.8ml l^{-1}, of sodium lactate syrup was set up. This experiment produced lower concentrations of iron sulphides than the original experiment, as insufficient lactate limited sulphate reduction. By day 10, only 20% of the available sulphate was reduced unlike the 61% reduced in the original experiment; and sulphate reduction and TRIS production rates were much lower. Both the maximum sulphate reduction and TRIS production rates are now between days 4 and 8 rather than between days 2 and 4 (Table VII). In the experiment containing high lactate concentrations, sulphate concentrations increased slightly between days 4 and 8, due to oxidation, and was reduced by day 10 (Table VII). Oxidation increased in experiments where sulphate concentrations have become limiting and the concentrations of hydrogen sulphide decreased, allowing the effect of oxygen leaking in during sampling to be observed.

Table VII - Sulphate reduction and TRIS production rates in mM day^{-1} for experiments with high and low lactate concentrations

	Sulphate Reduction Rates		TRIS Production Rates	
Time Period	Low Lactate	High Lactate	Low Lactate	High Lactate
Day 0-2	0.44	2.77	0.17	0.02
Day 2-4	0.67	5.77	0.26	5.87
Day 4-8	2.46	0	0.66	3.48
Day 8-10	0.09	0.29	0.83	4.82

The concentrations of reduced sulphide produced in this experiment (Figure 3.11) was at least 50% less than the original experiment (Figure 3.2). The reduced sulphide species were dominated by pyritic sulphide by day 2, but this was replaced by acid-volatile sulphides over time. Again an increase in TRIS occurred between days 8 and 10 (3.9mM to 5.3mM) due to an increase in the concentration of elemental sulphur in the vial. This increase corresponded to a decrease in pyrite

concentrations. However, there is a discrepancy between the concentrations of TRIS produced and sulphate reduced, indicating that there was probably a large concentration of thiosulphate, and other intermediate sulphur compounds, present in this experiment.

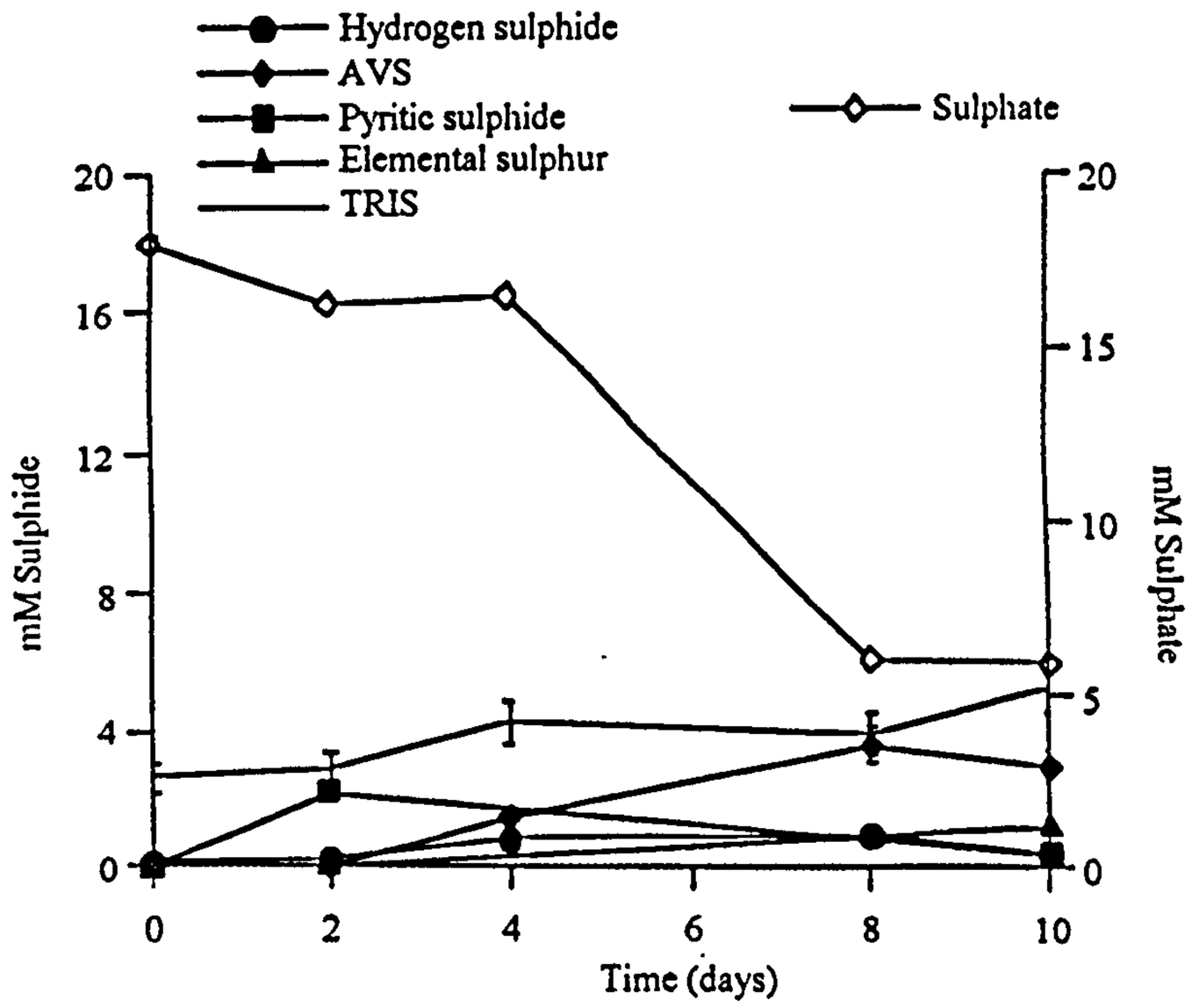

Figure 3.11 - Distribution of sulphate and reduced sulphide species in an experiments containing low lactate.

3.C.5 - The effect of changing sulphate concentrations on the production of pyrite and other reduced sulphur species.

In order to determine the effect of the consumption of sulphate during the burial of organic particles within a sediment column, an experiment was designed using slightly different sampling treatments and sulphate concentrations for the media which was used to top the vials. These were;

NT- the vials were not topped after sampling, so the headspace increased over time, (This models the top of the sediment where some interchange of oxygen occurs.) (Figure 3.12A)

SO- the vials were topped with the same media as they had been inoculated with, (This models an anoxic open system where both sulphate and organic matter are available and do not become limiting.)(Figure 3.12B)

LS- the media had half the normal amount of sulphate and was topped with the same media. (Some sulphate limitation occurs in this system.)(Figure 3.12C)

and TS- the vials were topped with a mineral salts solution (This models a system where both sulphate and organic matter become limiting).(Figure 3.12D)

Figure 3.12 - Distribution of sulphate and reduced sulphur species in experiments which had different sulphate concentrations throughout the experiment (A - an experiment which has not been topped after sampling, B - an experiment which has been topped with a sulphate medium after sampling, C - an experiment which has been made with a medium containing half the concentrations of sulphate and was topped after sampling and D - an experiment which was topped with a mineral salt solution after sampling)

A

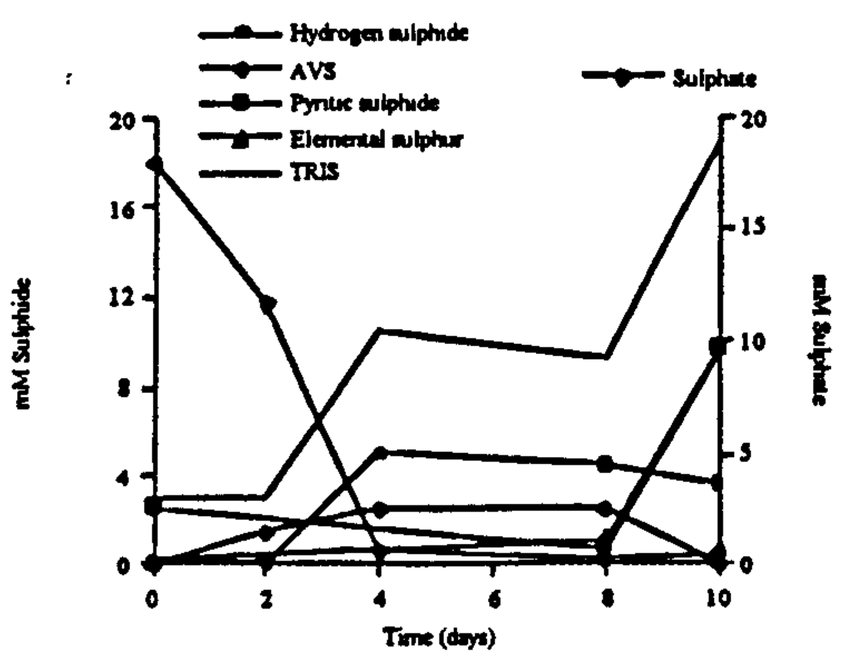

B

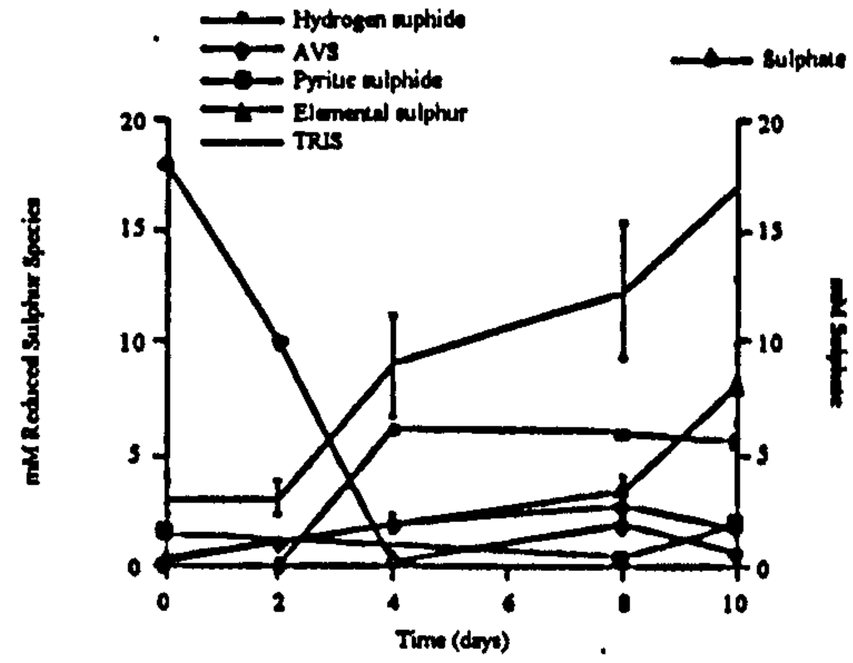

C

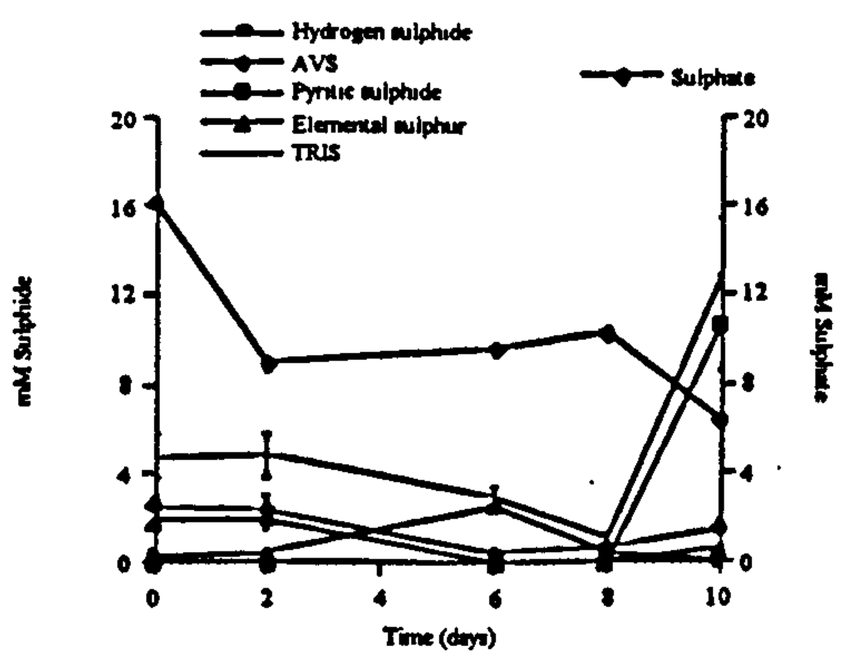

D

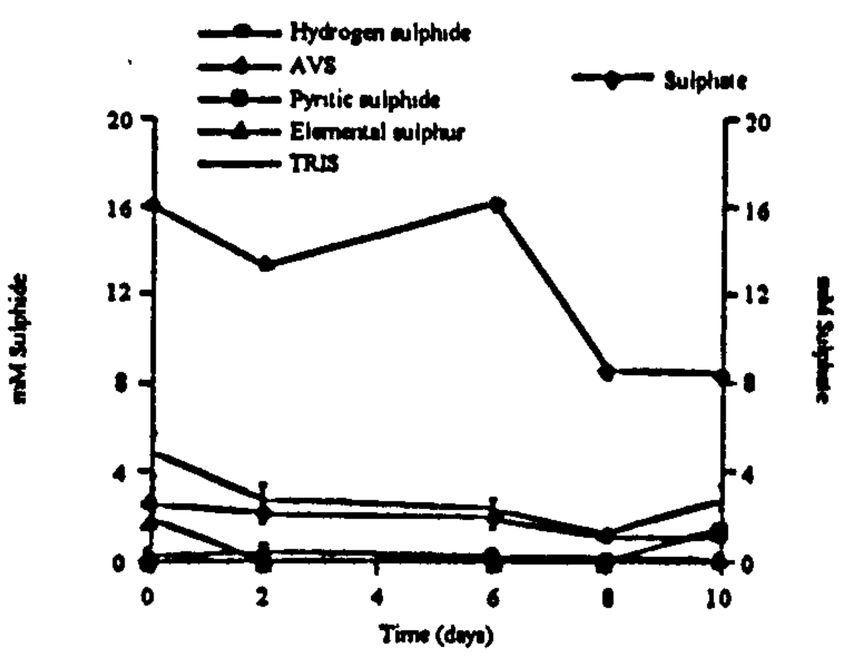

These experiments produce similar patterns in sulphate and TRIS concentrations. All four show an initial lag in the production of hydrogen sulphide between days 0 and 2, and an increase in the concentration of TRIS after day 8.

However, until day 10, reduced sulphur species in the experiments which were not topped or were topped with normal medium were dominated by hydrogen sulphide, while AVS and elemental sulphur dominated the low-sulphate-topped and salt-topped experiments. However, on day 10, all the experiments were dominated by pyritic sulphide or elemental sulphur. In the non-topped and topped experiments, this was due oxygen leaking into the experiments which reacted with hydrogen sulphide to form elemental sulphur. In the low-sulphate and salts-topped experiments sulphate reduction was limited and the reduced sulphur species were dominated by pyritic sulphide. Thiosulphate, or another intermediate sulphur compound, was also generated by oxidation of hydrogen sulphide in these experiments. The amount of oxygen leaking into the experiments increased when the headspace increased or the rate of sulphate reduction decreased. When this occurred in the experiments, pyrite concentrations increased.

3.C.6 - The effect of changing the medium type on the production of pyrite and other reduced sulphur species

In order to prevent the pH from changing during incubation a medium containing additional phosphate buffer was designed (appendix 6), which prevented the pH falling below 6. This medium showed a different behaviour to that of normal Postgates medium. 1.2mM pyrite was produced in buffered media; this was less than in unbuffered media (2.9mM). However, lactate-rich media still produced more pyrite than normal media. Furthermore, the concentration of TRIS was slightly lower in each group of experiments than in the corresponding unbuffered group. It is unlikely, therefore, that buffering the media enhanced pyrite production, but that it merely reduced the physiological stress of low pH on the bacteria (Pfennig, 1984).

Experiments were also run using a different pH buffering system to Postgates medium. Widdels medium (appendix 6) utilises a buffer using hydrogen sulphide and sodium bicarbonate, while Postgates utilises a system using ferrous sulphate and ascorbic acid. The experiments using Widdels growth medium (Figure 3.13) produced similar concentrations of TRIS as the experiments using lactate rich Postgates medium (Figure 3.2). However, the ratio of pyritic sulphide to TRIS was consistently larger in this experiment (0.423 compared to 0.329), and the ratio of acid-volatile sulphide to pyritic sulphide was smaller (0.291 compared to 0.745).

Table VIII - A comparison of the sulphate reduction and TRIS production rates for experiments using Postgates and Widdels media

	Sulphate Reduction Rates		TRIS Production Rates	
Time Period	Postgates Expt	Widdels Expt	Postgates Expt	Widdels Expt
Day 0-2	2.77	0.48	0.02	1.37
Day 2-6	5.77	0.51	5.87	-0.07
Day 6-8	-0.38	3.18	3.48	1.07
Day 8-10	0.29	0.51	4.82	0.56

Sulphate reduction and TRIS production rates are lower than those in Postgates experiment (Table VIII), meaning that the Widdels medium produced an environment which was slightly more suited to producing pyrite. This may have been due to the higher pH maintained throughout the experiment; the lowest value is 6.92 on day 8, or to the hydrogen sulphide buffering system, which may facilitate iron sulphide precipitation by keeping the partial pressure of hydrogen sulphide in the vial high.

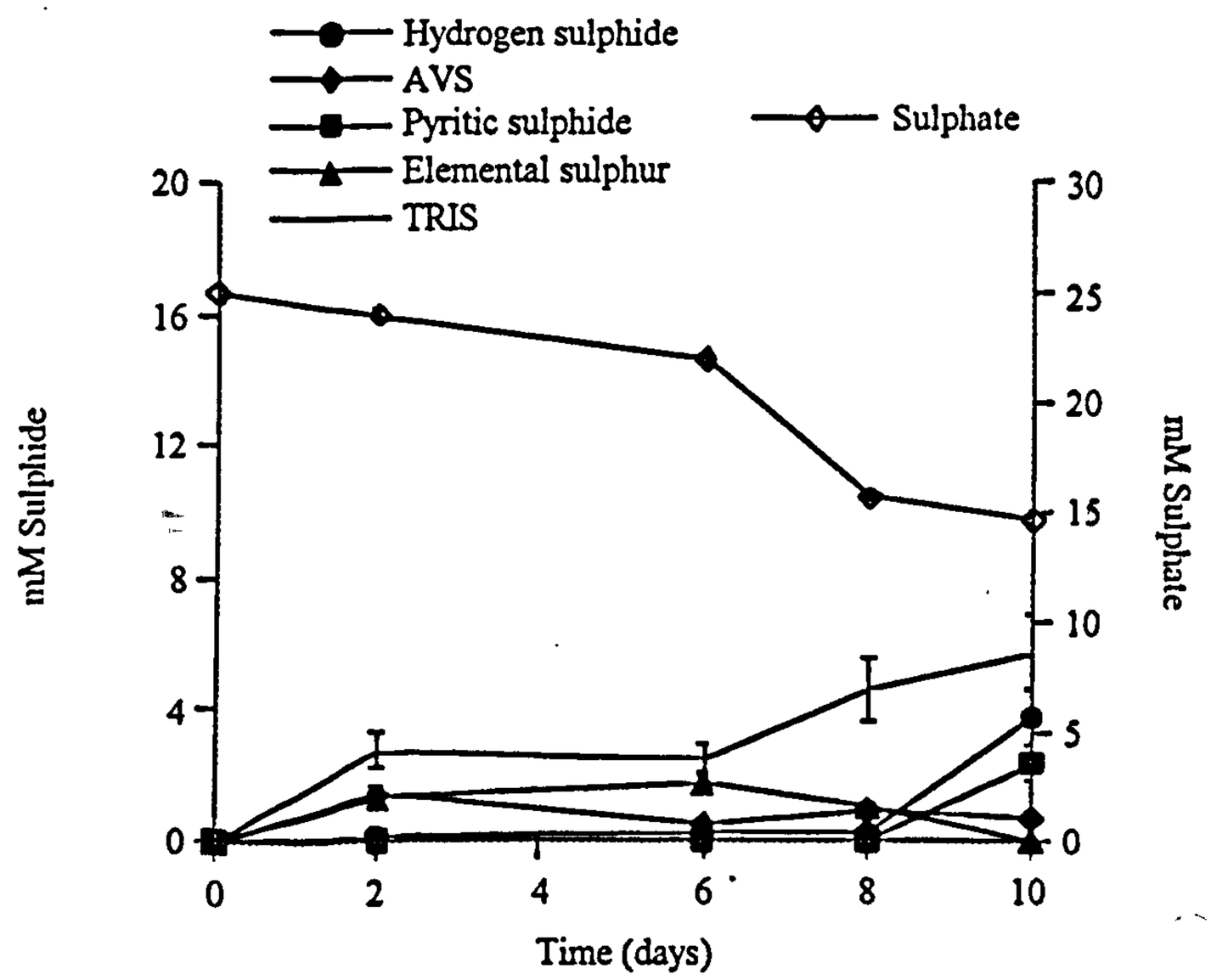

Figure 3.13 - The concentrations of sulphate and reduced sulphur species in an experiment utilising Widdels medium

3.C.7 - The effect of changing substrate and bacterial strain on the production of pyrite and other reduced sulphur species

Desulfobacter lactus is another strain of sulphate-reducing bacteria, which utilises acetate as a substrate which is reduced to carbon dioxide. Every mole of sulphate reduced requires one mole of acetate, but acetate is reduced at a much slower rate than that at which *Desulfovibrio desulfuricans* metabolises lactate and reduces sulphate. This experiment was run to see if slower sulphide production would facilitate better pyrite production, and whether the different substrate would affect pyrite production.

After 10 days, pyrite production in the *Desulfobacter* experiments only reached one quarter of the concentration of that in the experiments using Widdels medium and *Desulfovibrio*, despite the vials having the same concentration of substrate and twice the concentration of acetate. The average concentration of pyrite in *Desulfobacter* vials, after this incubation time, was 0.3746 µmoles per litre. The ratio of acid-volatile sulphide to pyritic sulphide (AVS/PS) was greater than that of the experiments using Widdels medium and *Desulfovibrio* (0.549 versus 0.173) indicating that the sulphate reduction rates did not facilitate the formation of pyrite.

Material in these vials did not form organic films as seen in *Desulfovibrio desulfuricans* vials. Instead, the sulphides formed as discrete particles, which may be due to either the change in substrate or organism. Conversely, *Desulfobacter lactus* may not produce as much extra-cellular polysaccharides as *Desulfovibrio desulfuricans.*

3.C.8 - The effect of sealing the experimental vials on the production of pyrite and other reduced sulphur species

The diffusion of oxygen into the experiments sealed with neoprene septa obviously affected the reduced sulphur species produced. The reduced sulphur species in the neoprene sealed experiments tended to be dominated by elemental sulphur and hydrogen sulphide, and have low iron sulphide concentrations. Elemental sulphur concentrations increase between days 8 and 10, due to oxygen leaking into the experiment when the septa was pierced during sampling. To determine whether this oxygen affected the reduced sulphur pool the grey neoprene septa sealing the vials were replaced with thicker buytl septa pierced by a large bore needle. Samples were taken through a three-way tap attached to the needle. Experiments were run

using lactate-rich and low lactate Postgates media, so that the effect of a closed system on different sulphate reduction rate could be observed.

Figure 3.14 - Distribution of sulphate and reduced sulphide species in : A - an experiment containing lactate-rich Postgates medium and sealed with a butyl septa, B - an experiment containing lactate-rich Postgates medium and sealed with a neoprene septa, C an experiment containing low lactate Postgates medium and sealed with a butyl septa, and D - an experiment containing low lactate Postgates medium and sealed with a neoprene septa

A

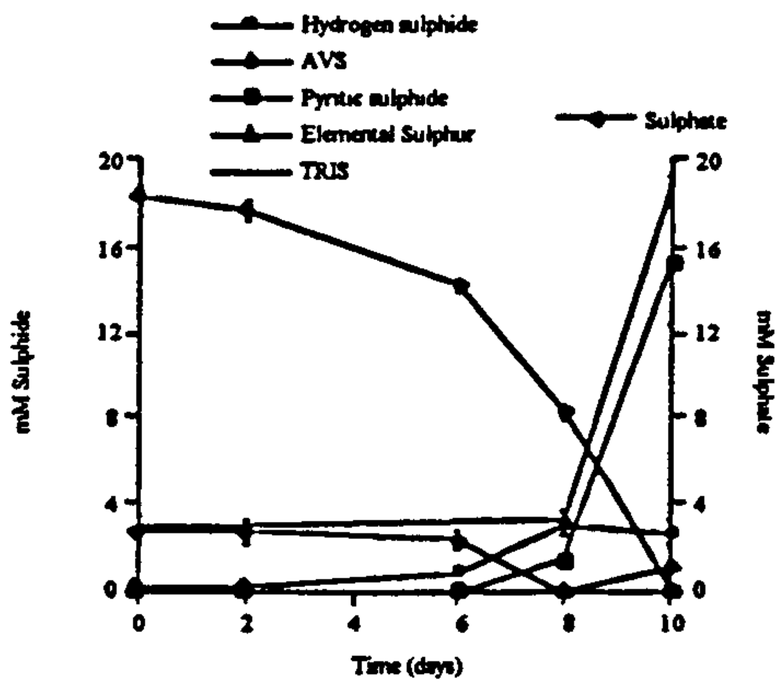

B

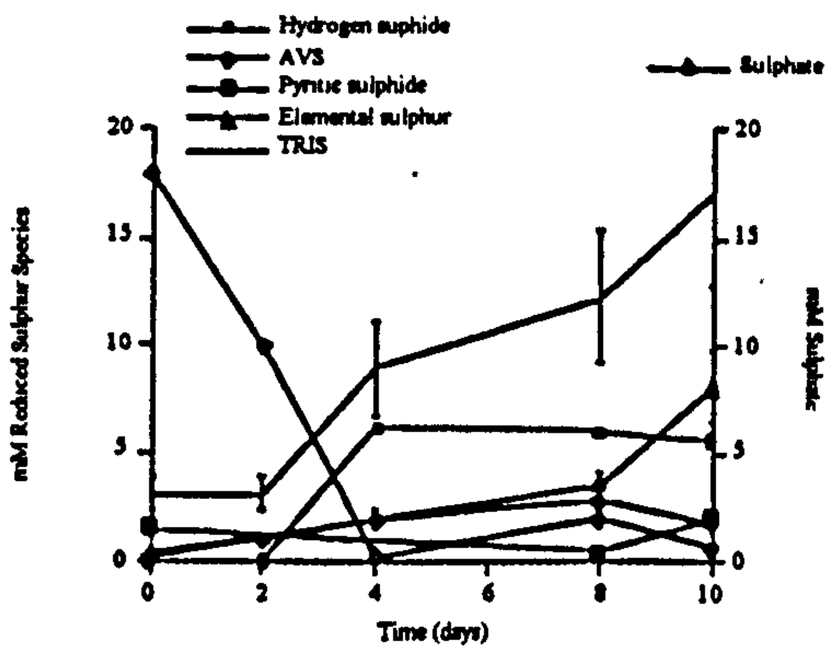

C

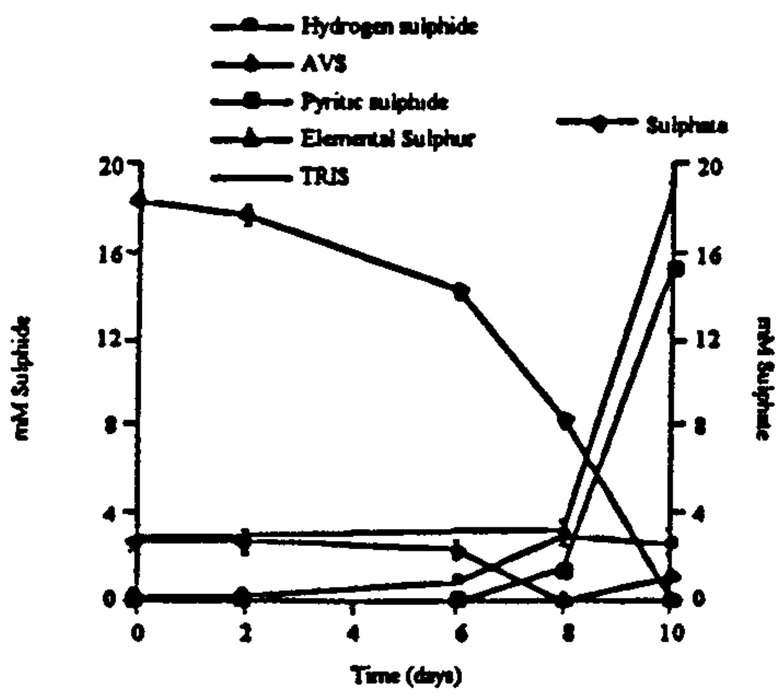

D

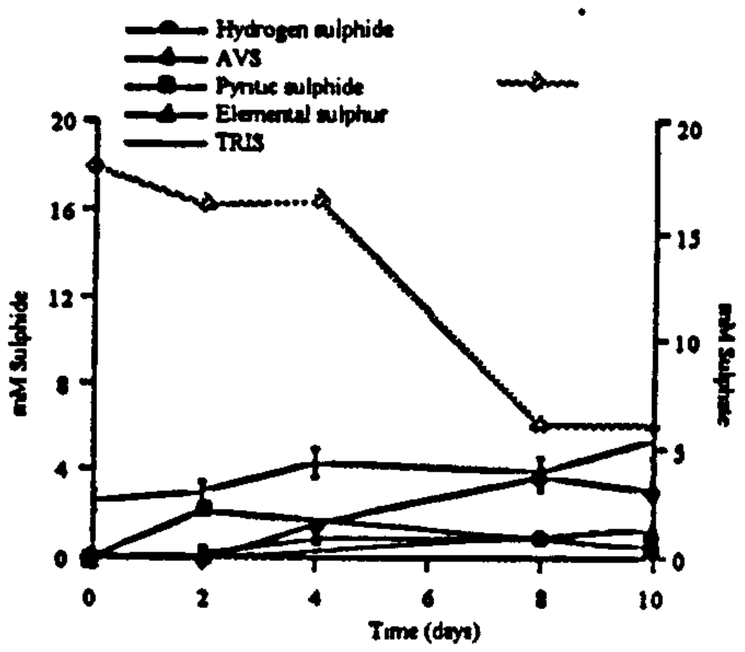

The experiment containing lactate-rich medium and sealed with a butyl septa (Figure 3.14A) produced a similar concentration of TRIS to the experiment sealed with a neophrene septa (Figure 3.14B). However, the pattern of reduced sulphur species produced differed between the experiments. In the experiment sealed with the butyl septa acid-volatile sulphide was the dominant reduced sulphur species until day 10, whereas in the experiment sealed with the neoprene septa hydrogen sulphide was

the dominant species. At the end of the incubation period, pyritic sulphide was the dominant reduced species in the experiment sealed with the butyl septa, while in the experiment sealed with a neoprene septa the dominant reduced sulphur species was elemental sulphur. The ratios of AVS/TRIS and PS/TRIS indicated that the iron sulphide species formed a larger proportion of reduced sulphur pool in the experiment sealed with a butyl septa than in the experiment sealed with a neophrene septa. The rate of sulphate reduction was similar over the whole incubation time in both experiments (Table IX).

Table IX- Sulphate reduction rates for butyl and neoprene sealed vials

	Lactate-rich Postgates		Lactate-poor Postgates	
Time Period	Butyl Septa	Neoprene Septa	Butyl Septa	Neoprene Septa
Day 0-2	0.32	2.77	0.16	0.44
Day 2-6	0.87	5.77	0.60	0.67
Day 6-8	2.99	0	3.01	2.46
Day 8-10	4.05	0.29	7.97	0.09

The experiments containing low lactate Postgates produced similar amounts of TRIS, however like the lactate-rich experiments iron sulphides formed a larger proportion of the reduced sulphur pool in the experiment sealed with a butyl septa (Figure 3.14C). Acid-volatile sulphide concentrations were greater than pyritic sulphide concentrations throughout the experiment, due to the smaller iron:hydrogen sulphide ratio produced by lowering the concentration of bacterial substrate in these experiments. The sulphate reduction rate for the experiment sealed with a butyl septa were greater than those in the experiment sealed with a neoprene septa as the buytl septa meant that there was no oxidation between days 8 and 10 (Table IX).

3.C.9 - Pyrite formation without bacterial metabolism

A series of experiments were run using 5mM ferrous sulphate and several different types of media; an inorganic solution, lactate-rich Postgates medium, buffered lactate rich Postgates medium, low lactate Postgates medium and buffered low lactate Postgates medium (appendix 4). These were set using a combation of aged and new media and precipitates from bacteria cultures which have been 'killed' using formalin or high temperatures and pressures. The experiments were then injected with 6mM sodium sulphide solution, and incubated at 25°C. 6mM was chosen to be the concentration of sulphide because it will not inhibit the metabolism of sulphate-reducing bacteria. Changes in the concentrations of reduced sulphur species are shown in Table X.

Table X - Concentrations of Hydrogen sulphide (H2S), Acid-volatile sulphides (AVS), Pyritic sulphide (PS), Elemental Sulphur (ES) and the total reduced sulphur compounds (TRIS) in experiments injected with sodium sulphide solution.

Autoclaved	H2S	AVS	PS	ES	TRIS
Inorganic solution					
Sodium Chloride	0.00	0.00	1.29	0.00	1.29
New medium					
Lactate-poor Postgates	0.05	3.66	0.00	1.60	5.31
Lactate-rich Postgates	0.00	6.79	0.00	0.51	7.30
Buffered Lactate-poor Postgates	0.00	0.00	0.00	0.00	0.00
Buffered Lactate-rich Postgates	0.00	0.00	0.00	0.23	0.23
New medium with live bacteria					
Lactate-poor Postgates	1.06	6.36	0.67	0.78	8.87
Lactate-rich Postgates	0.00	0.00	0.00	1.41	1.41
Buffered Lactate-poor Postgates	0.19	10.15	5.82	0.00	16.17
Buffered Lactate-rich Postgates	1.70	13.13	0.00	0.00	14.84
New medium with precipitates					
Lactate-poor Postgates	0.00	0.00	0.00	0.00	0.00
Lactate-rich Postgates	0.00	0.00	0.00	0.00	0.00
Buffered Lactate-poor Postgates	0.00	1.00	0.14	0.00	1.14
Buffered Lactate-rich Postgates	0.00	0.00	0.00	0.00	0.00
Old medium with new bacteria					
Lactate-poor Postgates	0.00	0.00	0.00	0.00	0.00
Lactate-rich Postgates	0.45	0.00	0.00	0.22	0.67
Buffered Lactate-poor Postgates	0.00	0.00	0.00	0.00	0.00
Buffered Lactate-rich Postgates	0.00	0.00	2.52	0.47	2.99
Old medium with precipitates					
Lactate-poor Postgates	0.00	2.25	7.56	0.03	9.84
Lactate-rich Postgates	0.92	0.78	0.00	0.36	2.06
Buffered Lactate-poor Postgates	0.00	0.59	0.00	0.00	0.59
Buffered Lactate-rich Postgates	0.47	0.75	0.00	0.00	1.23

Formaline	H2S	AVS	PS	ES	TRIS
Old medium with live bacteria					
Lactate-poor Postgates	0.04	0.00	0.00	0.00	0.04
Lactate-rich Postgates	0.04	0.00	0.00	0.29	0.33
Buffered Lactate-poor Postgates	0.08	0.00	0.00	0.00	0.08
Buffered Lactate-rich Postgates	0.07	0.00	0.00	0.00	0.07
Old medium with live bacteria and precipiates					
Lactate-poor Postgates	0.08	0.00	0.00	0.00	0.08
Lactate-rich Postgates	0.04	0.00	0.00	0.88	0.92
Buffered Lactate-poor Postgates	0.08	0.00	0.00	0.00	0.08
Buffered Lactate-rich Postgates	0.07	0.00	0.00	0.00	0.07
Old medium with precipitates					
Lactate-poor Postgates	0.04	0.00	0.00	1.08	1.12
Lactate-rich Postgates	0.06	0.00	0.00	0.00	0.06
Buffered Lactate-poor Postgates	0.04	0.00	0.00	0.00	0.04
Buffered Lactate-rich Postgates	0.07	0.00	0.00	0.00	0.07

Pyrite formation occurred in one quarter of new media with precipitates experiments, although the concentration of iron sulphides produced is small when compared to the concentrations produced in the control experiment (new medium with live bacteria). Pyrite did not occur in the new medium, which was dominated by AVS in experiments where oxidation did not occur. Pyrite also formed in the sodium chloride solution, where the pH was around 7.8 indicating that the reation to form pyrite could proceed without bacteria if oxidation does not occur. The old medium with new bacteria produced pyrite, although the concentration is half that produced in the new medium with live bacteria. The old medium with precipitates produced the highest concentration of pyrite, probably due to the availablity of precursor compounds, such as AVS. This produced more pyrite than the new medium with precipitates experiment because the precipitates were still in equilibrium with the medium, and did not disolve. Only 28% of the experiment produced any pyrite; this is lower than the percentage of experiments producing pyrite in the other experiments (81%). Furthermore, the bacteria in those experiments preferred the unbuffered, lactate-rich medium, but the formation of pyrite does not occur in that medium in these experiments. Pyrite formation only occurred if low redox levels were maintained throughout these experiments, and was enhanced by the presence of precuror compounds in the spent medium and precipitates. If oxidation occurs in the experiment pyrite does not form, and these cases show that bacteria are essential to maintain sufficiently high sulphide concentrations, under higher redox conditions.

The experiments where bacteria were killed using formalin differ from the other experiments, as there was no increase in the concentration of acid-volatile sulphide or pyrite. This was due to formalin inhibiting the reaction of sulphide with iron. These results indicate that bacteria are required in these experiments in order to maintain the concentration of sulphide and the redox throughout the duration of the experiment. The presence of organic compounds and biofilm seem to prevent the formation of pyrite.

3.C.10 - The effect of combinations of variables on the production of pyrite and other reduced sulphur species in bacterial cultures

Many groups of experiments were run using combinations of the variables described in the previous section in order to determine their effect on pyrite production. Although each experiment was prepared in such a way that the environmental conditions were suitable for pyrite formation, 21 out 110 cases did not

contain any pyrite, although they did contain acid-volatile sulphide and other reduced sulphur species. The most pyritic sulphide was produced in an experiment containing mackinawite and lactate-rich Postgates medium, and sealed using butyl rubber septa. This experiment produced 18.34mM of pyritic sulphide, unlike the equivalent experiment with neophrene septa which produced no pyritic sulphide, and shows the importance of oxygen in inhibiting the formation of pyrite, despite the requirements for an oxidising agent such as elemental sulphur in the reaction.

3.D - Discussion

In order for sulphate-reducing bacteria to metabolise they require an anoxic environment at a neutral pH. Any changes to these conditions alter the rate of sulphate reduction and the rate of TRIS production. All the experiments were prepared to be anaerobic and at neutral pH at the beginning of the experiment, therefore the differences between the amount of pyrite produced and the proportion of the reduced sulphur pool pyrite represents are dependant upon the concentrations of sulphate, organic matter and iron, and the potential for oxidation. In an anaerobic environment containing an actively growing population of sulphate-reducing bacteria the variables which have the greatest effect on the amount of pyrite produced in the experiment are those defined by Berner (1967;1970;1980) as controlling pyrite formation in anoxic sediments. These are the concentrations of sulphate, organic matter and reactive iron. Altering the concentration of bacterial substrate appears to have the greatest effect on the amount of TRIS produced, as in its absence no sulphate reduction occurs. Sulphate concentrations have a similar effect, but the experiments in which sulphate concentrations were altered became substrate limiting before they became sulphate limiting. These two factors can be considered to work in parallel, with the one with the lowest concentration being the limiting factor in the sulphate reduction.

Although the concentrations of sulphate and bacterial substrate control the amount of sulphate reduction that occurs, and therefore the concentrations of TRIS produced, iron is essential for the production of iron sulphides. Iron concentrations do not affect the amount of TRIS produced unless the concentration of aqueous ferrous iron ions is such that sulphate reduction is inhibited by low pH. However, iron concentrations control the type of iron sulphide produced. When iron concentrations are high, in comparison with the concentrations of sulphate and bacterial substrates, then acid-volatile sulphides will be the dominant iron sulphide phase because the ratio of iron to hydrogen sulphide is high. Conversely, if the ratio

of iron to hydrogen sulphide is low, pyrite is the dominant iron sulphide phase. Iron and hydrogen sulphide concentrations produce good correlations with acid-volatile sulphide concentrations but not with pyritic sulphide concentrations. This is due to the reaction which forms pyrite from precursor compounds.

The type of iron and the effect of oxygen on the production of pyrite are related to each other. When ferrous sulphate was used in the experiment pyrite concentrations were low compared to hydrogen sulphide and elemental sulphur concentrations, and acid-volatile sulphide was slightly more abundant than pyritic sulphide. In comparison the experiment containing lepidocrocite produced less reduced sulphur compounds (TRIS), but a larger proportion was pyritic sulphide. Experiments containing lepidocrocite produce patterns of pyrite production which are more similar to those observed in sediments due to the presence of an oxide in the system. The group of experiments containing mackinawite produced the most pyritic sulphide, due to the presence of pyrite precursors, and because hydrogen sulphide produced by sulphate-reduction was not consumed to form AVS, but was utilised in the reaction to form pyrite (Drobner *et al.*, 1990; Rickard, 1997). The concentrations of acid-volatile sulphides in these experiments was generally low and the ratios of AVS/TRIS and AVS/PS are small. The highest concentrations of pyritic sulphides were produced in experiments using butyl rubber septa rather than neoprene septa because the thicker butyl bungs and different sampling system prevented oxygen leaking into the experiments and oxidising the reduced sulphur species. These experiments had higher PS/T ratios and lower AVS/PS ratios, indicating that a higher proportion of TRIS was pyritic sulphide and that the concentration of pyritic sulphide was greater than that of acid-volatile sulphide. From the trends in sediments and those observed in these experiments it is obvious that pyrite can be produced in environments with varying degrees of anoxia but that the majority of pyrite forms only when the concentration of oxygen or the oxidising potential of the sediment is very low, despite the requirement for an oxidising agent in the reaction.

The reaction mechanisms which form pyrite from acid-volatile sulphide precursors also vary, depending on the iron type and the potential for oxygen to diffuse into the vial. Several mechanisms for the reaction to form pyrite from precursor compounds are suggested (see Chapter 1)(shown in equations 3.3 to 3.7).

$$Fe^{2+}(aq) + H_2S(aq) \rightarrow FeS(s) + H_2(g)$$

$$H_2S(aq) + O^{2-}(aq) \rightarrow H_20(g) + S^{\bullet}(s)$$

$$FeS(s) + S^{\bullet}(s) \rightarrow FeS_2(s) \qquad \text{(Berner, 1984)}$$

$$FeS(s) + H_2S(g) \rightarrow FeS_2(s) + H_2(g)$$ (Rickard & Luther, 1996)

(Eq. 3.3 - 3.7)

The experiments containing ferrous sulphate and mackinawite do not contain an oxidising agent to form elemental sulphur, and it is therefore likely that the reaction mechanism proceeds via hydrogen sulphide oxidation, despite the relatively high pH of the experiments. However, in the experiments sealed with neoprene septa, oxygen diffuses into the reaction vessel, so that the FeS transformation via hydrogen sulphide is likely to have been replaced or is coexisting with transformation via elemental sulphur or polysulphide (which are more likely at neutral pH). The hydrogen sulphide reaction is probably the dominant mechanism in the experiments sealed with the thicker butyl septa as very little oxygen entered these reaction vessels. The rate of reaction for hydrogen sulphide (Rickard, Schoonen & Luther, 1995) is significantly greater than that of the reactions utilising elemental sulphur and polysulphide, and this will explain why the butyl septa sealed experiments produced a significantly higher pyritic sulphide concentrations, in a shorter time period, than the equivalent experiments sealed with neoprene septa. The lepidocrocite vials contained an oxidising agent in the form of the iron compound. Thus the reaction to form pyritic sulphide from acid-volatile precursor compounds is likely to proceed via the elemental sulphur or polysulphide pathways. These reactions are slower rhan the hydrogen sulphide mechanisms and hence less pyrite is produced in the buytl septa sealed experiments, than in the equivalent ferrous sulphate or mackinawite experiments. However, the availablity of an oxidising agent in the neutral pH means that pyrite represents a larger proportion of the reduced sulphur pool.

3.E - Conclusions

Cultures of sulphate-reducing bacteria produce pyrite rapidly, within 4 days, in a suitably anaerobic environment with a neutral pH. The sulphate-reducing bacteria metabolise sulphate and organic compounds to produce hydrogen sulphide, which reacts with oxidising agents to form a variety of reduced sulphur species, and with iron compounds to form iron sulphides. The controlling variables on the production of iron sulphides, and most importantly pyrite, can therefore be defined as the concentrations of available iron, sulphate and metabolisable organic matter (Berner, 1969; and subsequent workers). Although the precipitation of iron sulphides is controlled by the concentrations of these variables there is no correlation between them and the concentration of pyrite produced in a given environment. Furthermore,

the concentration of pyrite does not correlate with the concentrations of precursor compounds, or hydrogen sulphide. The formation of pyrite did however require a constant flux of hydrogen sulphide, to prevent oxidation and provide the oxidising agent for the reaction to form pyrite from acid-volatile sulphide precursors. This flux is provided by the sulphate-reducing bacteria, whose metabolic activities are controlled by the concentrations of sulphate and organic matter. The bacteria also provide a nucleation site for the iron sulphide precipitation, in their extra-cellular polysaccharides, which concentrates iron sulphides to form a mixed biofilm. These biofilms are similar to those observed a variety of sediementary environments (Bertolin *et al.*, 1993; Konhauser *et al.*, 1993) and on bivalve shells (Clark & Lutz, 1980).

The type of iron and the potential for oxygen to enter the reaction vessel affects the aount of pyrite formed and the proportion of TRIS representd by pyritic sulphide. This is due to the different reaction mechanisms operating under different environment conditions. When ferrous iron ions are present, pyrite is formed from acid-volatile sulphide precursors via a reaction which utilises hydrogen sulphide as the oxidising agent. This reaction is faster than the mechanisms using elemental sulphur or polysulphide as the oxidising agent (Rickard, Luther & Schoonen, 1995; Rickard, 1997), so that pyrite is formed more rapidly. By contrast, when oxygen enters the environment, less pyrite is produced and the neutral pH and low abundance of oxidising agents forms a smaller proportion of the redced sulphur pool. Ferric iron compounds oxidise hydrogen sulphide so that the reaction proceeds via the elemental sulphur or polysulphide mechanisms, which are slower than the hydrogen sulphide mechanism, but the availablity of an oxidising agent means that pyrite forms a greater proportion of the reduced sulphur pool.

Chapter Four
Physical controls upon Pyritization

4.A - Introduction

Pyritization in sediments is controlled by a complex interplay of the activity of bacteria and the chemistry of detrital material input into the sediment. These in turn are controlled by the chemical requirements of the pyritization reaction and the rate of consumption of the initial reagents, the distribution of which is modified by the physical characteristics of the sediment. The physical characteristics of a sediment affect the distribution and diffusion of sulphate, bacterial growth substrates, iron compounds and the movement of bacteria. The argillaceous sediments in which the majority of pyrite formation occurs have a low permeability that limits diffusion of organic compounds (Sansone, 1986) and inorganic ions, facilitating the formation of micro-environments. The development of micro-environments therefore plays an important role in the pyritization of organic material. The chemistry of micro-environments is affected by four factors: i) the rate of sedimentation and the development of anoxia, ii) the concentration of organic matter input into the sedimentary system, iii) the reactivity of the organic and inorganic particles and iv) the availability of electron acceptors for bacterial metabolism. These factors also control the preservation of individual organic particles by pyrite mineralisation.

The introduction of organic particles and their rate of burial is controlled by the rate of sedimentation. Decreases in sedimentation rate cause lower sulphate reduction rates. Rapid burial, however, results in the availability of high organic carbon concentrations for sulphate reduction as the system becomes closed to oxygen (Figure 1.2) and successive electron acceptors are consumed. Further burial moves the organic particle through different bacterial populations. These bacterial populations are zoned with depth from aerobic to nitrate reducers, manganese reducers, iron reducers, sulphate reducers and methane oxidisers (Figure 1.2), and their metabolism imposes geochemical stratification upon the sediment column. For pyrite to form, metabolizable organic compounds and suitable electron acceptors have to survive aerobic degradation to enable anaerobic sulphate reduction to become the dominant process in the sediment column.

Pyrite is unlikely to form in oxic sediments as little sulphate reduction will occur and the initial formed pyrite may not be preserved. Canfield (1994) suggested

that a high sedimentation rate is the most important factor in the preservation of an organic particle as it means that a higher concentration of easily metabolisable organic compounds are available for sulphate reduction. However, it is likely that rapid burial is not the only control (Hedges & Keil, 1995) as anaerobic processes breaking down organic compounds occur at a similar rate to aerobic processes (Hansen & Blackburn, 1991; Allison, 1988). Burrowing (Aller, 1983; 1994) disrupts the geochemical zonation of the sediment column as it aerates the sediments, despite mixing labile organic material in from the sediment surface. Additionally, individual organic particles can develop a series of concentric bacterial and geochemical zones equivalent to those imposed with depth in the sediment column (Figure 1.2). This means that sulphate reduction can occur within a sediment where the oxygen concentrations are low (25% saturation; Jørgensen, 1977) or where iron and manganese reduction are occurring. The only requirements are dysaerobic sediment and an organic particle sufficiently large to develop zonation.

4.B - The availability of organic and iron compounds

The amount and type of organic material and detrital iron which enters the sedimentary system varies with water depth. Organic content is inversely proportional to water depth (Jørgensen, 1983), which means it is highest in coastal waters. Mass mortalities can input very high concentrations of organic particles and are important in the geological record. The availability of the easily metabolizable compounds for bacterial utilisation are also variable as different organic compounds are utilised at different rates by different bacterial populations. The concentration of hydrogen sulphide in the sediment is therefore affected by the nature of the organic substrates available for bacterial metabolism as well as the concentration and distribution of these particles. Muscles and internal organs, for example, are rapidly degraded during metabolism by the action of either bacteria or scavengers. Low molecular weight organic compounds are more metabolisable than refractory chitin or cellulose and they are consumed rapidly by bacteria. To preserve these easily metabolisable tissues in pyrite, the development of an anaerobic micro-environment must be extremely rapid. This will allow the most metabolisable tissues to be utilised by sulphate-reducing bacteria rather than being consumed by other bacterial populations in the sediment column. In addition, the iron concentration of the sediment must be sufficiently high in and around the organic particle to precipitate the hydrogen sulphide produced during sulphate reduction.

Iron concentrations are affected in a similar way to organic carbon with detrital input controlling the concentration of iron in a sediment. The rate of reaction with hydrogen sulphide, and the availability of the iron compounds to bacteria, is then controlled by the type of iron mineral. Canfield *et al.* (1992) outlined how the reactivity of iron minerals towards sulphide varies with different mineral types. Similarly this indicates which minerals bacteria are capable of reducing; ferric oxyhydroxides, such as lepidocrocite, are the most available and silicates the least.

4.C - The effect of diffusion

Once hydrogen sulphide has been generated in a micro-environment it begins to precipitate by reacting with available iron minerals or ferrous ions generated by bacterial iron reduction. The main types of pyrite preservation, permineralization, mineral coats and mineral moulds , vary only in the distance between the site of decay and the point of pyrite precipitation. This distance is controlled by the concentration of iron and hydrogen sulphide in the micro-environment and the permeability of the sediment. Canfield and Raiswell (1991) suggested that the occurrence of the three main types of pyrite preservation depends on differences in the balance between the reservoirs of iron and hydrogen sulphide.

Permineralization occurs within the pore spaces in organic particles, and the less refractory material is the source of the organic material utilised by the bacteria. This type of pyritization is common in plant fossils where the pyrite infills the cells and the cell walls remain as carbonaceous layers. In mineral coats pyrite forms a thin layer on the outside of the organic material. This outlines the organic material and is the commonest form of pyrite preservation for degradable soft parts, although the internal organs may no longer be present. The pyrite coat may be due to the permineralization of a layer of bacteria which have colonized the surface of the organic particle.

The most common type of preservation is as a mineral mould. In this case pyrite is precipitated around the outside of the organic particle preserving only the outline of the fossil, with none of the soft tissues remaining. This is usually forms a much thicker layer than the mineral coats which are limited to a thin millimetre layer. Canfield and Raiswell (1991) suggested that this type of preservation is due to limited pyrite formation. The dominance of one form of preservation over another can be predicted using the concentration of the hydrogen sulphide reservoir and the iron

reservoir, and the rates of hydrogen sulphide and ferrous iron diffusion in water. The model suggested in Raiswell *et al.*, (1993) and Briggs *et al.*, (1996) allows the distance from the site of decay to the edge of the pyrite precipitation zone to be calculated. Thus pyrite formation can be controlled by the concentration of iron in the sediment surrounding the particle and the rate of diffusion of hydrogen sulphide out of, and iron into, the particle. Iron diffuses into the particle at a much slower rate than hydrogen sulphide. Thus if the concentration of hydrogen sulphide diffusing out of the site is greater than the concentration of iron diffusing in then pyrite formation should occur in a halo around the organic matter (Coleman and Raiswell, 1993). An inverse situation should cause pyrite to form within the organic particle (Briggs *et al.*, 1996). The conditions for pyrite formation can be expressed mathematically if the particle size and rate of sulphate reduction are defined (Raiswell *et al.*, 1993). In a sediment which has a high organic content and a low iron content pyrite formation will be centred upon the iron sources as pyritization is controlled by the rate of diffusion of hydrogen sulphide into the iron rich zone.

4.D - Experimental Aims

The experiments were designed using different combinations of organic particles (whole crustaceans, chitin fragments, carbonate, phosphate and lactate) to assess the preservational effect of high organic rich environments containing bacterial substrates in addition to particulate material. The main iron source used was ferrous sulphate, as the experiments outlined in Chapter 3 had shown that there is little difference in the amount of pyrite produced using lepidocrocite and ferrous sulphate as the iron source. Lepidocrocite was used in the experiments where iron was required to coat shrimps. Using these two types of iron also makes these experiments comparable with those in chapter 3. The experiments described in this chapter addressed the following questions:

a) Is decay necessary for pyritization?

b) Is there any difference between pyrite occurring in association with carbonate, chitin, phosphate or decaying crustaceans?

c) Is preservation enhanced when high concentrations of bacterial substrates are present in addition to more recalcicant organics?

and d) Is there any visible intimate association between the products of sulphate reduction and organic matter?

Other experiments were designed, taking into account the results described in Chapter 3, to test the theories put forward in Canfield and Raiswell (1991), Coleman and Raiswell (1993) and in Raiswell *et al.*, (1993) describing the relationships between iron and sulphide reservoirs and the precipitation of pyrite, and to answer the following questions:

e) Are sulphate-reducing bacteria required at the point of decay?

f) What effect does diffusion have on pyrite formation?

g) What is the effect of separating the iron source from the sulphide source?

The experiments were then divided into two separate types. Experiments in aqueous media were used to consider questions relating to bacteria and decay, while gel stabilised experiments were used to consider questions relating to diffusion and the separation of sulphide and iron pools and to test the reservoir hypothesis of Raiswell *et al.* (1993).

4.E - Aqueous Experiments

4.E.1 -Methods for Aqueous cultures

These experiments were carried out as in Chapter 3, with each vial containing either pieces of common limpet (*Patella vulgaris*) shell, phosphatic material, *Crangon crangon* moults, or whole carcasses of *Crangon crangon* or *Palaemon elegans*. The limpet shells were boiled in potassium hydroxide, washed and autoclaved. The phosphate fragments and chitin moults were also washed and autoclaved. The phosphatic material was from the Solenhofen Limestone, Germany (supplied by Dr Phil Wilby), and was included in order to see whether pyrite nucleation occurred preferentially on phosphate. The crustaceans were asphyxiated in an anaerobic atmosphere, but were not sterilised. The medium reciepe used is shown in Table , and was modified so that it was similar to that which produced the greatest amount of pyrite in the bacterial experiments, containing ferrous sulphate. The greatest amount of pyrite was produced in vials containing a ratio of iron:sulphate:lactate of 1:4:15. This was corrected in order to prevent sulphate

limitation and fermentation occurring in the vials and the ratio used was 1:7.5:15 as *Desulfovibrio desulfuricans* uses 1 mole of sulphate to 2 moles of lactate in its metabolism (See Table XI).

Table XI- Media Ingredients

Compound	gl^{-1}
Potassium phosphate	0.5
Ammonium chloride	1.0
Calcium chloride	0.1
Magnesium sulphate	2.0
Resazurin	0.0001
Thioglycolatic acid	0.1
Ascorbic acid	0.1
Sodium sulphate	10.5
Sodium lactate	21
Yeast extract	1.0

Three sets of experiments were prepared, by adding the sterile medium into vials containing the organic particle and a pre-weighed amount of iron sulphate (5mM +/- 0.1mmoles). Three sets of experiments were set up: A - inoculated with *Desulfovibrio desulfuricans* and lactate (17.7 gl^{-1}), B - inoculated with a mixed culture of sulphate reducing bacteria from the Severn Estuary grown in a medium containing homogenized shrimp and chitin fragments and lactate (17.7 gl^{-1}), and C - inoculated with the same culture but without lactate (Table XII). Uninoculated experiments were also set up as controls.

Table XII - Aqueous experiment variations

Set	Number					
		Lactate	Shrimp	Chitin	Carbonate	Phosphate
A	1	✓	✓			
A	2	✓		✓		
A	3	✓			✓	
A	4	✓				✓
B	1	✓	✓			
B	2	✓		✓		
B	3	✓			✓	
B	4	✓				✓
C	1		✓			
C	2			✓		
C	3				✓	

The experiments were incubated at 25°C and destructively sampled at 10 day intervals. During sampling, the organic particles were removed from the vials, washed in distilled water and broken in half. One fragment was dried chemically for SEM (see appendix 7 for method) and the other was placed in 10% zinc acetate prior to sequential chromous chloride digestions. A freshly-killed shrimp was also chemically dried for SEM.

Additional samples were taken from the medium of the experiment and these were stored in the same manner as the bacterial experiment samples (see Chapter 3). These samples were analysed in the same manner as those in Chapter 3 (outlined in appendix 5) in order to determine the concentration of the reduced sulphur species in the vial.

4.E.2 - Methods for Tubing Experiments

Additional experiments were carried out with a shrimp and sterile medium placed inside a length of dialysis tubing. The dialysis tubing was knotted before being placed in a sterile vial containing Postgates medium (table XI), 5mM ferrous sulphate, 17.7 gl^{-1} of lactate and 2ml of Severn Estuary bacterial inoculum (this is equivalent to Set B1; see 4.E.3.2). Once the ferrous sulphate had dissolved it would have been free to pass through the membrane as were any metabolites. Samples were taken from both inside and outside the tube, and both the shrimp and the tubing were distilled to determine the site of sulphide precipitation. Some fragments of the shrimp and the tubing were also prepared for examination under the SEM (see appendix 7).

4.E.3 - Results of Aqueous Experiments

These experiments compared the amount of sulphides produced in the surrounding medium to the amount precipitated on and inside the organic matter in the experiment. The experiments developed similarly to those in Chapter 3. Hydrogen sulphide and acid volatile sulphides were the initial formed products. Pyrite was produced in some experiments but unlike the experiments in Chapter 3, the concentrations are small. The concentrations of different pools are listed in appendix 9, and the SEM results are shown in Figures 4.1 to 4.5.

4.E.3.1 - Set A - *Desulfovibrio desulfuricans* and lactate experiments - *Desulfovibrio desulfuricans* only metabolises low molecular weight organic compounds (e.g. lactate) and hydrogen. It cannot, therefore, decay complex organic material although it can utilise some of the low molecular weight degradation products of other anaerobic bacteria. Initially, the experiments with *Desulfovibrio desulfuricans* and lactate developed a similar pattern of iron sulphides to those experiments in Chapter 3 irrespective of the type of organic particle present.

Days 4 and 12 - After 4 days the media had become black, except in the vial containing the whole shrimp where the black colouring was associated only with the carcass. By day 12 this experiment was also opaque with an iron sulphide biofilm. Chemically, by day 12, the medium in the shrimp experiment had a low concentration of hydrogen sulphide (1.2mM) and similar low concentrations of AVS and PS (0.2mM), while little sulphide was present on the organic matter. The other experiments contained higher concentrations of AVS (8mM in the experiment containing carbonate fragments, 4.5mM in the experiment containing phosphate and 12.9mM in the experiment containing chitin) while the concentrations of hydrogen sulphide and pyritic sulphide were similar to those in the shrimp experiment (A1).

The surfaces of all the organic particles showed various structures. All these substrates have flat areas which were coated with a black deposit. This deposit had a knobbly structure which on closer examination consists of bundles of *D. desulfuricans* coated with a membrane, with individual bacteria on the top of this biofilm. Areas of higher relief were observed to be larger agglomerations of bacteria, and also contained calcitic and/or iron phosphate crystals (Figure 4.2B, 4.3A, B and E). The sulphide composition of the biofilms indicated that pyrite had not yet formed after 12 days. The composition of the iron phosphate crystals was confirmed using the electron micro-probe on several samples of carbonate material. They are likely to be present because Postgates medium precipitates iron phosphate as a pH buffer.

After 22 days - After 22 days the different experiments become more distinct chemically. Little AVS was present in association with the organic fragments. The media had lower concentrations of AVS in the shrimp experiment, whereas the carbonate experiment contained 14.2mM and the phosphate and chitin experiment contained approximately 28mM. The concentrations of pyritic sulphide were all around zero. The shrimp showed no mineralization on the internal edges of the carapace, but was coated with a black film, and black blobs had developed on its appendages. Under the SEM, these black blobs were seen to be crystal bundles of

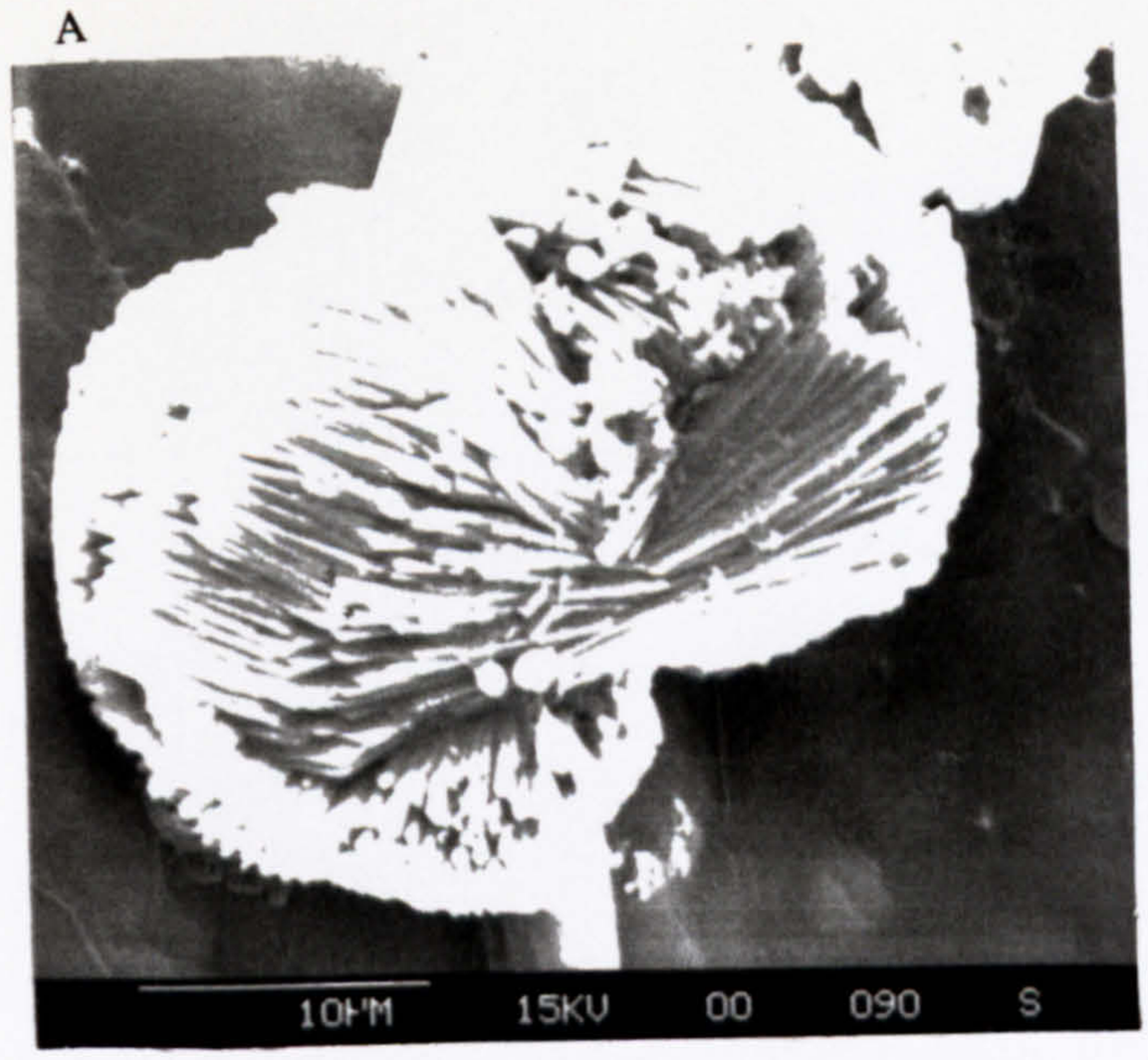

Figure 4.1 Structures found on the cuticle of a decaying shrimp in the aqueous experiment A; A - A calcium carbonate bundle on the cuticle surface, B - Bacteria in association with A, C - Calcium carbonate bundles on gill hairs, D - Antenna surrounded by calcium carbonate, E - 'Merguine nests' on the bacterial biofilm on the cuticle of a shrimp, F - More details of a 'merguine nest'.

A

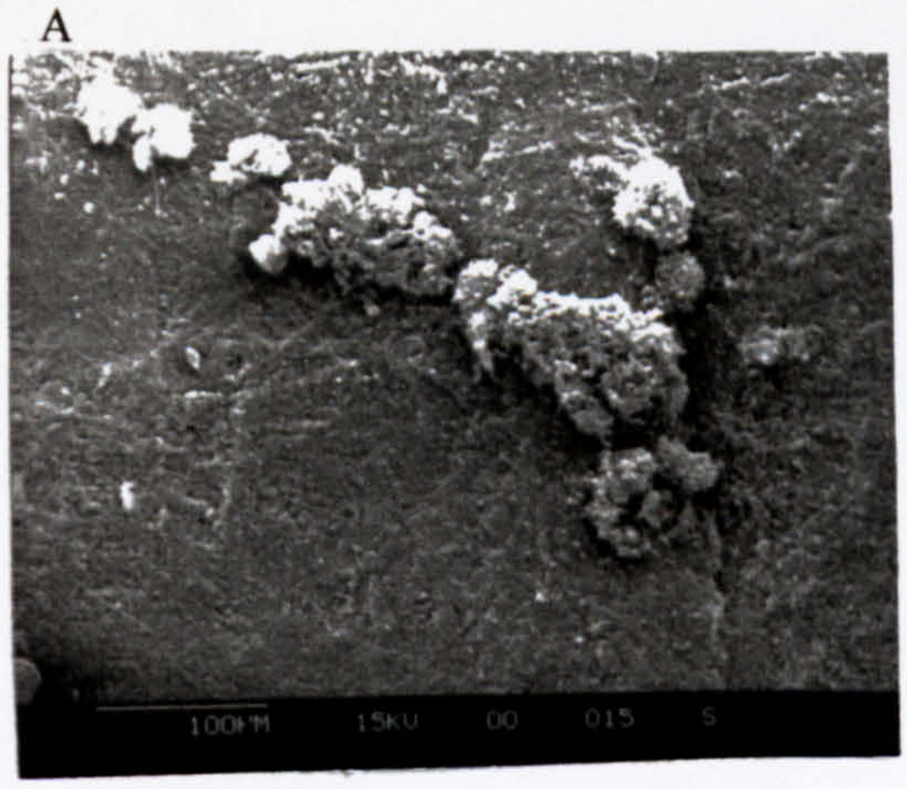

B

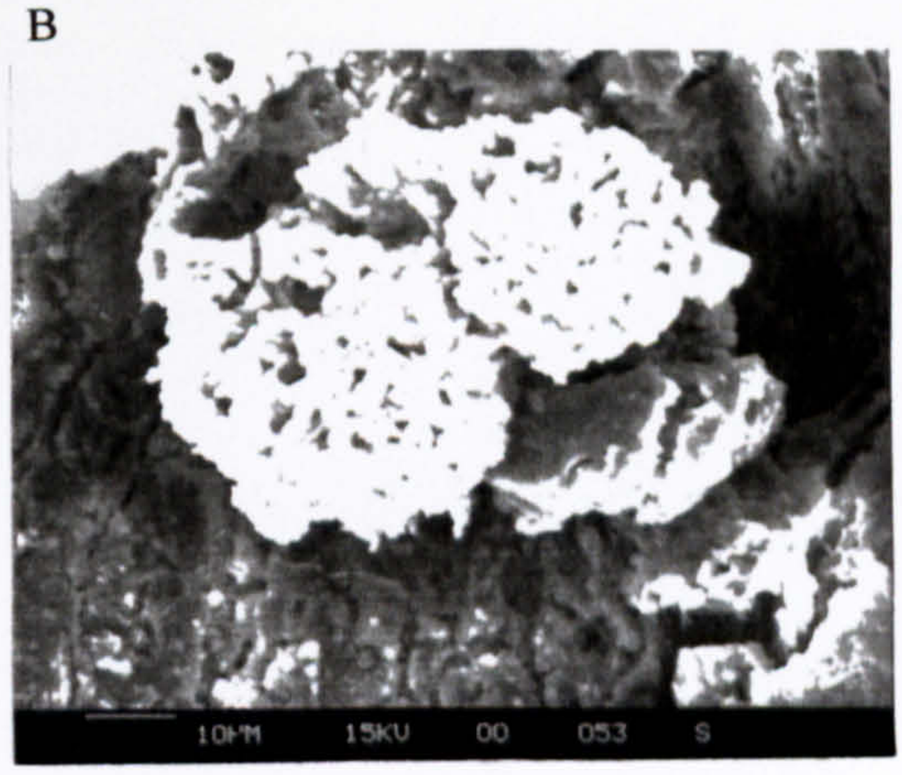

C

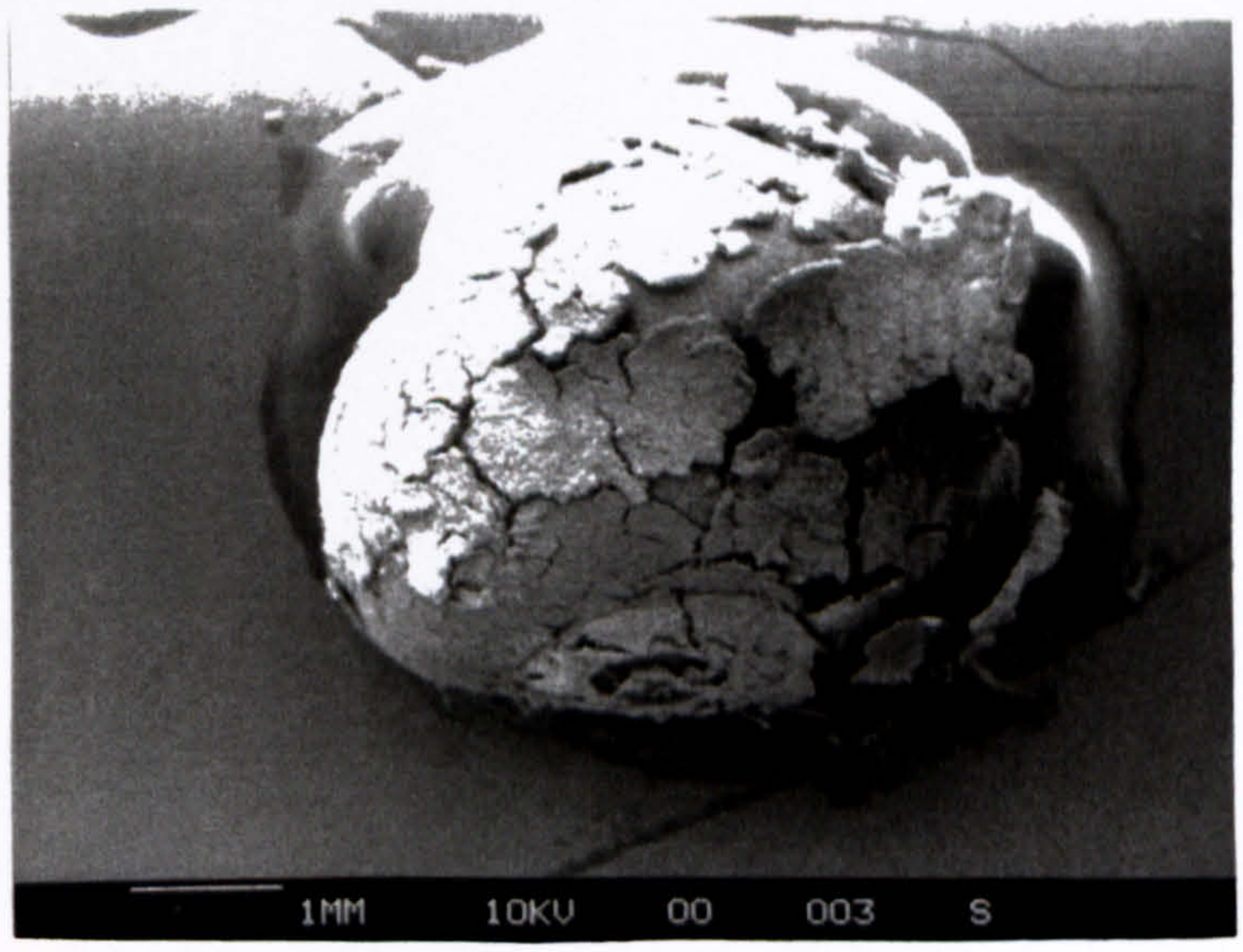

D

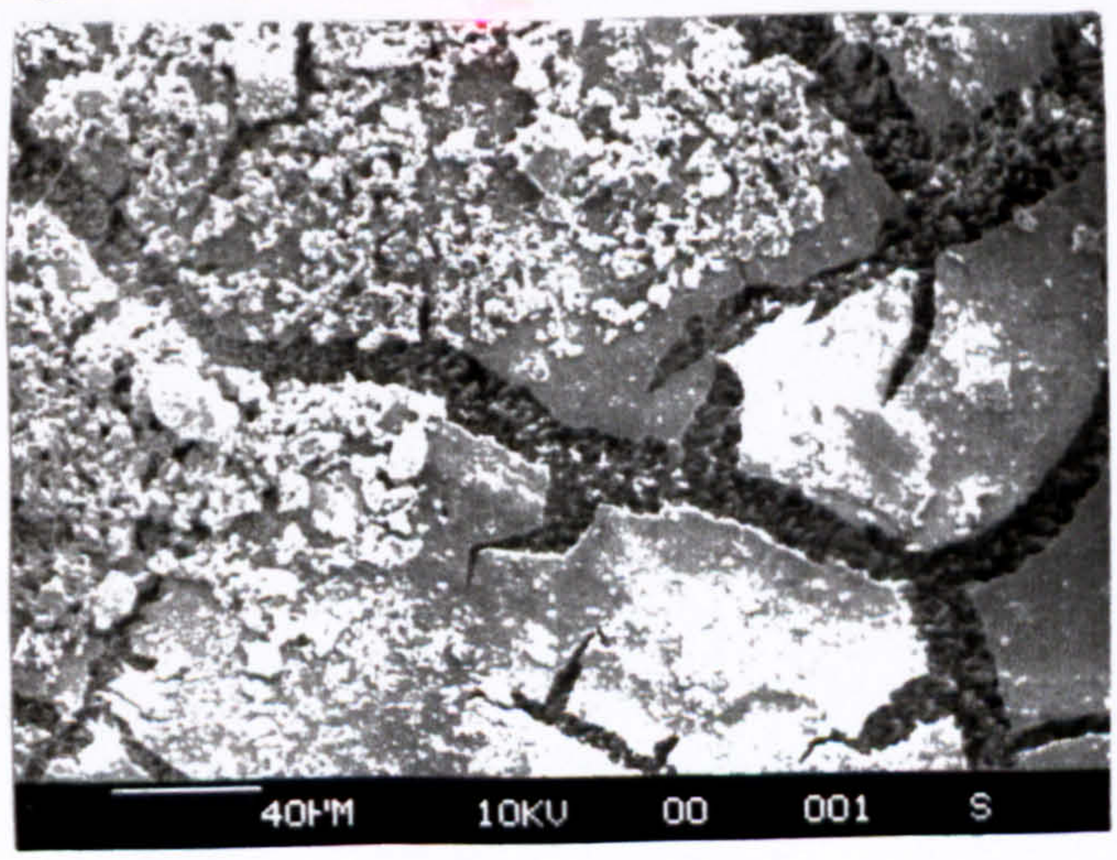

E

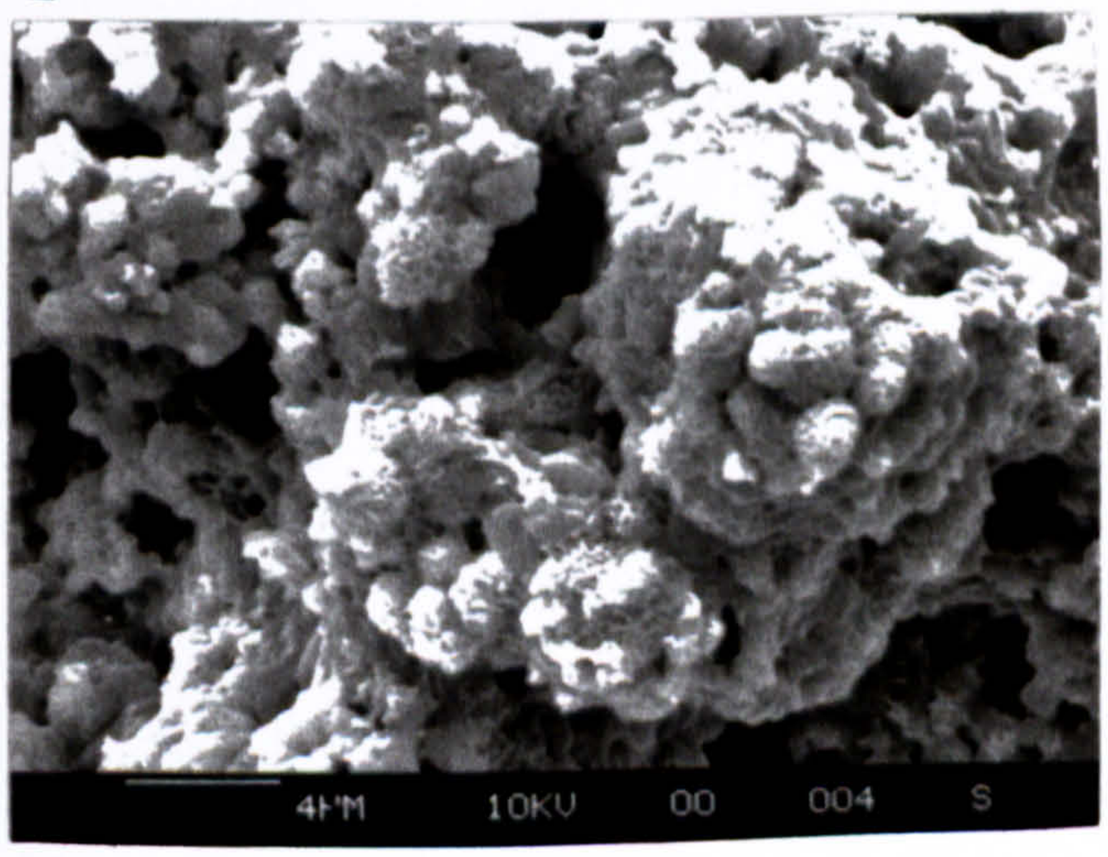

Figure 4.2 Structures on organic particles in aqueous experiment A; A - Surface of carbonate after 36 days, B - Details of higher relief agglomerations of bacteria, C - Surface of a periwinkle, D and E - Details of encrusting bacteria on the periwinkle

calcium carbonate which grew as dumb-bells and spheres on the gills and appendages (Figure 4.1C). Occasionally the crystal bundles coated the exterior of the appendages, as in the antenna shown in figure 4.1D. The control shrimp in uninoculated medium also had spherical growths associated with its gills and appendages (Figure 4.3C and D). These spheres are similar to those seen in Set C of the inoculated experiments (Figure 4.5D), and assumed to be formed by a similar change in the medium chemistry due to the decay of the shrimp by indigenous bacterial populations.

After 32 days - After another ten days, the interior of the shrimp carcass had become blackened as the soft tissues became liquified. Calcium carbonate was also found on the carapace of both the whole carcass and chitinous moult. On this surface the deposits were hemispherical crystal bundles of calcite (Figure 4.2E and F). Bacteria were found in association with these calcite deposits but the majority appeared to form the encrusting biofilm observed earlier in the experiment upon both the organic surface and the calcitic deposits. The biofilm contained both AVS and pyritic sulphide, when analysed in the electron micro-probe. In addition, chromous chloride digestions of the biofilms in the shrimp experiments (appendix 9) indicates that this biofilm contained pyritic and acid volatile sulphides, whereas on the carbonate, chitinous and phosphatic material varying concentrations of AVS were present. The medium of the experiments continued to contain a significant concentration of hydrogen sulphide (6.2mM on average) and AVS (10.2mM on average) although this begins to decrease by the later stages of the experiment as the amount of lactate decreases.

4.E.3.2 - Set B - Severn Estuary culture in a medium containing lactate.- Changes in the liquid composition - The concentration of sulphides after day 10 in this experiment (B:average of 20.3mM TRIS) is considerably higher than that of the *Desulfovibrio* experiment (A: average of 18.7 mM TRIS), as a natural population of bacteria utilises both the lactate and the labile organics from the shrimp. After 12 days there were high concentrations of hydrogen sulphide (7.7mM in the shrimp culture) and AVS (13.2mM in the shrimp culture) and lower concentrations of pyrite and elemental sulphur. High concentrations of AVS were found in association with all the organic particles except the phosphate. The concentration of AVS increased throughout the experiment up to day 22 (average approximately 25mM), although there was no significant increase in the concentration of pyrite (remaining around

A

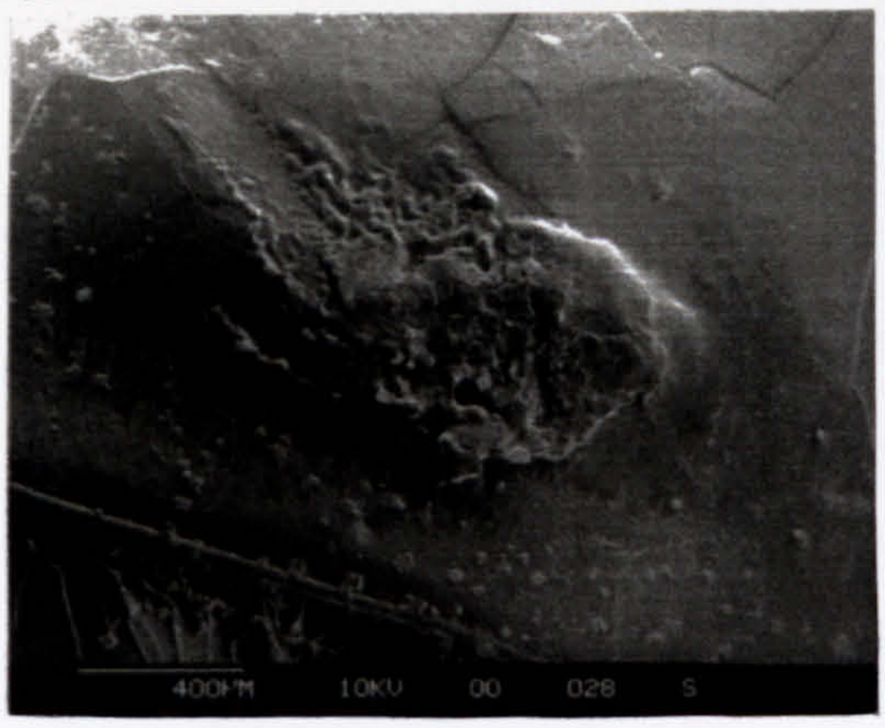

B

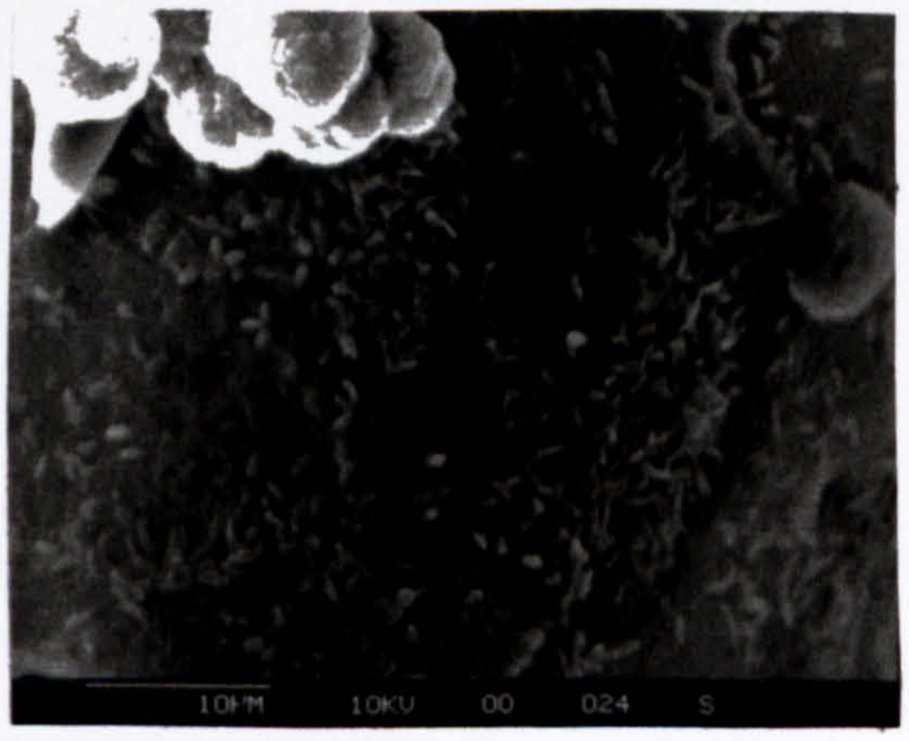

C

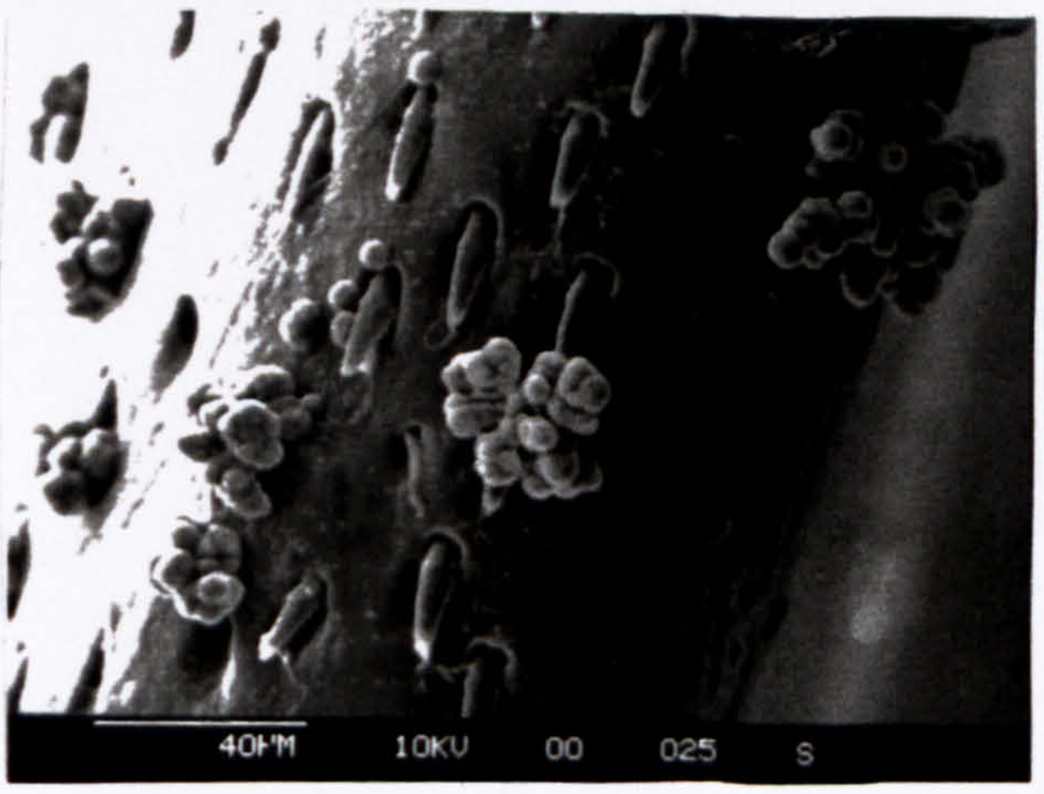

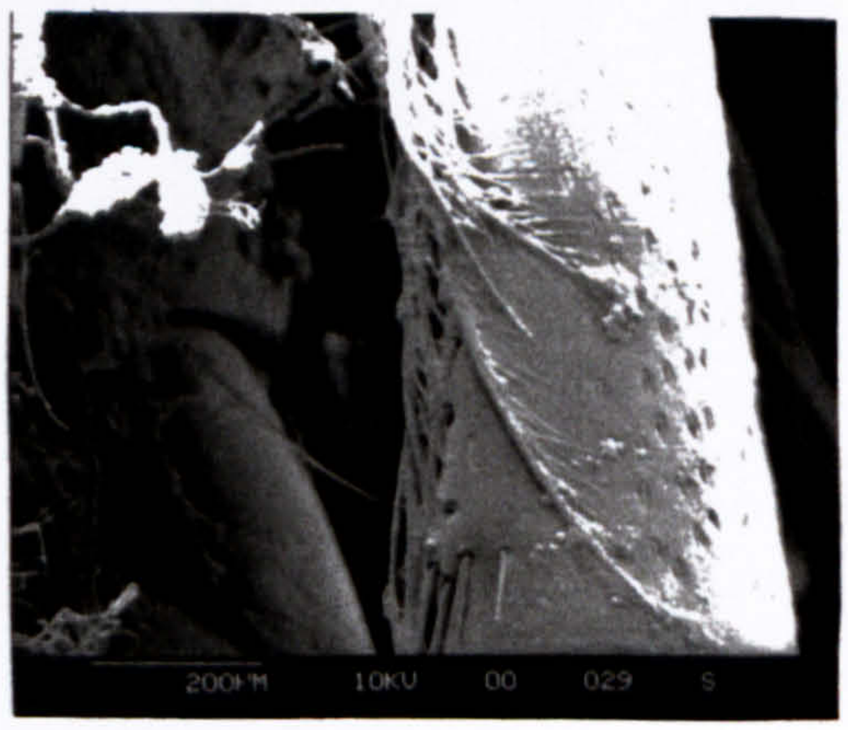

D

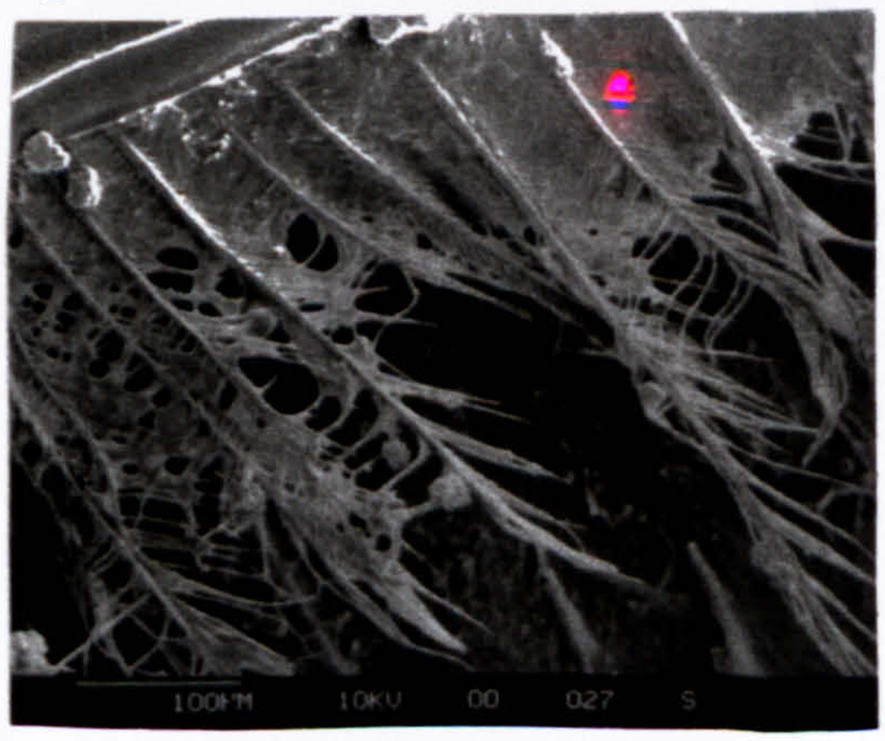

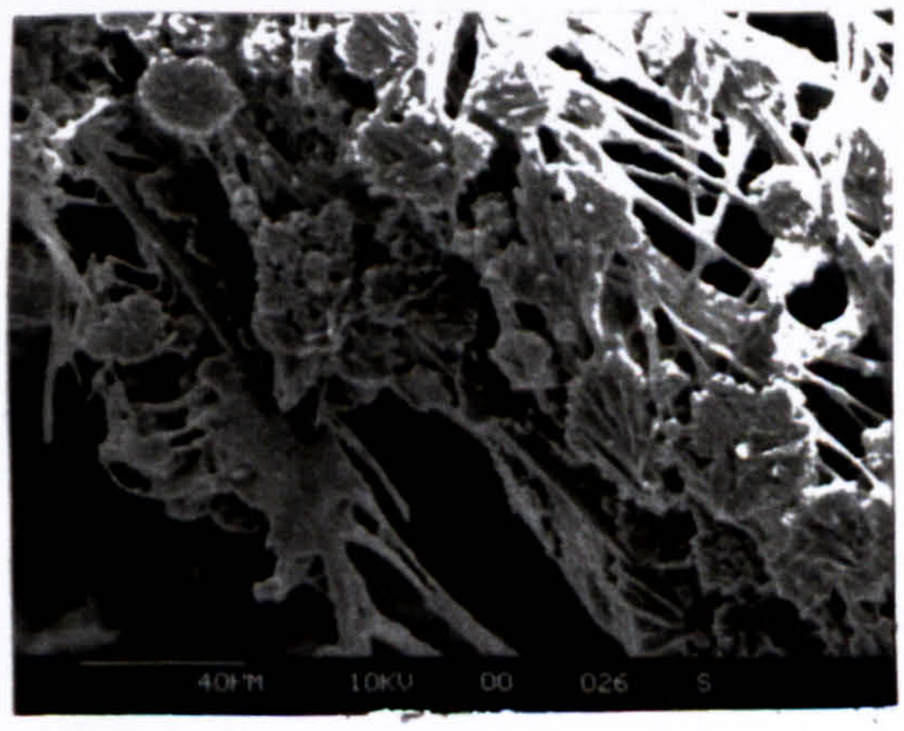

Figure 4.3- Structures on freshly killed and the experimental control shrimp; A - Cuticle surface, B - Close up the surface, C- surface of appendage, D - Gill hairs

A

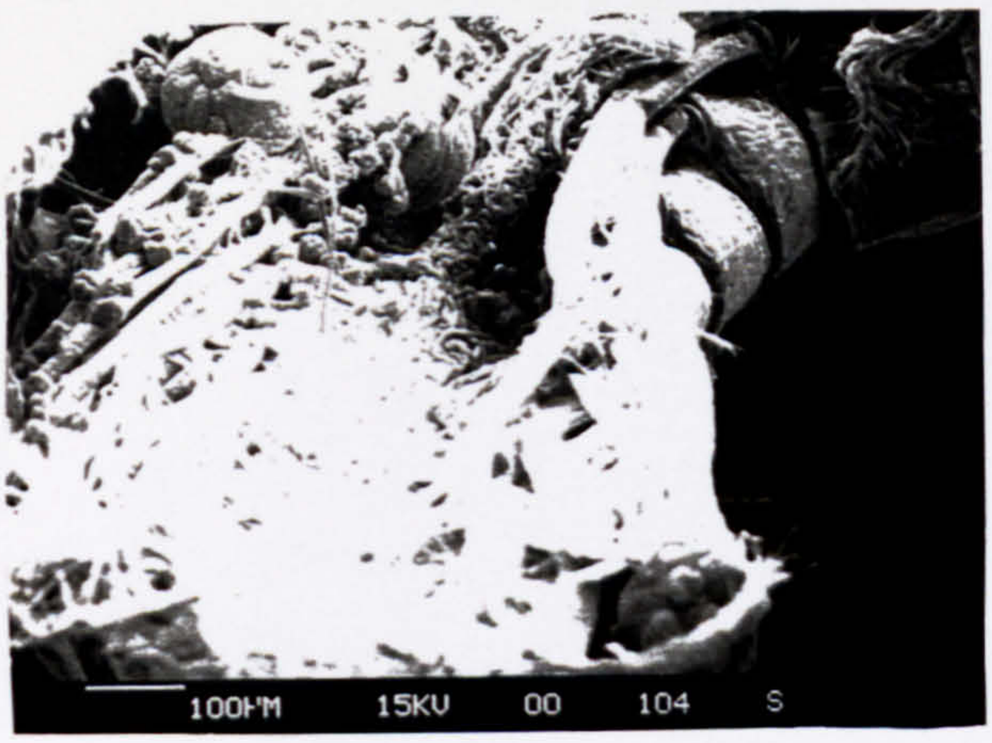

B

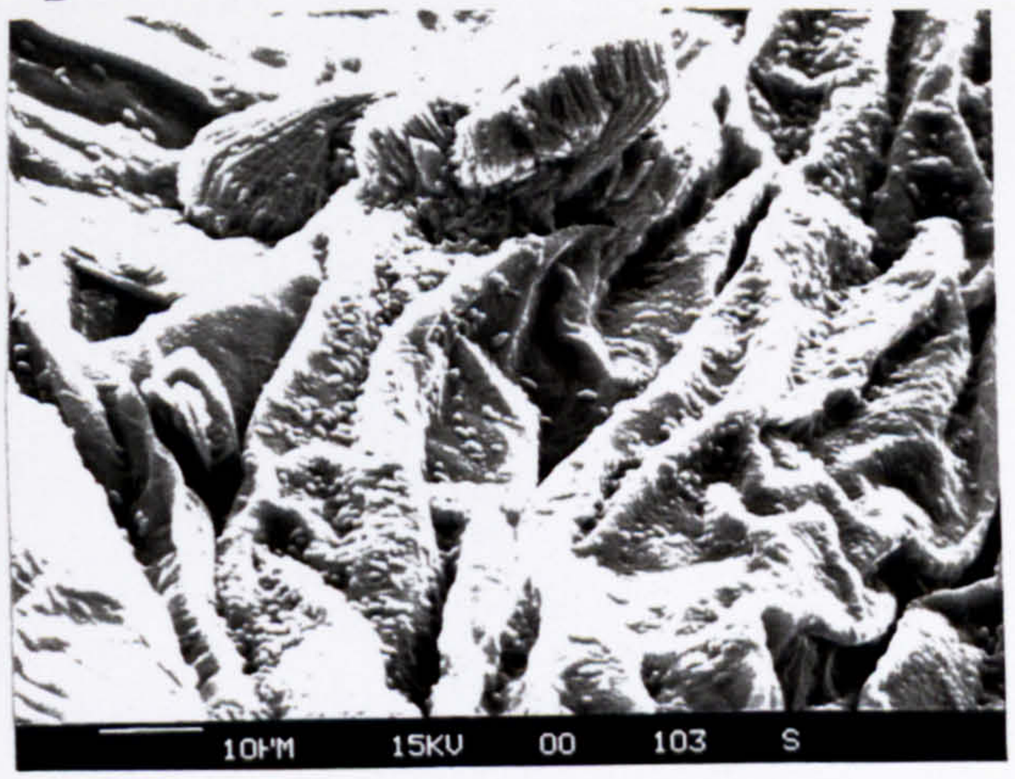

C

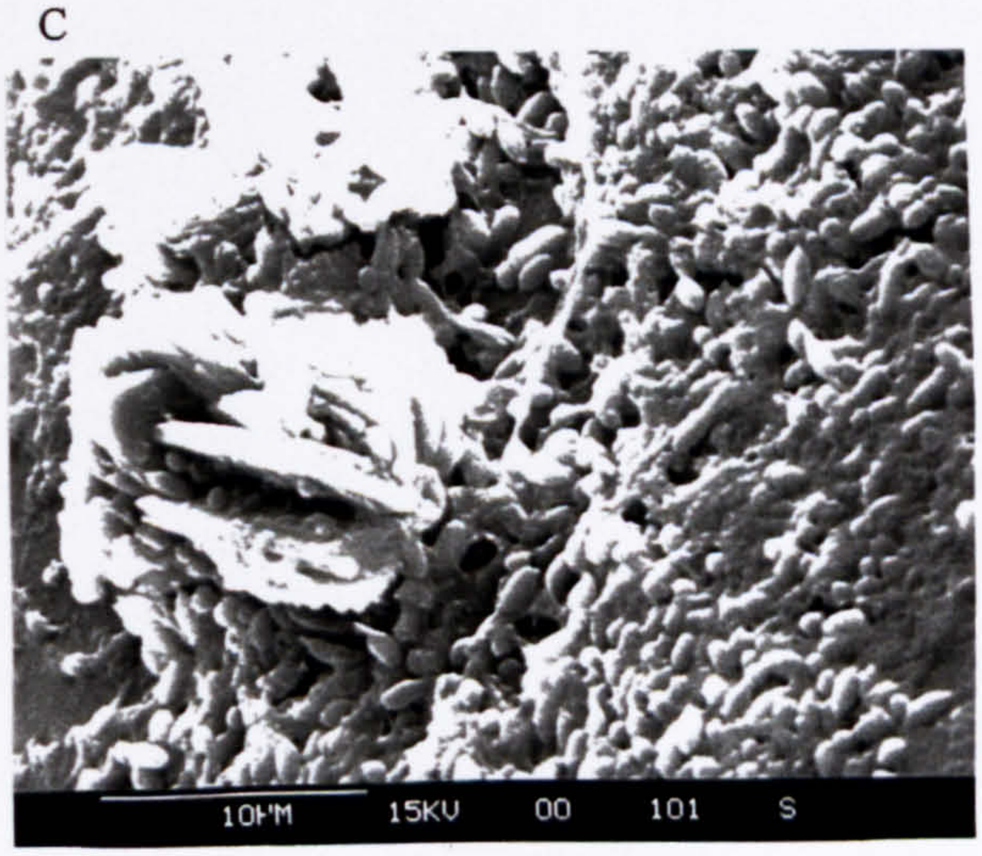

D

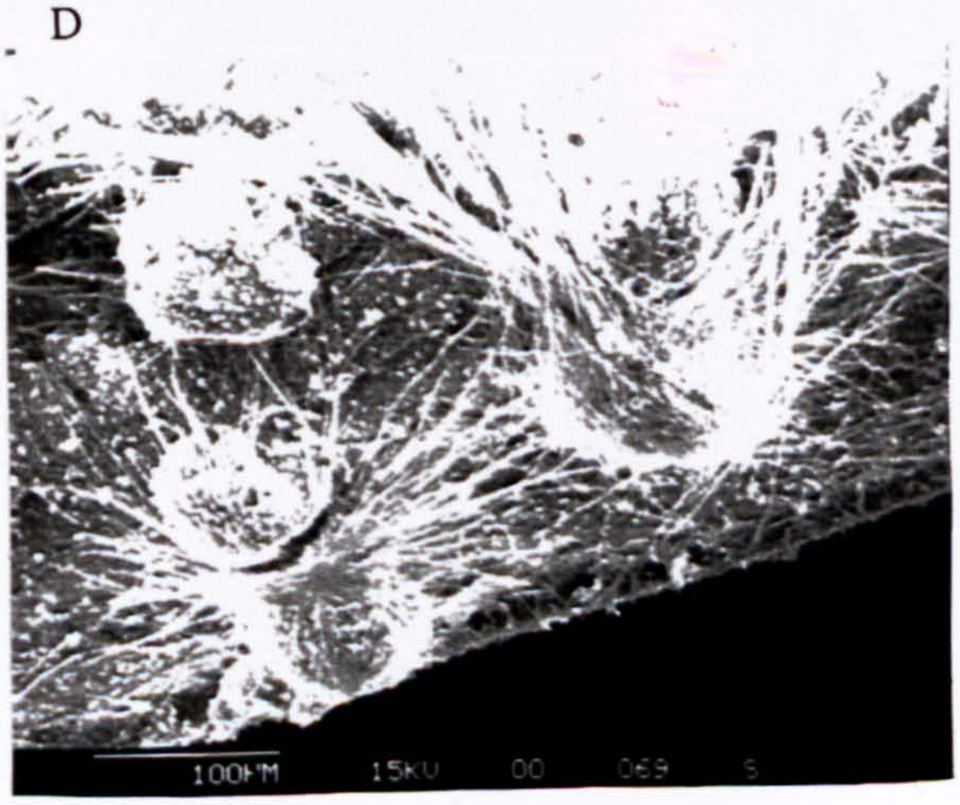

E

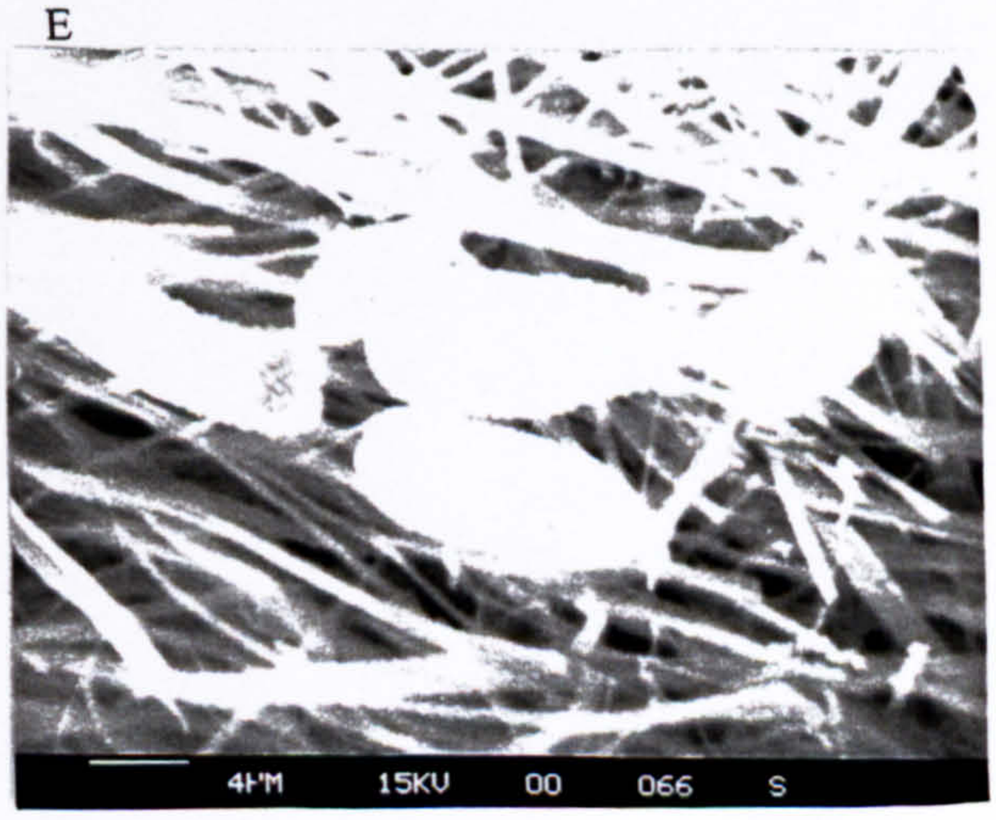

Figure 4.4 - Structures observed on shrimp carcasses in aqueous experiment B; A - Spherical calcium carbonate bundles on appendages, B - Carbonate and bacterial encrustations on the cuticle, C - Encrusting bacteria, D and E - Odd structures found on the carcass in aqueous experiment B.

A

B

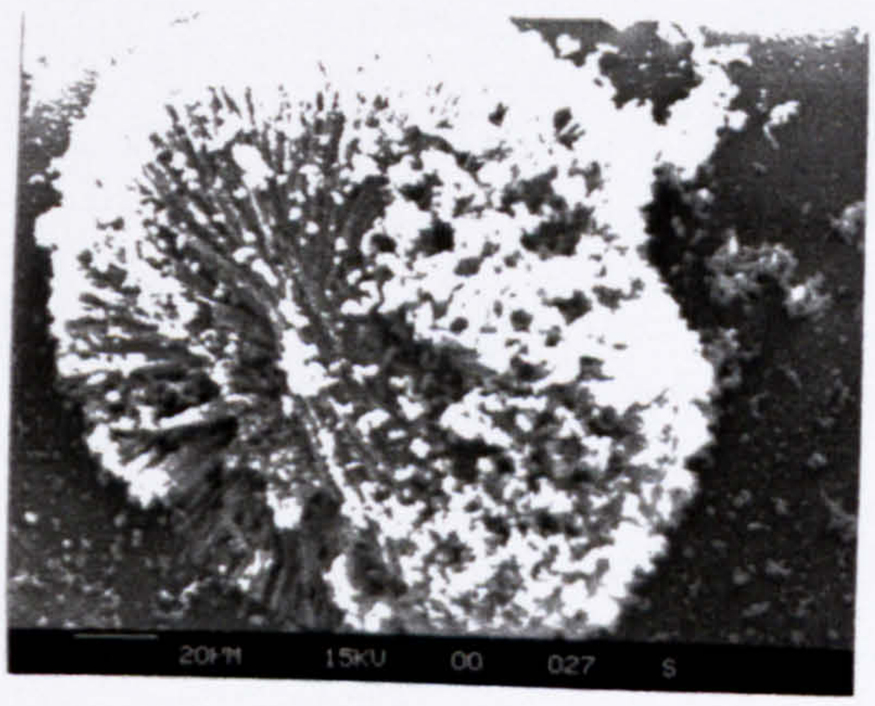

C

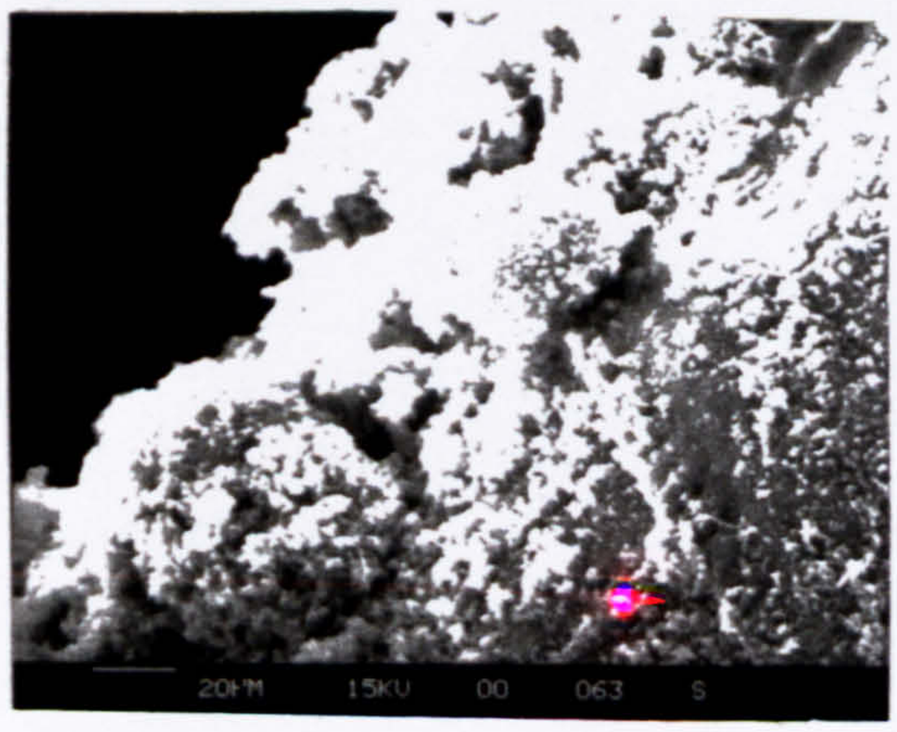

D

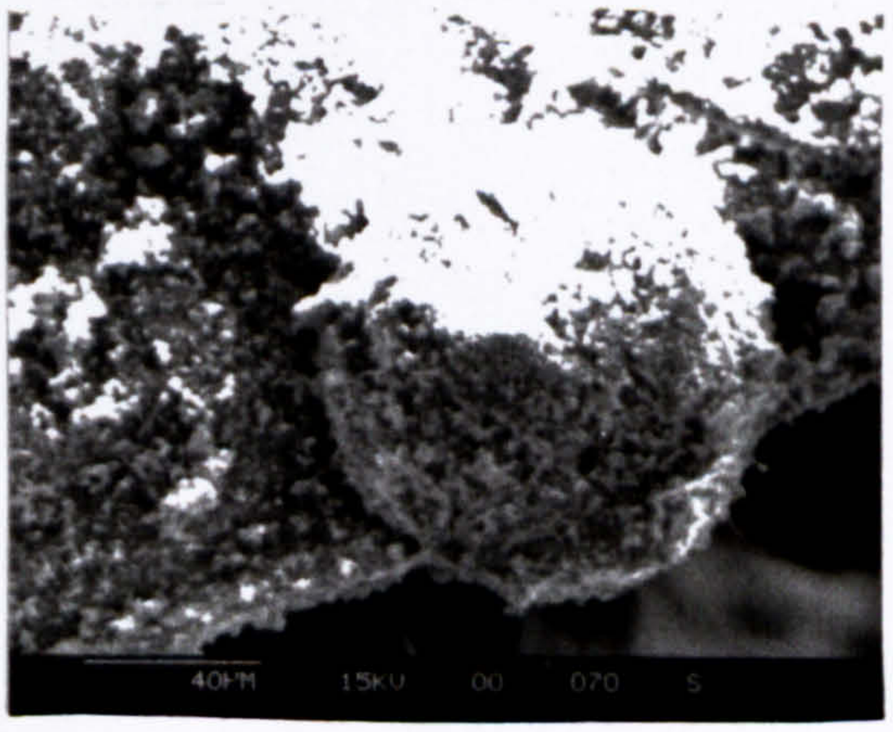

Figure 4.5 - Structures on organic particles in aqueous experiment B; A - Carbonate bundles on the carbonate fargments; B, C and D - Various carbonate stuctures on the Chitin fragments.

zero). After 34 days, these experiments contain similar concentrations of sulphide to those in the shrimp experiments in Set A as a result of sulphate limitation.

Changes associated with the solid substrates - As in set A, the organic particles rapidly became coated in a black biofilm (Figure 4.4B and C). In the shrimp experiment the head became separated from the abdomen and some black colouring was present inside the carapace and legs. Black films became more abundant after 22 days and started to coat the inside of the vials. Black blobs also appeared on the legs, gills and appendages as well as the carapace of the shrimp (4.4A). The surfaces of the organic particles in these experiments showed a much larger variety of structures than those seen in Set A, (see Figure 4.2 and 4.4) . However, the black biofilms full of encrusted bacteria are still present, as well as larger higher relief agglomerations of bacteria. In addition, the shrimp experiments contained spherical growths of calcium carbonate (Figure 4.4A), and a series of cross-shaped agglomerations made of flat crystals (Figure 4.4C). Similar structures were observed on carbonate and chitin, and to a lesser extent phosphate. Other structures include inorganic clusters of fibres (Figure 4.4D), fluffy spheres similar to those seen on fresh shrimps (Figure 4.3 and Figure 4.4D and 4.5C and D) and large knobbly bacteria-like organisms (Figure 4.4E).

4.E.3.3 - Set C - Severn Estuary culture in mineral salts.- This experiment had a average concentration of around 4mM AVS and 2.5mM hydrogen sulphide by day 10 (appendix 8) as the bacteria utilised any homogenised shrimp and labile organics from the inoculum. This is low compared to the previous two sets which contained lactate. The sulphide was precipitated upon the organic particles. After 35 days, AVS, pyrite and elemental sulphur were observed on both the carbonate and shrimp fragments as well as in the medium. However, these concentrations were lower than those observed in Set B (an average TRIS of 20.3mM in Set B compared to an average of 2.9mM in Set C). The chitin experiment had little sulphide material left due to oxidation from a leaking vial.

The macroscopic features of the organic particles are like those formed in sets A and B, although the black coating was less extensive. The bacteria coated with biofilm are also less extensive although the larger agglomerations of encrusted bacteria are still present (Figure 4.5 and 4.6B, C and D). The mineral deposits on the organic fragments contained fewer calcium carbonate dumb-bells. Other spherical structures resembled those seen on the freshly killed specimen where spherical growths associated with gills and hairs have a 'fluffy' tetxure.

A

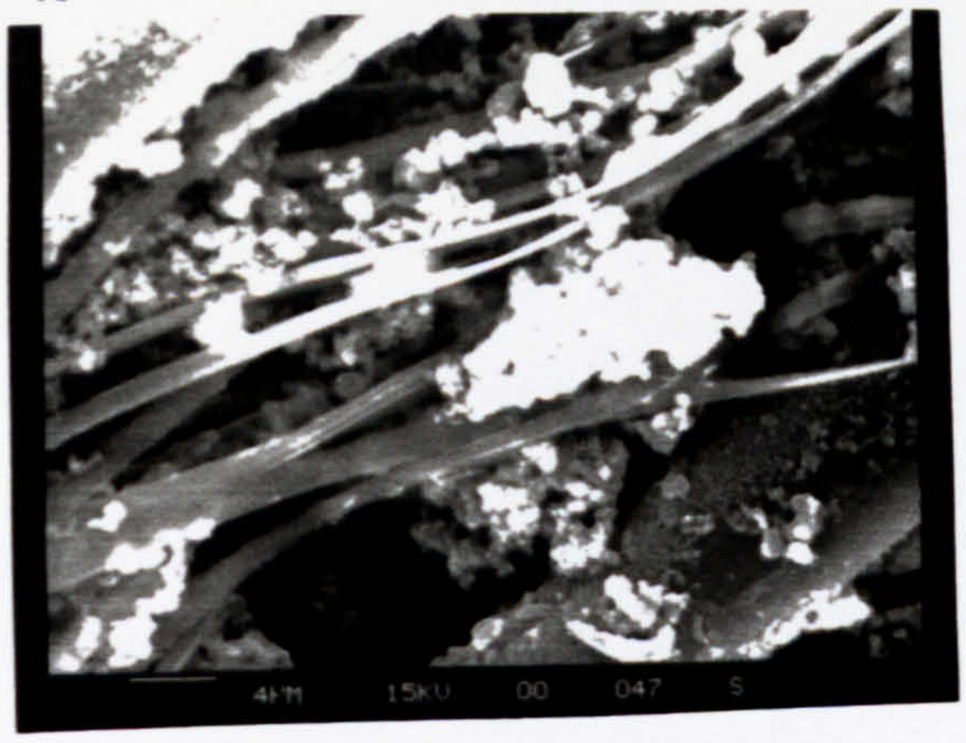

B

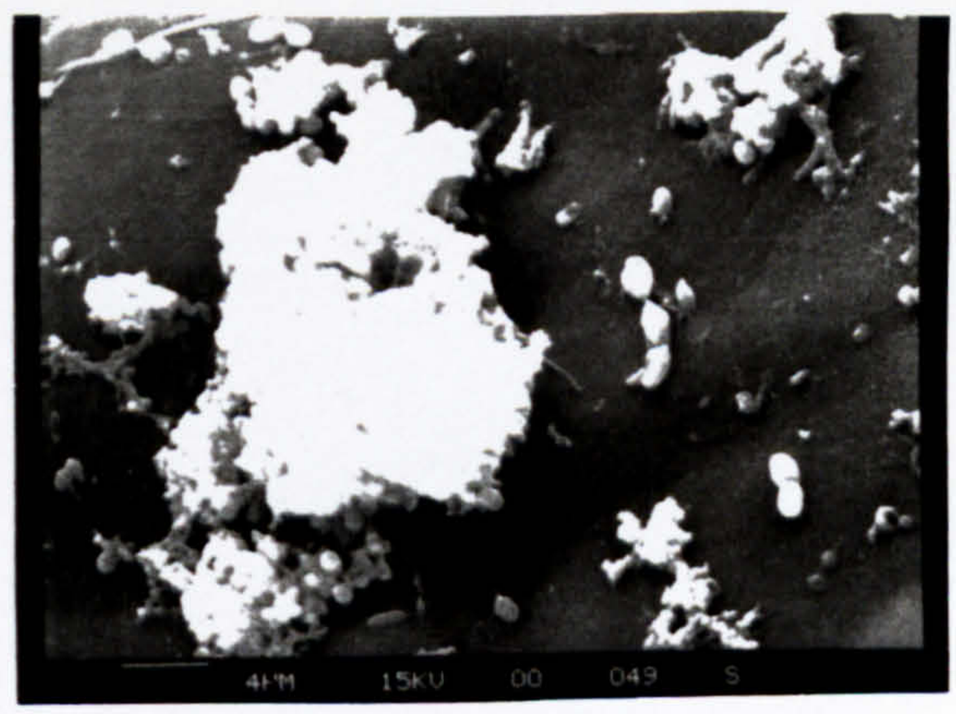

C

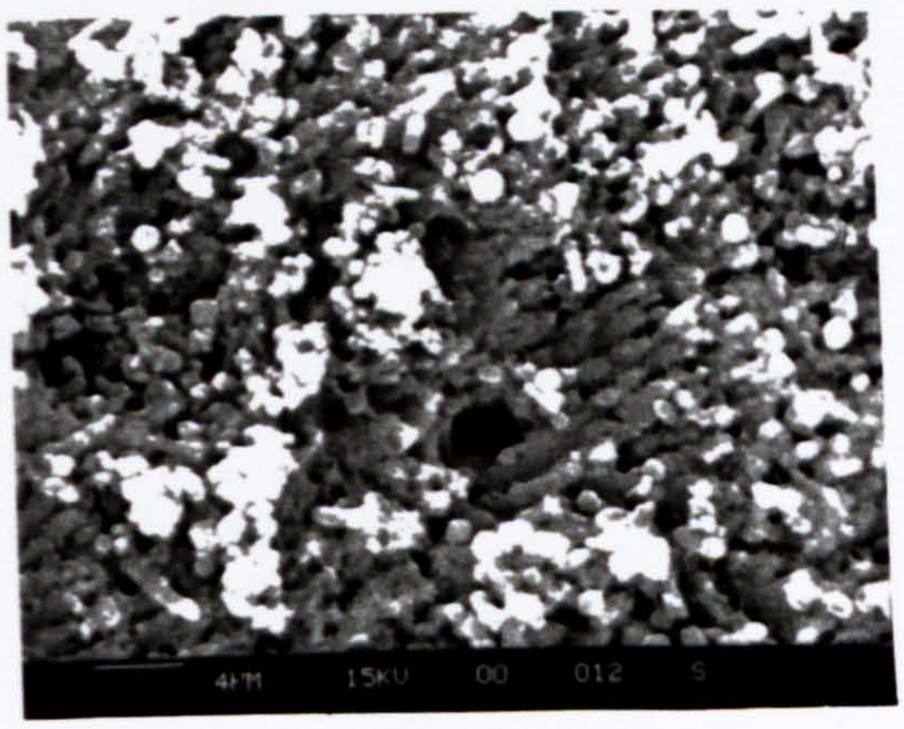

D

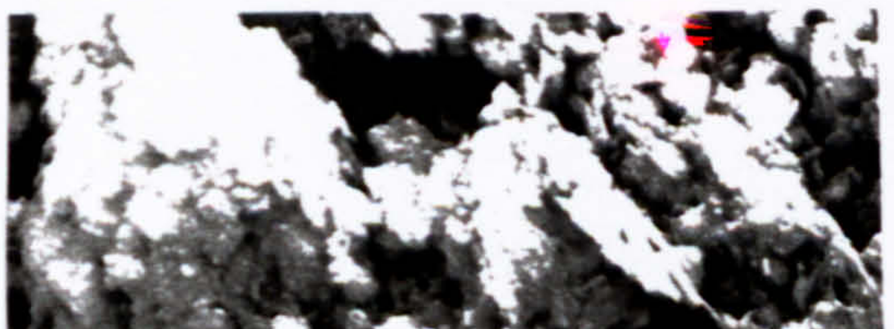

E

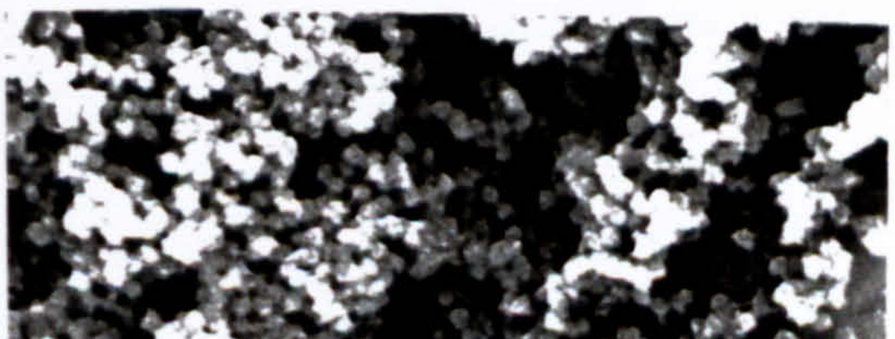

Figure 4.6 - Structures on shrimp carcasses in aqueous experiment C; A - Bacteria encrusting hairs, B - Bacteria cluster on carapace (low concentrations of bacterial encustation after 6 days), C - Surface of calcium carbonate bundles, showing bacteria on carbonate needles.

D, E - Structures on the surface of the shrimp within the visking tubing.

4.E.3.4 - Results of Dialysis Tubing Experiments

Initially the precipitation of AVS was confined to the outside of the dialysis tubing, while the interior contained no reduced sulphur compounds. Hydrogen sulphide was not found within the dialysis bag on day 12, as it was precipitated on the nucleation surface provided by the tubing (appendix 8). As the experiment continued the amount of AVS and pyrite found on both the shrimp and the tubing increased. The medium within the bag became black and cloudy like the medium outside it. After 36 days the medium inside the dialysis bag contained 4.8mM hydrogen sulphide, 3.2mM AVS and no pyrite, while the medium outside the bag contained 6.4mM hydrogen sulphide, 9.4mM AVS and 0.5mM pyrite. Black patches developed on the pink shrimp and these, when examined under the SEM, were poorly crystalline carbonate bundles (Figure 4.6D). Most of the mineralisation occurring on these shrimps was poorly crystalline and there were few encrusting bacteria present. Pyrite formed on the outside of the dialysis bag (3.2mM after 36 days) which was blackened. AVS was in association with the shrimp (0.5mM after 36 days). The tubing, however, was completely covered by both biofilms and agglomerations of bacteria (Figure 4.6 E).

4.E.3.5- Discussion of aqueous experiments

From these experiments it is possible to conclude that iron sulphides will form on any surface as long as the conditions required for sulphate reduction are met. There is no difference in the form of sulphides on any of the substrates and the bacteria provided a nucleation site for sulphides. The extra-cellular polysaccharides appear to be important as the majority of the sulphide is attached to substrates.

Locally, sulphides will also form without the presence of sulphate reducing bacteria, as long as the conditions and reactants required for pyritization are present, however the absence of sulphate-reducing bacteria means that the sulphides will not be associated with the surface of the organic particle.. In the dialysis tubing experiment, the shrimp does not develop encrusted biofilms as the bacteria are not using it as a surface, and the low concentrations of sulphides passing through the bag limit pyrite formation. This serves to illustrate that bacteria are not required for sulphides to form (Rickard, 1969b) although their presence seems to facilitate the precipitation of sulphides in the conditions used in these experiments. The formation of biofilms by bacteria has been suggested to influence the precipitation of carbonate minerals (Pedley, 1992 and Gerdes *et al.*, 1994) in sedimentary environments by

metabolically modifying the chemistry of their micro-environment. It seems probable that the extra-cellular polysaccharides produced by sulphate-reducing bacteria act in a similar way as the precipitation seems to be predominantly associated with them (Figures 4.1, 4.2, 4.4, 4.5 and 4.6A-C) and is limited when bacteria are excluded (4.6D and E). In sedimentary systems sulphate reducing bacteria are likely to be associated with particles of organic material and their combined production and nucleation of sulphide would facilitate pyritiztion.

Larger concentrations of pyrite are observed in the shrimp experiments as sulphate reduction continues, maintaining higher concentrations of pyritic sulphide and hydrogen sulphide. Similar concentrations of TRIS are produced in the experiments, with a maximum of 30mM, as the production of iron sulphides is limited by iron concentrations and sulphide by substrate and sulphate availability.

Similar structures were produced in all the experimental sets, although additional ones, such as 'fluffy' spherical crystal bundles (Figure 4.5D) and webs of fibres (Figure 4.4D), were observed in the sets using 'natural' populations of bacteria. Minerals were precipitated on the external surface of the shrimp carcasses within and over the sulphidized biofilms. Calcite is often associated with authigenic pyrite in sedimentary rocks. When hydrogen sulphide is precipitated as iron sulphide the increase in pH increases the degree of carbonate saturation in that micro-environment (Ben-Yaakov, 1973). Calcite and other carbonate minerals then begin to precipitate out (Canfield and Raiswell, 1991) which explains why the crystal bundles appear to cover some of the bacterial biofilm.

4.F - Gel Stabilised Experiments

4.F.1 - Methods

The use of a gel stabilised system allows diffusion fronts to be monitored during the decay of organic particles. They have been used by Wimpenny *et al.* (1986) to simulate the conditions in oil storage tanks, Mefarlane (1984) to simulate microbial processes in estuarine sediments, Nelson *et al.* (1986) to simulate oxygen and sulphide gradients and are currently being used by S.J. Bale (Bristol) to model the chemical gradients which develop around and within carcasses as decay occurs.

Experiments using agar stabilised systems were set up using a 30ml open ended tube. These tubes were plugged with inert buytl rubber bungs and autoclaved.

They were then filled under nitrogen with a sterile lactate-free Postgates medium (see Table VIII) containing 5% agar. Five sets of experiments were prepared. The sets varied in the amount of iron contained in the Postgates medium, the type of iron, and the positioning of this iron rich medium in relation to the carcass (a *Crangon crangon* or a *Palaemon elegans)*. The 5mM concentration of iron was selected as it had been used in the experiments in Chapter 3 and the aqueous experiments outlined in the previous section, and maintained pH between 6.2 and 7. Higher concentrations of iron sulphate also cause the agar solution to become opaque with iron phosphate precipitates. When the 5mM concentration is inserted in the equation for the radius of maximum pyrite precipitation proposed by Raiswell *et al.* (1993) a radius of 10.5 cm results. The equation relates the precipitation distance to the dimensions of the organic particle and amounts of sulphide and iron in the following manner:

$$R_{jmax} = \frac{a(D_S C_S + D_F C_F)}{D_F C_F} \qquad \text{Eq.4.1}$$

where R_{jmax} is the radius of maximum pyrite precipitation (cm), a is the radius of the 'shrimp' (assumed to be 0.5cm), D_S and D_F are the diffusion coefficients for dissolved sulphide (376 cm^{-2} yr^{-1} in seawater at normal seawater temperatures; Boudreau and Canfield, 1987) and dissolved iron (149 cm^{-2} yr^{-1} in seawater; Boudreau and Canfield, 1987) respectively and C_S and C_F are the concentrations of sulphide and iron in the reservoir in mols cm^{-3}. The concentration of sulphide used in this equation is 0.04M (4×10^{-5} mols cm^{-3}) and was the typical maximum sulphide concentration produced in similar agar experiments (S.J. Bale pers. comm.). The diffusion coefficients are assumed to be accurate but as the experiments were incubated at 20°C rather than sea water temperatures and in gel systems rather than in aqueous ones it is likely that the rate of diffusion is to be different. As the diffusion coefficients are likely to have changed in a similar way, ratios of the diffusion coefficients were also used in equations (Eq. 4.2), which also produced a radius of maximum pyrite precipitation of 10.5 cm.

$$R_{j\,max} = \frac{a\left(\frac{D_S C_S}{D_F} + C_F\right)}{C_F} \qquad \text{Eq. 4.2}$$

All the sets were inoculated with a mixed culture of sulphate-reducing bacteria from the Severn Estuary which had been incubated in a medium of Postgates salts and homogenized shrimp.

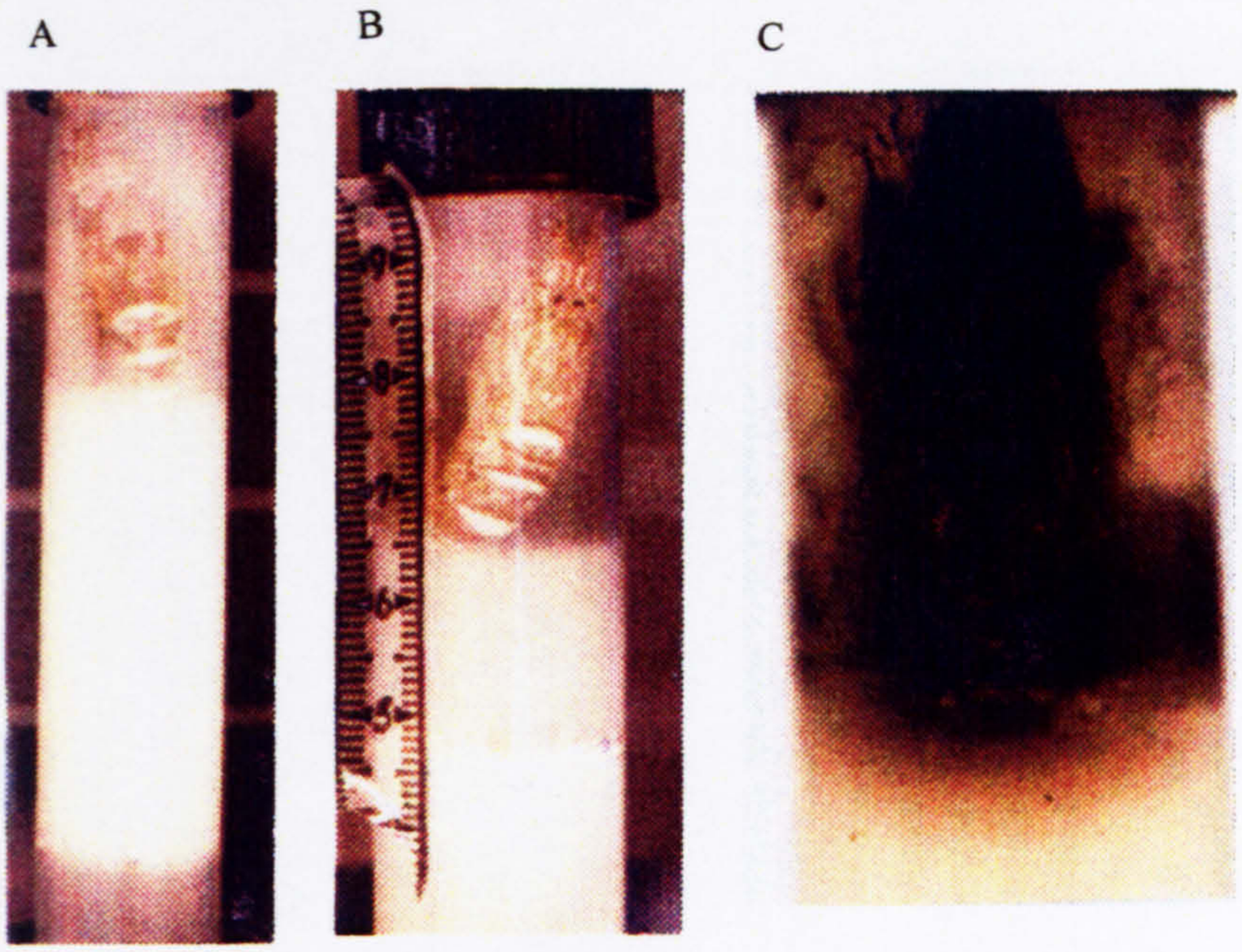

Figure 4.7 - Starting conditions of gel-stabilised experiments. A - gel with 5mM iron at the base of the tube; B - gel with 5mM iron surrounding the shrimp; C - Lepidocrocite covered shrimp.

Set 1 - These contained 15ml of a 5mM ferrous sulphate (5 x 10^{-6} mols cm^{-3}) dissolved in the Postgates medium and agar solution, which was placed under the shrimp.

Set 2 - These contained 15ml of 5mM iron in Postgates medium and agar solution, at the base of the tube. This placed the shrimp 4cm above the iron source (Figure 4.7A).

Set 3 - These contained 15ml of 5mM iron in Postgates medium and agar solution around the shrimp (Figure 4.7B).

Set 4 - These contained a 0.1mM iron in Postgates medium and agar solution around the shrimp (Figure 4.7C). Raiswell *et al.* (1993) stated that sedimentary iron concentrations rarely exceed 0.1mM so this was chosen as a reasonable concentration to compare to 5mM iron. A 0.1mM concentration of iron gives a radius of maximum pyrite precipitation of 505.2cm.

Set 5 - The shrimps in these experiments were coated in lepidocrocite before being suspended in a Postgates medium and agar solution (Figure 4.7D). The concentration of lepidocrocite used was higher than the concentration of ferrous iron used in sets 1 to 4. Approximately 4.5 grams (2.6 x 10^{-3} mols cm^{-3}) was weighed out and each shrimp was rolled in it prior to drying. This produced an R_{jmax} value of 0.53cm for a shrimp of 0.5cm in diameter.

Each experiment was duplicated six times as the sampling is destructive, and were incubated at 20°C. After photographing, the experiments were profiled with a sulphide microelectrode to determine the concentration and distribution of hydrogen sulphide ions prior to being extruded and sliced into 5mm sections from the top of the gel downwards. These sections were then digested in order to determine the concentration of other sulphur pools using chromous chloride digestions. Unlike the samples from the bacterial experiments, the gels were digested sequentially and as soon as possible after sampling as the slices oxidised quickly. The temperature of the initial acid digestion was 90°C as it had to be sufficient to melt the gel.

Fragments of the shrimps were also removed from the agar and chemically dried (see Appendix 8 for method) for SEM analyses.

4.F.2 - Results

The data are listed in Appendix 9, graphs are shown in Figures 4.8 to 4.12, and SEM photographs of the organic particles are shown in Figures 4.13 and 4.14.

AVS, pyritic sulphide and elemental sulphur profiles for each set of experiments show the diffusion of sulphide out of the shrimp into the gels and its transformation from AVS to pyrite. Hydrogen sulphide profiles are not included in the graphs as the concentrations of hydrogen sulphide measured never exceed 1mM.

4.F.2.1 - Set 1- Iron below shrimp - Set 1 experiments showed the development of a series of profiles for each reduced sulphide species from a peak below the 'shrimp' at 3.5cm to a profile with a large peak below the shrimp at 3cm depth, by day 6. After 10 days the concentration of sulphide had increased in the gel above 4.5cm depth, with large peaks in sulphide concentration up to the shrimp and smaller above it to the surface (Figure 4.8). The internal tissues within the carcass had become sloppy and white due to muscle shrinkage (Briggs and Kear, 1994), and there was no sulphide within the shrimp. The system became more pyrite dominated below the shrimp (%AVS/PS average 59%) and AVS dominated above and around it (%AVS/PS average 78%). The hydrogen sulphide concentration profile from the shrimp to the surface of the gel also showed an increase above the shrimp, although it was not possible to probe beneath the shrimp. The continuing diffusion of iron and sulphide throughout the gel system means that the black colour of AVS spreads further down the tube and the peaks become less distinct.

4.F.2.2 - Set 2- Iron at base of tube - The day three profile in this experiment showed an AVS peak at the base. This peak then moved up the gel as dissolved ferrous ions migrated from the reservoir into the iron free agar, and met sulphide diffusing downwards from the shrimp. Iron diffuses up the tube, before sulphide begins to leave the carcass. This is due to the time that it takes for sulphate reduction to start and for the concentrations of hydrogen sulphide to reach levels where it diffuses out of the carcass. Peaks subsequently developed around the shrimp and at approximately 6 cm where there was a visible change in the concentration of precipitated iron sulphides. The tube was clear above this 6cm point until day 17 when the whole tube became blackened (Figure 4.9-day 17). The precipitation front started to move closer to the shrimp from the iron source. After 67 days, the peak of sulphide concentration was at 4 cm and there was a gradual decrease in the amount of

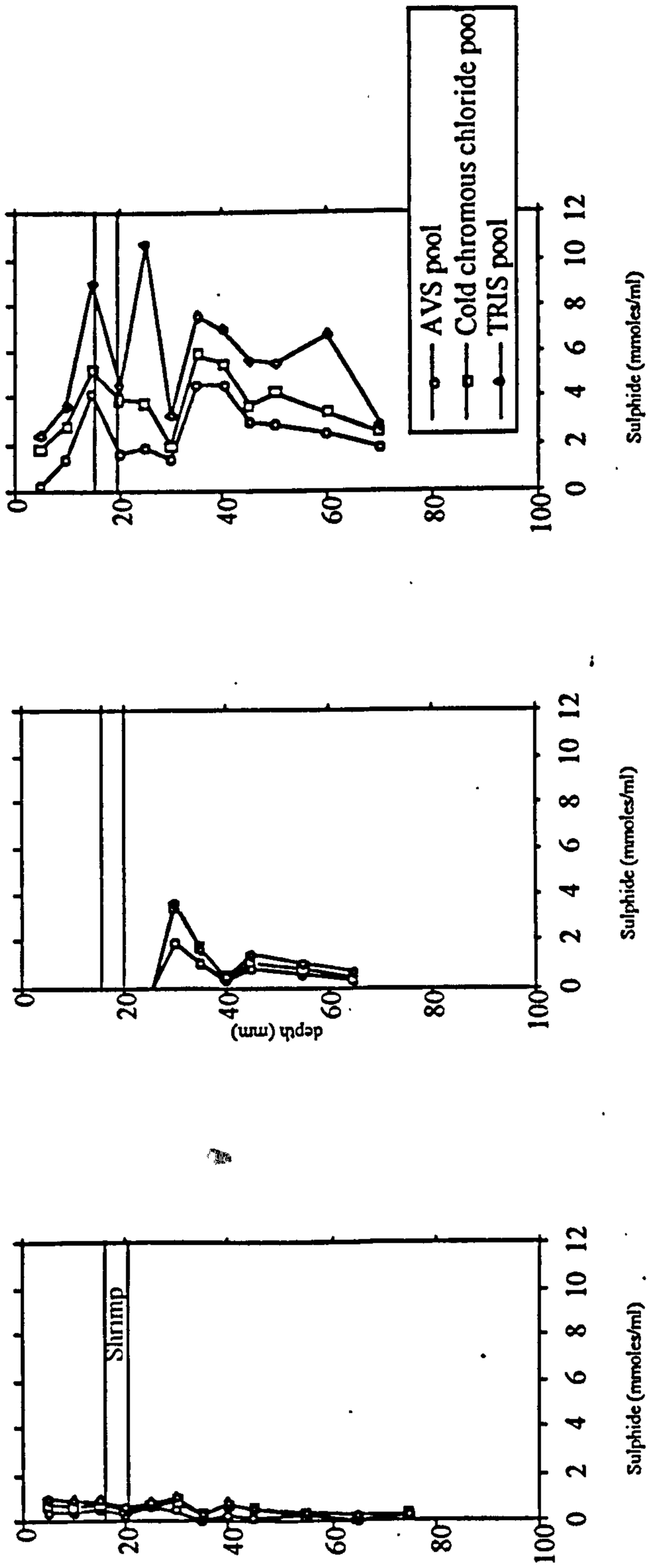

Figure 4.8 - Variations in the concentrations of reduced sulphur species in experiment 1. (AVS concentrations include acid-volatile sulphide and hydrogen sulphide concentrations. Chromous chloride concentrations contain AVS and pyritic sulphide concentrations, while TRIS concentrations contain the chromous chloride pool and elemental sulphur concentrations).

Figure 4.9 - Diagrams showing the changes observed in experiment set 2. The graphs show the changes in the cumulative concentrations of reduced sulphur species (AVS-circles; cold chromous chloride fraction-triangles; TRIS-filled triangles). The schematic diagrams show the changes in colour seen in the gel as iron sulphide precipitation occurs.

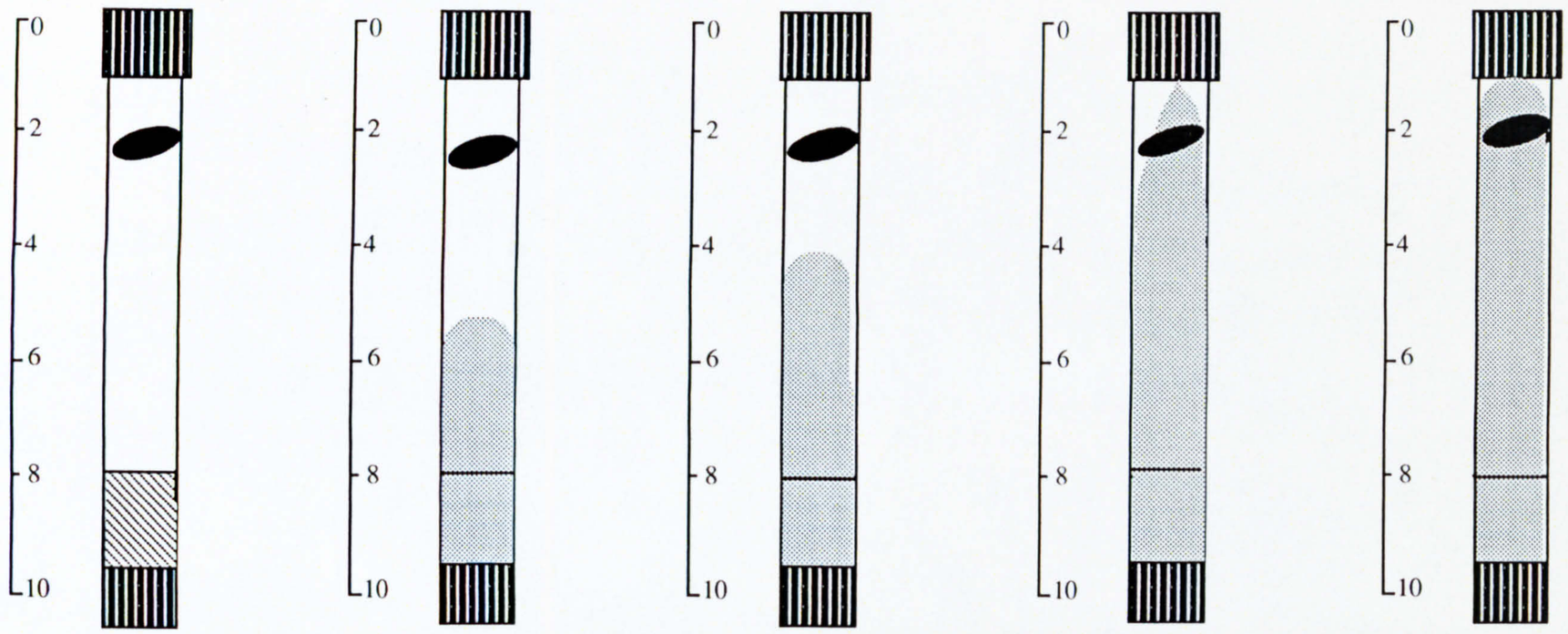

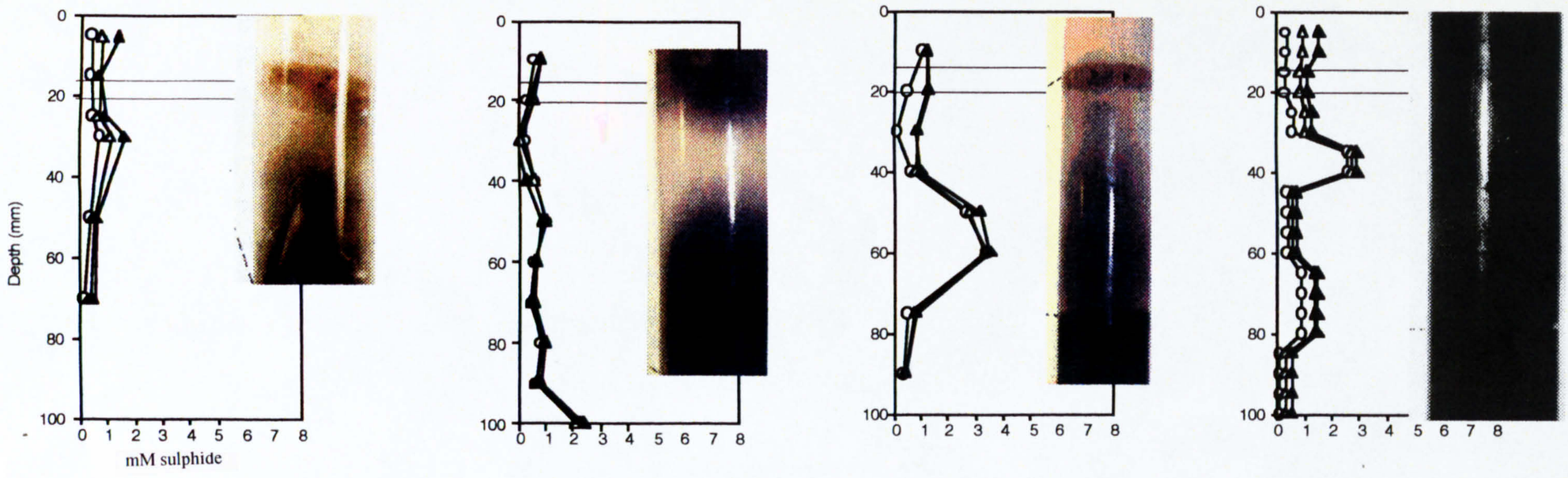

sulphide and hence in the blackening of the gel. The shrimp had no black mineralisation associated with it and the internal tissues became white and slushy. Little pyrite or elemental sulphur were observed in this experiment, and AVS remained the dominant reduced sulphide species.

4.F.2.3 - Set 3 - Iron surrounding shrimp - The majority of the precipitated sulphides in these experiments were found around the shrimp and below it into the iron rich layer beneath the shrimp. The development of peaks below the shrimp was similar to that seen in Set 1. The initial sulphide peak was found at 1cm depth. This peak remained throughout the experiment and additional sulphide peaks occurred beneath it (Figure 4.10). The internal tissues of the carcass became sloppy and remained white. No sulphides were observed and there was no precipitation of black minerals within the carcass or on the surface of the cuticle (Figure 4.14F and G). After 17 days pyrite became more abundant with an average %AVS/PS of approximately 345% rather than 833% of day 10, and this was replaced by elemental sulphur after 67 days due to some leakage around the top of the tube and a decrease in the concentration of hydrogen sulphide produced by the culture. Black colouring on day 67 was restricted to the iron rich layers and the shrimp had no black encrusting material, although calcite precipitation was observed on the carapace under the SEM (Figure 4.14).

4.F.2.4 - Set.4 - 0.1mM iron surrounding the shrimp - The initial precipitation of AVS occurred around the shrimp and this spread upwards so that the top 2cm became the zone of sulphide precipitation. The concentration of hydrogen sulphide also steadily decreased. The precipitates in the top 2 cm of this experiment were dominated by AVS (averages of 3mM AVS and 2mM pyritic sulphide after 17 days; Figure 4.11). After 67 days, AVS was still the dominant phase. The experiment profiles showed a large peak in the top 1 cm of the experiment, below which two smaller peaks were observed, one of which corresponded to the layer containing the shrimp. The shrimp still contained white liquified tissues and there was no external encrustation, although small concentrations of AVS were found in association with it (1.55mmoles ml^{-1} of shrimp). The other peak corresponded to the lower zone of the iron layer beneath the shrimp. Below this layer, sulphide concentrations decrease. The blackened colouring of the gel reflects this pattern as it decreases and disappears below the iron layer .

4.F.2.5 - Set 5 - Lepidocrocite coated shrimps - <u>The gels</u> **-** The association of iron with the shrimp meant that no hydrogen sulphide was measured in the gel above and

Figure 4.10 - Diagrams showing the changes observed in experiment set 3. The graphs show the changes in the cumulative concentrations of reduced sulphur species (AVS-circles; cold chromous chloride fraction-triangles; TRIS-filled triangles). The schematic diagrams show the changes in colour seen in the gel.

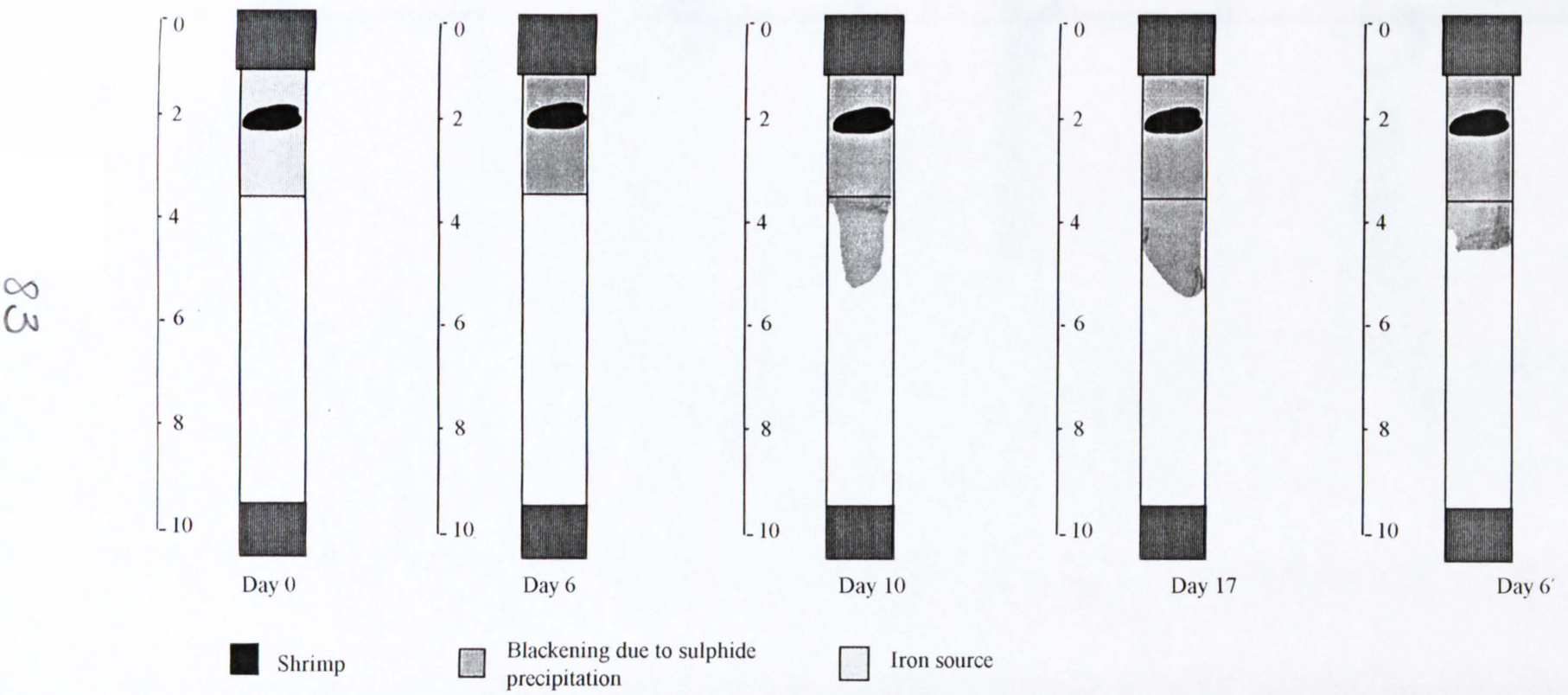

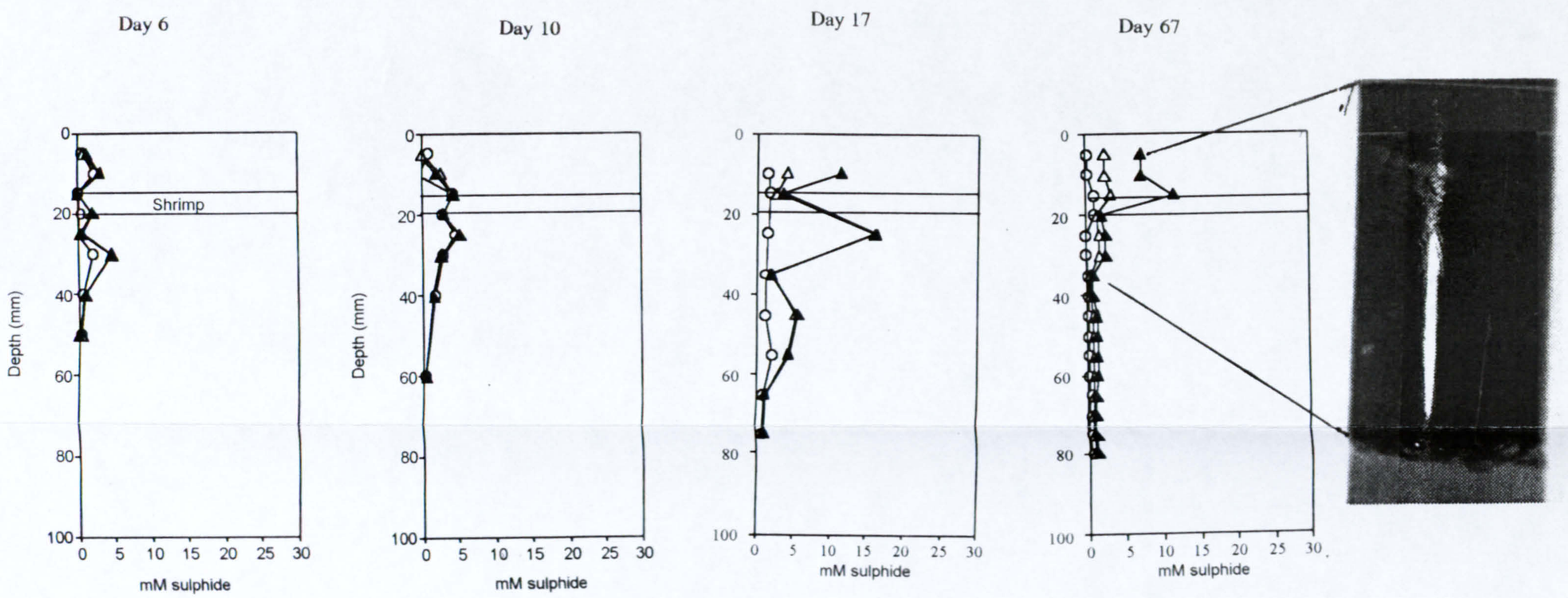

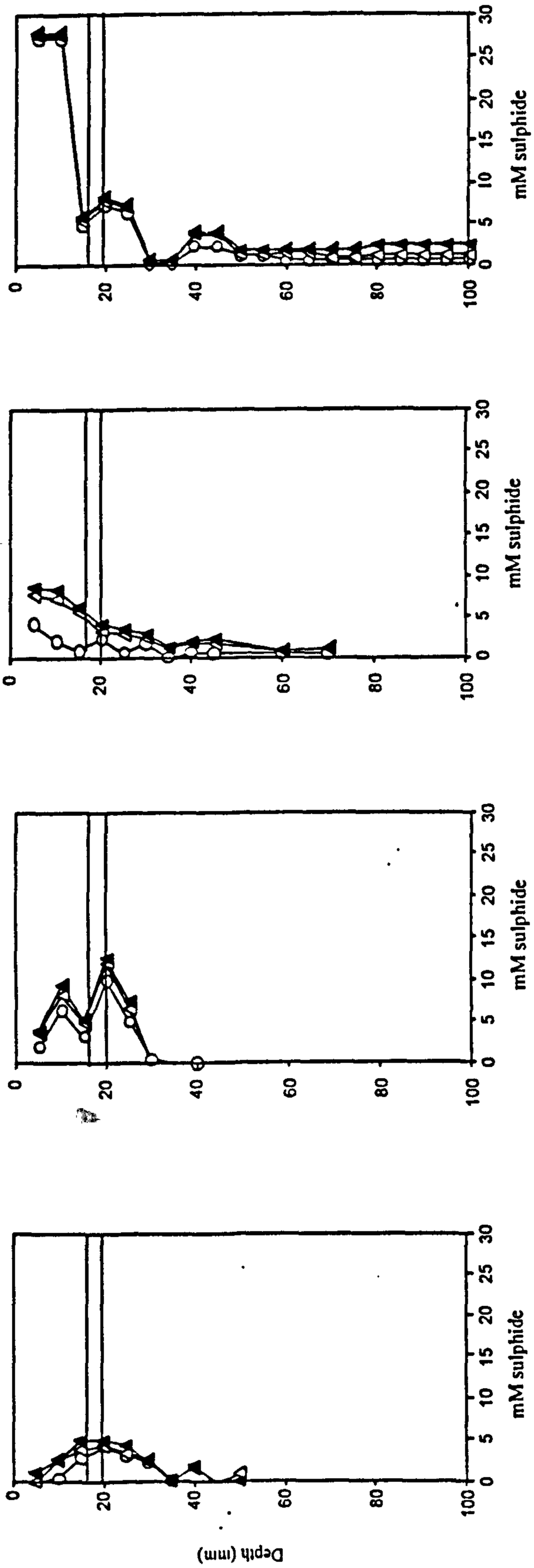

Figure 4.11 - Graphs showing variations in cumulative concentrations of AVS (circles), pyritic sulphide (triangles) and elemental sulphur (filled triangles) in gel-stabilized experiment set 4 - 0.1mM iron surrounding the shrimp

around the carcass. The sulphide peaks were also limited to the immediate vicinity of the shrimp and above and below it as some of the iron oxyhydroxide was reduced, by hydrogen sulphide or bacteria, to mobile ferrous ions. This was observed in the colour of the gel which started off black in the immediate vicinity of the carcass, and by day 10 was black above and below it (Figure 4.12). Unlike the other gel experiments, the iron sulphide pool was not dominated initially by AVS and then by pyrite as the concentration of sulphide increases. Pyritic sulphide concentrations in the gel remained larger than AVS concentrations from day 6 (an average of 0.42mM AVS and 1.6mM pyritic sulphide; Figure 4.12). Elemental sulphur concentrations were variable in the experiment but it is not the dominant phase unlike the case on day 67 of the set 3 experiments. Below the peaks there was a gradual decrease in the amount of solid sulphide measured. The width of this sulphide precipitation band increased throughout the experiment, and became gradually more prominent below the shrimp (Figure 4.12).

The carcasses - The carcasses in this experimental set, unlike the previous ones, did not contain white liquified muscle tissue. By day 67, the majority of the internal tissues of the shrimp had disappeared and the remainder had become blackened (Figure 4.13A). This blackened material was hard and when examined under the SEM was a cylinder with thick walls of irregular appearance. These walls were mineralized with crystal bundles of calcium carbonate, biofilms of iron sulphide and encrusting bacteria (Figure 4.13 and 4.14). High concentrations of sulphides were associated with the hardened material and the carcass, with AVS concentrations ranging from 1.69mmols ml^{-1} of shrimp to 22.59mmols ml^{-1} of shrimp and pyritic sulphide concentrations ranging from 5.99mmols ml^{-1} of shrimp to 13.78 mmols ml^{-1} of shrimp on day 67. This was much higher than the concentrations seen in set 4, with AVS concentrations of around 1.55mmols ml^{-1} of shrimp and pyritic sulphide concentrations of around zero. The exterior of the carcass was also very black and when examined under the SEM this was covered with encrusting bacteria (Figure 4.13) as in the experiments which used aqueous medium described in section 4.E.

4.F.3 - Using the data from the experiments

The distances at which sulphide precipitation occurs and the amount of sulphide produced can be used in the equations outlined by Raiswell et al. (1992) to calculate parameters such as the first order rate constant for sulphate reduction at this temperature. Other equations such as equation 4.1 can also be used to calculate the

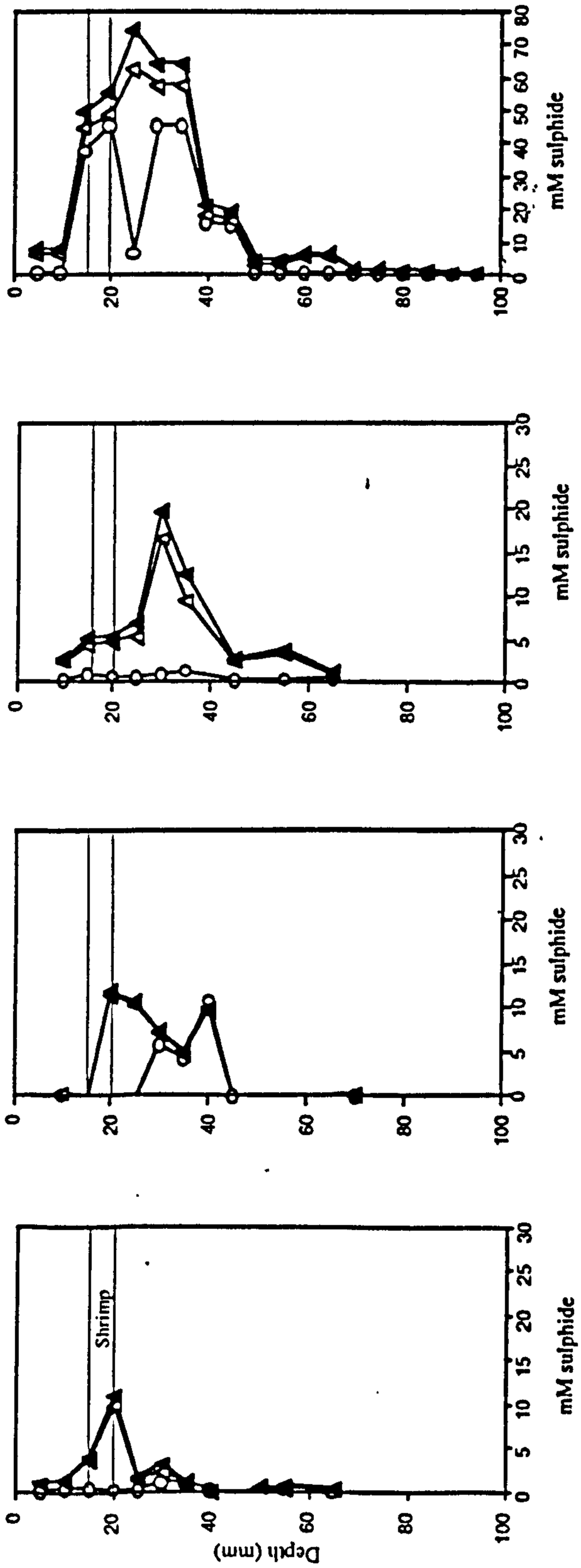

Figure 4.12 - Graphs showing variations in the cumulative concentrations of AVS (circles), pyritic sulphide (triangles) and elemental sulphur (filled triangles) in gel-stablised experiment 5 - lepidocrocite coated shrimps.

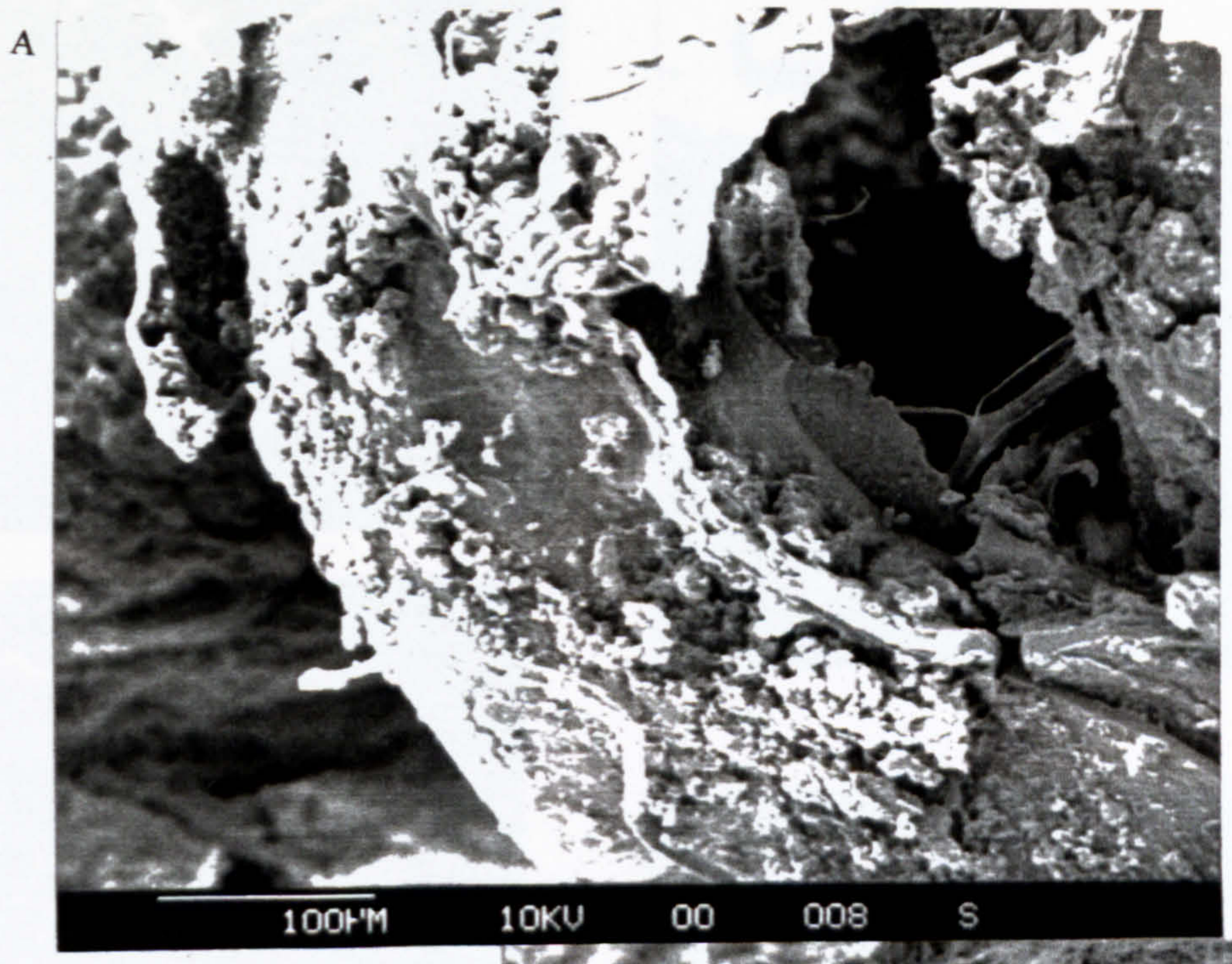

Figure 4.13 - Details of structures in association with the hard interior of the shrimp in gel experiment 5. A, B and C - details of the wall of the hardened interior

A

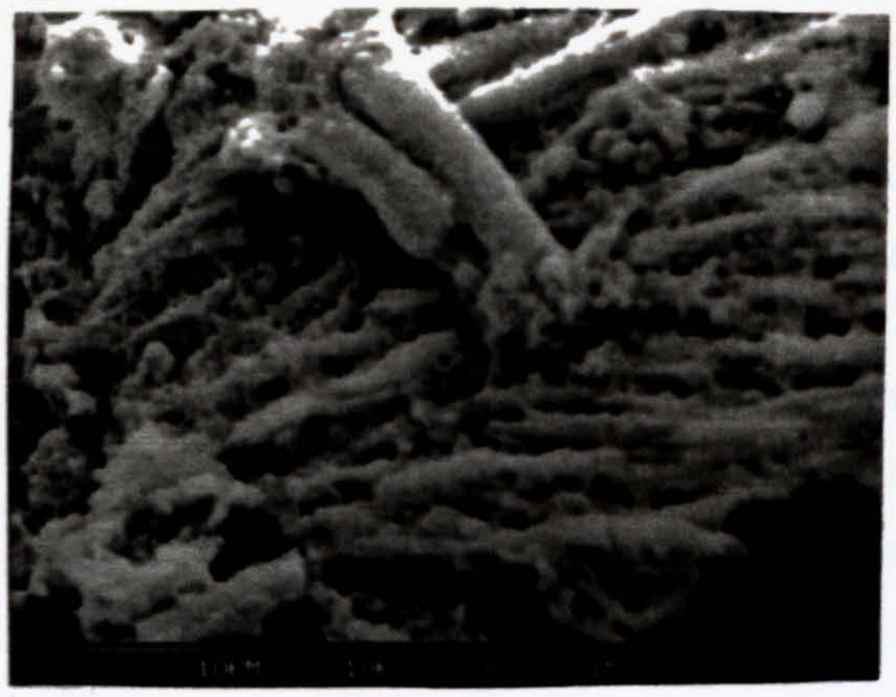

B

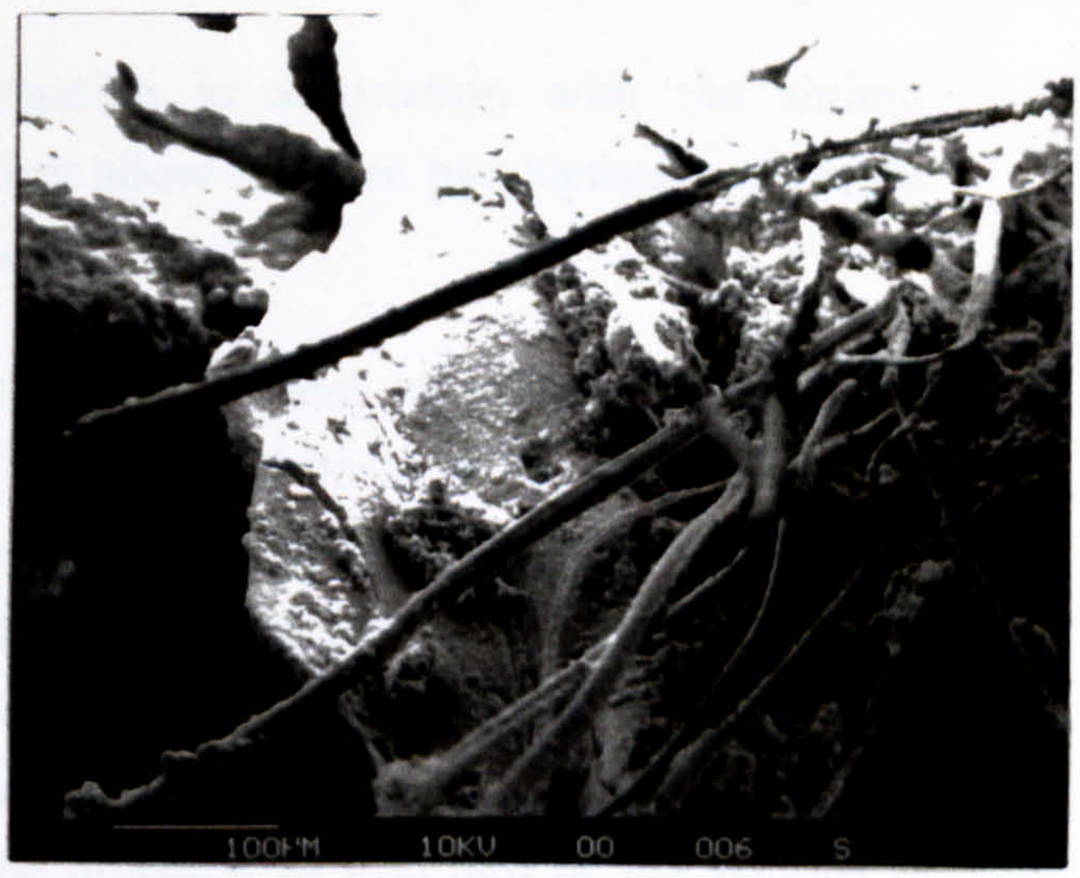

C

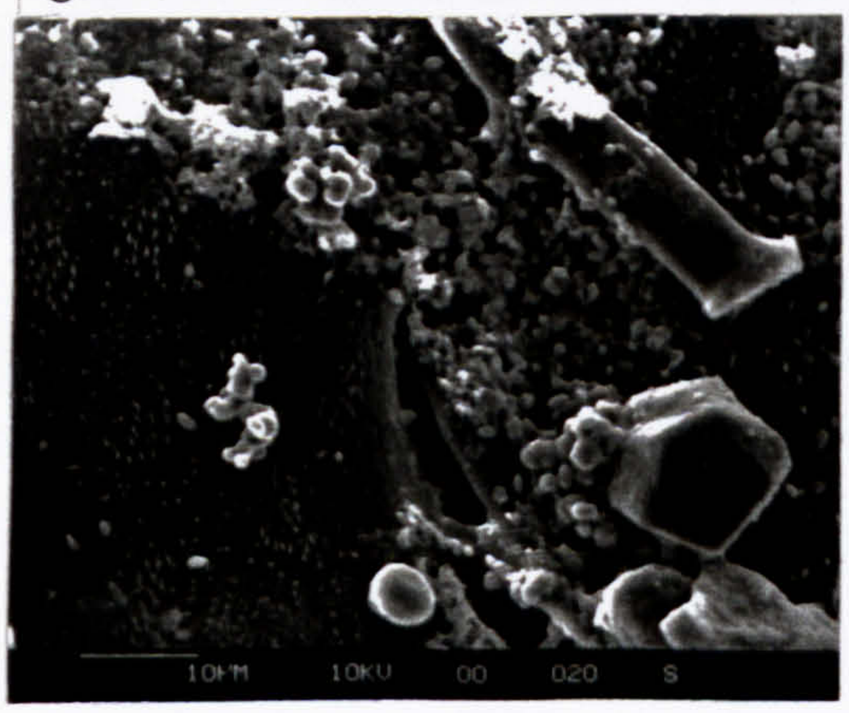

D

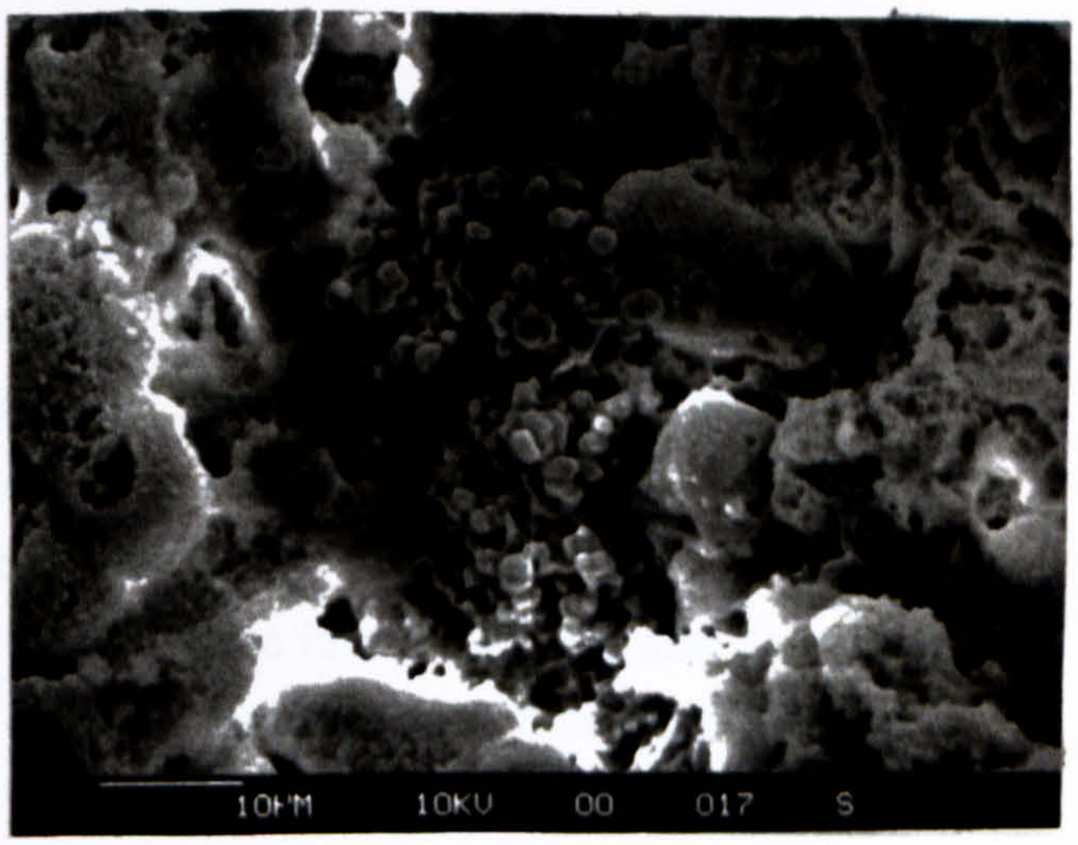

E

F

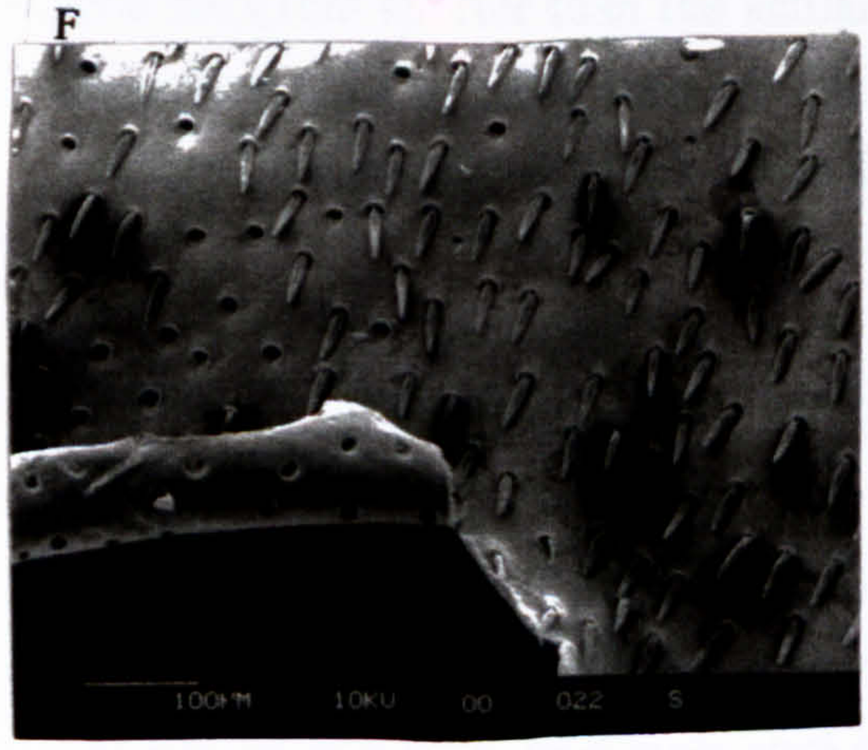

G

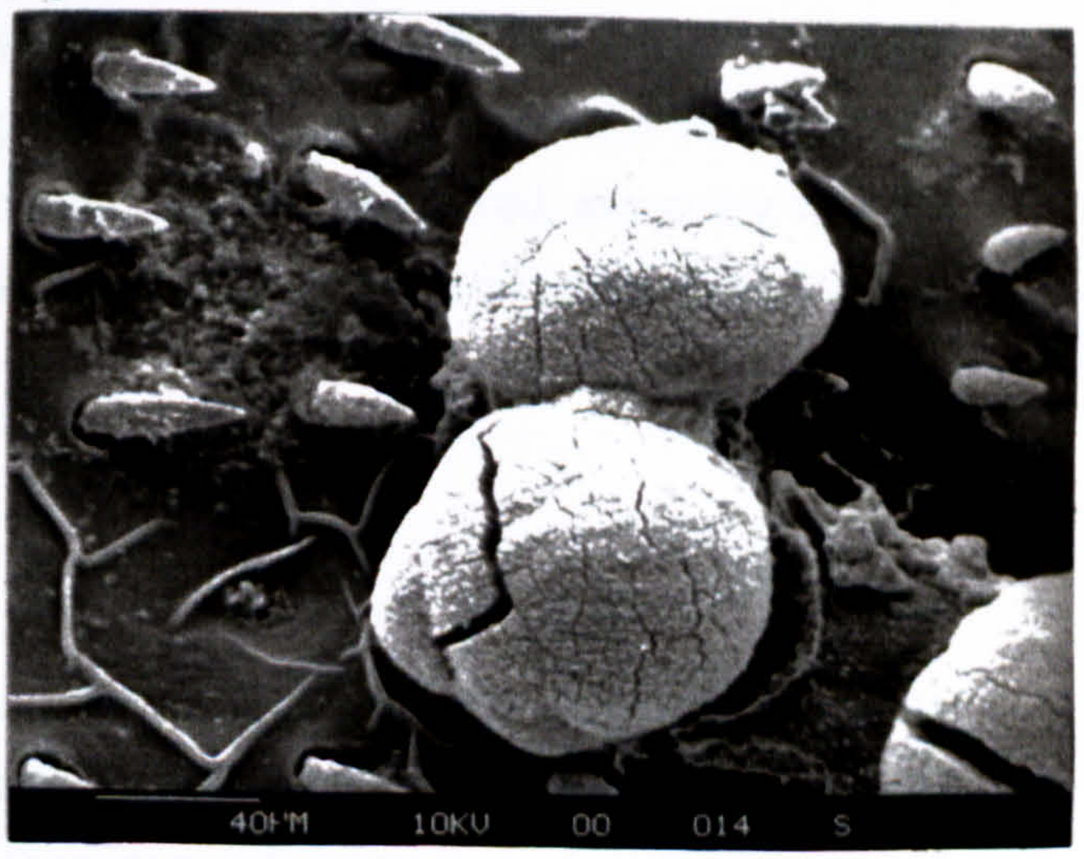

Figure 4.14 - A to E - Details of structures in association with the hard interior of the shrimp in gel experiment 5, F and G - cuticle from experiment 4.

amount of iron required for pyrite formation in association with the shrimp. Individual experimental sets are useful as they allow different parameters, such as the diffusion rate of iron in the gels, to be modelled.

Set 5, the lepidocrocite coated shrimps, is ideal to calculate the rate of sulphide generation and diffusion out of the shrimps because the majority of the sulphide appears to have been precipitated within a short distance of the carcass, causing the development of mineralization within the carcass. The precipitation distance is short, so that the radius of the shrimp, and the radius of the surface through which the hydrogen sulphide diffuses prior to precipitation may be assumed to be equal. This does not account for the diffusion of iron into or the regions of sulphate reduction within the shrimp.

After 67 days a concentration of 2.89×10^{-4} mols cm^{-3} of TRIS is observed. This relates to a rate of sulphate reduction of 1.8×10^{-3} mols cm^{-3} yr^{-1}, assuming that hydrogen sulphide is not being consumed by reducing ferric oxyhydroxide (lepidocrocite) to ferrous iron ions. If hydrogen sulphide is consumed by ferric iron reduction then the flux calculated will be too small, as it does not include the concentration of sulphide required to reduce 2.6×10^{-3}mols cm^{-3} of iron. Including this value will produce a rate of sulphide generation of 0.01 mols cm^{-3} yr^{-1}. It is likely that some ferric iron reduction occurred as iron diffuses into the shrimp and down the tube but it is difficult to estimate. Lower rates of hydrogen sulphide generation are produced in the experimental sets due to the greater rate of oxidation of hydrogen sulphide at the ends of the tubes, and the diffusion of hydrogen sulphide into these areas.

If a shrimp is considered to be a cylinder with a radius of 0.5 cm, and a length of 4 cm (1cm shorter than the actual length of the shrimps to allow for its tapering), then the flux of sulphide through this shrimp can also be calculated, assuming that the radius of the surface through which diffusion is occurring is equal to the radius of the shrimp.

$$\text{Sulphide.Flux} = \frac{a\pi r^2 l}{2\pi r^2 + l\pi 2r} \qquad \text{Eq.4.2}$$

where a is the rate of sulphide reduction, r is the radius of the shrimp and l is its length (Raiswell *et al.*, 1993). This produces a value of sulphide flux from its site of generation of 9.07 x 10-4 mols cm^{-2} yr^{-1} when iron reduction by hydrogen sulphide is not included.

The rate of sulphate reduction may also be used to calculate the first order rate constant (k) for sulphate reduction, using Berner (1964) equation which states:

$$k=R/-LG \qquad \text{Eq.4.3}$$

where L is the stoichiometric coefficient for sulphate reduction with respect to the number of moles of dissolved sulphide produced from organic matter (0.5) and G is the concentration of metabolizable organic matter. This equation produces values of k which are approximately 0.1 yr^{-1}. k values of similar magnitude are derived for each experimental set, and this value is consistent with rate constants obtained in other laboratory experiments (Middleburg, 1989).

4.F.4 - Discussion of gel stabilised systems

The gel stabilised systems provide a stable and visual method of observing the diffusion gradients associated with the decay by sulphate reduction of organic particles. Diffusion is an essential part of sulphide precipitation. The systems show a) the effect of having a limited iron pool in association with a large carcass (sets 1,3 and 4) and b) the effect of having a large iron pool in association with the carcass (set 5). In the first case, the amount and distance of sulphide precipitation is controlled by the availability of iron. As the concentration of hydrogen sulphide increases within the carcass, iron diffuses through the gel, so that iron sulphide precipitation is associated with the carcass initially, but over time, both iron and sulphide diffuse away from the decay site. The radius of iron sulphide precipitation occurs at is much greater than the thickness of the shrimp layer (Berner, 1969) but the Raiswell *et al.* (1993) equation produces values of maximum precipitation distances which are much higher than those actually achieved. For example, the equation predicted that the maximum precipitation distance for the experiment containing 0.1mM iron was 501cm (using the ratio of iron and sulphide diffusion coefficients). Instead of which the maximum depth of sulphide precipitation was 8.5 cm and the depth of maximum concentration was 4cm in a 12 cm tube (Figure 4.11-day 67). The depth of maximum sulphide precipitation is around 4cm in all four experiments. This is because the model used by Raiswell *et al.* (1993) assumes that no oxidation occurs in the system and that one of the reservoirs of reagents, in this case iron, is infinite. This is not the situation in the gel systems nor is it true in sedimentary systems where oxidation via oxide minerals is important, and low concentrations of iron will be rapidly consumed.

The effect of a large iron pool in association with the shrimp (set 5) was to precipitate higher concentration of sulphides in the area surrounding the organic particle, and within it. However, some iron began to diffuse away from the decay site down the tube and into the carcass. Sulphide precipitation became dispersed and, although the predicted R_{jmax} was around the 0.63cm for 67 days (TRIS 2.89×10^{-4} mols cm^{-3}; Iron 2.6×10^{-3} mols cm^{-3}). In this case Raiswell *et al.* (1993) model using ratios of diffusion coefficients gives a realistic radius of maximum pyrite precipitation, as the highest concentrations of pyrite are found within the carcass. Raiswell *et al.* (1993) suggested that 0.1 is a realistic value for the ratio of sulphide to iron in order to confine pyrite precipitation to the decay site. The ratio of sulphide to iron in the lepidocrocite gel experiment was 0.11, and pyrite formation occurred both outside and inside the carcass. This may have been because the concentration of hydrogen sulphide produced was greater than the measured concentration due to loss from diffusion out of the tube and oxidation by lepidocrocite. Assuming the sulphide to iron ratio needs to be less than 0.1 to confine pyrite to the carcass the experiment would require at least 3×10^{-3} mols cm^{-3} of ferrous iron. This is an extremely high concentration for sediments when the average concentration of reactive iron is 0.1mM (1×10^{-7} mols cm^{-3}; Raiswell *et al.*, 1993) and concentrations of 0.2mM (2×10^{-7} mols cm^{-3}) to 0.8mM (8×10^{-7} mols cm^{-3}) were measured for Tamar Estuary sediments (J.A.Kelly pers.comm.).

The diffusion of hydrogen sulphide and/or iron ions through the gel-stabilised experiments was affected by the precipitation of these ions. This meant that in all but set 4 of the gel-stablised experiments the rate of hydrogen sulphide diffusion was not proportional to time, and the maximum depth of the diffusion fronts oscillated back and forth. This is due to a system of reaction-transportation feedbacks (Ortoleva, 1994), which also formed two discrete iron sulphide peaks within an experiment. In experiment sets 1 to 4, the iron source was able to diffuse through the gel-stablised system before bacterial sulphate-reduction occurred. Therefore, as hydrogen sulphide diffused out of the carcass it entered an iron-rich environment. This coupled with the larger diffusion coefficient of hydrogen sulphide means that hydrogen sulphide can be regarded as a non-equilibriated fluid flowing through a iron-rich solid. The iron reacted with the hydrogen sulphide precipitating, in the first instance, acid-volatile sulphide. This process depleted both the hydrogen sulphide pool and the iron pool and additional ions diffused into the precipitation site. Under these conditions a form of self organisation called Liesegang banding occurred (Liesegang, 1913). This is a cycle of supersaturation, nucleation and depletion which occurs due to the repression of mineral nucleation at one point in space by the consumption of reagents at another

(Ortoleva *et al.*, 1987). Banding formed in all the experiments containing low iron concentrations, unlike the suggested occurrence of Liesegang banding in iron sulphide systems with an intermediate iron concentrations (Berner, 1969).

As the likely reaction mechanism for the formation of pyrite in these gel-stablised experiments is hydrogen sulphide oxidation (Eq.4.3), hydrogen sulphide is consumed by the reaction to precipitate acid-volatile sulphides and the reaction to convert acid-volatile sulphides to pyrite.

$$H_2S\ (g) + Fe^{2+}\ (aq) \longrightarrow FeS\ (s) + H_2\ (g)$$

$$FeS\ (s) + H_2S\ (g) \longrightarrow FeS_2\ (s) + H_2\ (g)$$

Eq .4.3

This consumption of hydrogen sulphide causes a diffusion gradient, bringing more hydrogen sulphide into the site of acid-volatile sulphide precipitation. This initially causes the reaction zone to become supersaturated with respect to acid-volatile sulphides and then to pyrite. The precipitation of pyrite in this zone of supersaturation causes the dissolution or diffusion of AVS precursors into the zone, in much the same way as the precipitation of AVS precursors causes hydrogen sulphide diffusion. These processes move the initial precipitation front backwards, forming a peak of iron concentrations behind it. As sulphate reduction continues, the hydrogen sulphide diffusion front moves down the tube. Once this has reached a sufficient distance from the initial zone, and the concentrations of hydrogen sulphide and acid-volatile sulphides are no longer limiting, a new zone of iron sulphide precipitation develops, producing banding. These bands developed significantly in experiment set 2 where the iron source was at the base of the tube, and they were observable in set 3 and 4 where they are poorly developed and closer together due to the association of the iron source with the carcass. Set 5, the lepidocrocite coated shrimps, differ from the other gel-stablised experiments as diffusion of iron and hydrogen sulphide are linked. The ferric iron ions can not diffuse away from the carcass until they have been reduced by hydrogen sulphide. This produced a large pyrite peak by day 6 because the reagents were concentrated spatially. However, as iron and sulphate reduction continues the iron sulphide peak migrated down the tube, illustrating the effect of the supersaturation-nucleation-depletion feedbacks (Ortoleva *et al.*, 1987).

4.G Sediment incubations

Experiments were set up in order to see if the processes of diffusion and precipitation observed in the gel-stablised experiments were observable in sediments. Sediment from the Severn Estuary (Aust Cliff, Avon, UK) was incubated in 10 cm plastic core tubes after mixing in iron and dried algae and removing as many *Nereis* as possible, which were sealed at one end with a rubber bung. One *Crangon crangon* carcass was then buried at approximately 5cm depth within the tubes. Tubes which did not contain carcasses were set up as a control. The sediment filled columns were incubated in a tank filled with sea water in a 15°C constant temperature room. This sediment was selected because it was easily accessible, and contains framboidal pyrite. It also has a high carbonate content which requires 10ml of 6M HCl for each AVS digestion.

The sediment was sampled by slicing the core into 1cm slices. A subsample of the slice was used for solid sulphide digestions and the remaining sediment centrifuged for porewater analysis of sulphate, hydrogen sulphide and in some cases iron concentrations. The sediment digestions were left to react for 4 hours. Half of the recovered remains of the carcass was examined under the light microscope and prepared for SEM analysis, while the rest was digested.

4.G.2 - Results of sediment incubations

After 4 days, the core profile shows an increase in all the reduced sulphur species analysed with depth (Figure 4.15A). The tube takes some time to develop anoxia and zones of sulphate-reduction. After 12 days, an increase in sulphide concentrations is observed below the carcass, which reflects the increased sulphate reduction occurring within it (Figure 4.15B). Higher concentrations of iron sulphides are found above and below the carcass as iron diffuses into the sediment surrounding it. This prevents AVS and pyrite precipitation in the rest of the sediment. The iron sulphides analysed are approximately 50% AVS and 50% pyritic sulphide after 12 days (12mM AVS and 9mM pyritic sulphide) but these precipitates are not found within the carcass. After 68 days, it is no longer possible to retrieve any fragments of the carcass, however, there is now a high concentration of iron sulphides below the layer which previously contained it. The sulphide species are AVS dominated (54mM AVS around the carcass) rather than pyritic (10mM) (Figure 4.15C). The increase in monosulphide rather than bisulphide species is due to the availability of iron oxides or oxyhydroxides. The concentration of pyrite within the core does increase from day

Figure 4.15 - Cumulative reduced sulphur species profiles from incubations of Severn Estuary sediments (● is acid-volatile pool, ■ is the cold chromous chloride pool and ◆ is the TRIS pool) (Appendix 10)

A - Sediment incubation after 4 days.

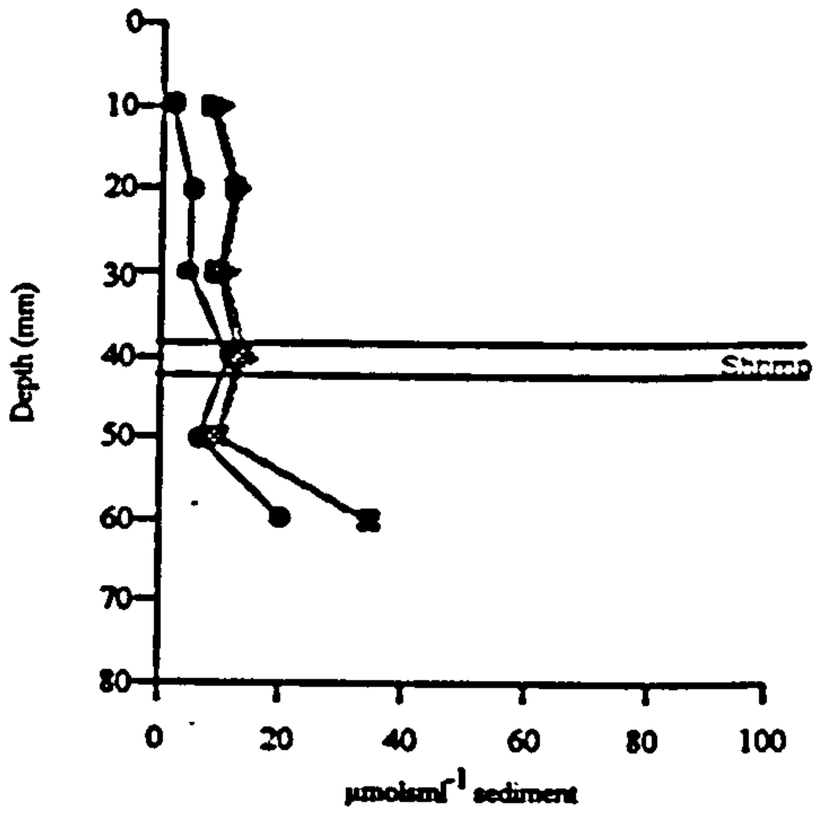

B - Sediment incubation after 12 days

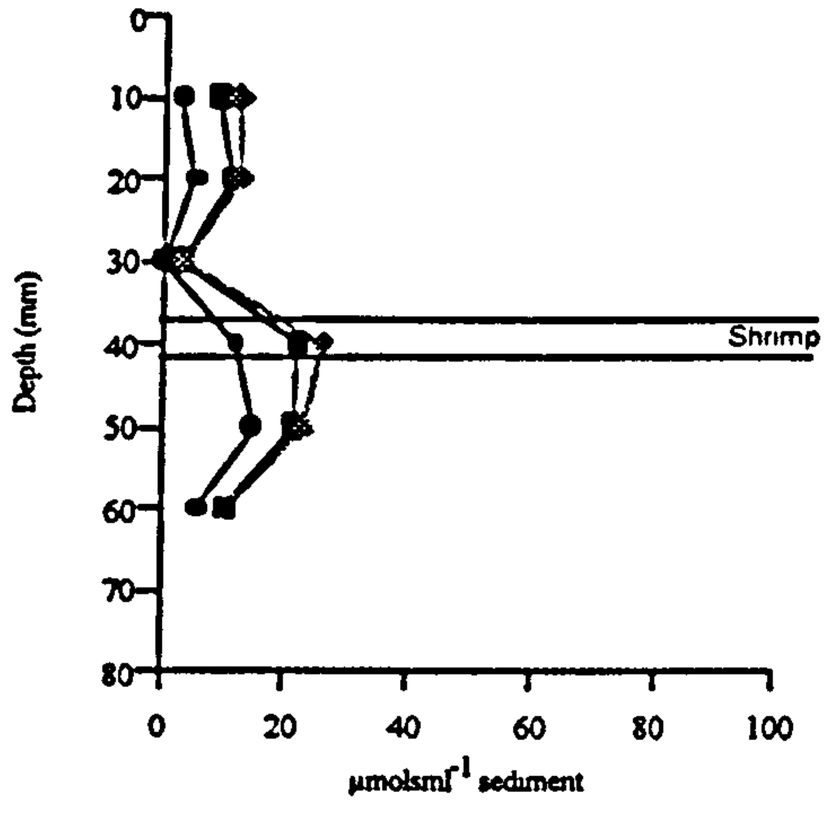

C - Sediment incubation after 68 days.

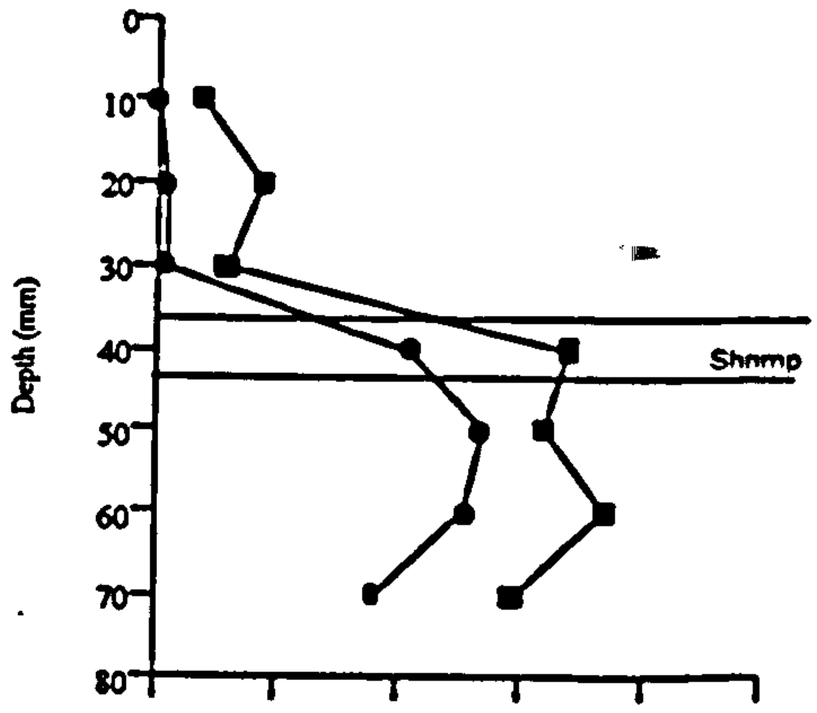

D - Sediment incubation after 12 days

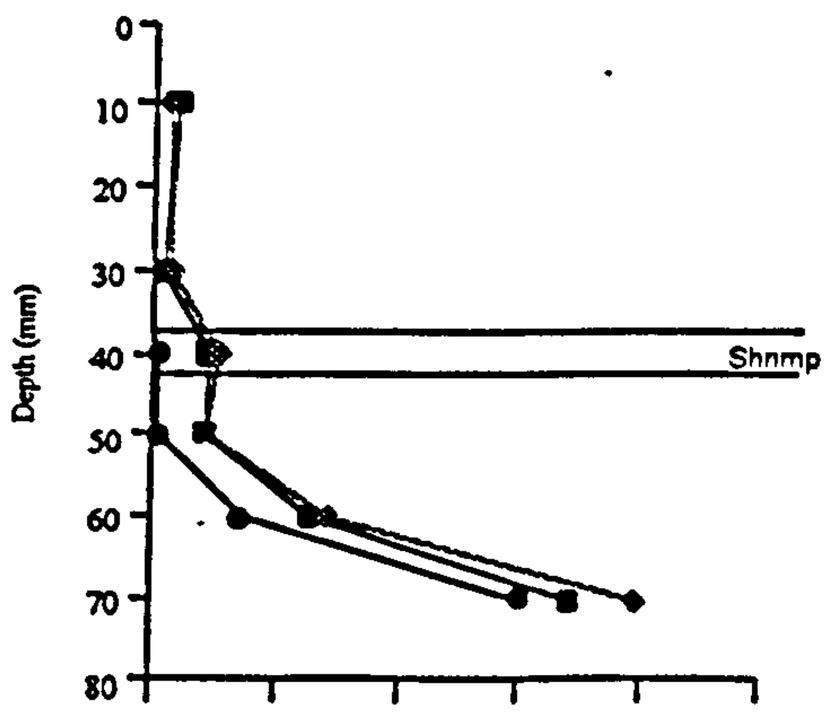

12 to day 68 but the increase is not as large as that of the AVS concentrations. The increased width of the iron sulphide peak is due to the reaction and precipitation of hydrogen sulphide as it moves through iron-rich sediments. This is similar to the profile seen in gel-stabilised experiments 1 to 4, as is the downward movement of hydrogen sulphide. This movement may be driven by oxygen diffusion into the top of the tube as the rate of sulphide production decreases, as the sediment incubation where bioturbation occurred develops a similar, but more extreme, profile (Figure 4.15D).

4.G.3 - Conclusions drawn from sediment incubations

The sediment profiles are very similar to those obtained from the gel experiments containing low iron concentrations. They show a peak of sulphide surrounding the carcass which widens over time, as hydrogen sulphide diffuses out of the carcass and precipitates to iron sulphides. Like the gel-stablised experiments, the diffusion of hydrogen sulphide can only be followed downwards as the upwards diffusive flux is oxidised. In general, these sediment incubations serve as a useful indicator that the gel-stablised experiments containing lower concentrations of iron relate well to systems containing sediment.

4.H - Conclusions of Physical controls.

Pyrite formation occurs in micro-environments within which the chemical requirements for the reaction are met and precipitation will occur on any suitable surface. There is no requirement for sulphate reducing bacteria to be present at the nucleation site in order for pyrite to form but the extra-cellular polysaccharides and biofilms formed by bacteria seem to play a role in nucleating pyrite. The tendency of bacteria to inhabit surfaces, and their association with organic matter in sediments, would also localise the production and precipitation of sulphides to sediment surrounding the organic particle.

The distribution of pyrite within the micro-environment does appear to be a balance between the reservoirs of iron and sulphide, as suggested in Canfield and Raiswell (1991), Coleman and Raiswell (1993) and Raiswell *et al.* (1993), and the diffusion of iron into the nucleation site is an important controlling factor in the pyritization of carcasses. The radius of maximum pyrite precipitation in environments

containng anomalously high concentrations of iron seems to be well defined by the model suggested by Raiswell *et al.* (1993), although pyrite will not be completely limited to the organic particle and the concentrations of iron used greatly exceed those found in sediments (Raiswell *et al.*, 1993; J.A. Kelly pers. comm.). In experiments with iron concentrations similar to those found in sediments the maximum precipitation distances predicted from the concentration of TRIS produced in the experiments containing high iron concentrations were larger than those observed in the experiments. This was due to the assumptions in Raiswell *et al.* (1993) model that the iron resevoir was infinite and that no oxidation occurred.

In the experiments containing low iron concentrations, the diffusion and precipitation of hydrogen sulphide and iron is subject to a negative feedback mechanism, caused by the consumption of hydrogen sulphide and iron ions. This produces oscillations in the depth that the diffusion front has reached, and multiple peaks of high iron sulphide concentrations in the tubes. The formation of these features seems to be similar to that described in Liesegang banding (Liesegang, 1913), where zones of supersaturation and precipitation of a mineral form in a system and cause the diffusion of reagents and precursor compounds from areas surrounding the zone (Ortoleva *et al.*, 1987; Ortoleva, 1994).

Chapter Five
Ancient Sediments and Pyritization

5.A - Introduction

Most pyrite occurs in association with biomineralized skeletons with a high preservation potential. It commonly infills calcium carbonate fossils such as ammonites and bivalves. The processes controlling pyritization in ancient sediments are thought to be the same as those in modern sediments, but they can be obscured by later diagenetic events, such as dissolution and precipitation by circulating fluids. The aim of this study was to determine the effects and controls upon pyritization in a short sequence of sediments, and also to discover whether features observed in gel experiments (such as diffusion horizons) could be determined from the rock record. The Lower Liassic Belemnite Marls (Lang, 1913) of Dorset, UK were selected as an easily accessible pyrite rich lithology to use as an example of ancient pyritization. The upper part of this lithological division contains two pyrite-rich bands, but the matrix is of the same lithology as the rest of the 2m section. As the section is composed of mudstones, all of which have experienced the same diagenetic sequence of shallow burial and weathering conditions; it is therefore likely that any differences in the lithologies are due to primary depositional events. This makes this section ideal for comparative work.

5.B - Stratigraphy of the Belemnite Marls

The Belemnite Marls of the Lower Lias of Dorset comprise an 80m sequence of laminated mudstones, characterised by predominantly pale grey marls. They lie stratigraphically above the dark, soft mudstones of the Black Ven Marls of the Charmouth region of Dorset and below the pale, crumbly mudstones of the green Ammonite Beds (Figure 5.1). The Belemnite Marls are exposed along the coast around the village of Seatown, approximately 6 miles east of Charmouth. They tend to have a higher calcite content (85% $CaCO_3$) than the surrounding lithologies (50-60% $CaCO_3$), as indicated by their relative hardness and pale colour. The marls also have a lower %TOC (1-5% rather than 9%) than the darker marl bands in the lower Lias of Dorset (Wilson *et al.*, 1958). The increased calcite content means that the

Belemnite Marls behave more like limestones in their resistance to weathering; they form the majority of the lower cliffs between Charmouth and Golden Cap. Unlike the other divisions of the Dorset Lias, the Belemnite Marls have only two distinct limestone beds, which occur at the very top and bottom of the unit. The shales between these two bands are divided into upper, middle and lower subzones (Wilson *et al.*, 1958) on the basis of colouring. This study is limited to the upper section of the upper zone, which is exposed near Seatown.

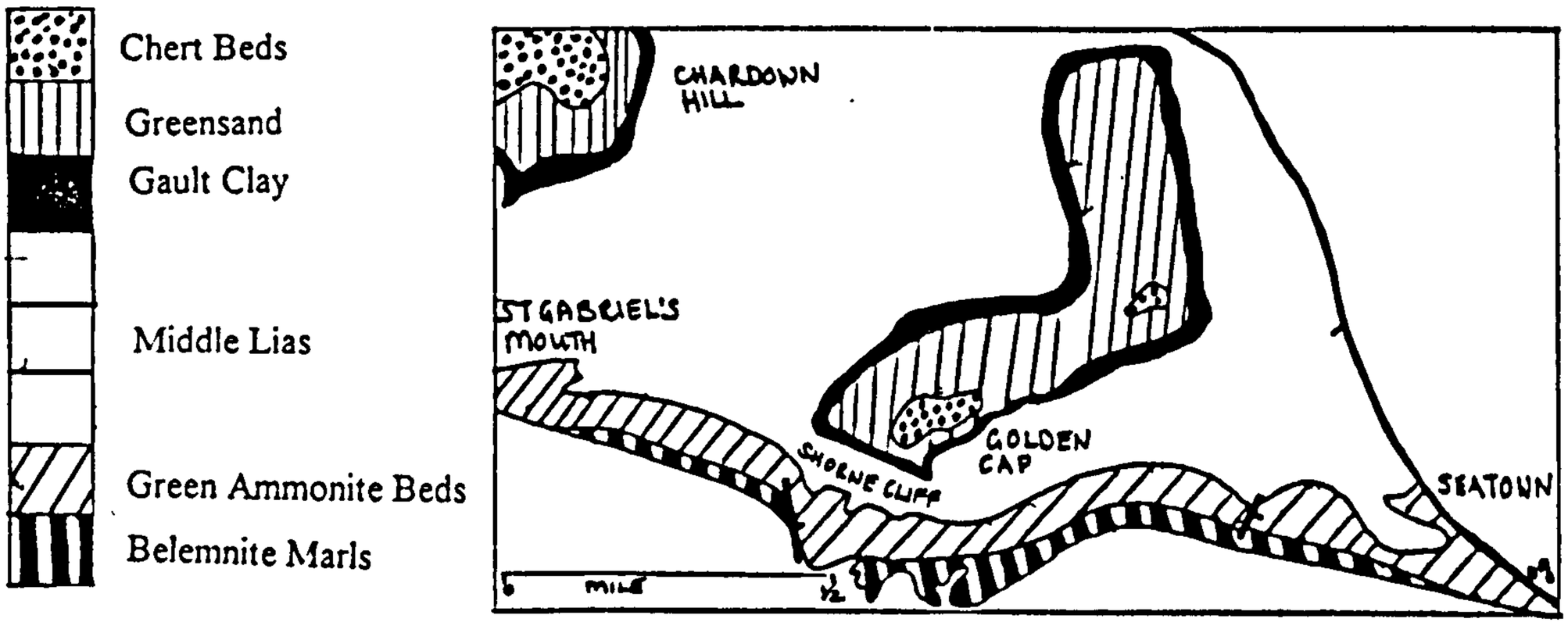

Figure 5.1 - Map of the area surrounding Golden Cap with stratigraphy (afrom Wilson *et al.*, 1958)

Two intensely pyritic bands, the Pyritic Marls, lie below the upper limestone band, the Belemnite Limestone, within a half metre succession of mudstones (Wilson et al., 1958). This section, which lies within the upper part of the *Tragophylloceras ibex* zone, also contains lens-shaped concentrations of calcareous fossils. These were classified as limestone bands by Lang and others (1928). These bands and the surrounding lithologies have been sampled, from the wave cut platform at Golden Cap, in order to carry out a geochemical and palaeontological assessment of the lithologies.

Samples were only collected from the top two metres of the Belemnite Marls because the rest of the sequence does not contain intensely pyritized bands (Figure 5.2). Samples were collected from the Green Ammonite Beds above the Belemnite Limestone, in order to determine if there are any significant differences between the depositional environment of these beds and those of the Belemnite Marls. Comparative samples were also collected from pyrite free limestone (as determined by chromous chloride digestions), as well as samples from pyritized and pyrite-free mudstones in the Black Ven Marls of Charmouth.

Figure 5.2 - Log of sampled section beneath Golden Cap, Dorset, UK

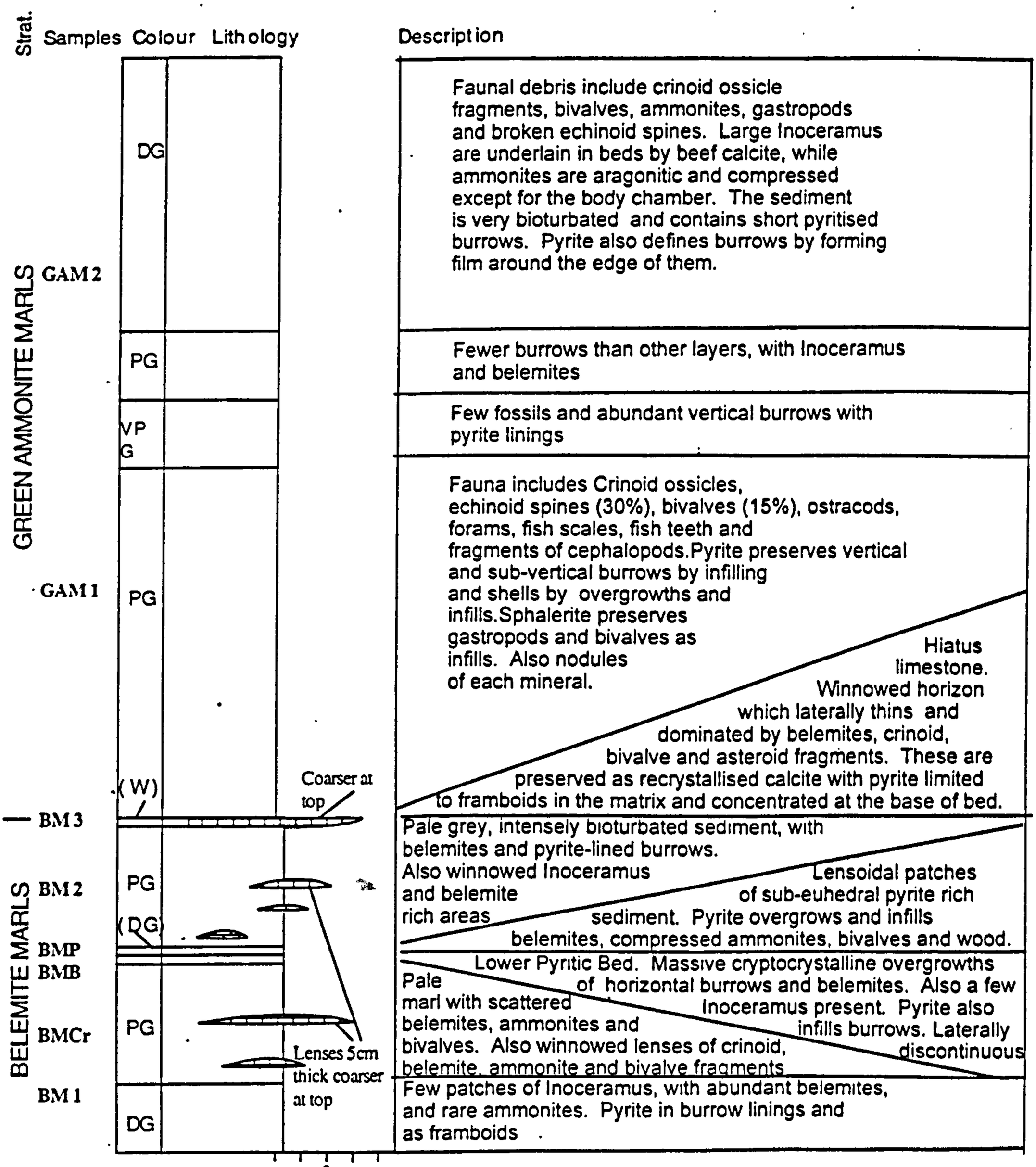

5.C - Lithologies and faunal elements collected from the Upper Belemnite Marls and the Lower Clays of the Green Ammonite Beds.

The Pyritic Marls, Crinoid Limestone, Crumbly Bed, Belemnite Shales and clays from the Lower Green Ammonite Beds (Lang *et al.*, 1928) were all sampled. The section was also logged in order to record any distinctive colour or sedimentation changes associated with the pyritization of the Pyritic Marls.

5.C.1 - The Basal Marls (BM1)

The lowermost part of the section consists of dark grey mudstone with isolated patches of the oyster-like bivalve, *Inoceramus*. These patches also contained broken fragments of *Inoceramus* and the marl is harder around them due to dissolution and precipitation of calcium carbonate from the shells. Ammonoids are rare but belemnite guards are abundant. Pyritic fragments are limited to small vertical burrows and scattered framboids. Trace fossils are limited to small (1 to 2cm depth) vertical burrows and some larger horizontal burrowing.

5.C.2 - The Crinoid Limestone (BMCr)

Ascending the section the marls become paler and scattered lenses of winnowed *Inoceramus* and belemnite fragments become more common. Pyrite is still limited to a few vertical burrows. Approximately 40 cm up the section the lenses of shelly debris coalesce to form a bed which is variable in thickness, and crinoid fragments begin to dominate the deposits. These lenses are the Crinoid Limestones of Lang *et al.*; considered to represent a storm scour infilled with a typical hardground fauna. The lenses are laterally variable; they consist of abundant fragments of belemnites, crinoids and bivalves with some wood and ammonites. The fragments show some degree of orientation, and the lenses appear to coarsen upwards due to a increase in the ratio of bioclasts to matrix. Some of the crinoid stems still show some articulation although the pieces of *Inoceramus* and ammonoids are broken in 2 to 3 cm long fragments. The quality of preservation of the faunal elements in the Crinoid Limestone is variable. Calcite recrystallisation has occurred in all the ammonoids, most of the belemnites and some of the crinoid fragments. Pyrite is limited to the matrix of the lenses, where it either occurs as scattered framboids or as a large

concentration of pyrite within or around organic fragments (Figure 5.3). Pyrite occurs in the highest concentrations at the base of the lenses.

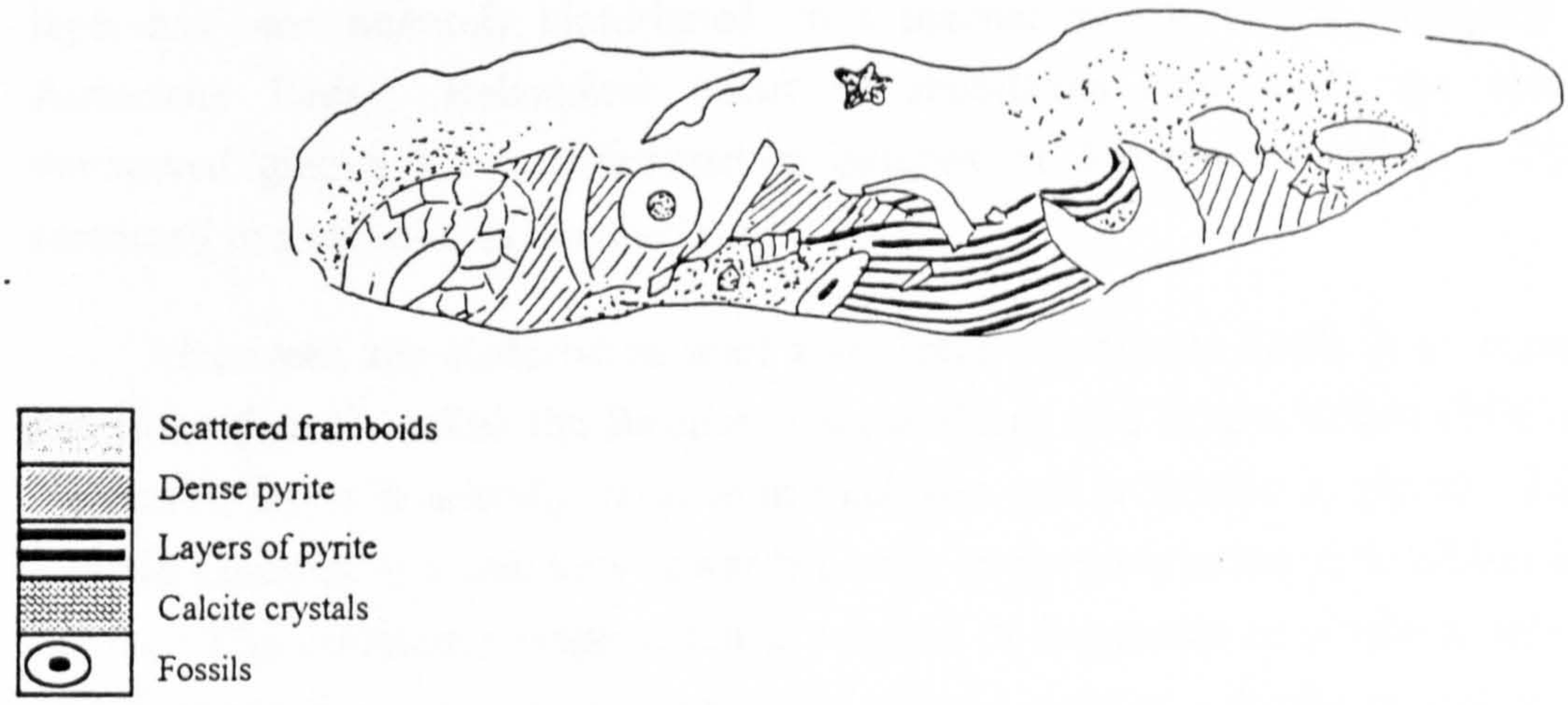

Figure 5.3 -Distribution of faunal debris and pyrite in the Crinoid Limestone

5.C.3 - The Pyritic Marls (BMB and BMP)

The Pyritic Marls crop out as pyrite rich layers within a dark grey mudstone. The lower pyritic marl (BMB) is a laterally discontinuous bed in which pyrite forms massive cryptocrystalline overgrowths and infills of large (up to 1cm in diameter) horizontal burrows. Calcareous fossils are rare; those present are mainly belemnites. Pyrite occurs as overgrowths on these. In all, pyrite constitutes 50% to 60% of this lithology. Approximately 15cm above the Lower Pyritic Marl, a second pyrite-rich layer outcrops, the Upper Pyritic Marl (BMP). Pyrite constitutes between 60% and 70% of the material present, and occurs mainly as overgrowths on calcareous and carbonaceous material. This pyrite forms massive cryptocrystalline agglomerates, although some may be are subhedral. Pyrite also occurs as framboids in the matrix and within woody material in the bed. The woody material has pyrite within its cells, and a random scattering of small calcite crystals on the upper surface. Again, pyrite is concentrated at the base of the bed. Other fossil remains include echinoid spines, belemnites, compressed ammonoids and *Inoceramus*.

5.C.4 - The Bioturbated Marls (BM2) and Belemnite Stone (BM3)

Above the pyritic marls is a 30cm wide band of pale grey marl (BM2). This layer has been intensely bioturbated, in a manner similar to the overlying Green Ammonite Beds. Belemnites occur in abundance throughout the mudstone; winnowed guards are concentrated in patches of *Inoceramus* debris. Pyrite is restricted to framboids in burrow linings.

Between the bioturbated marl and Green Ammonite Beds is a continuous limestone deposit, called the Belemnite Stone (Lang and others, 1928) (BM3). The Belemnite Stone is laterally variable in thickness and is lensoid in places. Like the Crinoid Limestone, it coarsens upwards due to an increase in the ratio of bioclasts to matrix. The calcareous organic debris consists of fragments of bivalves, belemnites and ammonoids, with a small number of crinoid ossicles. Pyrite is limited to the darker, less calcareous base of the bed, where it occurs as framboids in a pale grey marl matrix.

5.C.5 - The Lower Clays of the Green Ammonite Beds (GAM 1 and 2)

The lowermost unit of the Green Ammonite Beds, the Lower Clays, is made up of pale grey, crumbly marls. On disaggregation they yield a diverse fauna of petaloid crinoid ossicles, echinoid spines (30%), bivalve fragments, fish scales and fragments of cephalopods. Smaller faunal elements, such as gastropods, forams and ostracods have been preserved by an infilling of either pyrite or sphalerite (Figure 1.1). Pyrite also observed infills and lines burrows. Some areas have a greater number of pyritized burrows while others have patches of *Inoceramus* underlain by beef calcite. Large ammonites also occur in this lithology; they are compressed laterally except for the body chambers which are infilled by calcite.

5.D - Analytical Methods

5.D.1 - Hand Specimen Treatment.

Samples were polished and examined under a binocular microscope to determine the distribution of pyritic burrows, pyrite overgrowths and calcareous organic material. Several samples were also disaggregated to examine the small

organic fragments and the types of preservation in the microfauna. Material from these samples was removed for SEM.

5.D.2 - Chemical Methods

5.D.2.1 - Elemental Analysis - Samples for elemental analysis were dried, crushed to a fine flour and dissolved using the standard perchloric/hydrofluoric acid digestion method. These samples were then analysed using the ICP-MS for trace element concentrations, in order to determine their variance with respect to the Pyritic Marls, and using AA for the concentrations of the major elements, magnesium, calcium, manganese and total iron.

Acid soluble iron was extracted by placing 0.1g of sample in 5ml of 1M hydrochloric acid for 24 hours, and diluting 4ml of the centrifuged solution to 100ml (Leventhal & Taylor, 1990). This solution was then analysed on the AA, so that the concentration of oxides and non-pyritic iron could be determined. This method of determining the concentration of acid soluble iron was prefered over boiling samples in 12M HCl for 1 minute as it produced similar values for iron concentrations in Leventhal and Taylor (1990) and was more convenient to use in a crowded laboratory. However, this was prior to work by Raiswell *et al.* (1994) which demonstrated possible problems with using a cold 1MHCl digestion to calculate DOP-values, and commented on the lack of calibration between DOP-values calculated using cold 1HCl digestions and sediments of known palaeoenvironments.

5.D.2.2 - Sulphide Analysis - Three phases of sulphide analysis were performed on the crushed rock samples using the digestion sequence outlined in Chapter 2 (Figure 2.4). First a small subsample of powder was heated with excess 6N HCl in anaerobic conditions for 2 hours, in order to determine the amount of acid volatile sulphide (AVS). The AVS fraction of these samples may be either sphalerite, chalcopyrite or iron monosulphides, which are characteristically extracted by this technique (see Chapter Two). The concentrations of pyrite and elemental sulphur were determined using cold/hot chromous chloride digestions, using 25ml chromous chloride, 5ml ethanol and 10ml hydrochloric acid. The concentration of hydrogen sulphide released in each stage of the digestion was then determined by trapping the H_2S in zinc acetate to form zinc sulphide. This was analysed using the Cline (1969) methyl blue method.

5.D.2.3 - Percentage Total Organic Matter (%TOM) Measurements - %TOM was measured by heating the dry crushed rock powder in a furnace at 450°C for 24 hours. The weight loss was then measured. This method, however, also releases some inorganic carbon from carbonate minerals, oxdizes pyrite and causes the loss of structural water, and must therefore be regarded as an indicator of total organic matter. %TOC was claculated from %TOM using the following equation

$$\%TOC = (\%TOM \times 12) / 30 \qquad \text{Eq. 5.1}$$

5.E - Chemical Results

The chemical analyses of elemental abundances (Appendix 11) show correlations between minor and major element concentrations due to substitution in the crystal lattice. For example, copper, nickel and cobalt all substitute for ferrous iron in the pyrite crystal lattice and therefore peak in the Pyritic Marls, while strontium replaces calcium in the calcite lattice and is at low concentrations in these beds.

The Degree of Pyritization (DOP: Raiswell *et al.*, 1988) were calculated using the 1M HCl soluble iron and total reduced inorganic sulphide (TRIS) concentrations (Leventhal & Taylor, 1990) as the concentration of reactive iron. This may have underestimated the DOP-values, as the Leventhal & Taylor (1990) method used does not extract the goethite and haematite pools (Raiswell *et al.* ,1994) (Table XIII). The TRIS concentrations were used to calculate the DOP-values as elemental sulphur concentrations in all the samples, using both the method described and the selective digestion method (outlined in Chapter Two), were very small.

5.F - Discussion

The fauna of the Upper Belemnite Marls fits the criteria for an environment with restricted bottom water oxidation (Morris, 1979). It has also been suggested that the substrate was soupy (Sellwood, 1972; Savrda and Bottjer, 1991) due to the restriction of the benthos to *Inoceramus* and burrowing organisms. This faunal assemblage confirms that the overlying water column was aerobic and of normal marine salinity. However the occurrence of pyritized burrows throughout the section indicates that oxic-anoxic interface was close to the sediment water interface. The

Table XIII - Acid-volatile Sulphides (AVS), Total Reduced Inorganic Sulphide (TRIS), Total Organic Matter (TOM), Iron and Calcium concentrations and DOP values from the Belemnite Marls.

(GAM1 - Green Ammonite Marl, BM3 - Belemnite Stone , BM2 - Bioturbated Marls, BMP - Upper Pyritic Marl, BMB - Lower Pyritic Marl, BMCr - Crinoid Limestone, BM1 - Basal Marls)

		AVS			TRIS (elemental sulphur is negligible)		
Sample	Depth	µmols/g	g/g sample	% sulphide	µmols/g	g/g sample	% sulphide
GAM1	210	3.13	0.00	0.01	374.64	0.01	1.20
BM3	140	14.55	0.00	0.05	149.24	0.00	0.48
BM2	78	27.41	0.00	0.09	130.79	0.00	0.42
BMP	51	10.34	0.00	0.03	503.99	0.02	1.61
BMB	47	1.45	0.00	0.00	604.02	0.02	1.93
BMCr	34	6.45	0.00	0.02	103.78	0.00	0.33
BM1	0	10.67	0.00	0.03	137.33	0.00	0.44

		TOM					
Sample	Depth	weight loss	initial wght	%TOM	% TIS	%CaCO3	%TOC
GAM1	210	0.01	0.09	11.1	1.21	34.50	4.4
CGAM	140	0.01	0.08	12.5	0.52	0.47	5
BM3	78	0.00	0.09	0	0.51	67.30	3.6
BMB	51	0.01	0.11	9.1	1.65	16.47	0
BMN	47	0.01	0.10	10	1.94	12.17	4
BMCr	34	0.01	0.15	6.7	0.35	43.10	2.7
BM1	0	0.00	0.08	0	0.47	92.80	0

Sample	Depth	ppm Fe (Total)	%Fe (Total)	mols Fe (Total)	ppm Fe (HCl)	%Fe (HCl)	mols Fe (HCl)
GAM1	210	23533	2.35	0.0004	11800	1.18	0.0003
BM3	140	37266	3.73	0.0007	8200	0.82	0.0002
BM2	78	16166	1.62	0.0003	11200	1.12	0.0002
BMP	51	96000	9.60	0.0017	12800	1.28	0.0003
BMB	47	109866	10.99	0.0020	8600	0.86	0.0002
BMCr	34	28600	2.86	0.0005	87500	8.75	0.0019
BM1	0	16900	1.69	0.0003	13200	1.32	0.0003

Sample	Depth	DOP	DOS
GAM1	210	0.56	0.56
BM3	140	0.42	0.45
BM2	78	0.32	0.36
BMP	51	0.61	0.62
BMB	47	0.74	0.74
BMCr	34	0.05	0.05
BM1	0	0.30	0.31

Where DOS is the Degree of Sulphidization and DOP is the Degree of Pyritization

aerobic nature of the overlying water column is reflected in the generally low DOP-values (average 0.40) values throughout most of the section (Raiswell *et al.*, 1988) and the distribution of values when %Total Inorganic Sulphide (%TIS) and %Total Organic Carbon (%TOC) are plotted (Figure 5.4). This places all seven samples from the section within or around the normal marine field (Berner, 1964). Although, the DOP-values may have been underestimated, the biota and carbon-sulphur plot support the conclusions drawn from the DOP-value. The Pyritic Marls have higher DOP values (0.73 and 0.61; Table XIII) which means that the bottom water conditions were restricted in relation to the rest of the sequence (Raiswell *et al.*, 1988).

Figure 5.4 - Distribution of sulphur and organic carbon concentrations (%S and %TOC) in the Belemnite Marls

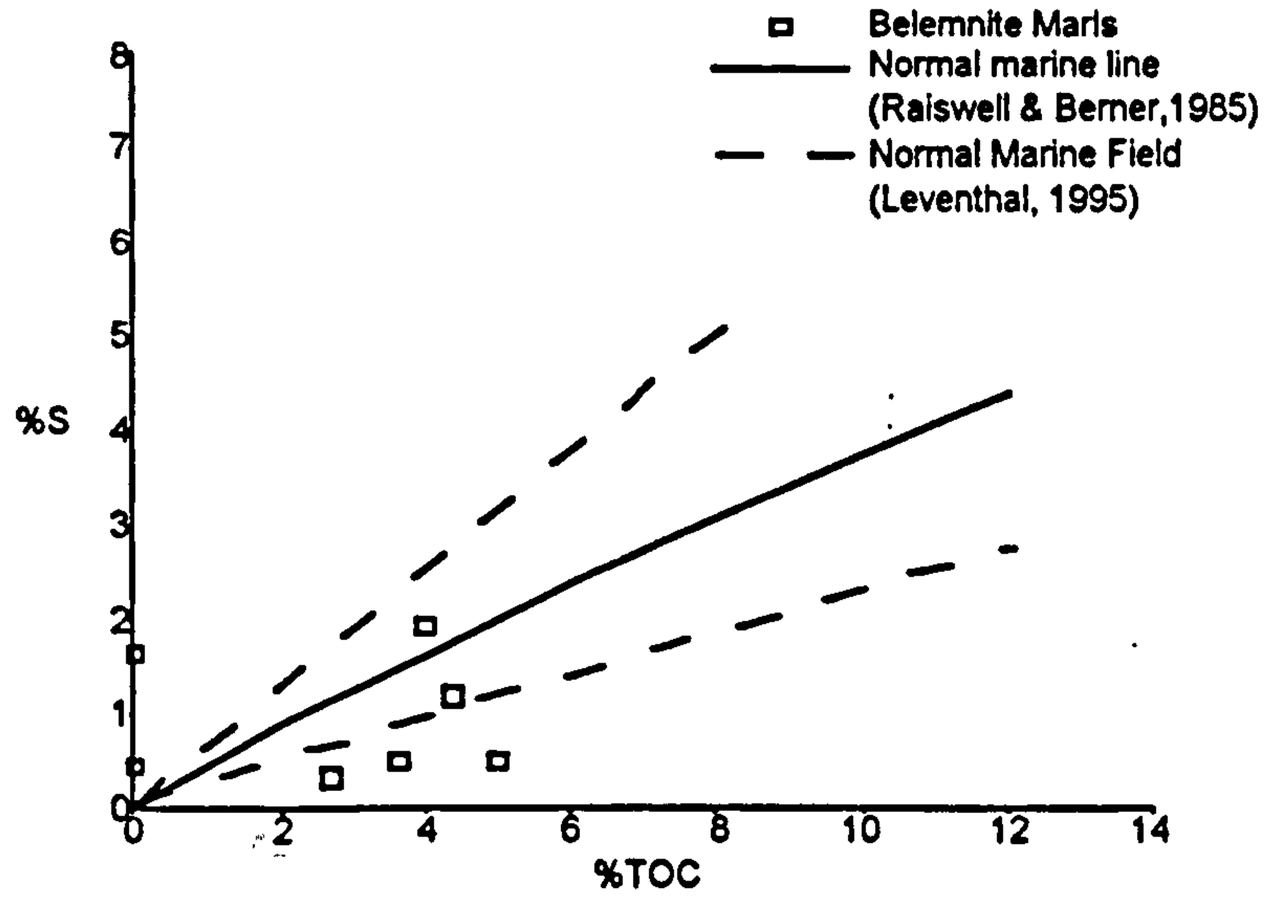

The DOP values from this sequence of mudstones have a range from 0.05 to 0.7. A plot of DOP against %TOM produces a positive trend through the origin which is indicative of authigenic pyrite formation (Raiswell and Berner, 1985). The DOS values are also similar as the percentage of acid-volatile minerals is low in the sequence despite the occurrence of sphalerite in the Green Ammonite Marls.

Iron concentrations remain similar throughout the sequence except in the Pyritic Marls, where they peak to around 10% total iron and 1% HCl-soluble iron. The concentration of reactive iron (HCl-soluble iron and pyritic iron) also peaks in

these beds (Upper Pyritic Marl - 2.7%; Lower Pyritic Marl - 2.5%), while the surrounding sediments have lower concentrations (Bioturbated Marl - 1.4%; Basal Marl - 1.7%). The limestone bands have lower concentrations of reactive iron than the shales. The lower concentrations of reactive iron in the marls surrounding the Pyritic Marls indicates that iron was leached from these beds into the Pyritic Marls during later diagenesis.

Figure 5.5 - Distribution of %TOM, %$CaCO_3$, % Total Fe and %TRIS in the Belemnite Marls.

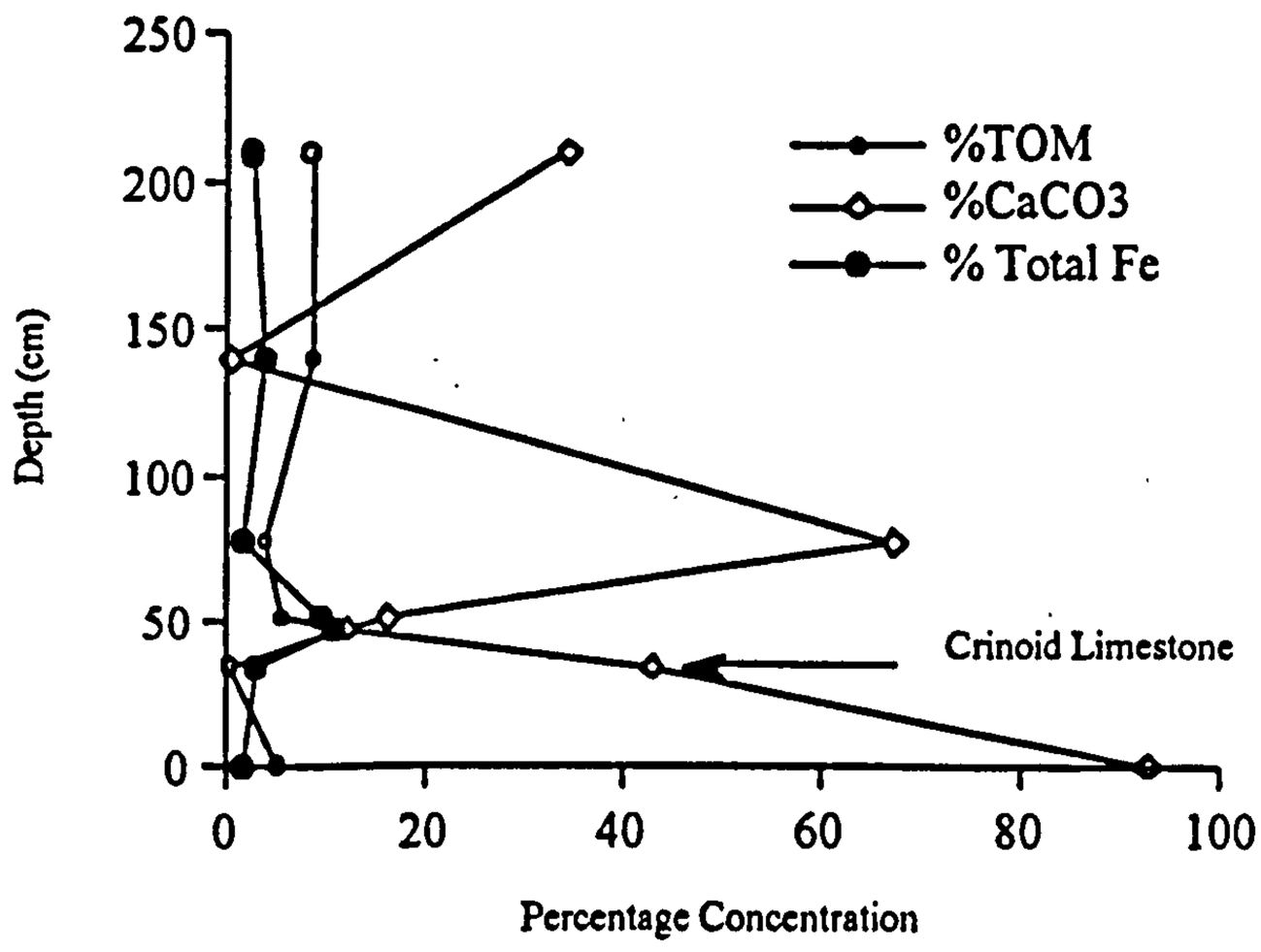

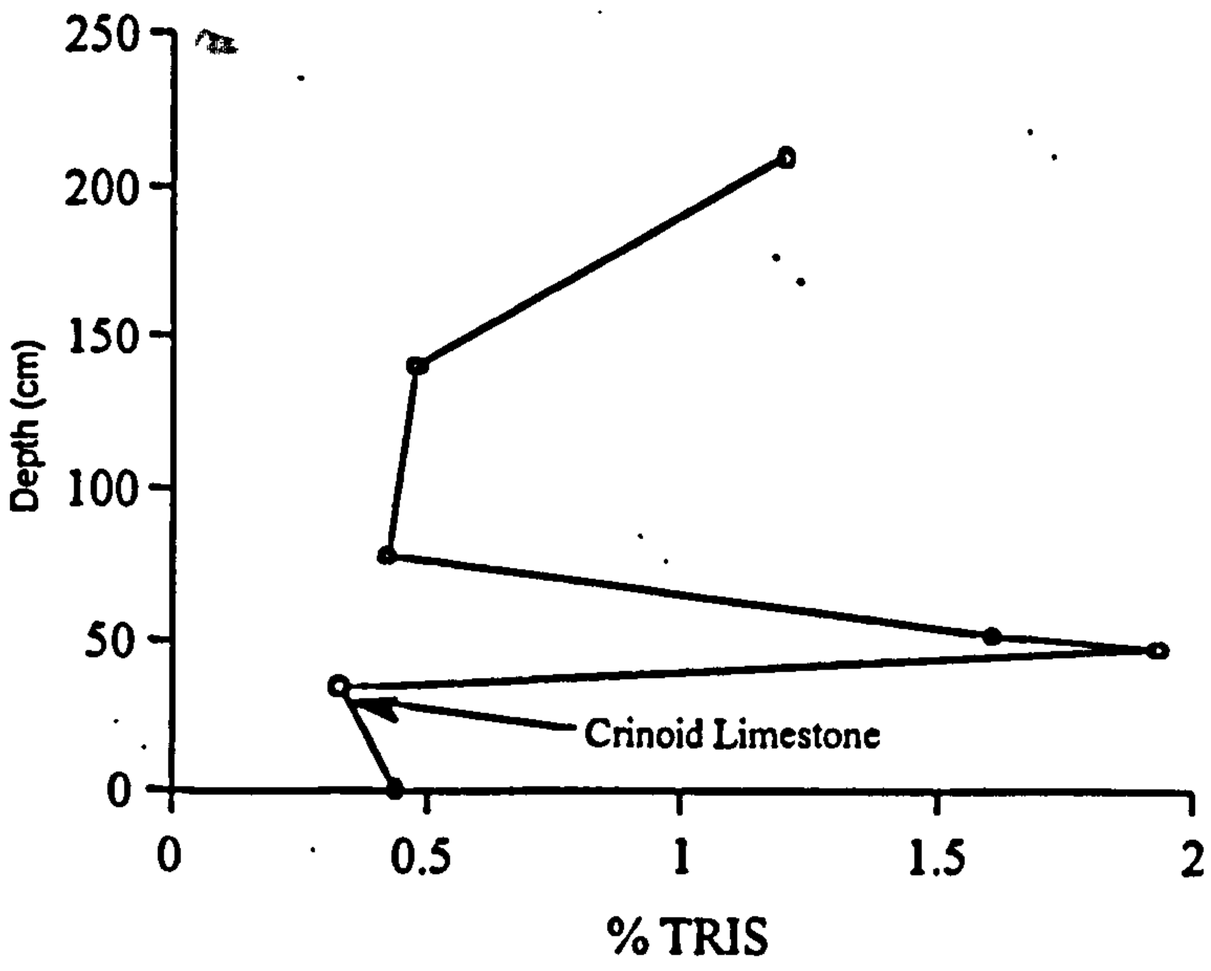

5.F.1 - The Limestone Bands

The marls are disrupted by events which washed in a high concentration of calcareous bioclasts. These increased the calcium carbonate content of specific beds and the dissolution and precipitation of calcium carbonate from these bioclasts form limestone bands such as the Crinoid Limestone and the Belemnite Stone. The limestone bands are dominated by asteroid crinoids, belemnites and *Inoceramus*, with some wood debris. The fragments include organisms which are not found within the rest of the sequence, indicating that the bioclasts were transported from a different area of the basin prior to deposition. Sellwood (1972) suggested that the faunal debris within the limestone bands had been washed in from other areas of the basin by a storm. The bioclasts were deposited into scours because these allochthonous deposits have sharply defined bases. However, the sharply defined bases of these beds could also have developed from the sudden influx of debris without requiring a scour to be formed, especially as the limestones are laterally continuous.

The Crinoid Limestone and Belemnite Stone have low %TOM and high $\%CaCO_3$ values (Figure 5.4). The occurrence of pyrite at the base of the bed is probably an effect of transportation processes, however, the high abundance and overgrowths of fossil suggests that later pyritization occurred *in situ*. However the low TRIS concentrations also indicates that aerobic rather than anaerobic decay was dominant. The Belemnite Stone at the top of the sequence differs from the Crinoid Stone in being characterised by a high AVS concentration (27.41µmols g^{-1} compared to 10.34µmols g^{-1} in the Crinoid Limestone) which coincides with peaks in lead and nickel. This, combined with a high calcium content and little pyrite, is due to the availability of minerals, such as lepidocrocite, which react rapidly with hydrogen sulphide. The sediment immediately above this, in the Green Ammonite Beds, also has a high AVS content (14.5µmols g^{-1}) which coincides with peaks in nickel and chromium. The change from the marls containing pyritized burrows to the clays containing limestone nodules and higher concentrations of AVS is indicative of a change in the sedimentation to shallower conditions.

5.F.2 -The Lower Pyritic Marl

The %TOM peaks in the Lower Pyritic Marl (Table XIII), which is a lensoid deposit containing a high concentration of belemnites, pyritized burrows and a few fragments of *Inoceramus*. As these bioclasts are found throughout the marls below the pyrite band, this deposit does not relate to an influx of debris but to an accumulation of indigenous organisms, which was then scavenged. The sediment

conditions must have been anoxic at the sediment-water interface to facilitate anaerobic decay and pyrite production. It is also possible that the high concentration of organic matter would have facilitated the formation of an anoxic water column at some stage. Conversely, a suddenly anoxic water-column could have been the mechanism which caused the accumulation of the organic matter which was then scavenged by infaunal organisms once the anoxic boundary had lowered to within the sediment column.

Trace elements which have a peak concentration coinciding with this pyritic layer are lanthanium, niobium, germanium, nickel, copper, lead, chromium, cerium and vanadium. Nickel and copper are substituted into the pyrite matrix, but lead and lanthanium have ionic radii which are too large to allow substitution into the crystal lattice in the place of ferrous iron (Appendix 11).

5.F.3- The Upper Pyritic Marl

The Upper Pyritic Marl is similar in character to the Crinoid Limestone and Belemnite Stone and must also be a deposit of allochthonous material. However, the debris must have come from a different part of the basin from that of the Crinoid Limestone as there are fewer crinoid fragments, and different trace elements peak in the sediment. The Upper Pyritic Marl also differs from the other autochthonous deposits in having a higher TRIS concentration, implying that the dominant decay process was anaerobic, rather than aerobic as in the Crinoid Limestone. As the environment in which deposition occurred is likely to have been anoxic, there need not have been any difference in the character of this deposit during transportation from that of the limestone bands.

The Upper Pyritic Marl has a lower %TOM and contains a higher concentration of acid-volatile sulphide than the Lower Marl. This correlates with a zinc peak, which must be derived from the external source of the debris in the lensoid deposits, as it is not observed in high concentrations in the rest of the sequence (Figure 5.6). The elements which show a peak in the Lower Pyritic Marl are depleted in the Upper, while magnesium, barium and cobalt are present in higher concentrations confirming that they have a different source. Nickel and copper remain high compared to the rest of the sequence.

Figure 5.6 - Some variations in trace element distribution in the Belemnite Marls (the Upper Pyritic Marl is at 51cm depth).

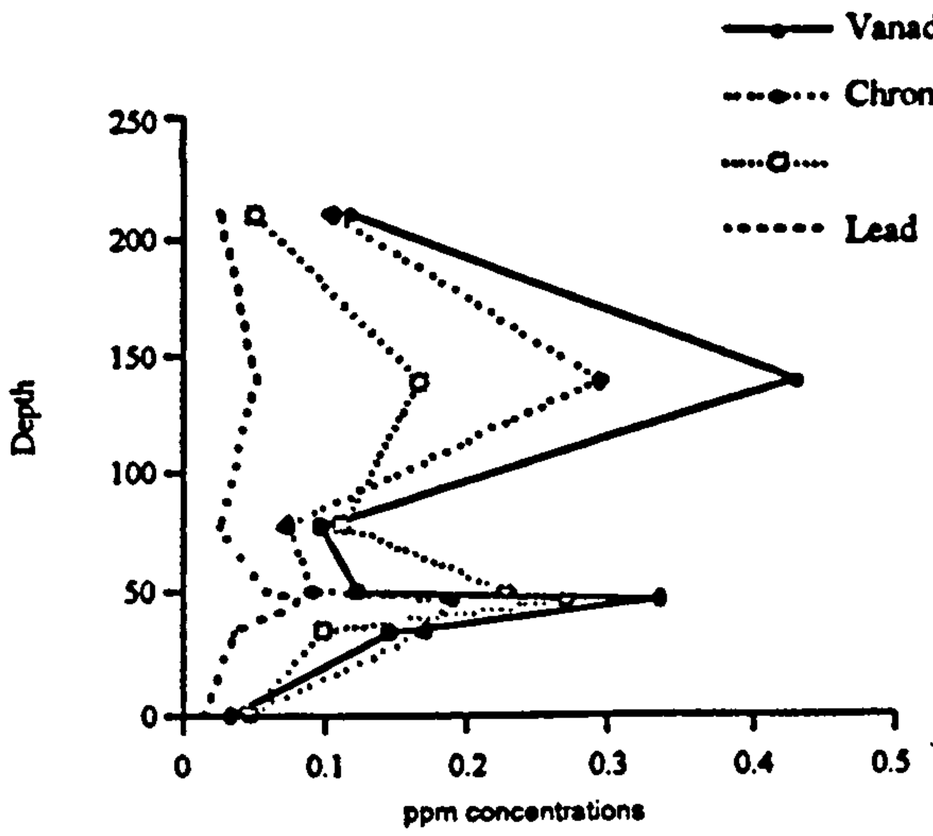

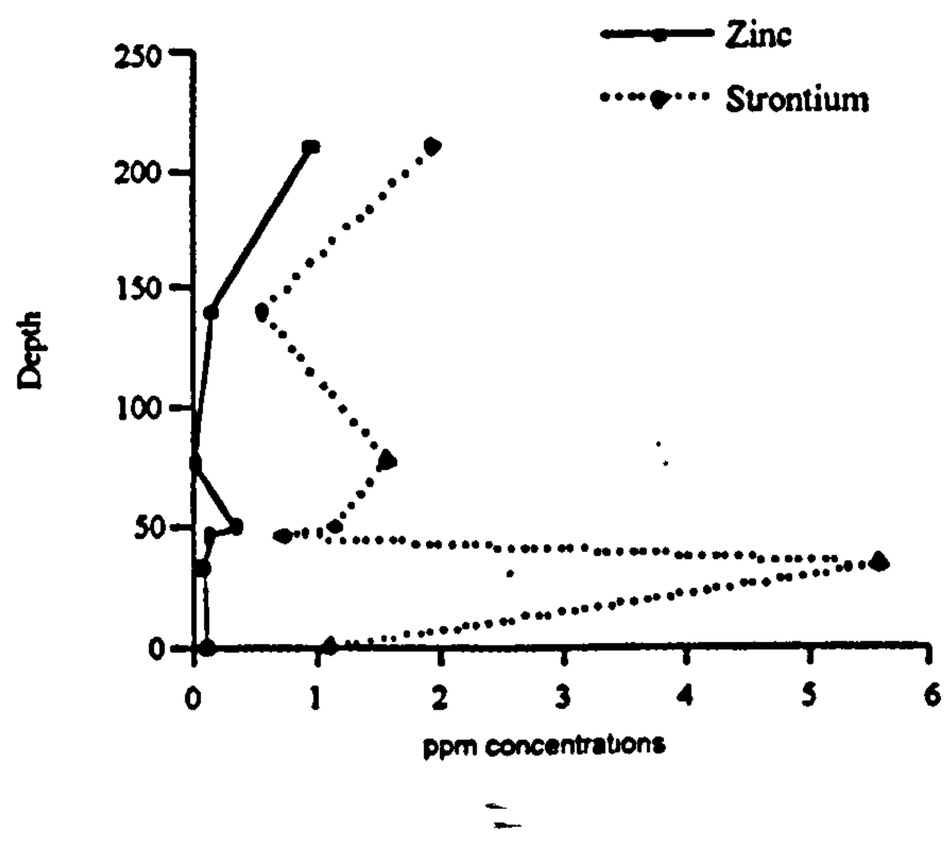

5.G - Conclusions

The Upper Belemnite Marls of Dorset, UK, represent a sequence of soupy sediments colonised by burrowing organisms and oysters. The sediment column was anoxic near the sediment-water interface as pyritization in burrows is commonplace. It is also likely that the water columns was periodically anoxic; allowing the accumulation of indigenous organisms and the production of highly pyritic bands such as the Lower Pyritic Marls. However, the anoxic water column can not have been present for long periods of time as the Lower Pyritic Marl also contains large numbers of pyritized burrows.

The Upper Belemnite Marls also contain several "limestone" bands. These bands are characterised by the occurrence of fragments of crinoids, bivalves and pieces of wood. These represent influxes of debris, such as those found on talus slopes, and were deposited, after transportation, under predominantly aerobic (Belemnite Stone) or anaerobic (Upper Pyritic Marl) conditions. The Crinoid Limestone appears to represent a band in which both aerobic and anaerobic conditions occurred, as it has a pyritic base, and a calcite cemented top.

Iron concentrations in the sediments are consistent throughout the sequence, except in the Pyritic Marls which contain five times the average total iron concentration. This appears to indicate that the Pyritic Beds may have leached some iron from surrounding sediments during later diagenesis to allow late pyrite growth and that, in addition to high concentrations of organic matter, they must also have contained higher concentrations of iron in order for the layers to become so pyritic.

Chapter Six

Summary Discussion and Conclusions

Pyrite is an important mineral in fossil preservation, and in argillaceous sediments, with many different forms found in association with organic particles. It is confined to argillaceous sediments as the low permeability facilitates the rapid development of an anaerobic environment when metabolisable organic material is present. Authigenic pyrite formation, which forms the majority of pyrite found in association with organic particles, is attributable to the metabolic activities of sulphate-reducing bacteria. Under anaerobic conditions sulphate-reducing bacteria metabolise sulphate and low molecular weight organic compounds, producing hydrogen sulphide and bicarbonate ions. The hydrogen sulphide produced reacts with iron compounds forming iron monosulphides (FeS) which then react with either elemental sulphur, polysulphide or hydrogen sulphide to form pyrite (see review in Chapter One). The intimate association between sulphate-reducing bacteria and the production of pyrite constrains the environmental conditions under which pyrite formation occurs. Sulphate-reducing bacteria grow best under anaerobic, neutral pH conditions, at seawater salinities and at low temperatures. This means that a study using bacterial cultures is automatically constrained by these limits, although there can be some variation in these parameters, as some bacterial strains such as *D. desulfuricans* can metabolise under dysaerobic conditions. In experiments with actively growing cultures of sulphate-reducing bacteria, pyrite formed after 3-4 days. This is much more rapid than the majority of the reaction times reported in the literature for the neutral pH range used (Schoonen and Barnes, 1994 - 6-8 days; Rickard, 1969 - six months), although faster precipitation of more crystalline material is observed at lower pH (Schoonen and Barnes, 1994; Roberts, Walker & Buchanan, 1969; Berner, 1970; Allen *et al*, 1914). Bacterial precipitation of pyrite is more rapid due to the constant flux of hydrogen sulphide produced by bacteria.

Under the conditions required for bacterial metabolism, pyrite formation is thought to be controlled by the concentration and reactivity of sulphate, metabolisable organic matter and iron minerals (Berner, 1969). Organic matter availability is the dominant control in terrigenous normal marine sediments (Berner, 1970), as in barren sediments sulphate reduction does not take place. However, although, pyrite

production is controlled by the availability of iron, sulphate and organic compounds, there is no correlation between the concentrations of these reagents and the concentration of pyrite. This is unlike hydrogen sulphide concentrations which are controlled by the concentrations of sulphate and organic matter; these reagents act in a manner interdependant of each other until one or the other reaches low concentrations (Westrich and Berner, 1984).

Once an actively metabolising culture of sulphate-reducing bacteria is present in an environment, then the concentration of pyrite in a sediment will be controlled by the availability of reactive iron minerals, such as lepidocrocite, goethite and haematite (Canfield, 1989). Generally, high concentrations of iron limit the formation of pyrite in a sediment because hydrogen sulphide is rapidly consumed by the reaction to form iron monosulphides. AVS-dominated environments were modelled using cultures of sulphate-reducing bacteria. The type of iron compound and the potential for oxygen to enter the reaction vessel affected the concentration and rate of pyrite production, as the presence of oxygen or an oxide mineral changed the reaction forming pyrite from the iron monosulphide precursors. Experiments containing ferrous sulphate and the iron monosulphide, mackinawite, have no oxidising potential when sealed, and the reaction to form pyrite is therefore dominated by the hydrogen sulphide oxidation (Drobner *et al.*, 1990; Rickard, 1997). In the experiments containing lepidocrocite, this iron oxyhydoxide oxidised hydrogen sulphide to produce elemental sulphur, which then reacted with iron monosulphides to form pyrite, despite the continuing oxidation of elemental sulphur back to sulphate (Canfield & Berner, 1987). A similar reaction occurred in experiments where oxygen leaked into the vial. The change between a reaction dominated by hydrogen sulphide oxidation to elemental sulphur oxidation meant that the rate of pyrite production slowed (Rickard, 1997) and that the ratio of the concentration of pyrite to the total concentration of reduced sulphur species increased.

Iron concentrations also had an important effect on the precipitation of pyrite in association with organic particles. Low iron concentrations in an environment means that sulphide generated within a carcass diffuses out into the surrounding sediment producing haloes of iron sulphide. The diffusion of hydrogen sulphide away from, and iron towards, the site of iron sulphide precipitation is affected by a negative feedback reaction, where the precipitation of acid-volatile sulphides in one area prevents the precipitation of acid-volatile sulphide in front of this point. This feedback mechanism is further complicated by the formation of pyrite where the consumption of acid-volatile sulphides forms a diffusion gradient into the zone of pyrite precipitation, imposing bands of acid-volatile sulphides and pyrite similar to the

Liesegang Banding observed in rocks (Ortoleva, 1994). These bands are more distinct when iron concentrations are low because iron diffusion gradients are less important. When iron concentration are higher, iron diffuses into the zone of precipitation and the bands become compressed around the decay site. However the diffusion of iron into the carcass does produce a zone where iron, acid-volatile sulphides and pyrite are limited around the decay site. This means that the pyritization of whole organisms and soft tissues is limited to sediments which would generally be considered AVS-dominated (Gagnon *et al.*, 1995; Boesen & Postma, 1988) rather than pyritic, and that the process of pyrite precipitation will form an iron diffusion gradient into the decay site.

The pyrite formed in the bacterial experiments was poorly crystalline and was associated with both the bacterial cells and the extra-cellular polysaccharides, that bacteria produced as a means of attachment and protection against extreme conditions (Bleckinsopp & Costerton, 1991). These films are identical to the 'oil-like' film observed by Rickard (1969) in his experiments containing bacteria and ferric iron compounds. The 'biofilms' were observed in both both ferrous and ferric iron experiments; contained both pyrite and acid-volatile sulphide compounds, and when examined using an acridine orange stain were shown to form a large clump containing live and dead bacterial cells and extra-cellular polysaccharides. They are likely to have been formed when iron was bonded to the bacterial cell wall, as the negatively charged cell wall is likely to attract cations. The bonding of iron to bacterial cell walls has previously been suggested as a mechanism for (Fe, Al) silicate precipitation in Amazonian river sediments (Konhauser *et al.*, 1993). When shrimp carcasses and pieces of carbonate are placed in vial containing a metabolising culture of sulphate-reducing bacteria they rapidly became colonised by the bacteria. Iron sulphides were precipitated, as part of a biofilm, on the outside of the organic particles and within the shrimp carcasses, once muscle shrinkage had occurred. Calcium carbonate bundles, similar to those described by Briggs and Kear (1994), also formed around shrimp appendages and inside the carcass. The precipitation of iron sulphide biofilms is similar to the mechanisms for the formation of mineral coats suggested by Wuttke (1983) and Davis and Briggs (1995). The textures (Figures 4.1, 4.2, 4.4, 4.5 and 4.6) formed also resemble those described in Pleistocene polychaete burrows (Thomsen and Vorren, 1984).

Although the colonisation of decaying organic particles by bacteria results in the formation of small scale mineral coats, and probably provides a nucleation site for further pyrite growth (Hudson 1967, 1982), this process will not facilitate the preservation of soft tissues or whole organisms. In order for this type of preservation

to occur, hydrogen sulphide produced by sulphate-reducing bacteria within a carcass must be precipitated as iron sulphides within it. This process requires rapid burial so that the metabolisable organics within the carcass are available for sulphate reduction, and so that the risk of disaggregation of the carcass by bioturbation and scavengers is minimised (Canfield, 1994). The rate of decay in anaerobic sediments is not slower (Jørgensen, 1982; Canfield, 1989; Allison, 1988), and rapid burial may have to be combined with a reduction in decomposition rates (Canfield, 1989) to allow preservation to occur. Once rapid burial has occurred, anaerobic conditions will rapidly develop and iron needs to be abundant in the surrounding sediment. In order to pyritize an organic particle with a similar rate of hydrogen sulphide production as a shrimp (6×10^{-6} mols cm^{-3} day^{-1}) a concentration of iron at least ten times that of hydrogen sulphide is required. Such high concentrations of iron greatly exceed those observed in most marine sediments (Canfield, 1989; Raiswell *et al.*, 1993), despite the diffusion of iron through the sediment. It is likely, therefore that an unusual depositional event should be associated with exceptionally pyritized fossils. In Beecher's Trilobite Bed (Ordovician, USA) it is suggested that the organisms were rapidly buried by small scale slumps (Cisne, 1973; Bartels and Bassel, 1990) which deposited iron-rich sediments. Sulphate reduction was suggested to have been repressed in the majority of the sediment by the lack of easily metabolised organic matter so that the environment was dominated by iron reduction (Raiswell et *al.*, 1993). However, this is unlikely as iron-reducing bacteria utilise easily metabolisable as well as recalcitrant organic matter (Lovely *et al.*, 1993) and a mass mortality in a marine sediment is unlikely to occur without burying easily metabolisable organic material along with the more recalictrant. Therefore some other control must have affected the system causing it to be iron-dominated. Despite rapid burial, an anaerobic environment may not have been formed immediately, and the system may have had a higher Eh than sulphate-reducing bacteria prefer. The higher redox suppressed sulphate reduction in the majority of the sediment, as it does in the modern sediments of the Amazon shelf (Aller, Mackin and Cox, 1986). The interior of the carcasses, due to their membranes and the colonisation of their surfaces by iron carrying bacteria, become anaerobic allowing sulphate reduction to occur. The coincidence of sulphate and iron reduction in marine sediments is not unusual, with the highest rates of sulphate reduction being observed in iron-dominated sediments (Goldhaber & Kaplan, 1974). Recent work has also shown that bacterial iron reduction is more important than previously realised and that the simultaneous reduction of iron and sulphate is likely under a wide range of sediment environments (Chapelle & Lovely, 1992; Postma & Jakobsen, 1997). Alternatively, if the influx of fine coastal sediment containing high concentrations of reactive iron minerals

(Canfield et *al.*, 1992) these would have altered the sediment chemistry so that iron reduction was energetically more favourable than sulphate reduction, despite the development of an anaerobic environment (Postma & Jakobsen, 1997). This would occur if the iron oxide and hydroxide minerals washed in with the sediments were microbially available (Lovely and Phillips, 1986). The larger carcass would then become micro-environments of sulphate reduction (Aller, 1986), due to the higher pH within the carcass and the limited availability of ferric iron compounds. The formation of such micro-environments in a heterogeneous sediment allows sulphate reduction to occur in an open system with abundant iron, as is suggested by the stable sulphur isotopes of the trilobite legs in Beecher's Trilobite Bed (Briggs *et al.*, 1991) to be the conditions under which pyritization started in this deposit. As the system becomes closed to the water column, and iron reduction becomes organic limited, sulphate reduction can then continue within the carcasses, until either sulphate or organic matter became limiting. This would the produce stable isotope signatures similar to those seen in the Hunsrück Slate (Briggs *et al.*, 1996). In both cases the overall process of pyritization must have been terminated by lack of organic matter as suggested by Briggs *et al.* (1991).

Interpretating the controls upon pyritization in ancient sediments is complicated as the diagenetically altered sediment records the end result of a process which may have had many different routes. In environments where sulphate-reduction is not limited by the concentrations of sulphate or organic matter, pyrite concentrations are controlled by the iron compounds. High iron concentrations means that a sediment is dominated by iron monosulphides, while changing the valancy of the iron ions changes the rate of pyrite formation by changing the dominate reaction. The ratio of dissolved iron to hydrogen sulphide concentrations determining the distance from the decaying organism that pyrite is precipitated. Low iron concentrations result in the dispersal of the initial pyrite precipitate around the decay site, forming concentric rings around the carcass. High iron concentrations confine the precipitation to the decay site, as suggested by Raiswell *et al.* (1993) and Briggs *et al.* (1996), and produce infills of the organism. Bacteria play a role in the precipitation of iron sulphides around the carcass as the formation of iron sulphide biofilm from extra-cellular polysaccharides limits some pyrite formation to the area colonised by bacteria. The diffusion of iron into and sulphide out of decaying organisms is also important as it produces bands of sulphide precipitation around decaying organic matter, zones of iron-barren sediment around deposits where sulphide production is localised and sulphide mineralization on iron minerals.

References

Allen, E.T., *et al.*, **1912**, The mineral sulphides of iron, *American Journal of Science*, **33**, p. 169-236.

Allen, E.T., J.L. Crenshaw, and H.E. Merwin, **1914**, Effect of acidity and temperature in the formation of marcasite (FeS2) and wurtzite (ZnS): a contribution to the genesis of unstable forms, *American Journal of Science*, **38**, p. 393-431.

Aller, R.C., **1982**, The effects of macrobenthos on the chemical properties of marine sediment and overlying water, In:*In: Animal-sediment relations. The biogenic alteration of sediments;* , P.L. (McCall & Tevesz, J.S. Eds.), Ed.; Plenum Press: Topics in Geobiology, Vol. 2; p. 96-102.

Aller, R.C., J.E. Mackin & R. T. Cox, Jnr., **1986**, Diagenesis of Fe and S in Amazon Inner Shelf muds: Apparent dominance of Fe reduction and implications for the genesis of ironstones, *Continental Shelf Research*, **6**, p.263-289

Aller, R.C., **1994**, Bioturbation and remineralization of sedimentary organic matter: effects of redox oscillation, *Chemical Geology*, **114**, p. 331-345.

Allison, P.A., **1988**, The role of anoxia in the decay and mineralisation of proteineous macrofossils, *Palaeobiology*, **14**, p. 139-154.

Bak, F., & Pfennig, N., **1991**, Sulfate-reducing bacteria in the littorial sediment of Lake Constance, *FEMS Microbiology Ecology*, **85**, p. 43-52.

Bak, F., & Pfennig, N., **1991**, Microbial sulphate reduction in littorial sediment of Lake Constance, *FEMS Microbiology Ecology*, **85**, p. 31-42.

Bartels, C. & G. Brassel, **1990**, Fossilien im Hunsrückshiefer - Dokumente des Meeresleben im Devon, Idar- Oberstein, Museum Idar-Oberstein, 232 ps.

Bender, M.L., & Hedge, D.T., **1984**, The fate of organic carbon reaching the seafloor; a status report, *Geochem., Cosmochem. Acta*, **48**, p. 977-986.

Berner, R.A., **1962**, Iron sulfides formed from aqueous solution at low temperatures and atmospheric pressure, *American Journal of Science*, , p. 293-305.

Berner, R.A., **1964**, Distribution and diagenesis of sulfur in some sediments from the Gulf of California, *Marine Geology*, **1**, 117-140

Berner, R.A., **1967**, Diagenesis of iron sulphide in recent marine sediments, In:*Estauries: sediments and sedimentation;* , G.H. Lauff, Ed.; AAAS: Washington,

Berner, R.A., **1969**, Migration of iron and sulphur within anaerobic sediments during early diagenesis, *Amer. Jour. Sci.*, **267**, 19-21

References

Berner, R.A., **1970**, Sedimentary pyrite formation., *Amer. Jour. Sci.*, **268**, p. 1-23.

Berner, R.A., **1971**, Principles of Chemical Sedimentology, In:*Principles of Chemical Sedimentology.*; Editor, Ed.; Mc-Graw Hill Inc.: 240 pgs.

Berner, R.A., **1984**, Sedimentary pyrite formation: an update, *Geochem. Cosmochem. Acta*, **48**, 605-615.

Berner, R.A., & Westrich, J.T., **1985**, Bioturbation and the early diagenesis of carbon and sulfur, *Amer. Jour. Sci.*, **285**, p. 193-206.

Bertolin, A., P. Frizzo, and G. Rampazzo, **1995**, Sulphide speciation in surface sediments of the Lagoon of Venice : a geochemical and mineralogical study, *Marine Geology*, **123**

Bertrand, P., Lallier-Verges, E., & Boussafir, M., **1993.**, Enhancement of both accumulation and anoxic degradation of organic carbon controlled by cyclic productivity: a model, *Advances in Organic Geochemistry.*

Beveridge, T.J., Forsberg, C.W., Doyle, R.J., **1982**, Major sites of metal-binding in bacillus-licheniformis walls, *J. Bacteriology*, **150**, 3, 1438-1448

Blenkinsopp, S.A. and J.W. Costerton, **1991**, Understanding bacterial biofilms, *Tibtech*, **9**, p. 138-143.

Boesen, C., & Postma, D., **1988**, Pyrite formation in anoxic environments of the Baltic, *Am. J. Sci*, **288**, p. 575-603.

Boudreau, B.P., & Westrich, J.T., **1984**, The dependance of bacterial sulfate reduction on sulfate concentration in marine sediments, *Geochem., Cosmochem. Acta*, **48**, p. 2503-2516

Boudreau, B.P., & Canfield, D.E., **1993**, A comparrison of closed and open system models for porewater pH and calcite saturation state, *Geochim. Cosmochim. Acta*, **57**, p. 317-334.

Briggs, D.E.G., S.H. Bottrell, and R. Raiswell, **1991**, Pyritization of soft-bodied fossils: Beecher's Trilobite Bed, Upper Ordovician, New York State, *Geology*, **19**, p. 1221-1224

Briggs, D.E.G. and G.D. Edgecombe, **1992**, The Gold Bugs, *Natural History*, **11**, p. 37-42.

Briggs, D.E.G., & A.J. Kear, **1994**, Decay and mineralization of shrimps, *Palios*, **9**, p.431-456

Briggs, D.E.G., Raiswell, R., Bottrell, S.H., Hatfield, D. and Bartels, C., **1996**, Controls on pyritization of exceptionally preserved fossils: An analysis of the Lower Devonian Hunsrück Slate of Germany, *Bulletin Geological Society America*, **296**, p.633-636

Bryan, G.W. and W.J. Langton, **1992**, Bioavailability, accumulation and effects of heavy metals in sediments with special reference to United Kingdom

estuaries: a review, *Environmental Pollution*, **76**, p. 89-131.

Canfield, D.E., Raiswell, R., Westrich, J.T., Reaves, C.M., & Berner, R.A., **1986**, The use of chromium reduction in the analysis of reduced inorganic sulfur in sediment and shales, *Chemical Geology*, **54**, p. 149-155.

Canfield, D.E. & R.A. Berner, **1987**, *Geochimica Cosmochimica Acta*, **51**, p. 645-659

Canfield, D.E., **1989**, Reactive iron in marine sediments., *Geochem., Cosmochem. Acta*, **53**, p. 619-632.

Canfield, D.E., **1989**, Sulphate-reduction and oxic repiration in marine sediments-implications for organic carbon preservation in euxinic environments, *Deep-Sea Research Part A-Oceanographic research papers*, **36**, p. 121-138.

Canfield, D.E., & Raiswell, R., **1991**, Pyrite formation and fossil preservation, In:*In: Taphonomy: Releasing the data locked in the fossil record, Vol.9 of Topics in Geobiology;* , P.A. Allison & Briggs, D.E.G. (Eds.); p. 337-387.

Canfield, D.E., R. Raiswell, and S. Bottrell, **1992**, The reaction of sedimentary iron minerals towards sulphide, *American Journal of Science*, **292**, p. 659-683.

Canfield, D.E., **1994**, Factors influencing organic carbon preservation in marine sediments, *Chemical Geology*, **114**, p. 315-329.

Chanton, J.P. and C.S. Martens, **1985**, The effects of heat and stannous chloride addition on the active distillation of acid volitile sulfide from pyrite-rich marine sediment samples, *Biogeochemistry*, **1**, p. 375-383.

Chapelle, F.H., & Lovely, D.R., **1990**, Competitive exclusion of sulphate reduction by Fe(III)-Reducing bacteria: a mechanism for producing discrete zones of high iron ground water., *Ground Water*, **30**.

Cisne, J.L., **1973**, Beecher's Trilobite Bed revisited: Ecology of an Ordovician deep water fauna, *Postilla*, **160**, 25 p.

Clark, G.R., & Lutz, R.A., **1980**, Pyritization in the shells of living bivalues, *Geology*, , p. 268-271

Cline, J.D., **1969**, Spectroscopic determination of hydrogen sulphide in natural waters, *Limnol. Oceanogr.*, **14**, p. 454-458.

Coleman, M.L., & Raiswell, R., **1995**, Sources of carbonate and origins of zonations in pyritiferous carbonate concretions: evaluation of a dynamic model, *American J. Science*, **295**, p.282-302

Coleman, M., Hedrick, D.B., Lovely, D.R., White, D.C. & Pye, K., **1993**, Reduction of Fe(III) in sediments by sulphate-reducing bacteria, *Nature*, **361**, p. 436-438.

Cornwell, J.C. and J.W. Morse, **1987**, The characterisation of iron sulphide minerals in anoxic marine sediments, *Marine Chemistry*, **22**, p. 193-206.

Costerton, J.W., R.T. Irvin, and K.-J. Cheng, **1981**, The bacterial glycocalyx in nature and disease, *Annual Review of Microbiology*, **35**.

Cragg, B.A., Harvey, S.M., Fry, C.J., Herbert, R.A., & Parkes, R.J., **1992**, Bacterial biomass and activity in deep sediment layers of the Japan Sea, Hole 798B, In:*In; Proceedings of the Ocean Drilling Program, Scientific Results;* , K.A. Pisciotto Ingle, J.C., von Breymann, M.t., Barron, J. et al (Eds.), Ed.; **127/128**; p. 761-776.

Davis, P.G. and D.E.G. Briggs, **1995**, Fossilization of feathers, *Geology*, **23**, p. 783-786.

Davison, W., **1979**, Soluble inorganic ferrous complexes in natural waters, *Geochim. Cosmochim .Acta*, **43**, p. 1693-1696.

Deer, W.A., R.A. Howie, and J. Zussman, **1966**, An introduction to the rock-forming minerals, In:*An introduction to the rock-forming minerals.*; Longman: London, 528 pgs.

Drobner, E., Huber, H., Wachtershauser, G., Rose, D., & Stetter, K.O., **1990**, Pyrite formation linked with hydrogen evolution under anaerobic conditions, *Nature*, **346**, p. 742-744.

Ferris, F.G., W.S. Fyfe, and J.J. Beveridge, **1987**, Bacteria as nucleation sites for authigenic mineral s in a metal-contaiminated lake sediment, *Chemical Geology*, **74**, p.*225-232.*

Fisher, I.S.J., **1986**, Pyrite replacement of mollusc shells from the Lower Oxford Clay (Jurassic) of England, *Sedimentology*, **33**, p. 575-585.

Fisher, I.S.J., **1986**, Pyrite formation in bioturbated clays from the Jurassic of Britain, *Geochem. Cosmochem. Acta*, **50**, p. 517-523.

Fossing, H., & Jørgensen, B.B., **1989**, Measurement of bacterial sulfate reduction in sediments; evaluation of a single step chromium reduction method., *Biogeochemistry*, **8**, p. 205-222.

Froelich, P.N., *et al.*, **1979**, Early oxidation of organic matter in pelagic sediments of the eastern equatorial Atlantic: suboxic diagenesis, *Geochimica et Cosmochimica Acta*, **43**, p. 1075-1090.

Fry, J.C., **1990**, Evaluation of bacterial numbers using acridine orange staining, *Methods in Microbiology*, **22**, 41-85

Furukawa, Y. and H.L. Barnes, **1995**, Reactions forming pyrite from precipitated amorphous ferrous sulfide, In:*Geochemical transformations of sulphur;* , M.A. Vairavamurthy and M.A.A. Schoonen, Ed.; American Chemical Society: Washington, **612**; p. 194-205.

Gagnon, C., A. Mucci, and E. Pelletier, **1995**, Anomalous accumulation of acid-volatile sulphides (AVS) in a coastal marine sediment, Saguenay Fjord, Canada, *Geochimica et Cosmochimica Acta*, **59**, p. 2663-2675

Gardener, L.R., **1973**, Chemical models for sulfate reduction in closed anaerobic marine environments, *Geochem. Cosmochem. Acta*, **37**, p. 53-68.

Gibson, G.R., Parkes, R.J., & Herbert, R.A., **1987**, Evaluation of viable counting procedures for the enumeration of sulfate-reducing bacteria in estuarine sediments, *Journal of Microbiological Methods*, **7**, p. 201-210

Gerdes, G., *et al.*, **1994**, Structural diversity of biogenic particles in microbial mats, *Sedimentology*, **41**.

Goldhaber, M.B., & Kaplan, I.R., **1974**, The Sulphur Cycle, *In : The Sea (ED. E.D. Goldberg)*, Wiley Interscience, Vol. **5**, p. 569-655

Hansen, L.S. and T.H. Blackburn, **1991**, Aerobic and anaerobic mineralization of organic material in marine sediment microcosms, *Marine Ecology*, **75**, p. 283-291.

Hedges, J.L. and R.G. Keil, **1995**, Sedimentary organic matter preservation-an assessment and speculative sythesis, *Marine Chemistry*, **49**, p. 81-115.

Howarth, R.W., & Jorgensen, B.B., **1984**, Formation of ^{35}S-labelled elemental sulphur and pyrite in coastal marine sediments (Limfjorden and Kysing Fjord, Denmark) during short-term $^{35}SO_4^{2-}$ reduction measurements, *Geochem. Cosmochem. Acta*, **48**, p. 1807-1818.

Hudson, J.D., **1967**, The elemental composition of the organic fraction, and the water content of some Recent and fossil mollusc shells, *Geochimica Cosmochimica Acta*, **31**, p. 2361-2378

Hudson, J.D., **1982**, Pyrite in ammonite bearing shales from the Jurassic of England and Germany, *Sedimentology*, **29**, p. 639-667.

Issatchenho, B.L., **1912**, The deposits of iron sulfide in bacteria, In:*The deposits of iron sulfide in bacteria.*; Editor, Ed.; Bull. Jord. Inmp. Bot., Vol. **12**; : St Petersburg

Jørgensen, B.B., **1977**, Bacterial sulfate reduction within reduced micro-niches of oxidised marine sediments, *Mar. Biol.*, **41**, p. 7-17.

Jørgensen, B.B., **1982**, Ecology of the bacteria of the sulphur cycle with special reference to anoxic-oxic interface environments, *Phil. Trans. Roy. Soc. Lond.*, **B298**, p. 543-561.

Kelly, J.A., **1992**, *The determination of aid volatile sulphides in marine sediments and their relevance to the bioavailability of heavy metals*, MSc Thesis, Leeds University:

Kenrich, P., & Edwards, D., **1988**, The anatomy of Lower Devonian, Gosslinga brecanersis (Heard) based on pyritized axes with some comments on the permineralization process, *Bot. Jour. Limean Soc.*, **97**, p. 95-123.

Kohen, M.E., *et al.*, **1989**, Early incorporation of polysulphides in sedimentary organic matter, *Nature*, **341**, p. 640-641.

Konhauser, K.O., *et al.*, **1993**, Metal sorption and mineral precipitation by bacteria in two Amazonian river systems: Rio Solimões and rio Negro, Brazil, *Geology*, **21**, p. 1103-1106.

Krairaponond, N., DeLaune, R.D., & Patrick, W.H., **1992**, Distribution of organic and reduced sulfur forms in marsh soils of coastal Louisiana., *Org. Geochem.*, **18**, p. 489-500.

Krauskopf, K.B., **1982**, Introduction to geochemistry, McGraw-Hill International Editions, 617 pages

Kríbek, J., **1975**, The origin of framboidal pyrite as a surface effect of sulphur grains, *Mineral. Deposita*, **10**, p. 389-396.

Lang, W.D., **1913**, The Lower Pliensbachian-Carixian-of Charmouth, *Geological Magazine*, **5**, p. 401-412.

Lang, W.D., *et al.*, **1928**, The Belemnite Marls of Charmouth, a series of the Lias of the Dorset Coast, *Quarterly Journal of the Geological Society*, **84**, p. 179-257.

Leventhal, J., **1995**, Carbon-sulfur plots to show diagenetic and epigenetic sulfidization in sediments, *Geochimica et Cosmochimica Acta*, **59**, p. 1207-1211.

Leventhal, J., & Taylor, C., **1990**, Comparrison of methods to determine degree of pyritization, *Geochim., Cosmochim Acta*, **54**, p. 2621-2625.

Liesegang, R.E., **1913**, Geologische Diffusionen, Dresden and Leipzig, Steinkopff, 180 pages

Lovely, D. R. & Phillips, E.J., **1986**, Organic matter mineralization with reduction of ferric iron in anaerobic sediments, *Appl. Environ. Microbiol.*, **52**, p.683-689

Lovely, D.R., Roden, E.E., , Phillips, E.J.P., & Woodward, J.C., **1993**, Enzymatic iron and uranium reduction by sulfate-reducing bacteria, *Marine Geology*, **113**, p. 41-53

Luther, G.W., A.E. Giblin, and R. Varsolona, **1985**, Polarographic analysis of sulfur species in marine porewaters, *Limnology and Oceanography*, **30**, p. 727-736.

Luther, G.W., *et al.*, **1986**, Inorganic and organic sulfur cycling in salt-marsh pore waters, *Science*, **232**, p. 746-749.

Luther, G.W., **1991**, Pyrite sythesis via polysulphide compounds, *Geochem., Cosmochem. Acta*, **55**, p. 2839-2849.

Luther, G.W. and T.G. Ferdelmann, **1993**, Voltametric characterisation of iron (III) sulfide complexes in laboratory solutions and in marine waters and porewaters, *Science*, **276**, p. 1154-1163.

Macfarlane, G.T., Russ, M.A., Keith, S.M., & Herbert, R.A., **1984**, Simulation of microbial processes in estuarine sediments using gel-stablised systems, *J. General Microbiology*, **130**, p. 2927-2933

Marnette, E.C., Van Breemen, N., Hordijk, K.A., & Cappenberg, T.E., **1993**, Pyrite formation in freshwater systems in the Netherlands, *Geochim., Cosmochim. Acta*, **57**, p. 4165-4177.

Middelburg, J.J., **1989**, A simple rate model for organic matter decomposition in marine sediments, *Geochim., Cosmochim. Acta*, **53**, p. 1577-1581.

Morris, K.A., **1979**, A classification of Jurassic marine sequences and an example from the Toarcian (Lower Jurassic) of Great Britain, *Palaeogeography, palaeoclimatograph and palaeoecology*, **26**, p. 117-126.

Morse, J.W., Millero, F.J., Cornwell, J.C., & Rickard, D., **1987**, The chemistry of hydrogen sulphide and iron sulphide systems in natural waters, *Earth Science Review*, **24**, p. 1-42.

Morse, J.W. and J.C. Cornwell, **1987**, Analysis and distribution of iron sulfide minerals in Recent anoxic marine sediments, *Marine Chemistry*, **22**, p. 55-69.

Mossman, J.-R., Aplin, A.C., Curits, C.D., & Coleman, M.L., **1991**, Geochemistry of inorganic and organic sulphur in organic-rich sediments from the Peru margin, *Geochem. Cosmochem. Acta*, **55**, p. 3581-3592.

Nedwell, D.B., **1984**, The input and mineralization of organic carbon in anaerobic aquatic systems, *Advances in Mcrobial Ecology*, **7**, p. 93-131.

Oenema, O., **1990**, Pyrite accumulation in salt-marshes in the Eastern Scheldt, Southwest Wethertands, *Biogeochemistry*, **9**, p. 75-98.

Ortoleva, P.J., **1994**, Geochemical Self-Organization, Oxford University Press, 411 pages

Ortoleva, P.J., Merino, E., Moore, C., & Chadam, J., **1987**, Geochemical self-organization I: reaction-transport feedbacks and modelling approach, *American Journal of Science*, **287**, p. 979-1007.

Overnell, J., Harvey, S.M., & Parkes, R.J., **1995**, A biogeochemical comparison of sea loch sediments. Manganese and iron contents, sulphate reduction and oxygen uptake rates, *Oceanologica Acta*, **19**, p. 41-55.

Parkes, R.J., & Buckingham, W.J., **1986**, The flow of organic carbon through aerobic respiration and sulphate-reduction in in-shore marine sediments, Proc. IV-ISME, p. 617-624.

Parkes, R.J., *et al.*, **1994**, Deep bacterial biosphere in Pacific Ocean sediments, *Nature*, **371**, p. 410-413.

Pedley, M., **1992**, Freshwater (phytoherm) reefs: the role of biofilms and their bearing on marine reef cementation, *Sedimentary Geology*, **79**, p. 255-274.

Pfennig, N., **1984**, Microbial behaviour in the natural environment., In:*The Microbe, 1984;* , D.P. Kelly and N.G. Carr, Ed.; Syposium for the Society of General Microbiology; Cambridge University Press: Cambridge, II - Prokaryotes and Eukaryotes; p. 23-50.

Pfennig, N., & Widdel, F., **1982**, The bacteria of the sulphur cycle, *Phil. Trans. Roy. Soc. Lond.*, **B298**, p. 433-441.

Postgate, J., **1979**, The sulphate-reducing bacteria, In:*The sulphate-reducing bacteria.*; Editor, Ed.; Cambridge University Press

Postma, D., & Jakobsen, R., **1996**, Redox zonation: equilibrium constraints on the Fe (III)/SO_4 reduction interface, *Geochimica et Cosmochimica Acta*, **60**, p: 3169-3175.

Pruden, G. and C. Blommfield, **1968**, The determination of ferrous sulfide in soil in the presence of ferric oxide, *Analyst*, **93**, p. 532-534.

Psenner, R., **1983**, The origin of pyrite in Recent sediments of the Piburg Lake (Piburgsee, Tirol, Austria), *Schweizerische zeitschrift Fur hydrologie-Swiss Journal of Hydrology*, **45**, p. 219-232.

Raiswell, R., **1982**, Pyrite texture, isotope composition and the availablity of iron, *Amer. Jour. Sci.*, **282**, p. 1244-1263.

Raiswell, R., & Berner,R.A., **1985**, Pyrite formation in euxinic and semi-euxinic sediments, *Amer. Jour. Sci.*, **285**, p. 710-724.

Raiswell, R., Buckley, F., Berner, R.A., & Anderson, T.F., **1988**, Degree of pyritization of iron as a palaeoenvironmental indicator of bottom water oxygenation, *Jour. Sed. Pet.*, **58**, p. 812-819.

Raiswell, R., *et al.*, **1993**, A simple 3-dimensional model of diffusion-with-precipitation applied to localised pyrite formation in framboids, fossils and detrital iron minerals, *Geology*, **113**, p. 89-100.

Rice, C.A., M.L. Tuttle, and R.L. Reynolds, **1993**, The analysis of forms of sulfur in ancient sediments and sedimentary rocks: comments and cautions, *Chemical Geology*, **107**, p. 83-95.

Rickard, D.T., **1969**, The chemistry of iron sulphide formation at low temperatures., *Stockholm contributions to geology*, **23**, p. 67-95.

Rickard, D.T., **1969**, The microbiological formation of iron sulphides, *Stockholm Contributions to Geology*, **20**, p. 49-66.

Rickard, D.T., **1970**, The origin of framboids, *Lithos*, **3**, p. 269-293.

Rickard, D.T., **1975**, Kinetics and mechanism of pyrite formation at low temperatures, *Amer. Jour. Sci.*, **275**, p. 636-652.

Rickard, D.T., **1989**, Experimental concentration-time curves for the iron(III) sulphide precipitation process in aqueous solutions and their interpretation., *Chemical Geology*, **78**, p. 315-324.

Rickard, D.T., **1995**, Kinetics of FeS precipitation :Part 1. Competing reaction mechanisms, *Geochimica et Cosmochimica Acta*, **59**, p.4367-4379.

Rickard, D.T., 1997, Kinetics of pyrite formation by the H_2S oxidation of iron (II) monosulfide in aqueous solutions between 25°C and 125°C: the rate equation, *Geochimica et Cosmochimica Acta*, **61.**

Rickard, D.T., M.A.A. Schoonen & G.W. Luther III, 1995, Chemistry of iron sulphides in sedimentary environments, In:*Geochemical transformations of sulphur;* , M.A. Vairavamurthy and M.A.A. Schoonen, Ed.; American Chemical Society: Washington, **612**; p. 168-193.

Rickard, D.T., & Luther, G.W., 1997, Kinetics of pyrite formation by the H_2S oxidation of iron (II) monosulfide in aqueous solutions between 25°C and 125°C: the mechanism, *Geochimica et Cosmochimica Acta*, **61.**

Roberts, W.M.B., A.L. Walker, and A.S. Buchanan, 1969, The chemistry of pyrite formation in aqueous solution and its relation to the depositional environment, *Mineral.Deposita*, 4, p. 18-29.

Savrda, C.E., & Bottjer, D.J., 1991, Oxygen-related biofacies in marine strata: an overview and update, In:*Modern and ancient continental shelf anoxia;* , R.V. Tyson & Pearson, T.H., Ed.; Geological Society Special Publication; London, 58; p. 201-219.

Schimmelmann, A., & Kastner, M., 1993, Evolutionary changes over the last 1000 years of reduced sulphur phases and organic carbon in varved sediments of the Santa Barbara Basin, California, *Geochim., Cosmochim. Acta*, 57, p. 67-78.

Schoonen, M.A.A., & Barnes, H.L., 1991, Reactions forming pyrite and marcasite from solution:I. Nucleation of FeS2 below 100°C, *Geochem. cosmochem. acta*, 55, p. 1495-1504.

Schoonen, M.A.A., & Barnes, H.L., 1991, Reactions forming pyrite and marcasite from solution:II. Via FeS precursors below 100°C, *Geochem. cosmochem. acta*, 55, p. 1505-1514.

Sellwood, B.W., 1972, Regional environmental changes across a lower Jurassic stage boundary in Britain, *Palaeontology*, 15, p.125-157.

Sweeney, R.E. and I.R. Kaplan, 1973, Pyrite framboid formation: Laboratory sythesis and marine sediments, *Economic Geology*, 68, p. 618-634.

Taylor, P., Rummery, T.E., & Owen, D.C., 1979, Reactions of iron monosulfide solid with aqueous hydrogen sulfide up to 160°C, *J. Inorg. Nucl. Chem.*, 41, p.1683-1687

Taylor, P., 1980, The sterochemistry of iron sulfides- a structural rationale for the crystallisatin of some metastable phases from the aqueous solution., *American Mineralogoist*, 65, p. 1026-1030.

Thode-Anderson, S., & Jorgensen, B.B., **1989**, Sulfate reduction and the formation of ^{35}S-labelled FeS, FeS_2 and S^o in coastal marine sediments, *Limnol. Oceanogr.*, **34**, p. 793-806.

Thomsen, E., & T.O. Vorren, **1984**, Pyritization of tubes and burrows from Late Pleistocene continental shelf sediments off North Norway, *Sedimentology*, **31**, p.481-492.

Troelsen, H., & Jørgensen, B.B., **1982**, Seasonal dynamics of elemental sulfur in two coastal sediments, *Esturine, Coastal and Shelf Science*, **15**, p. 255-266.

Wada, H., **1977**, The sythesis of gregite from a polysulphide solution at about 100°C, *Bulletin of the Chemical Society of Japan*, **50**, p.2615-2617.

Wang, Q. and J.W. Morse, **1995**, Laboratory simulation of pyrite formation in anoxic sediments, In:*Geochemical transformations of sulphur;* , M.A. Vairavamurthy and M.A.A. Schoonen, Ed.; American Chemical Society: Washington, **612**; p. 206-223.

Westrich, J.T., & Berner, R.A., **1984**, The role of sdimentary organic matter in bacterial sulphate reduction; the G model tested, *Limnol. Oceanogr.*, **29**, p. 236-249.

Widdel, F., **1988**, Microbiology and ecology of sulfate and sulfur-reducing bacteria, In:*The biology of anaerobic micro-organisms,;* , A.J.B. Zehnder, Ed.; Series in ecological and applied microbiology; Wiley Interscience, J. Wiley & Sons: London,

Wilson, V., Welch, F.B.A., & Green, W.G., **1958**, Geology of the country around Bridport and Yeovil, In:*Geology of the country around Bridport and Yeovil.*; Editor, Ed.; Memoirs of the Geological Survey of Great Britain, HMSO: London, 239 pgs.

Wimpenny, J.W.T., *et al.*, **1981**, A gel-stablisied model ecosystem for the investigation of microbial growth in spatially ordered solute gradients,. *Journal o General Microbiology*, **127**, p. 277-287

Wuttke, M., **1983**, "Weichteik-Erhaltung" durcg lithifizierte Mikroorrganismen bei mitteleozanen Vertebraten aus den Ölschiefern der "Grube Messel" bei Darnstadt, *Senckenbergiana Lethaea*, **64**, p. 509-527

Yaakov, S.B., **1973**, pH buffering of pore water in Recent anoxic marine sediments, *Limnol. Oceanogr.*, **18**, p. 86-94.

Zhabina, N.N. and I.I. Volkov, **1978**, A method of determination of various sulfur compounds in sea sediments and rocks, In:*Environmental biogeochemistry and geomicrobiology;* , W.E. Krumbein, Ed.; Ann Arbor Science: *3. Methods, metals and assessment*; p. 735-746.

Appendix One
Abbreviations Used

PS - Pyritic sulphide.

AVS - Acid Volatile Sulphide.

H_2S - Hydrogen Sulphide.

ES - Elemental Sulphur.

TRIS -Total reduced inorganic sulphide.

SO_4 - sulphate

Fe - iron.

FeS - mackinawite.

[x] - the concentration of x.

DOP - degree of pyritization.

DOS - degree of sulphization.

Treatment Types

NT - not topped.

SO - topped with sulphate medium.

NS - topped with sulphate-free medium.

LS - medium used for experiment and topping has a sulphate concentration of 50% of the normal medium.

TS - topped with sulphate free marine salts.

Appendix Two
Preparation of the Jones Reductor column

This column is used to reduce the chromic chloride solution to chromous chloride, which is then used in the pyritic sulphide and elemental sulphur digestions. It is prepared by mixing 300g of zinc with 300ml of 2% mercuric chloride solution and 2 ml of concentrated nitric acid. This was stired with a glass rod until all the zinc had become silvery and the metal had become heavy to stir. The zinc was then washed several times by decantion and carefully transfered into a glass column filled with water, trying to minimise the number of air spaces remaining.

In order to reduce chromous chloride the column was first primed with 5% HCL solution. 1M Chromous chloride in 0.5N HCl was then introduced into the column and is slowly drawn through it until it turns peacock blue. The solution is then used in pyritic sulphide, elemental sulphur and TRIS digestions.

Appendix Three
Preparation of artifical compounds

Iron Sulphides

Amorphous FeS - 6.5g of $Fe(NH_4)_2(SO_4)_2.6H_2O$ was mixed with 7g of $Na_2S.9H_2O$ in 400ml of deoxygenated, distilled water at room temperature (Cornwell and Morse, 1987). The residue was filtered, washed and stored in a vial under nitrogen.

Gregite - 6.5g of $Fe(NH_4)_2(SO_4)_2.6H_2O$ was mixed with 7g of $Na_2S.9H_2O$ in 400ml of deoxygenated, distilled water. This was boiled overnight before washing in deoxygenated distilled water (Cornwell and Morse, 1987). It was then stored in a vial under nitrogen.

Pyrite - 6.5g of $Fe(NH_4)_2(SO_4)_2.6H_2O$ was mixed with 7g of $Na_2S.9H_2O$ in 400ml of deoxygenated, distilled water in a duran bottle. 10ml of polysulphide solution and 3g of flowers of sulphur were added to the duran bottle and the headspace flushed with nitrogen. It was then sealed and heated for for days at 65°C and a further four days at 85°C.

The residue was filtered, washed in 1M HCl and deoxygenated water before drying overnight at 90°C. It was then extracted several times with dichloromethane (Cornwell and Morse, 1987) and stored in a vial under nitrogen.

Sulphur Compounds

Elemental Sulphur - collodial suspension - 1g of flowers of sulphur was boiled in 50ml of acetone for three minutes. This acetone solution was then mixed with water in a ratio of 1:3 (Fossing, 1989)

- Flowers of sulphur - A sulphur saturated solution of dichloromethane was evaporated and then the product washed with deoxygenated, distilled water.

Polysulphide solution - A solution of 1M sodium sulphide and 0.5M of elemental sulphur was boiled. This was then removed from the heat, cooled and filtered.

Iron Oxyhydroxides

Lepidocrocite - Sodium hydroxide solution was added to a suspension of ferric oxalate in order to obtain a ratio of OH/Fe of 1.5. The solution was then oxidated with carbon dioxide free air and washed with sodium hydroxide.

An alternative method of making lepidocrocite (Lovely and Phllips, 1986) was also used. A solution of 0.4M ferric chloride was prepared and sufficient sodium hydroxide added to bring the pH up to 7. This was then washed with deionised water until the chloride ion concentration was less than 1mM.

Appendix Four
Media Receipes

The media used in the bacterial experiments in Chapter Three was based on the receipes in Table (Widdels, 1988), and the different variations of in the constituents of the media are also listed. Media were autoclaved and cooled under either oxygen free nitrogen (Postgates) or nitrogen/carbon dioxide (Widdels), prior to dispensing into autoclaved 100ml vials which contained either 0.14g of ferrous sulphate, 0.05 g of lepidocrocite, or 0.05 g of amorphous iron monosulphide.. In the experiment containing 15mM 0.42g/100ml of ferrous sulphate or 0.15g/100ml of lepidocrocite were put in the experiment. The headspaces were then flushed with the appropriate gas and the vials were sealed with grey neoprene septa or blue butyl stopper, pierced with 1.1mm gauge needles and 3-way taps.

Table XIV: Media Recipes

Postgates B medium (Based on DSM 63)		**Widdels Medium (based on DSM 363)**	
Compound	g/l	Compound	g/l
Potassium phosphate	0.5	Potassium dihydrogen phosphate	0.2
Ammonium chloride	1.0	Ammonium chloride	0.3
Calcium chloride	0.1	Calcium chloride	0.15
Magnesium sulphate	2.0	Magnesium chloride	3.0
Resazurin	0.0001	Sodium chloride	1.0
Thioglycolatic acid	0.1	Potassium chloride	0.5
Ascorbic acid	0.1	Sodium bicarbonate	2.5
Sodium sulphate	0.545	Sodium sulphide	0.4
Yeast extract	1.0	Sodium sulphate	2.29
		Sodium acetate	2.5
		Resazurin	0.1
		Sodium selenate	0.2
		Vitamin solution	0.1
		Trace Element solution	0.1

Appendix Four

Media Variations

Lactate-rich Postgates Medium - 17.5ml per litre of Postgates salts of 60% DL lactic acid solution (sodium salt).

Lactate-rich Widdels Medium - 22.3ml per litre of lactic acid.

Lactate-poor Postgates Medium - 2.8ml per litre of lactic acid.

Lactate-poor Widdels Medium - 2.8ml per litre of lactic acid.

Acetate Widdels Medium- 2.5g per litre of sodium acetate trihydrate.

Sulphate-free Medium - All the compounds containing sulphate were removed from the medium and 17.5ml per litre of lactic acid was added.

Low Sulphate Medium - 17.5ml per litre of lactic acid and half the quantity of sulphates, so that the sulphate reduction potential was reduced by 50%.

Salts - The medium was made without any organic compounds or sulphates.

Buffered Medium - 34.9g per litre potassium hydrogen phosphate (dibasic salt) and 27.22g per litre potassium dihydrogen phosphate were added to the lactate-rich and lactate-poor Postgates medium.

Inorganic solution- This solution was a 5mM solution of sodium chloride.

Appendix Five

Methods for determining the concentrations of dissolved sulphide, sulphate and thiosulphate ions

A5.1 - Sulphide Titration

It was necessary to determine the exact molarity of the sulphide solutions analysed during these experiments. Solutions used in the modified sulphide assay (Cline, 1969) were standardized against a sulphide solution prepared using 100ml of degassed water and 0.753g of sodium sulphide. This was then reacted with an acidified iodine solution and titrated against thiosulphate in order to determine its molarity. 2ml of the sulphide solution was mixed with 10ml of a 0.02N iodine solution and 5ml of a 6N HCl solution in triplicate 250ml flat bottom flasks. Three additional mixtures were also prepared substituting distilled water for the sulphide solution to make control solutions. The flasks were placed in the dark for five minutes and then titrated against 0.02 N thiosulphate solution. Starch solution was used to clarify the end point of the reaction. The solution changed from yellow to pale yellow, then to blue-black when the starch was added. As the blue-black colour disappeared the end-point was reached. The volume of thiosulphate solution used in the blanks is greater than that used in the titrations using sulphide as the iodine reacts with sulphide to produce iodine ions and elemental sulphur (Kelly, 1992). The molarity of the sulphide solution was then calculated by:

*Normality of sulphide = ((volume of thiosulphate for blank-volume of thiosulphate for sample)*0.02 / volume of sulphide standard*

Molarity of sulphide solution = Normality of sulphide solution / 2 Eq. A5.1

A5.2 - Methods for determining the concentration of Reduced Sulphur Species in cultures.

Acid Volatile Sulphide (AVS) concentrations 2ml of experimental sample stored in zinc acetate were used in each digestion and the

procedure followed that outlined for aqueous samples in Chapter 2. 100µl from the zinc acetate trap was then used in the sulphide assay (Appendix 4) to calculate the AVS content of the sample (Chapter Two).

Pyritic sulphide (PS) and elemental sulphur (ES) concentrations 2ml of each experimental sample was used in each digestion. The procedure followed was as for aqueous samples in Chapter 2. 100µl from each zinc acetate trap was taken and analysed for sulphide. The cold digestion is used to calculate the concentration of pyritic sulphide while the trap used during heating is used to calculate the concentration of elemental sulphur.

A5.3 - Bacterial Direct Counts (AODC) Samples fixed in 4% filter-sterilized formalin were used in order to determine changes in the bacterial population. These were vortex mixed to suspend all the particles and then 10µl of the solution was placed in a sterlin vial with 10ml of 0.1µm filtered 2% formalin. 50µl of acridine orange was added to the vial and this was mixed thoroughly. After 3 minutes the mixture was filtered onto a black polycarbonate membrane (Nucleopore Cat. No. SN116060). This filter was washed with additional filter sterilised formalin and mounted on a glass slide using paraffin. The slide was examined under epifluorescent blue light (Zeiss filter set at 487909) using a 100x/1.30 Plan-Neofluor oil immersion objective. Bacteria were counted in a minimum of 100 fields or to 200 cells, and the numbers calculated using the following equation:

$$\textit{No. of bacteria per ml sample} = \frac{\textit{Average no. per view} * 3.463x10^{8}}{a * v} \qquad \text{Eq. A5.1}$$

where $3.463x10^{8}$.is the effective filtration area of the membrane, a is the area of the field of view in μm^2 and v is the volume of sample filtered in µl. This can then be converted into the number of bacteria per ml.

A5.4 - Modified Sulphide Assay (after Cline, 1969)

100µl of 10% zinc acetate solution was pipetted into 7 @ 1.5ml eppendorfs. 1ml of sulphide stock was diluted with 9ml of distilled, degassed water, and 10µl, 30µl, 50µl, 100µl, 150µl and 200µl of this solution were then added to the zinc acetate (Table XII). One eppendorf remained as the blank. Acidified ferrous chloride

solution (60g per litre 50% HCl) and N, N - Dimethyl-p-phenylene diamine sulphate (40g per litre in 50% HCl) were mixed together in equal quantities and 100µl was pipetted into each eppendorf. 100µl of a sample fixed in zinc acetate was pipetted into an eppendorf to which 100µl of mixed reagent was added (Table XV).

The colour was left to develop for 40 mins, before making the volume up to 1ml with distilled water. This was left again for 5 minutes prior to 208µl being pipetted into 5ml of distilled water. The intensity of the colour was measured spectrophotometrically (CECIL CE292, Digital Ultraviolet Spectrophotometer) at 670 nanometers. The intensity of the standards minus that of the blank should then form a straight line when plotted against concentration. The equation of this line is:

$$molarity = gradient * absorption + intercept \qquad \text{Eq.A5.3}$$

and can be used to calculate the concentration of sulphide in the samples.

Table XV- Proportions of sulphide solution, reagent and water required in the sulphide assay

µl		ZnAc µl	Complex	H_2O
	0	100	100	800
	10	100	100	790
	30	100	100	770
	50	100	100	750
	100	100	100	700
	150	100	100	650
	200	100	100	600
Samples	**100**	**100**	**800**	

A5.5 - Determination of Sulphate and Thiosulphate Ion concentrations

Samples were stored in zinc acetate and centrifuged to remove particulate material. 100µl of solution was pipetted into 9.9ml of MilliQ water. This was then injected into an ion exchange liquid chromatography system (Dionex 4000i, Dionex Ltd., UK.) using an Ion Pac AG4A (PN 37042) column coupled to a micro-membrane and an AG4A guard column (Dionex Ltd.).

Appendix Six
Chapter Three results

These tables list the results from the bacterial incubations discussed in Chapter Three. Table contains the data from the bacterial incubations under different starting conditions, and table contains the data from the aged experiments.

Appendix Six

Data from the Incubations of Sulphate-Reducing Bacteria

Experiment	Group	Medium	Ibung	Bacteria		Treatment	Iron	mmols free sulphide	2.00	4.00	8.00	10.00	mmols Monosulphides	2.00	4.00	8.00	10.00	mmols pyritic sulphide	2.00	4.00	8.00	10.00	mmols elemental sulphide	2.00	4.00	8.00	10.00	TRIS	2.00	4.00	8.00	10.00	pH	2.00	4.00	8.00	10.00	Sulphate	4.00	8.00	10.00	Sulphate	2.00	4.00	8.00	10.00	substrate	2.00	4.00	8.00	10.00	% S recovered	4.00	8.00	10.00
3		Postgates	grey	Ivibrio	lactate	INS	F		0.08		0.95	1.04		0.00		3.56	4.16		0.00		9.39	10.87		0.00	2.61	3.12	0.00	0.08	0.00	16.51	19.20	7.00	7.15		5.72	6.88	6.99		19.92		7.00	7.15		17.57	17.57	17.57	17.57		78.72	86.59	103.91	114.30		120		99	182	139
3		Postgates	grey	Ivibrio	lactate	INT	F		0.03		1.25	1.23		0.00		2.40	2.93		0.00		11.05	10.28		0.00	1.15	1.70	0.00	0.03	0.00	15.89	16.14	6.90	7.12		5.80	6.75	6.45		16.12		8.42	1.89		17.57	17.57	17.57	17.57		71.57	71.57	71.57	71.57		92		48	101	103
3		Postgates	grey	Ivibrio	lactate	INT	F		0.00		1.61	1.44		0.00		4.71	3.63		1.04		9.01	9.77		0.00	3.09	1.20	0.00	1.05	0.00	18.43	16.04	7.00	6.74		6.85	7.06	7.14		16.93		7.85	1.92		17.57	17.57	17.57	17.57		71.57	71.57	71.57	71.57		102		45	116	102
3		Postgates	grey	Ivibrio	lactate	ISO	F		0.04		1.75	1.53		0.00		4.71	2.42		0.00		10.24	10.41		0.00	2.96	0.89	0.00	0.00	0.04	0.00	19.65	15.25	7.00	6.36		6.04	6.82	6.79		17.94		12.78	1.99		17.57	19.33	21.08	24.60	26.36	71.57	78.72	86.59	103.91	114.30		93		61	88	65
3		Postgates	grey	Ivibrio	lactate	ISO	F		0.03		1.76	1.42		0.00		3.77	3.19		1.04		7.09	8.19		0.00	2.02	0.97	0.00	1.07	0.00	14.64	13.78	6.90	7.04		6.07	7.02	7.02		16.29		14.16	2.12		17.57	19.33	21.08	24.60	26.36	71.57	78.72	86.59	103.91	114.30		90		67	68	60
3		Postgates	grey	Ivibrio	lactate	INS	L		0.05		1.17	1.02		0.00		3.58	2.32		0.00		0.00	7.05		0.00	2.41	1.30	0.00	0.05	0.00	7.16	11.72	7.00	6.72		6.50	6.79	6.99		21.21		22.88	22.07		2.51	17.57	17.57	17.57	17.57	71.57	78.72	86.59	103.91	114.30		121		130	166	81
4		Postgates	grey	Ivibrio	lactate	ISO	F		0.07		2.07	1.53		0.00		5.22	5.28		0.00		8.43	8.90		0.00	3.15	3.74	0.00	0.07	0.00	18.87	19.46	6.90	7.12		6.18	6.45	6.52		14.61		2.63	1.90		0.00	17.57	19.33	21.08	24.60	26.36	71.57	78.72	86.59	103.91	114.30		76		12	84	74
4		Postgates	grey	Ivibrio	lactate	INT	L		0.02		1.48	1.40		0.05		3.32	3.32		1.16		10.55	11.94		0.03	1.85	1.92	0.00	1.26	0.00	17.20	18.58	6.90	7.21		6.30	7.00	7.02		15.34		11.35	2.04		2.04	17.57	17.57	17.57	17.57	71.57	71.57	71.57	71.57	71.57		94		65	110	117
4		Postgates	grey	Ivibrio	lactate	INS	L		0.07		1.14	1.04		0.08		4.41	3.44		0.00		10.87	10.99		0.00	3.27	2.40	0.00	0.15	0.00	19.68	17.88	6.90	7.12		6.30	6.78	6.65		16.69		6.00	1.99		2.04	17.57	17.57	17.57	17.57	71.57	78.72	86.59	103.91	114.30		96		34	123	113
4		Postgates	grey	Ivibrio	lactate	INT	F		0.00		0.93	1.53		0.00		4.80	3.45		1.04		7.67	7.87		0.00	3.87	1.05	0.00	1.05	0.00	17.27	13.90	7.00	6.34		6.21	6.75	6.82		9.96		7.40	1.63		1.60	17.57	17.57	17.57	17.57	71.57	71.57	71.57	71.57	71.57		63		42	108	84
4		Postgates	grey	Ivibrio	lactate	ISO	L		0.09		1.73	1.44		0.00		3.44	3.14		0.00		6.74	7.80		0.00	1.71	0.93	0.00	0.09	0.00	13.62	13.32	7.00	6.69		6.98	6.97	7.05		9.96		6.91	0.00		0.00	17.57	19.33	21.08	24.60	26.36	71.57	78.72	86.59	103.91	114.30		52		33	55	51
4		Postgates	grey	Ivibrio	lactate	INS	L		0.08		1.40	1.32		0.05		5.63	2.34		0.00		5.98	6.76		0.00	4.23	1.02	0.00	0.13	0.00	17.25	11.45	7.00	6.70		6.81	6.98	6.79		16.18		7.14	1.98		2.39	17.57	17.57	17.57	17.57	71.57	78.72	86.59	103.91	114.30		93		41	109	79
7		Postgates	grey	Ivibrio	normal	INS	F	0.15	0.24	0.19	0.54	0.31	0.02	0.00	1.25	8.27	1.39		2.25			0.80		0.08		7.24	2.52	2.69	5.07	3.36	10.14	6.90	6.99		6.93	7.02	7.01		14.92		10.50	1.94		1.41	17.57	17.57	17.57	17.57	17.57	19.08	20.99	23.09	27.70	30.47		100		89	30	66
7		Postgates	grey	Ivibrio	normal	INT	F	0.08	0.15	0.05	0.38	0.34	0.45	0.18	4.49	2.58	7.17		1.91			0.00		0.21		0.75	2.65	2.62	4.15	4.28	7.96	7.80	5.94		6.01	6.39	6.21		12.47		17.07	7.50		7.01	17.57	17.57	17.57	17.57	17.57	19.08	19.08	19.08	19.08	19.08		87		121	67	85
7		Postgates	grey	Ivibrio	normal	ISO	L	0.13	0.19	0.18	0.63	0.24	0.23	0.07	1.60	1.01	1.94		2.09			2.19		0.13		2.89	2.56	5.41	3.19	3.53	7.71	7.80	6.10		6.09	6.41	6.39		16.02		16.63	4.04		4.50	17.57	19.33	21.08	24.60	26.36	19.08	20.99	23.09	27.70	30.47		111		94	31	46
7		Postgates	grey	Ivibrio	normal	ISO	L	0.19	0.28	1.19	0.80	0.23	0.20	0.31	3.94	4.19	2.55		2.18			0.14		0.00		4.22	2.52	2.77	4.32	4.36	7.58	7.80	6.20		6.77	6.80	6.75		17.20		17.25	6.59		5.13	17.57	19.33	21.08	24.60	26.36	19.08	20.99	23.09	27.70	30.47		103		102	44	48
7		Postgates	grey	Ivibrio	normal	ISO	L	0.08	0.11	0.38	1.00	0.42	0.27	0.28	1.27	4.32	2.86		2.09			0.30		0.04		3.10	2.48	2.77	3.02	0.00	7.08	7.80	6.09		6.30	6.30	6.47		18.05		13.37	7.06		7.50	17.57	19.33	21.08	24.60	26.36	19.08	20.99	23.09	27.70	30.47		108		78	29	55
7		Postgates	grey	Ivibrio	normal	ISO	F	0.11	0.35	1.22	0.80	0.35	0.24	0.00	3.84	5.25	1.38		2.17			1.23		0.13		3.47	2.65	2.94	4.49	2.82	6.87	7.80	6.28		6.75	6.86	6.74		15.58		17.31	3.66		3.91	17.57	19.33	21.08	24.60	26.36	19.08	20.99	23.09	27.70	30.47		96		103	26	41
7		Postgates	grey	Ivibrio	normal	INS	L	0.23	0.29	1.45	0.74	0.24	0.30	0.04	0.00	6.95	3.73		1.91			0.00		0.29		1.84	2.69	2.77	4.28	4.07	5.66	7.00	6.30		6.29	6.87	6.76		10.32		1.47	1.57		1.50	17.57	17.57	17.57	17.57	17.57	19.08	20.99	23.09	27.70	30.47		75		33	32	41
7		Postgates	grey	Ivibrio	normal	ISO	F	0.11	0.23	0.49	1.13	0.46	0.02	0.00	3.52	4.46	3.84		2.35			0.00		0.04		0.33	2.52	2.94	0.00	4.45	5.03	7.80	6.22		6.42	6.78	6.64		16.23		14.19	6.46		6.80	17.57	19.33	21.08	24.60	26.36	19.08	20.99	23.09	27.70	30.47		103		86	48	42
7		Postgates	grey	Ivibrio	normal	ISO	F	0.19	0.40	0.77	0.93	0.41	0.25	0.00	5.48	2.09	3.72		2.12			0.00		0.04		0.00	2.61	2.89	0.00	3.65	3.99	7.80	6.13		6.12	6.31	6.48		17.01		18.05	5.14		5.50	17.57	19.33	21.08	24.60	26.36	19.08	20.99	23.09	27.70	30.47		103		86	48	42
8		Postgates	grey	Ivibrio	haclate	ISO	F	0.15	0.06	5.11	4.57	3.72	0.00	1.46	2.55	2.57	0.00		2.66			0.78	9.64		0.17		1.21	9.68	2.98	2.94	10.43	9.13	22.92	7.80	6.78		6.91	6.83	7.06		11.6513627		0.66103037	0.25530957		0.57386785	17.57	17.57	17.57	17.57	17.57	71.57	71.57	71.57	71.57	71.57		63		53	134	
8		Postgates	grey	Ivibrio	haclate	ISO	F	0.14	0.00	5.87	4.84	4.73	0.19	0.85	0.21	3.55	4.77		2.40			0.00	0.21		0.25		4.85	3.01	2.98	3.07	7.66	12.48	12.73	7.80	6.94		6.74	6.69	6.70		10.3544609		0.66581952	2.39543689		0.52294067	17.57	19.33	21.08	24.60	26.36	71.57	78.72	86.59	103.91	114.30		69		40	60	51
8		Postgates	grey	Ivibrio	haclate	ISO	F	0.00	0.10	5.66	5.35	4.57	0.33	0.95	2.67	2.19	0.50		2.40			0.01	5.65		0.25		4.68	10.33	2.98	3.02	9.51	12.23	21.05	7.80	6.83		6.92	6.76	6.83		14.1129856		0.15599857	0.03097877		0.03302981	17.57	19.33	21.08	24.60	26.36	71.57	78.72	86.59	103.91	114.30		89		46	53	62
8		Postgates	grey	Ivibrio	haclate	ISO	F	0.03	0.11	6.92	7.55	7.55	0.62	1.46	2.25	2.68	0.00		0.00			1.06	0.00		0.71		0.81	11.02	3.19	3.11	9.44	12.10	17.50	7.80	7.07		7.19	6.87	6.80		5.36672116		0.13838727	2.46724222		0.58376542	17.57	19.33	21.08	24.60	26.36	71.57	78.72	86.59	103.91	114.30		44		45	59	69
8		Postgates	grey	Ivibrio	haclate	ISO	L	0.07	0.22	5.37	5.37	5.66	0.46	0.76	1.11	1.05	2.01		0.00			2.88	0.00		0.42		0.00	1.74	2.94	3.23	8.78	8.55	9.26	7.80	6.54		6.78	6.75	6.89		16.3258921		1.09262011	0.05643534		0.68737069	17.57	19.33	21.08	24.60	26.36	71.57	78.72	86.59	103.91	114.30		101		47	35	38
8		Postgates	grey	Ivibrio	haclate	ISO	L	0.06	0.15	5.71	4.93	4.85	0.47	1.16	2.71	1.29	2.86		0.00			4.00	2.26		0.46		0.00	0.63	2.90	3.02	6.48	9.93	10.60	7.80	6.34		6.92	6.96	6.96		10.9862251		0.74292483	0.18747925		0.53529923	17.57	19.33	21.08	24.60	26.36	71.57	78.72	86.59	103.91	114.30		73		34	43	42
9		widdels	grey	bacter	lactate	INT	L	0.05	0.01	0.00	0.00	0.02	1.84	1.66	1.49	2.84	2.88		1.11		1.00		0.02	0.30		0.33		0.31	3.30	1.66	2.82	2.84	3.23	6.98	6.91		6.94	6.99	7.06				13.25			13.31	12.12	12.12	12.12	12.12	12.12	18.38	18.38	18.38	18.38		14		133	23	136
9		widdels	grey	bacter	lactate	INT	F	0.18	0.04	0.03	0.03	0.04	1.54	1.34	1.24	1.52	1.46		1.09		0.79		1.19	0.31		0.33		0.29	3.11	1.38	2.40	1.55	2.98	6.98	7.13		7.15	7.16	7.22				13.62			15.08	12.12	12.12	12.12	12.12	12.12	18.38	18.38	18.38	18.38	18.38		11		132	13	149
9		widdels	grey	bacter	lactate	ISO	F	0.00	0.01	0.00	0.00	0.00	1.76	1.83	1.72	2.17	2.34		0.40		1.79		0.90	0.32		0.34		0.26	2.50	1.83	3.85	2.17	3.51	6.98	7.00		6.95	7.00	7.17				12.31			15.46	12.12	13.34	14.67	17.60	19.36	18.38	20.22	22.24	26.69	29.36		14		110	12	98
9		widdels	grey	bacter	lactate	ISO	L	0.20	0.04	0.03	0.04	0.01	1.35	1.28	1.41	1.74	1.76		0.90		0.90		0.56	0.33		0.36		0.30	2.78	1.33	2.69	1.78	2.63	6.98	7.15		7.11		7.42				12.53			12.40	12.12	13.34	14.67	17.60	19.36	18.38	20.22	22.24	26.69	29.36		10		104	10	78
9		widdels	grey	bacter	lactate	INS	L	0.02	0.01	0.00	0.00	0.00	1.70	1.83	1.94	2.28	2.39		0.46		1.82		0.45	0.36		0.34		0.39	2.54	1.83	4.20	2.28	3.24	6.98	7.22		7.00	7.06	7.10				13.20			12.94	12.12	12.12	12.12	12.12	12.12	18.38	20.22	22.24	26.69	29.36		15		144	19	133
9		widdels	grey	bacter	lactate	INS	L	0.15	0.05	0.04	0.02	0.01	1.78	1.11	1.40	1.30	1.38		0.00		1.09		0.52	0.29		0.37		0.29	2.24	1.16	2.90	1.33	2.19	6.98	7.02		7.23		7.29		11.60			12.17	12.12	12.12	12.12	12.12	12.12	18.38	20.22	22.24	26.69	29.36		10		120	11	119
11		bufferred	grey	Ivibrio	normal	ISO	L	0.00	0.00	0.01		0.01	4.82		0.00	0.01			0.15		1.96	6.77		1.19		0.56	0.31	1.19	0.16	0.00	2.78	12.41	7.80	6.17		5.99	5.89	6.10		17.82			18.37	17.57	19.33	21.08	24.60	26.36	19.08	20.99	23.09	27.70	30.47		93		0	11	117
11		bufferred	grey	Ivibrio	normal	ISO	F	0.00	0.00	0.14		0.90	1.44		0.04	1.26	4.49		0.23		0.83	5.80		0.00		0.50	0.31	0.00	0.41	0.00	3.50	12.03	7.80	6.17		6.05	6.12	6.34		21.44			20.58	17.57	19.33	21.08	24.60	26.36	19.08	20.99	23.09	27.70	30.47		113		0	14	124
11		bufferred	grey	Ivibrio	normal	INT	F	0.00	0.00	0.09		1.04	1.32		0.04	1.02	5.65		0.38		1.51	2.03		0.13		0.89	0.50	0.13	0.50	0.00	4.26	9.50	7.80	6.79		6.79	6.76	6.86		22.18			14.62	17.57	17.57	17.57	17.57	17.57	19.08	19.08	19.08	19.08	19.08		129		0	24	137
11		bufferred	grey	Ivibrio	normal	INT	L	0.00	0.00	0.03		0.83	0.44		0.00	0.68	0.17		0.00		3.09	5.80		0.00		0.25	0.25	0.00	0.03	0.00	4.85	6.65	7.80	6.07		5.40	5.32	5.27		23.93			9.89	17.57	17.57	17.57	17.57	17.57	19.08	19.08	19.08	19.08	19.08		136		0	28	94
11		Postgates	grey	Ivibrio	lactate	ISO	F	0.00	0.00	0.03		0.08	0.10		0.05		0.00	0.38		0.00		0.60	5.80		0.00		0.38	0.31	0.00	0.08	0.00	1.06	6.59	7.80	5.58		5.76	5.88	6.01		23.42			19.49	17.57	19.33	21.08	24.60	26.36	71.57	78.72	86.59	103.91	114.30		122		0	4	99
11		bufferred	grey	Ivibrio	lactate	INT	L	0.00	0.00	0.03		0.07	0.00		0.00	0.44	2.66		0.00		1.96	3.01		0.00		0.50	0.00	0.00	0.03	0.00	2.97	5.67	7.80	6.07		5.80	6.25	6.40		25.29			12.62	17.57	17.57	17.57	17.57	17.57	71.57	71.57	71.57	71.57	71.57		144		0	17	104
11		bufferred	grey	Ivibrio	normal	ISO	F	0.00	0.00	0.00		0.05	0.00		0.04	1.93	0.79		0.00		0.00	1.73		0.00		0.38	0.00	0.04	0.00	1.98	3.25	7.80	5.58		5.98	6.14	6.24		22.66			10.17	17.57	19.33	21.08	24.60	26.36	19.08	20.99	23.09	27.70	30.47		117		0	8	51
11		bufferred	grey	Ivibrio	normal	INT	F	0.00	0.00	0.03		0.08	0.13		0.04	0.04	0.30		0.00		0.00	2.11		0.38		0.31	0.38	0.07	0.00	0.12	2.85	7.80	6.79		6.79	6.85	6.81		17.16			13.41	17.57	17.57	17.57	17.57	17.57	19.08	19.08	19.08	19.08	19.08		98		0	1	93
11		bufferred	grey	Ivibrio	lactate	INT	F	0.00	0.00	0.12		0.04	0.03		0.02	0.00	0.80		0.08		1.20	1.35		0.00		0.44	0.06	0.00	0.21	0.00	1.68	2.25	7.80	6.75		6.67	6.80	6.86		19.88			18.07	17.57	19.33	21.08	24.60	26.36	71.57	78.72	86.59	103.91	114.30		104		0	7	77
11		bufferred	grey	Ivibrio	lactate	INT	F	0.01	0.01	0.06		0.02	0.10		0.00	0.00	0.25		0.30		0.90	1.51		0.19		0.56	0.31	0.00	0.36	0.00	1.48	2.03	6.98	7.02		7.23	7.25	7.29		17.40		18.26	12.56	17.57	17.57	17.57	17.57	17.57	71.57	71.57	71.57	71.57	71.57		101		104	8	83
11		Postgates	grey	Ivibrio	lactate	INT	F	0.00	0.00	0.01		0.02	0.02		0.00	0.00	0.01		0.15		0.98	0.00		0.00		0.50	0.00	0.00	0.20	0.00	0.02	1.51	7.80	5.85		5.59	5.45	5.95		20.57			12.01	17.57	17.57	17.57	17.57	17.57	71.57	71.57	71.57	71.57	71.57		118		0	0	77
11		Postgates	grey	Ivibrio	normal	INT	F	0.00	0.00	0.03		0.06	0.01		0.00	0.00	0.05		0.00		0.00	0.83		0.00		0.50	0.00	0.03	0.00	0.00	1.39	7.80	5.85		5.40	6.24	6.08		22.85			16.05	17.57	17.57	17.57	17.57	17.57	19.08	19.08	19.08	19.08	19.08		130		0	0	99
11		bufferred	grey	Ivibrio	lactate	ISO	L	0.00	0.00	0.03		0.00	0.00		0.00	0.00	0.00		0.23		0.60	0.25		0.00		0.19	0.25	0.26	0.00	0.00	0.79	7.80	6.79		6.42	6.11	6.60		12.96			14.62	17.57	19.33	21.08	24.60	26.36	71.57	78.72	86.59	103.91	114.30		68		0	0	58
11		bufferred	grey	Ivibrio	lactate	ISO	F	0.00	0.00	0.23		0.02	0.00		0.00	0.00	0.38		0.00		0.00	0.15		0.06		0.13	0.06	0.23	0.00	0.02	0.65	7.80	6.79		6.06	6.32	6.17		20.34			18.27	17.57	19.33	21.08	24.60	26.36	71.57	78.72	86.59	103.91	114.30		106		0	0	72
11		bufferred	grey	Ivibrio	lactate	INT	F	0.00	0.00	0.06		0.00	0.00		0.00	0.00	0.01		0.23		0.15	0.44				0.25	0.44	0.29	0.00	0.00	0.41	6.98	7.22		7.00	7.06	7.10		19.81		19.41	16.88	17.57	17.57	17.57	17.57	17.57	71.57	71.57	71.57	71.57	71.57		114		110	0	98
11		Postgates	grey	Ivibrio	normal	ISO	F	0.00	0.00	0.06		0.00	0.00		0.00	0.02	0.02		0.15		0.15	0.00				0.06	0.00	0.21	0.00	0.05	0.28	7.80	6.75		6.77	6.82	6.87		23.94			13.46	17.57	19.33	21.08	24.60	26.36	19.08	20.99	23.09	27.70	30.47		125		0	0	52
12		postgates	grey	Ivibrio	lactate	INT	F	0.24	0.22	0.21	0.03	0.04	2.41	2.43	2.74	1.53	1.51		0.00		0.00	4.65		0.12		0.00	0.00	0.00	0.16	2.77	2.65	2.95	1.56	6.37	7.80	5.14		5.31	5.75	5.94		22.67		21.83	10.89		9.83	17.57	17.57	17.57	17.57	17.57	56.71	56.71	56.71	56.71	56.71		144		141	71	92
12		postgates	grey	Ivibrio	lactate	INT	L	0.26	0.33	2.97	3.11	4.03	2.39	2.22	6.20	7.35	7.36		0.00		0.00	0.26	0.00	3.03		0.00	0.00	0.00	0.14	2.65	2.55	9.46	10.46	14.56	7.80	5.14		5.35	5.85	5.28		16.33		17.42	12.61		11.19	17.57	17.57	17.57	17.57	17.57	56.71	56.71	56.71	56.71	56.71		119		153	131	147
12		postgates	grey	Ivibrio	lactate	ISO	F	0.24	0.21	0.87	3.03	2.59	2.71	2.64	2.25	-1.39	1.07		0.00		0.00	1.39	15.32		0.00	0.00	0.00	0.03	0.00	2.85	3.12	3.05	18.98	7.80	5.93		5.91	6.33	5.96		15.58			21.49	17.57	19.33	21.08	24.60	26.36	56.71	62.38	68.62	82.34	90.58		95		15	12	154
12		postgates	grey	Ivibrio	lactate	INS	L	0.26	0.24	0.63	2.30	2.61	2.72	2.81	2.29	9.42	5.87		0.00		0.00	6.46	0.00	8.19		0.00	0.00	0.00	0.04	2.99	3.05	9.41	11.71	16.70	7.80	5.89		5.84	6.82	6.85		19.92	16.39	9.03	1.14		17.57	19.33	21.08	24.60	26.36	56.71	62.38	68.62	82.34	90.58		119		122	84	68
12		postgates	grey	Ivibrio	lactate	INS	F	0.24	0.41	1.19	0.09	0.03	2.41	2.38	1.83	1.42	1.29		0.00		0.00	0.00	0.00	0.00		0.00	0.00	0.00	0.00	2.65	2.79	3.02	1.52	1.32	7.80	5.14		5.31	5.75	5.94		22.67	21.83	10.89	9.83		17.57	17.57	17.57	17.57	17.57	56.71	62.38	68.62	82.34	90.58		145		141	71	63
12		postgates	grey	Ivibrio	lactate	INS	L	0.26	0.24	2.21	2.19	2.20	2.72	2.95	0.68	5.03	0.00		0.00		0.00	2.99	0.00	8.78		0.00	0.00	0.00	0.00	2.97	3.19	5.92	7.22	11.05	7.80	5.14		5.45	6.18	6.67		18.33	17.69	8.19	0.09		17.57	17.57	17.57	17.57	17.57	56.71	62.38	68.62	82.34	90.58		122		134	84

Concentrations of reduced sulphur species, and sulphate and pH values from experiments containing ferrous sulphate and 17.5 ml per litre lactic acid in Postgates medium, inoculated with *Desulfovibrio desulfericans*, and incubated for 163 days

Time (hrs)	pH	Sulphate (mM)	H_2S (mM)	AVS (mM)	Pyritic sulphide (mM)	Elemental Sulphur (mM)	TRIS (mM)
0	7.8	19.46	0.26	2.79	3.09	1.25	7.38
42	5.29	15.69	0.23	2.92	2.86	2.12	7.88
140	5.77	13.64	0.34	2.75	2.85	0.00	5.95
194	5.84	8.13	0.27	1.68	3.05	0.53	5.54
237	6.9	8.09	0.12	1.19	3.66	2.69	7.66
1008	6.82	5.01	1.36	5.89	5.96	0.00	13.21
1824		5.03	0.58	9.05	16.89	1.34	27.86
2712		4.86	0.59	22.04	16.02	3.16	41.82
3912		4.77	3.63	12.92	11.12	0.72	28.41

Appendix Seven
Chemical Drying for Scanning-Electron Microscopy

Samples for the SEM and the microprobe were prepared using a chemical drying technique. This fixed the specimens in 1% glutaraldehyde in 100mM cacodylate at pH 7. The specimen was then left for 5 minutes prior to washing with distilled water. After a further five minutes a series of washes in ethanol (70% ethanol- 2 five minute washes, 80% - 2 five minute washes, 95% - 2 five minute washes and 100% - 3 ten minute washes) were used to dehydrate the samples. The final stage was a wash in Hexamethyldisilizane (HMDS) for five minutes. The sample was then left to air dry in the anaerobic cabinet prior to mounting on stubs.

Appendix Eight
Results of the aqueous fossilization experiments.

This table lists the data generated in the aqueous fossilization experiments, in the form of the concentrations of sulphide determined using different procedures. The digestion results from the organic material are listed under solids.

Solids after washing in distilled water	Weight	AVS absorbance	AVS mmols/ml	AVSmmols/g	Cold chromous chloride absorbance	PS mmols/ml	PS mmols/g	Hot chromous chloride absorbance	Sulphur mmols/ml	Sulphur mmols/g	Total cold chromous chloride (mmols/ml)	TRIS (mmols/ml)	Total cold chromous chloride (mmols/g)	TRIS (mmols/ml)
Shell (Set A -day 36)	0 870	0 119	1 038	5 966	0 029	0 000	0 000	0 024	0 000	0 000	1 038	1 038	5 966	5 966
Shell (Set B - day 12)	0.750	0 219	3 286	21 909	0 048	0 000	0 000	0 038	0 000	0 000	3 286	3 286	21 909	21 909
Shell (Set B - day 22)	0 720	0 306	8.718	60 542	0 029	0 000	0 000	0 065	0 369	2 561	8 718	9 087	60 911	63 472
Shell (Set C - day 10)	0 030	0 111	1.962	327 073	0 027	0 000	0 000	0 033	0 000	0 000	1 962	1 962	327 073	327 073
Shell (Set C -day 22)	0 140	0.134	1 645	58 754	0 029	0 000	0 000	0 031	0 000	0 000	1 645	1 645	58 754	58 754
Chitin (Set A - day 22)	0 030	0 069	0.167	27 763	0 033	0 000	0 000	0 024	0 000	0 000	0 167	0 167	27 763	27 763
Chitin (Set B - day 12)	0 030	0 269	4 442	740.334	0 069	0 000	0 000	0 050	0 000	0 000	4 442	4 442	740 334	740 334
Chitin (Set B - day 12)	0 020	0.134	1 322	330 440	0 037	0 000	0 000	0 039	0 000	0 000	1 322	1 322	330 440	330 440
Chitin (Set C - day 10)	0 020	0 081	0 923	230.780	0 034	0 000	0 000	0 027	0 000	0 000	0 923	0 923	230.780	230 780
Phosphate (Set B -day 3(	0.020	0 078	0.289	72 146	0 023	0 000	0 000	0 021	0 000	0 000	0 289	0 289	72 146	0 023
Shrimp (Set A - day 12)	1.117	0 069	0 000	0 000	0 058	0 000	0 000	0 034	0 000	0 000	0 000	0 000	0 000	0 000
Shrimp (Set A - day 22)	1.000	0 056	0.057	0 285	0 048	0 000	0 000	0 025	0 000	0 000	0 057	0 057	0 285	0 285
Shrimp (Set A - day 36)	1.285	0 042	0 000	0 000	0 061	0 027	0 106	0 030	0 000	0 000	0 106	0.106	0 030	0 030
Shrimp (Set B - day 12)	1.100	0 249	3 980	18 090	0 045	0 000	0 000	0 095	0 420	1 909	3 980	5 889	18 090	18 999
Shrimp (Set B - day 36)	1 204	0.103	0 759	3 153	0 028	0 000	0 000	0 033	0 000	0 000	0 759	0 759	3 153	0 028
Shrimp (Set C - day 10)	0 930	0 068	0 473	2 542	0 032	0 000	0 000	0 019	0 000	0 000	0 473	0 473	2 542	2 542
Shrimp (Set C - day 22)	0 730	0.016	0 000	0 000	0 031	0 000	0 000	0 038	0 000	0 000	0 000	0 000	0 000	0 000

Medium	Hydrogen sulphide absorbance	PS mmols/ml	AVS absorbance	AVS mmols/ml	Cold chromous chloride absorbance	PS mmols/ml	Hot chromous chloride absorbance	ES mmols/ml	Total cold chromous chloride (mmols/ml)	TRIS (mmols/ml)
Set A (shell) - day 12	0 997	7 089	0 367	8 058	0 034	0 184	0 034	0 184	8 242	8 426
Set A (shell) - day 22	1 234	13 623	0 882	14 233	0 037	0 000	0 034	0 000	14 233	14.233
Set A (shell) - day 36	0 975	6.358	0.705	12 188	0 035	0 000	0 042	0 000	12 188	12 188
Set B (shell) - day 12	1.468	10.718	0 118	2 170	0 038	0 278	0.042	0 373	2 449	2 822
Set B (shell) - day 22	1.194	13.161	0.783	12 517	0.029	0 000	0 048	0 000	12 517	12 517
Set C (shell) - day 36	1 250	8 297	0 647	11 117	0 082	0 685	0 064	0.353	11 802	12 154
Set C (shell) - day 10	0.168	1.312	0.105	1.755	0 045	0 000	0 019	0 000	1 755	1.755
Set C (shell) - day 22	0.175	0 716	0 093	0.888	0.026	0 000	0 048	0.057	0 888	0 945
Set A (phosphate) - day 12	0.179	0.787	0 215	4 464	0 031	0 113	0 025	0 000	4 577	4 577
Set A (phosphate) - day 22	1.188	13.091	0 878	28.534	0.053	0 000	0 031	0 000	28 534	28 534
Set A (phosphate) - day 36	0 918	5 956	0 598	10 212	0 023	0.000	0.031	0 000	10 212	10 212
Set B (phosphate) - day 12	1.104	7.914	0 527	11 842	0 042	0 373	0 037	0 255	12 215	12 470
Set B (phosphate) - day 22	0 964	10.505	0 919	29 955	0 029	0 000	0 047	0 000	29 955	29 955
Set B (phosphate) - day 36	0 938	6 097	0 404	6 630	0.027	0.000	0 048	0 057	6 630	6 687
Set A (chitin) - day 12	0.309	1.789	0 572	12 906	0 034	0.184	0 028	0.042	13 090	13.132
Set A (chitin) - day 22	1.338	14.824	0 858	27.842	0 039	0 000	0 042	0.000	27 842	27 842
Set A (chitin) - day 36	0 846	5.448	0 501	8 421	0 028	0.000	0 031	0 000	8.421	8 421
Set B (chitin) - day 12	1.372	9 979	0.655	14.869	0.091	1.532	0 028	0.042	16.401	16.443
Set B (chitin) - day 22	1.438	15.976	0 781	25 174	0.036	0.000	0.022	0 000	25.174	25.174
Set B (chitin) - day 36	1.088	7.155	0.986	17.376	0 024	0 000	0.153	1.996	17.376	19.372
Set C (chitin) - day 10	0.061	0 077	0.065	0.369	0.048	0.000	0.026	0.000	0 369	0 369
Set C (chitin) - day 22	0.191	0.829	0 094	0 907	0.026	0.000	0.026	0.000	0 907	0.907
Set A (shrimp) - day 12	0.237	1.234	0 032	0.137	0.036	0 231	0.032	0.137	0.368	0.504
Set A (shrimp) - day 22	0.038	0.000	0.046	0.000	0 026	0 000	0.022	0.000	0.000	0 000
Set A (shrimp) - day 36	1.163	7.684	0.761	13 222	0.03	0 000	0.026	0.000	13.222	13.222
Set B (shrimp) - day 12	1.082	7.744	0 837	17.570	0.063	0.000	0 098	0.490	17.570	18 060
Set B (shrimp) - day 22	0.99	10.805	0.777	25 035	0.026	0 000	0.033	0.000	25.035	25.035
Set B (shrimp) - day 36	1.18	7 804	0.78	13.572	0.026	0 000	0.069	0.000	13.572	13.572
Set C (shrimp) - day 10	0.429	4.326	0.235	6.258	0.029	0.000	0.053	0 000	6 258	6.258
Set C (shrimp) - day 22	1.012	6.618	0.109	1.184	0.019	0.000	0.037	0.000	1.184	1.184

Solids after washing	Free sulphide absorbance	FS mmols/ml	AVS absorbance	AVS mmols/ml	Cold chromous chloride absorbance	PS mmols/ml	Hot chromous chloride absorbance	ES mmols/ml
Day 10 -shrimp	0.039	0.000	0.029	0.000	0.024	0.000	0.024	0.000
Day 10 - bag	0.174	4.145	0.056	0.057	0.109	1.893	0.109	0.864
Day 24 -shrimp	0.064	0.079	0.039	0.000	0.021		0.021	
Day 24 - bag	1.166	19.286	0.045	0.000	0.423	6.336	0.423	6.336
Day 36 - shrimp			0.090	0.533	0.040		0.040	
Dy 36 - bag			0.850	13.779	0.240	3.147	0.830	13.430

Medium	Free sulphide absorbance	FS mmols/ml	AVS absorbance	AVS mmols/ml	Cold chromous chloride absorbance	PS mmols/ml	Hot chromous chloride absorbance	ES mmols/ml
Day 10 -outside bag	0.166	1.289	0.037	0.000	0.031	0.000	0.02	0.000
Day 10 - inside bag	0.044		0.039	0.000	0.03	0.000	0.024	0.000
Day 24 -outside bag	0.519	3.142	0.526	8.132	0.081	0.376	0.033	0.000
Day 24 - inside bag	0.224	1.062	0.457	6.929	0.046	0.000	0.038	0.000
Day 36 - outside bag	0.98	6.393	0.6	9.421	0.09	0.533	0.03	0.000
Day 36- inside bag	0.76	4.842	0.24	3.147	0.05	0.000	0.03	0.000

Appendix Nine

Results of the gel- stablised experiments.

This table lists the data generated in the gel-stablised experiments, in the form of the concentrations of sulphide determined using different procedures. These results were used in the diagrams in Chapter Four.

Appendix Nine

Data for Experiment 1

Day 10

mm	AVS abs	AVS(mmoles/ml)	Cold CrCl Abs	Cold CrCl (mmoles/ml)	Pyrite (mmoles/ml)	Hot CrCl abs.	Hot CrCl (mmols/ml)	TRIS (mmoles/ml)
0.0000								
1.0000								
2.0000								
3.0000								
4.0000								
5.0000	0.030000	0.37500	0.030000	0.37500	0.75000	0.027000	0.23400	0.98500
6.0000								
7.0000								
8.0000								
9.0000								
10.000	0.030000	0.37500	0.028000	0.28100	0 65600	0.028000	0.28100	0.93800
11.000								
12.000								
13.000								
14.000								
15.000	0.033000	0.51600	0.027000	0.23400	0.75000	0.026000	0.18800	0.93800
16.000								
17.000								
18.000								
19.000								
20.000	0.029000	0.32800	0.026000	0.18800	0 51600	0.024000	0.094000	0.61000
21.000								
22.000								
23.000								
24.000								
25.000	0.035000	0.61000	0.024000	0.094000	0.70300	0.024000	0.094000	0.79700
26.000								
27.000								
28.000								
29.000								
30.000	0.032000	0.46900	0 031000	0.42200	0 89100	0.025000	0.14100	1.0320
35.000	0.024000	0.094000	0.026000	0.18800	0.28100	0.023000	0.047000	0.32800
40.000	0.028000	0.28100	0.032000	0.46900	0.75000	0.023000	0.047000	0.79700
45.000	0.025000	0.14100	0 031000	0.42200	0.56300	0.022000	0.0000	0.56300
50.000								
55.000	0.027000	0.23400	0.023000	0.047000	0.28100	0.024000	0.094000	0.37500
60.000								
65.000	0.024000	0.094000	0.022000	0.0000	0.094000	0.025000	0.14100	0.23400
70.000								
75.000	0.027000	0.23400	0 023000	0.047000	0 28100	0.022000	0.0000	0.28100

"Day 8 ·

mm	AVS abs	AVS(mmoles/ml)	Cold CrCl Abs	Cold CrCl (mmoles/ml)	Pyrite (mmoles/ml)	Hot CrCl abs.	Hot CrCl (mmols/ml)	TRIS (mmoles/ml)
0.0000								
1.0000								
2.0000								
3.0000								
4.0000								
5.0000	0.021000	-0.16700	0.019000	-0.27800	-0.44400	0.020000	-0.22200	-0.66600
6.0000								
7.0000								
8.0000								
9.0000								
10.000	0.023000	-0.056000	0.023000	-0.056000	-0.11100	0.023000	-0.056000	-0.16700
11.000								
12.000								
13.000								
14.000								
15.000	0.023000	-0.056000	0 024000	0.0000	-0.056000	0.016000	-0.44400	-0.50000
16.000								
17.000								
18.000								
19.000								
20.000	0.023000	-0.056000	0.017000	-0.38900	-0.44400	0.020000	-0.22200	-0.66600
21.000								
22.000								
23.000								
24.000								
25.000	0.019000	-0.27800	0.018000	-0.33300	-0.61100	0.023000	-0.056000	-0.66600
26.000								
27.000								
28.000								
29.000								
30.000	0.059000	1.9430	0.052000	1.5540	3.4970	0.026000	0.11100	3 6080
35.000	0.044000	1.1100	0.035000	0.61100	1.7210	0.023000	-0.056000	1.6650
40.000	0.030000	0.33300	0.027000	0.16700	0.50000	0.024000	0.0000	0.50000
45.000	0.038000	0.77700	0.030000	0.33300	1.1100	0.029000	0.27800	1.3880
50.000								
55.000	0.035000	0.61100	0.028000	0.22200	0.83300	0.028000	0.22200	1.0550
60.000								
65.000	0.031000	0.38900	0.025000	0.056000	0 44400	0.028000	0.22200	0.66600

Day 18

mm	Sulphide (mg/ml)	Sulphide (mmoles/ml)	AVS abs	AVS(mmoles/ml)	Cold CrCl Abs	Cold CrCl (mmoles/ml)	Pyrite (mmoles/ml)	Hot CrCl abs.	Hot CrCl (mmols/ml)
1.0000e-07	0.012000	0.00038000							
1.0000	0.014000	0.00044000							
2.0000	0.015500	0.00048000							
3.0000	0.017000	0.00053000							
4.0000	0.021000	0.00066000							
5.0000	0.021700	0.00068000	0.021000	0 28000	0.030000	1.5400	1.8200	0.023000	0.56000
6.0000	0.024100	0.00075000							
7.0000	0.025000	0.00078000							
8.0000	0.024700	0.00077000							
9.0000	0.025500	0.00080000							
10.000	0.027200	0.00085000	0.029000	1.4000	0.029000	1.4000	2.8000	0.025000	0.84000
11.000	0.028900	0.00090000							
12.000	0.029100	0.00091000							
13.000	0.030700	0.00096000							
14.000	0.032000	0.0010000							
15.000	0.033300	0.0010400	0.049000	4 2000	0 026000	0.98000	5.1810	0.046000	3.7800
16.000	0.035400	0.0011100							
17.000	0.035700	0 0011200							
18.000	0.035500	0.0011100							
19.000	0.036300	0.0011300							
20.000	0.037800	0.0011800	0.031000	1.6800	0.035000	2.2400	3.9200	0.023000	0.56000
21.000	0.038000	0.0011900							
22.000	0.038500	0.0012000							
23.000	0.039000	0.0012200							
24.000	0.039900	0.0012500							
25.000	0.040400	0.0012600	0.032000	1.8200	0.033000	1.9600	3.7800	0.068000	6 8610
26.000	0.040500	0.0012700							
27.000	0.040500	0.0012700							
28.000	0.040800	0.0012800							
29.000	0 040800	0.0012800							
30.000	0.041000	0 0012800	0.029000	1.4000	0.023000	0.56000	1.9600	0.028000	1.2600
35.000			0.051000	4.4810	0 029000	1.4000	5.8810	0.031000	1.6800
40.000			0.051000	4.4810	0.026000	0.98000	5.4610	0.030000	1.5400
45.000			0.040000	2.9400	0.024000	0.70000	3.6400	0.033000	1.9600
50.000			0.039000	2.8000	0 029000	1.4000	4 2000	0.028000	1 2600
55.000									
60.000			0.037000	2 5200	0 025000	0.84000	3.3600	0.043000	3 3600
65.000									
70.000			0 032000	1.8200	0 024000	0.70000	2.5200	0.021000	0.28000

Appendix Nine

Data for experiments 2, 3, 4 and 5

Day 6 - solids data*

AVS

Cold CrCl2

Depth (mm)	B	C	D	E	5mM Fe in base	5mM Fe around shrimp	0.1mM Fe around shrimp	Lepidocrocite coated shrimp	J	K	L	M	5mM Fe in base	5mM Fe around shrimp
5	0.031	0.033	0.026	0.031	0.43053	0.60274	-0.16189	0.20348	0.031	0.028	0.031	0.041	0.43053	0.17221
10		0.055	0.03463	0.035		2.4971	0.46874	0.49578		0.033	0.057	0.04		0.60274
15	0.035	0.028	0.069	0.036	0.38748	0.17221	2.9803	0.56885	0.034	0.024	0.043	0.073	0.34442	-0.17221
20		0.032	0.62	0.033		0.51664	43.245	0.34963		0.043	0.028	0.161		1.4638
25	0.038	0.024	0.072	0.032	0.51665	-0.17221	3.1995	0.27656	0.031	0.032	0.033	0.046	0.21527	0.51664
30	0.035	0.051	0.062	0.044	0.77495	2.1526	2.4688	1.1535	0.031	0.054	0.032	0.043	0.43053	2.411
35			0.033	0.042			0.34963	1.0073			0.029	0.029		
40		0.041		0.031		0.6458		0.20348		0.031		0.027		0.21527
45			0.024	0.026			-0.15405	-0.16189			0.027	0.026		
50	0.046	0.036		0.027	0.43053	0.43053		-0.088819	0.032	0.028		0.026	0.12916	0.086105
55				0.034				0.4227				0.034		
60														
65				0.031				0.10174				0.037		
70	0.035				0.19374				0.036				0.21527	
75														
80														

Hot CrCl2

0.1mM Fe around shrimp	Lepidocrocite coated shrimp	R	S	T	U	5mM Fe in base	5mM Fe around shrimp	0.1mM Fe around shrimp	Lepidocrocite coated shrimp
0.20348	0.93423	0.033	0.032	0.043	0.028	0.60274	0.51664	1.0804	-0.015744
2.1034	0.86115		0.026	0.032	0.031		0	0.27656	0.20348
1.0804	3.2726	0.026	0.027	0.042	0.033	0	0.086106	1.0073	0.34963
-0.015744	9.7032		0.029	0.036	0.043		0.25832	0.56885	1.0804
0.34963	1.2996	0.032	0.029	0.042	0.031	0.25832	0.25832	1.0073	0.20348
0.27656	1.0804	0.032	0.028	0.025	0.042	0.51664	0.17221	-0.23497	1.0073
0.057331	0.057331			0.024	0.031			-0.30804	0.20348
	-0.088819		0.03		0.03		0.17221		0.13041
-0.044408	-0.16189			0.025	0.026			-0.23497	-0.16189
	-0.16189	0.032	0.014		0.041	0.12916	-0.51665		0.93423
	0.4227				0.023				-0.38112
	0.32083				0.032				0.13828
		0.033				0.15068			

AVS Concentrations

Cold CrCl2 cores

Depth (mm)	B	C	D	E	5mM Fe in base	5mM Fe around shrimp	0.1mM Fe around shrimp	Lepidocrocite coated shrimp	J	K	L	M	5mM Fe in base	5mM Fe around shrimp
5		0.043	0.058	0.029		0.9567	1.9134	-0.4766		0.013	0.053	0.037		-0.9567
10	0.039	0.022	0.127	0.042	0.60096	-0.38268	6.3142	0.29788	0.03	0.076	0.059	0.039	0.21463	3.0614
15		0.095	0.077	0.035		4.2733	3.1252	-0.11915		0.028	0.053	0.029		0
20	0.033	0.073	0.184	0.029	0.34341	2.8701	9.9497	-0.4766	0.031	0.03	0.062	0.239	0.25755	0.12756
25		0.102	0.107	0.029		4.7197	5.0386	-0.4766		0.035	0.051	0.222		0.44646
30	0.032	0.074	0.035	0.136	0.30048	2.9339	0.44646	5.8979	0.02	0.027	0.018	0.061	-0.21463	-0.06378
35			0.027	0.109			-0.06378	4.2894			0.022	0.051		
40	0.039	0.081	0.028	0.22	0.60096	1.6902	0	10.902	0.024	0.024	0.02	0.022	-0.042926	-0.12751
45				0.039				0.11915				0.029		
50	0.048			0.034	0.98729			-0.17873	0.025			0.024	0	
55														
60	0.038	0.055	0.021	0.031	0.55803	0.43053	-0.11162	-0.17873	0.026	0.032	0.017	0.033	0.042926	0.063755
65														
70	0.037			0.038	0.51511			0.029787	0.024			0.05	-0.042926	
75														
80	0.044				0.81559				0.028				0.12878	
85														
									0.025				0	

0.1mM Fe around shrimp	Lepidocrocite coated shrimp	R	S	T	U	5mM Fe in base	5mM Fe around shrimp	0.1mM Fe around shrimp	Lepidocrocite coated shrimp
1.5945	0		0.021	0.033	0.03		-0.44646	0.3189	-0.41703
1.9772	0.11915	0.025	0.019	0.047	0.028	0	-0.57402	1.2118	-0.53618
1.5945	-0.4766		0.03	0.036	0.032		0.12756	0.51024	-0.29788
2.1685	12.034	0.021	0.028	0.037	0.046	-0.1717	0	0.57402	0.53618
1.4669	11.021		0.031	0.044	0.042		0.19134	1.0205	0.29788
-0.6378	1.4298	0.021	0.024	0.022	0.04	-0.1717	-0.25512	-0.38268	0.17873
-0.38268	0.83405			0.02	0.033			-0.51024	-0.29788
-0.51024	-0.89363	0.019	0.03	0.023	0.032	-0.25755	0.06378	-0.3189	-0.29788
	-0.4766				0.032				-0.29788
	-0.77448	0.022			0.033	-0.12878			-0.2383
-0.17539	-0.11915	0.027	0.03	0.027	0.033	0.085851	0.03189	-0.0015945	-0.11915
	0.38724	0.027			0.027	0.085851			-0.29787
		0.026				0.042926			
		0.029				0.1717			
		0.032				0.30048			

Hot CrCl2 cores

"Day 17 - solids data"

AVS concentrations

Cold CrCl2 Concs

Depth (mm)	B	C	D	E	5mM Fe in base	5mM Fe around shrimp	0.1mM Fe around shrimp	Lepidocrocite coated shrimp	J	K	L	M	5mM Fe in base	5mM Fe around shrimp
5			0.091				4.1136				0.08			
10	0.044	0.049	0.052	0.032	1.0961	1.3935	1.9159	0.39445	0.028	0.069	0.113	0.094	0.14437	2.5832
15		0.041	0.03	0.035		1.8353	0.67621	0.95796		0.032	0.105	0.081		0.76462
20	0.034		0.057	0.033	0.50128		2.1977	0.84526	0.039		0.036	0.091	0.7987	
25		0.05	0.028	0.032		1.453	0.56351	0.78891		0.27	0.057	0.102		14.54
30	0.028		0.048	0.036	0.14437		1.6905	1.0143	0.038		0.029	0.299	0.73922	
35		0.045	0.018	0.044		1.1556	0	1.4651		0.039	0.038	0.166		0.7987
40	0.037		0.029		0.67973		0.61986		0.028		0.037		0.14437	
45		0.044	0.027	0.032		1.0961	0.50716	0.39445		0.093	0.037	0.094		4.0109
50	0.071				2.7022				0.027				0.084887	
55		0.06		0.037		2.0479		0.53535		0.06		0.124		2.0479
60	0.083		0.039		3.416		0.41329		0.025		0.031		-0.034082	
65		0.043		0.042		1.0366		0.6762		0.027		0.036		0.084887
70			0.033				0.42263				0.03			
75	0.039	0.042			0.53247	0.97715			0.032	0.027			0.25487	0.084887
80														
85														
90														

Hot CrCl2 Concs

0.1mM Fe around shrimp	Lepidocrocite coated shrimp	R	S	T	U	5mM Fe in base	5mM Fe around shrimp	0.1mM Fe around shrimp	Lepidocrocite coated shrimp
3.4937				0.035				0.95796	
5.3533	2.1414	0.025	0.147	0.036	0.034	-0.034082	7.223	1.0143	0.45081
4.9025	3.5501		0.033	0.029	0.033		0.88358	0.61986	0.84526
1.0143	4.1136	0.025		0.034	0.028	-0.034082		0.90161	0.56351
2.1977	4.7335		0.03	0.03	0.048		0.26334	0.67621	1.6905
0.61986	15.835	0.025		0.026	0.072	-0.034082		0.45081	3.0429
1.127	8.3399		0.025	0.02	0.072		-0.034082	0.1127	3.0429
1.0707		0.029		0.023		0.20386		0.28175	
1.0707	2.1414		0.034	0.028	0.033		0.50128	0.56351	0.42263
		0.032				0.38231			
	2.9866		0.028		0.033		0.14437		0.42263
0.24422		0.028		0.031		0.14437		0.24219	
	0.50715		0.026		0.029		0.025403		0.30993
0.53533				0.026				0.2254	
		0.027	0.026			0.056591	0.025403		
		0.025				-0.022721			

'Day 67 - solids data'

AVS concentrations

Cold CrCl2 concs

Depth (mm)	B	C	D	E	5mM Fe in base	5mM Fe around shrimp	0.1mM Fe around shrimp	Lepidocrocite coated shrimp	J	K	L	M	5mM Fe in base	5mM Fe around shrimp
5					0.35837	0.35837	27.192	0.7999					0.59649	2.2396
10	0.023	0.023	0.073	0.038	0.35837	0.35837	27.192	0.7999	0.033	0.102	0.027	0.192	0.59649	2.2396
15		0.03	0.107	0.606	0.31074	1.0501	4.7172	38.456		0.057	0.02	0.124	0.52505	2.336
20	0.021	0.061	0.159	0.722	0.31074	1.2632	7.1937	45.983	0.03	0.022	0.019	0.068	0.52505	0.33455
25			0.14	0.119	0.59649	0.14405	6.2889	6.8549			0.021	0.874	0.4298	1.6442
30	0.033	0.014			0.59649	0.14405	0.13453	45.774	0.026	0.077			0.4298	1.6442
35			0.0136	1.4242	2.5967	0.33455	0.13453	45.774			0.025	0.388	0.12024	0.2393
40	0.117	0.022			2.5967	0.33455	2.1443	16.243	0.013	0.018			0.12024	0.2393
45			0.098	0.514	0.38159	0.19109	2.1443	16 243			0.069	0.097	0.16727	0.7983
50					0.38159	0.19109	1.0013	0.8319					0.16727	0.7983
55			0.05	0.039	0.38159	0.19109	1.0013	0.8319			0.02	0.084	0.16727	0.7983
60	0.04	0.024			0.38159	0.19109	0.40599	0.6048	0.022	0.075			0.16727	0.7983
65			0.025	0.032	0.89355	0.46499	0.40599	0.6048			0.049	0.177	0.46499	0.29825
70					0.89355	0.46499	0.6103	0.28035					0.46499	0.29825
75			0.034	0.022	0.89355	0.46499	0.6103	0.28035			0.015	0.055	0.46499	0.29825
80	0.083	0.047			0.89355	0.46499	0.5957	0.29785	0.047	0.033			0.46499	0.29825
85				0.017	0.09584		0.5957	0.29785				0.046	0.17918	
90					0.09584		0.5957	0.29785					0.17918	

0.1mM Fe around shrimp	Lepidocrocite coated shrimp	R	S	T	U	5mM Fe in base	5mM Fe around shrimp	0.1mM Fe around shrimp	Lepidocrocite coated shrimp
0.45362	5.796					0.59649	4.7161	0.31074	1.7404
0.45362	5.796	0.033	0.206	0.021	0.067	0.59649	4.7161	0.31074	1.7404
0.57386	7.1793		0.185	0.018	0.086	0.31074	8.432	0.47861	4.7136
0.52623	3.5456	0.021	0.03	0.019	0.112	0.31074	0.52505	0.52623	6.4007
0.62148	55.846			0.015	0.197	0.28693	0.83462	0.33573	11.916
0.40599	12.155	0.02	0.043			0.28693	0.83462	0.14405	6.4125
0.40599	12.155			0.014	0.211	0.19168	0.35837	0.14405	6.4125
1.4537	2.7137	0.016	0.023			0.19168	0.35837	0.35837	2.5839
1.4537	2.7137			0.023	0.093	0.13656	0.34587	0.35837	2.5839
0.28693	2.2919					0.13656	0.34587	0.47743	1.3185
0.28693	2.2919			0.028	0.054	0.13656	0.34587	0.47743	1.3185
0.9775	5.309	0.019	0.037			0.13656	0.34587	0.47743	0.8968
0.9775	5.309			0.028	0.041	0.10774	0.48875	0.47743	0.8968
0.16786	1.351					0.10774	0.48875	1.0013	0.21546
0.16786	1.351			0.05	0.02	0.10774	0.48875	1.0013	0.21546
0.47665	1.059	0.017	0.049			0.10774	0.48875	1.2942	0
0.47765	1.059				0.013	0.26252		1.2942	0
0.47765	0.44258					0.26252		1.2942	0.08569
0.47765	0.4258				0.016	0.26252		1.2942	0.08569
0.47765		0.03				0.26252		1.2942	
0.47765				0.171				1.2942	

Hot CrCl2 Concs

Appendix Ten
Results from the analysis of sediment incubations

This table lists the reduced sulphur pool data from the sediment incubations.

Aust incubation after 4 days

cm depth	Hydrogen sulphide (mM)	AVS (mM)	PS (mM)	ES (mM)
0-1		2.2126	5.7537	1.2388
1-2		5.134	6.9045	0.97321
2-3		4.8684	4.4258	1.5044
3-4		11.508	1.4159	1.0617
4-5		6.816	2.5667	0.53058
5-6		20.449	13.898	0.35353
6-7				

Aust incubation after 12 days

cm depth	Hydrogen sulphide (mM)	AVS (mM)	PS (mM)	ES (mM)
0-1		3.0093	5.6651	3.629
1-2		5.311	5.7537	1.3273
2-3		0.087945	3.0979	0.53058
3-4		11.951	9.8259	4.1602
4-5		14.96	6.6389	0.97321
5-6		6.0193	4.3372	0.17647
6-7				

Aust incubation after 68 days

cm depth	Hydrogen sulphide (mM)	AVS (mM)	PS+ES(mM)
0-1	0	<0.0001	7.3031
1-2	0	1.5944	15.662
2-3	<0.0001	1.4925	10.157
3-4	<0.0001	41.861	26.264
4-5	<0.0001	53.686	10.463
5-6	0	51.035	23.308
6-7	0	36.05	23.002

Aust incubation after 12 days (bioturbated)

cm depth	Hydrogen sulphide (mM)	AVS (mM)	PS (mM)	ES (mM)
0-2		0	5.2503	0
2-3		0	3.6061	1.4921
3-4		0.7874	7.9515	2.0793
4-5		0.55252	7.834	<0.0001
5-6		14.176	11.592	2.6665
6-7		59.979	8.7736	10.77